

Synthesis and mass spectrometry based characterization of chemical tools to explore FK506 binding proteins

Synthese und massenspektrometrie-basierte Charakterisierung von chemischen Werkzeugen zur Erforschung von FK506 bindenden Proteinen

Zur Erlangung des Grades eines Doktors der Naturwissenschaften (Dr. rer. nat.)

Genehmigte Dissertation von Tim Heymann aus Groß-Umstadt

Tag der Einreichung: 31.03.2022, Tag der Prüfung: 09.05.2022

1. Gutachten: Prof. Dr. Felix Hausch
2. Gutachten: Prof. Dr. Franz-Josef Meyer-Almes
Darmstadt 2022



TECHNISCHE
UNIVERSITÄT
DARMSTADT

Fachbereich Chemie
Clemens-Schöpf-Institut
Arbeitskreis Hausch

Synthesis and mass spectrometry based characterization of chemical tools to explore FK506 binding proteins

Synthese und massenspektrometrie-basierte Charakterisierung von chemischen Werkzeugen zur Erforschung von FK506 bindenden Proteinen

Genehmigte Dissertation von Tim Heymann

1. Gutachten: Prof. Dr. Felix Hausch
2. Gutachten: Prof. Dr. Franz-Josef Meyer-Almes

Tag der Einreichung: 31.03.2022

Tag der Prüfung: 09.05.2022

Darmstadt 2022

Bitte zitieren Sie dieses Dokument als:

URN: urn:nbn:de:tuda-tuprints-214415

URL: <http://tuprints.ulb.tu-darmstadt.de/21441>

Dieses Dokument wird bereitgestellt von tuprints,

E-Publishing-Service der TU Darmstadt

<http://tuprints.ulb.tu-darmstadt.de>

tuprints@ulb.tu-darmstadt.de

Die Veröffentlichung steht unter folgender Creative Commons Lizenz:

Namensnennung – Weitergabe unter gleichen Bedingungen 4.0 International

<https://creativecommons.org/licenses/by-sa/4.0/>

Erklärungen laut Promotionsordnung

§8 Abs. 1 lit. c PromO

Ich versichere hiermit, dass die elektronische Version meiner Dissertation mit der schriftlichen Version übereinstimmt.

§8 Abs. 1 lit. d PromO

Ich versichere hiermit, dass zu einem vorherigen Zeitpunkt noch keine Promotion versucht wurde. In diesem Fall sind nähere Angaben über Zeitpunkt, Hochschule, Dissertationsthema und Ergebnis dieses Versuchs mitzuteilen.

§9 Abs. 1 PromO

Ich versichere hiermit, dass die vorliegende Dissertation selbstständig und nur unter Verwendung der angegebenen Quellen verfasst wurde.

§9 Abs. 2 PromO

Die Arbeit hat bisher noch nicht zu Prüfungszwecken gedient.

Darmstadt, 31.03.2022

T. Heymann

Acknowledgements

First and foremost I would like to thank my family and friends for their continued support during my education and doctoral thesis. I thank Felix Hausch who gave me a lot of freedom during my thesis and allowed me to use a substantial amount of financial resources for consumables and acquiring new instruments. I thank all my colleagues at the TU Darmstadt for the productive working atmosphere. I especially thank Patrick Purder and Andreas Voll for contributing synthetic intermediates for this thesis, Matthias Brauser and Johann Primožic for our productive cooperations and for measuring NMR spectra for me, and Thomas Nehls for the valuable discussions about analytical chemistry with me. I am indebted to Alexander Schießler for allowing me to use the mass spectrometers of the mass spectrometry department and providing very helpful technical support. Many thanks go to Christian Meyners for providing me with protein constructs and valuable advice about biochemistry. I thank Thomas Geiger and Wisley Oki Sugiarto for measuring NanoBRET and FP assays for me respectively.

Zusammenfassung

Die FK506 bindenden Proteine (FKBPs) sind eine Proteinfamilie, die zu den Immunophilinen gehören und interessante Wirkstoffziele. FKBP51 ist in Säugetieren mit Stresskrankheiten, metabolischen Krankheiten und chronischem Schmerz assoziiert. Mikrobiische und parasitische FKBPs sind wichtig für die Vervielfältigung von Pathogenen, wodurch deren Inhibitoren anti-infektiös wirken.

Obwohl die Effekte von FKBP Deletion oder Inhibierung mit Liganden gut charakterisiert sind, sind die für die beobachteten Effekte verantwortlichen Mechanismen unklar und die Literatur dazu oft kontrovers. Um dieses Problem zu lösen, wurden mehrere chemische Werkzeuge sowie MS-basierte Methoden zu deren Charakterisierung und späteren Analyse innerhalb dieser Thesis entwickelt.

Die Entwicklung einer Synthese von SAFit2 im Gramm-Maßstab machte das bisher beste verfügbare chemische Werkzeug für FKBP51 in großen Mengen verfügbar und erlaubt damit breit angelegte *in vivo* Experimente zur weiteren Erforschung von FKBP51 in Säugetieren wie Mäusen.

Die Entwicklung einer Synthese für einen Diazirin-Synthesebaustein machte das Kopeln dieses photoreaktiven Bausteins mit beliebigen Proteinliganden oder Molekülen möglich. Dies erlaubt ein breites Spektrum von neuen photoreaktiven Liganden mit vielfältigem Nutzen, wie die Cystein-reaktiven photoaktiven Bausteine und die photoreaktiven Liganden, die in dieser Arbeit synthetisiert wurden, zeigen. Eine simple intakte Proteinmassenanalyse durch LCMS wurde entwickelt. Ergänzend mit einer einfachen top-down Methode wird das Analysieren von *in vitro* Experimenten mit photoreaktiven Crosslinkern ermöglicht, was die schnelle Identifikation von markiertem Protein mit hoher Selektivität erlaubt. Eine komplexere bottom-up Proteomics-Methode ermöglicht die Verwendung und Analyse von photoreaktiven FKBP Liganden in Zellen, was das Identifizieren von Proteinbindungspartnern und alternativen Bindungspartnern von Liganden ermöglicht. Dies ist durch herkömmliche gezielte Methoden, wie Western Blotting, nicht möglich. Beide Methoden in Kombination mit den photoreaktiven chemischen Werkzeugen bilden eine leistungsstarke Toolbox, um FKBPs in Zellen zu erforschen.

Abstract

The FK506 binding proteins (FKBPs) are a protein family belonging to the immunophilins and are interesting drug targets. FKBP51 is associated with stress-related diseases, metabolic diseases and chronic pain which makes it an interesting drug target. Microbial or parasitic FKBPs (Mips) are important for the replication of pathogens and thus inhibitors for Mips are anti-infective.

While the effects of addressing FKBPs by knockout or with FKBP ligands are well characterized, the underlying mechanisms leading to the observed effects on the cell level are unclear and the literature is often controversial. To address this problem, several chemical tools and MS based methods for their characterization and later use have been developed in this thesis.

The development of a gram scale SAFit2 synthesis makes this so far best chemical tool for FKBP51 available for extensive *in vivo* experiments, allowing further study of FKBP51 inhibition in animals.

The development of a synthesis for a diazirine building block allows coupling of this photoreactive warhead to almost any given ligand or molecule of choice via a linker. This allows a broad spectrum of new photoreactive ligands with versatile use, as demonstrated by the photoreactive ligands and cysteine reactive photo labels synthesized and used for photoaffinity labeling in this thesis. Development of a simple protein intact mass LC-MS analysis supplemented by a top-down approach allows assessment of *in vitro* experiments performed with chemical crosslinkers, facilitating rapid identification of labeled proteins with high confidence. A more sophisticated bottom-up proteomics approach allows the use and analysis of photoreactive FKBP ligands in cells, enabling the identification of protein binding partners and ligand off-targets otherwise not possible by targeted methods such as western blotting. Both LC-MS based methods in combination with the photoreactive chemical tools make up a powerful toolbox for the analysis of FKBPs.

Table of Contents

Acknowledgements	v
1 Introduction	1
1.1 FK506 binding proteins (FKBPs)	1
1.2 FKBP ligands	4
1.2.1 Development of FKBP51 selective ligands	4
1.2.2 Macrocyclic FKBP ligands	5
1.3 Photoaffinity labels (PALs) in biochemistry	6
1.3.1 Structure of PALs	6
1.3.2 Use of photoaffinity labels to identify protein binding partners	6
1.4 Liquid chromatography electrospray ionization mass spectrometry (LC-ESI-MS)	7
1.4.1 Components and properties of LC-MS systems	7
1.4.2 Mass analyzers in ESI MS	9
1.4.3 Proteomics	12
1.4.4 Footprinting of proteins	13
2 Aim	15
3 Results and discussion	17
3.1 Gram scale synthesis of SAFit ligands	17
3.2 SAFit1-like lactam derivatives as ligands for FKBP51	26
3.3 Analysis of FKBP ligand binding by oxidative footprinting	30
3.4 Photo affinity labels (PALs) to explore FKBP5	33
3.4.1 Cysteine reactive photo crosslinker	33
3.4.2 Stable isotope labeled pBpa	35
3.4.3 Photo reactive ligands (PRLs) for FKBP5	37
3.5 Analysis of a tetrapeptidic organocatalyst	45
4 Conclusion	49
5 Materials and methods	51
5.1 NMR	51
5.2 HRMS	51
5.3 LC-MS	51
5.4 HPLC	51
5.5 Chiral HPLC	52
5.6 UHPLC-MS	52
5.7 GC-MS	52

5.8	Flash chromatography	52
5.9	Manual column chromatography	53
5.10	Preparative HPLC	53
5.11	Solvents and reagents	53
5.12	FKBP protein constructs	53
5.13	Fluorescence polarization assay	53
5.14	NanoBRET assay	54
5.15	Protein LCMS	54
5.15.1	Oxidative footprinting	54
5.15.2	Intact protein mass measurements by LC-MS	54
5.15.3	Top down analysis	55
5.15.4	Bottom up proteomics	55
5.16	General procedures	56
5.16.1	Organic synthesis	56
5.16.2	Solid phase synthesis	56
6	Experimental procedures	59
6.1	Crosslinking of PRL in vitro	59
6.2	Crosslinking of PRL in HEK cells	60
6.3	Organic syntheses	61
	References	161

1 Introduction

1.1 FK506 binding proteins (FKBPs)

FK506 binding proteins (FKBPs) belong to the class of immunophilins and have at least one domain with high sequence homology to FKBP12, the first known member.^[1] In mammals, FKBP12 is a 12 kDa protein with a peptidyl-prolyl *cis-trans* isomerase (PPIase) activity that binds the natural ligands FK506 (see **Figure 1**) and rapamycin.^[2,3] This in turn results in the formation of ternary gain-of-function complexes with calcineurin, a protein important for T-cell activation^[4,5], and the FRB domain of mTOR, a kinase involved in cell growth and cell proliferation^[2,6], respectively. Both of these complexes lead to immunosuppressive effects and are induced only in the presence of their respective ligands. For this reason, FK506 and rapamycin are used as drugs to stop allograft rejection in organ transplant patients.^[7-9]

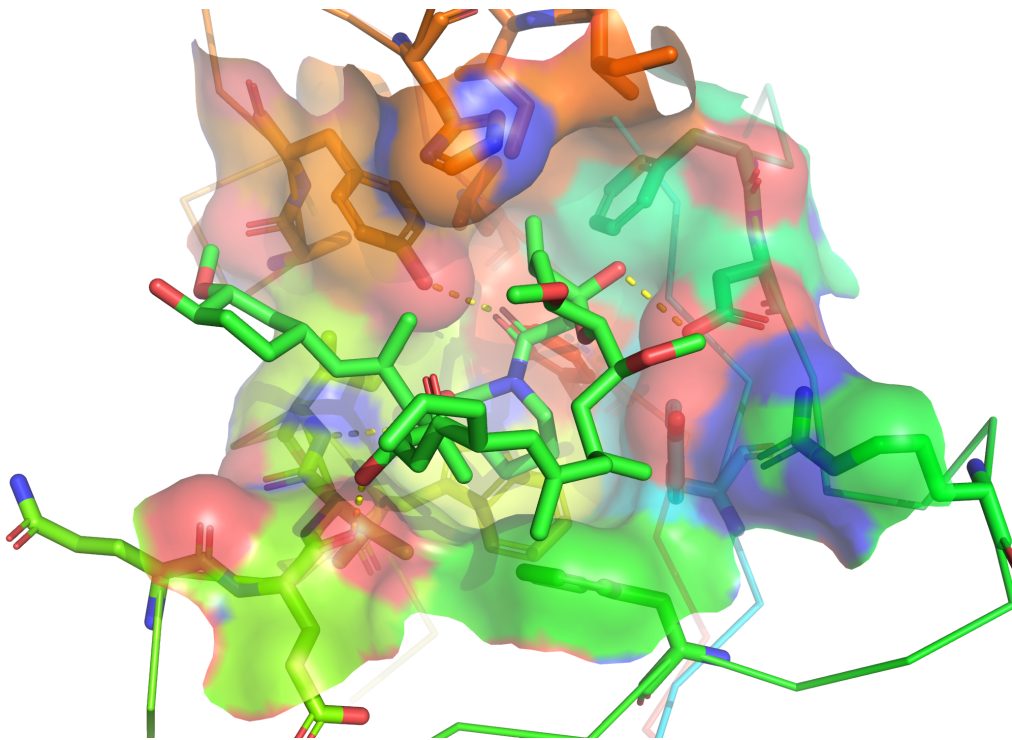


Figure 1: Complex of FK506 with human FKBP12 (pdb: 1FKF). Hydrogen bonds are indicated by yellow dashed lines.^[3]

Aside from the immunosuppressive effect, FKBP12 and its homologue FKBP12.6 were

shown to be essential for mammalian life since they play an important role in the fine tuning of the excitability of smooth and heart muscles together with ryanodine receptors (RyRs).^[10–12] Knock-out of FKBP12 in mice led to severe cardiac defects resulting in an embryonic lethal phenotype.^[13,14] This is attributed to a non-functioning ryanodine receptor which modulates intracellular Ca^{2+} -signaling in myocytes to evoke muscle contraction. FKBP12.6 seems to share this function, but is specialized to control the cardiac muscle stimulation in mammals by forming complex with RyR2. On the other hand, FKBP12 is present in complex with RyR1 in skeletal muscles.^[10,15] These findings are highly controversial though, as various studies about FKBP12 and FKBP12.6 and their interaction with RyRs lead to contradicting findings, leaving the details unclear.^[1]

Other FKBP of importance in mammals are FKBP51 and FKBP52 which both consist of three domains, an *N*-terminal FK1 domain and FK2 domain with high homology to FKBP12 and a C-terminal tetratricopeptide repeat-domain (TPR-domain) as shown in **Figure 2**. Both proteins share high sequence homology in the FK1 domain which exhibits a PPIase function. The FK1 domain of both proteins bind FK506 and rapamycin with weaker affinity compared to FKBP12^[16], while the homologous FK2 domains do not, and no valid biological function is known so far.^[17,18] The TPR domain facilitates FKBP51 activity as a cochaperone for HSP90 in the form of a docking site.^[19,20]

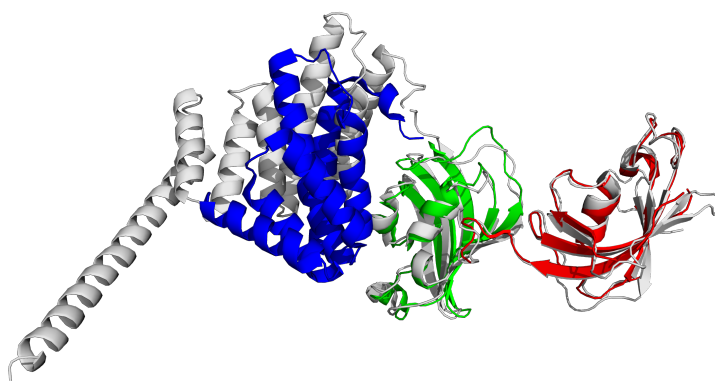


Figure 2: Superimposed protein structures of FKBP51 (pdb: 1KT0), shown in blue (FK1 domain), green (FK2 domain), and red (TPR domain) and FKBP52 (pdb: 1Q1C and 1P5Q) shown in gray demonstrating their high homology.

FKBP51 emerged as a promising drug target for stress related diseases^[21–28], obesity^[29,30], and chronic pain^[31–33] based on studies with knockout mice. On the other hand, FKBP52 knockout led to severe side effects in impaired sex organ development, demonstrating the need of selective ligands for FKBP51.^[34,35]

SAFit2 was the first synthesized selective FKBP51 ligand with an acceptable pharmacological profile for *in vivo* studies in rodents as a chemical tool and exhibits a selectivity of >10000 for FKBP51 over FKBP52 with a nanomolar affinity.^[28] Studies with SAFit2 in mice phenocopied the results of FKBP51 knockout mice resulting in increased stress coping behavior^[28], antidiabetic effects as well as attenuated weight gain^[30], resistance

to chronic pain^[31,33] and NF κ B driven inflammatory pathways^[27]. This clearly validated FKBP51 as a drug target and lead to further advances in ligand development of FKBP51 selective ligands.^[36-40]

FKBP51 is believed to regulate the glucocorticoid (GR) receptor by a negative feedback loop within the HPA axis as shown in **Figure 3**. This hypothesis initially resulted from the observed FKBP51 overexpression in squirrel monkeys^[41,42] causing low GR sensitivity and was later supported by single nucleotide polymorphisms in the FKBP5 gene encoding FKBP51 in patients with depression.^[43,44] Within this model FKBP51 acts as a cochaperone with HSP90 downregulating GR sensitivity towards glucocorticoids, like cortisone, resulting in enhanced stress coping ability.^[45] On the other hand, FKBP52 is believed to cause the opposite effect by upregulating the sensitivity of the GR resulting in lowered stress coping ability.

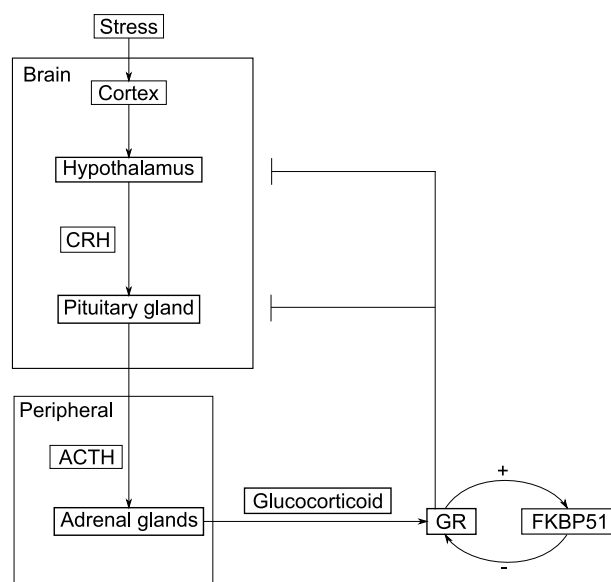


Figure 3: Schematic functioning of the HPA axis involving FKBP51: Stress registered by the cortex can lead to HPA-axis activation by increasing the production and secretion of corticotropin-releasing hormone (CRH) in the hypothalamus. This, in turn, activates the pituitary gland which releases adrenocorticotropic hormone (ACTH) into the bloodstream. ACTH activates the adrenal glands to release glucocorticoids like cortisol. Glucocorticoids itself regulate the release of CRH and ACTH by a negative feedback mechanism together with the glucocorticoid receptor (GR). FKBP51 regulates the GR by a negative feedback loop as a cochaperone together with HSP90.^[41,45-47]

While this model is supported by detection of the interaction between FKBP51 and the GR by a cryo-EM structure of a HSP90-FKBP51-p23 complex and a crosslinking analysis, the question of how FKBP51 interacts with other proteins in this complex still remains unclear.^[48]

Aside from mammals, FKBP51s present in microbes or parasites (also called Macrohpa-

ge infectivity potentiators, Mips) are important for replication of pathogens which makes Mip inhibitors in turn potentially anti-infective.^[49] As these proteins usually do not affect cell growth, the selectivity pressure for developing resistances is much lower than for proteins which are vital for cell growth and proliferation.^[50] Studies have shown, that pan selective FKBP ligands have antimalarial, antilegionellal, and antichlamydial properties in cellular models of infectivity, making them Mip inhibitors.^[51]

1.2 FKBP ligands

1.2.1 Development of FKBP51 selective ligands

FKBP ligands were developed with the natural compounds rapamycin and FK506 as a starting point in an attempt to generate chemical tools to study FKBP, with the ultimate aim to develop orally available drugs.^[1] The first synthetic ligand for FKBP (SLF) no longer induced ternary complex formations and showed no immunosuppressive effects.^[52,53] Based on this initial breakthrough several improvements followed, which ultimately led to two different ligand classes: High affinity, pan-selective bicyclic ligands^[54] and FKBP51 selective SAFit ligands as shown in **Figure 4**.

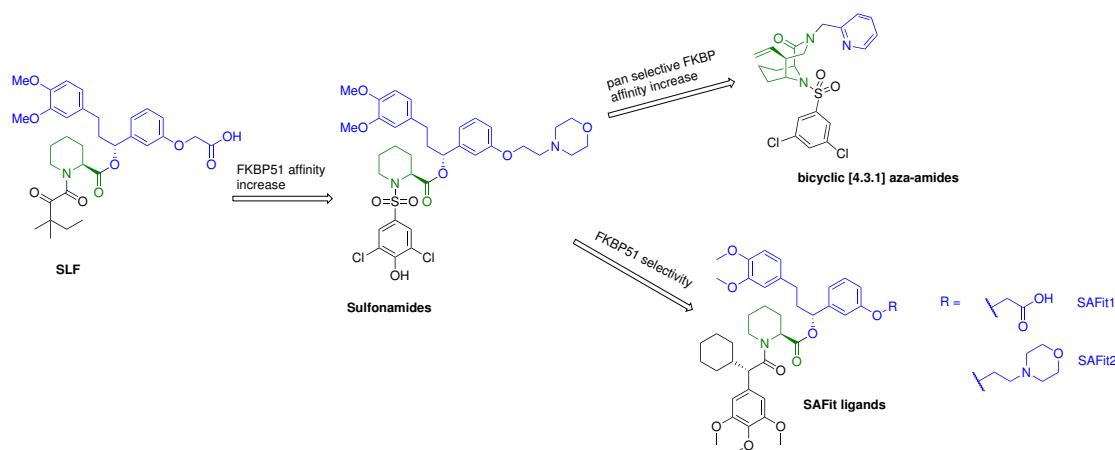


Figure 4: Major development steps of FKBP ligands starting from the first synthetic ligand for FKBP (SLF). Structural building blocks are color coded (blue top group, green core group, black bottom group): Increase of FKBP51 affinity was achieved with Sulfonamides^[55], followed by a further pan-selective affinity increase with [4.3.1] aza-amides by introducing a bicyclic core structure^[54], and development of FKBP51 selective SAFit ligands^[28].

SAFit ligands derive their selectivity from an induced fit mechanism involving the displacement of F67 which flips out of the binding pocket to accommodate the cyclohexyl moiety of the C⁹ position. In FKBP52 this conformational change is strongly disfavored compared to FKBP51 because the surrounding amino acids are significantly more bulky. SAFit1 was meant to be used as a non-brain permeable drug to specifically address metabolic disease

without affecting the brain by designing the ligand with a carboxylic acid that greatly reduces its permeability for the blood-brain barrier but also for cell membranes.^[28]

1.2.2 Macrocyclic FKBP ligands

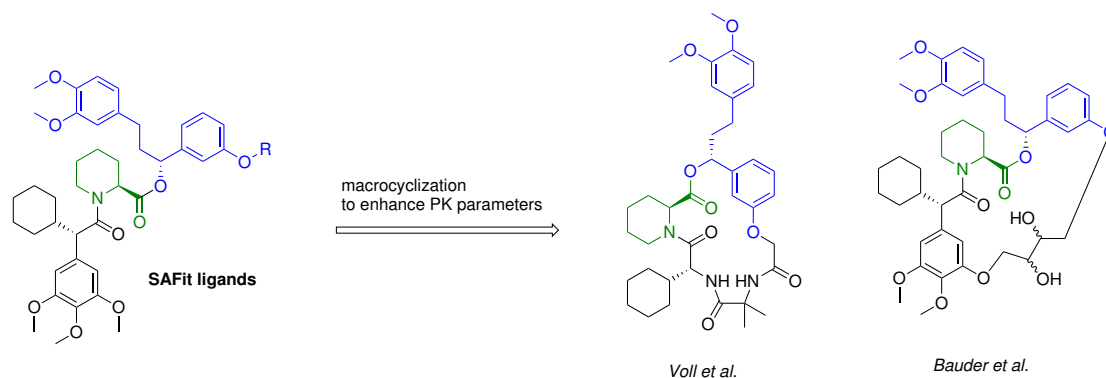


Figure 5: Developed macrocycles based on SAFit ligands to enhance PK parameters like cell permeability while maintaining ligand affinity and selectivity.^[39,40]

Optimizing SAFit ligands with the ultimate goal to create not just a chemical tool but a drug to address above mentioned diseases in humans has been an actively pursued challenge over the last years resulting in several structure activity relationship (SAR) studies.^[36,38] However, significantly reducing the molecular weight while keeping affinity and selectivity to enhance the pharmacological profile of SAFit ligands has not been achieved after several attempts. This prompted the development of macrocyclic SAFit like ligands^[39,40] shown in **Figure 5** which bypassed the requirement for smaller ligands and resulted in enhanced pharmacological properties, such as cell permeability.^[56–58] Although these ligands were capable of increasing selectivity with comparable affinities to those of SAFit, their synthesis became even more complex, limiting the amounts available for *in vivo* studies. For this reason, SAFit2 remained the gold standard as a chemical tool to explore FKBP51 functions in *in vivo* studies.^[1]

1.3 Photoaffinity labels (PALs) in biochemistry

1.3.1 Structure of PALs

Photocrosslinkers are commonly used tools in chemical biology to study protein-protein interactions^[59] and identifying ligand-protein binding partners^[60]. Several photoreactive groups activated with UV irradiation at different wavelengths are shown in **Figure 6**, but only diazirines, benzophenones and aryl azides are commonly used. Photoreactive chemical tools typically consist of three parts, the photoreactive group, an affinity/specificity unit, and a reporter tag. The photoreactive group generates a highly reactive species to form a covalent bond with molecules in proximity.^[61] Affinity/specificity units can either be unselective, such as cysteine reactive moieties^[62] or selective, such as protein specific ligands^[63]. Reporter tags in the form of fluorophores, biotin, or radiolabels are often introduced after photo-crosslinking using a bioorthogonal handle, like an alkyne or azide group, within the photocrosslinker compound.^[64]

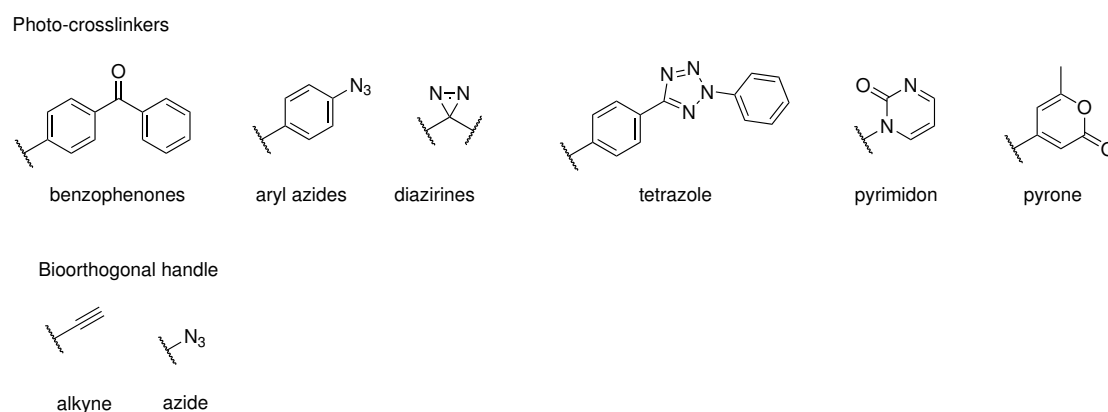


Figure 6: Photocrosslinkers and bioorthogonal handles for introducing reporter tags used in chemical biology.^[61]

Diazirines are the most popular choice among photo reactive groups because of their small size, chemical stability, superior crosslinking reactivity, and most importantly the longwave UV 365 nm used to activate diazirines, reducing the damage to the biological system compared to other photo reactive groups requiring lower wavelengths.^[65] After crosslinking, proteins can be analyzed by LC-MS or fluorescence imaging to elucidate binding interactions of protein interactomes or crosslinking sites of the target protein.^[59,66]

1.3.2 Use of photoaffinity labels to identify protein binding partners

In practice, photoaffinity labels are often used to fish for drug targets and study the interactome of ligands^[67] or to study protein-protein interactions^[68] in cells. While for small molecules ligands the incorporation of a photoreactive group can simply be accomplished during the synthesis resulting in a photoreactive ligand (PRL), incorporation of photo affinity labels in proteins is more difficult and can be achieved by site specific labelling,

e.g. using cysteines^[69], or by incorporating unnatural amino acids during protein biosynthesis^[70,71]. After introduction of the photoaffinity label, crosslinking is induced upon UV irradiation leading to the formation of covalent bonds between the photoaffinity label and a protein in proximity as shown in **Figure 7**. Notably, the crosslinking yields of the popular diazirine PALs are typically under 10 % because the reactive carbene intermediate can be quenched by the solvent water.^[72] On the other hand, benzophenones can crosslink more efficiently because they are not quenched by reaction with water.^[73]

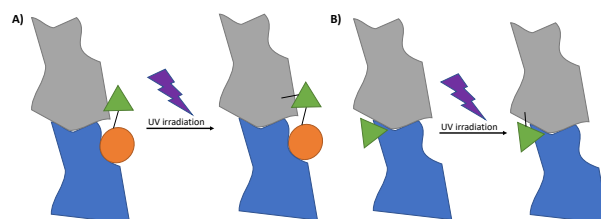


Figure 7: Concept of photo-crosslinkers for photoaffinity labeling to study protein binding partners: **A)** a ligand (orange circle) equipped with a photoreactive warhead (green triangle) via a linker binds its protein (blue) and crosslinks another protein (gray) forming a complex with the target protein upon UV irradiation. **B)** A protein is directly labeled with a photoreactive warhead and crosslinks a protein binding partner in proximity upon UV irradiation.

1.4 Liquid chromatography electrospray ionization mass spectrometry (LC-ESI-MS)

1.4.1 Components and properties of LC-MS systems

Over the last decades, mass spectrometry has taken a vital position in biochemistry after ESI and MALDI ionization techniques were introduced that allowed the soft ionization of proteins and peptides.^[74–76] Applications of mass spectrometry range in the analysis of isolated proteins or metabolites to analyzing complex mixtures from cells or tissue, so called proteomics or metabolomics, aiming to analyze the entire proteome or metabolome respectively.^[77,78] For complex samples, mass spectrometers are typically operated with online liquid chromatography (LC) systems to allow sensitive and robust analysis using the LC separation together with the mass over charge (m/z) separation of the analytes in the mass spectrometer. This allows specific identification and quantification of entire proteomes with high sensitivity.^[79] Major advantages compared to western blotting are the much higher linear dynamic range^[80,81] as well as the ability to use untargeted LC-MS methods which does not require beforehand knowledge of the proteins to be analyzed.^[82]

With the advance in technology of high resolution mass spectrometry^[83] and the improvement of liquid chromatography to use higher pressure^[84], liquid chromatography mass spectrometry (LC-MS) has taken a vital role in the analysis of biomolecules and especially proteins.^[85] In this analysis technique, analytes dissolved in a liquid matrix are

separated by an analytical column containing a stationary solid phase, such as C18 silica particles, before they are introduced into the ion source of a mass spectrometer where the analytes are ionized and then analyzed depending on their mass over charge (m/z) ratio.^[77] **Figure 8** shows the components of a modern LC-MS.

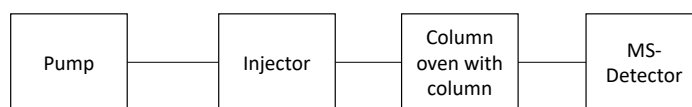


Figure 8: Components of a typical LC-MS system.^[86]

Performance of LC systems mainly depend on their tolerated back pressure, as analytical LC columns achieve a higher plate count N with smaller particles sizes that result in higher back pressures.^[87] Additionally, the use of smaller particles size columns allows faster flow rates and therefore faster analysis at higher chromatographic resolution as demonstrated by the van Deemter plots in **Figure 9**.^[88]

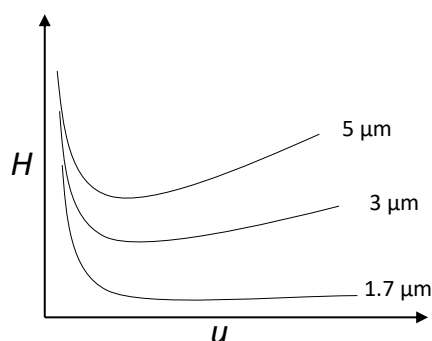


Figure 9: Typical van Deemter curves for LC columns with different silica particle sizes showing the dependence of the height of a theoretical plate H in dependence of the linear velocity of the mobile phase u . The inner diameter of the particles is indicated in μm .^[89]

Therefore, it is desirable to use LC systems capable of withstanding high pressures. Advances in the development of LC allow pressures of up to 1300 bar with sub 2 μm silica particle columns in modern ultra high pressure liquid chromatography (UHPLC) systems.^[90] For maximum sensitivity, nano LC systems are utilized together with mass spectrometers, maximizing sample concentration.^[91]

Mass spectrometers are sensitive detectors for ions generating very specific signals for their mass over charge (m/z) adding another dimension of analyte separation to the already powerful chromatographic separation of modern UHPLC systems.^[77] In order to analyze molecules with a mass spectrometer, it is first necessary to ionize the molecules in an ion source. This is commonly achieved by electrospray ionization (ESI), that allows soft ionization of small and large molecules, such as proteins, by charging them with multiple

charges without any fragmentation, enabling preservation of non covalent bonds.^[74,86] Figure 10 shows the components of a mass spectrometer coupled to an LC system.

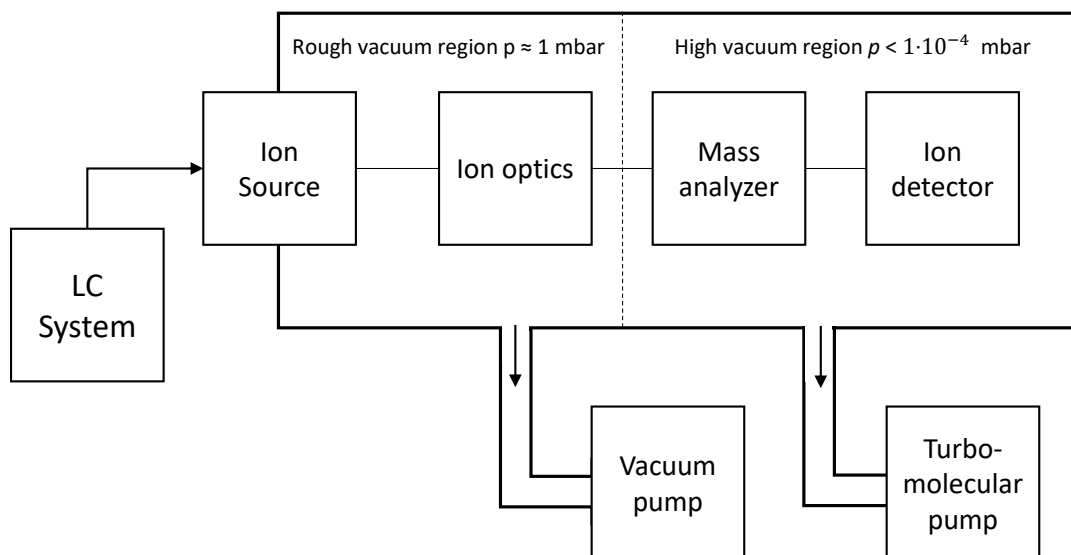


Figure 10: Components of a mass spectrometer coupled to an LC system. The vacuum pumps generate a vacuum gradient, with a rough vacuum region starting at a pressure of about $p = 1$ mbar close to the orifice of the ion source along the ion optics, dropping to below $p > 1 \times 10^{-4}$ mbar in the high vacuum region where the mass analyzer and ion detector are situated.^[92]

Analytes arriving from a LC system in the ESI ion source are sprayed from a thin emitter tip and ionized into the gas phase by applying a high voltage to the emitter tip. During this process the liquid surface forms a Taylor cone from which small charged droplets are sprayed. With the aid of heated nitrogen gas the solvent in the droplets is removed until the electrostatic repulsion leads to a Coulomb explosion, thereby releasing ions into the gas phase.^[74] These ions then enter the orifice of the mass spectrometer and are separated from neutral molecules and compressed into an ion beam by the ion optics, thereby transitioning from atmospheric pressure inside the ion source into the rough vacuum region (1 mbar) of the ion optics. This ion beam is then passed on into the high vacuum region of the mass analyzer, where ions are separated according to their m/z and detected by a detector.^[93] Most detectors are based on electron multipliers and are able to detect very small amounts of ions to the point that almost individual ions can be detected in some modern mass spectrometers.^[94]

1.4.2 Mass analyzers in ESI MS

The performance of ESI mass spectrometers strongly depends on their mass analyzer. The most widely used MS analyzer in modern mass spectrometers is the quadrupole mass analyzer.^[95] As the name suggests, this mass analyzer consists of four rods to which an oscillating radio frequency (RF) voltage with a direct current (DC) offset is pairwise appli-

ed. For this system, stable trajectories of ions depending on their m/z exist only for certain ratios of RF and DC voltages. The stable region for these voltage ratios can be determined by solving the Mathieu **Equation 1** in x and y direction, the plane perpendicular to the orientation of the quadrupole rods.^[96]

$$\frac{d^2u}{d\xi^2} + (a_u - 2q_u \cos 2\xi) \quad (1)$$

$$a_u = \frac{8eU}{mr_0^2\omega^2} \quad (2)$$

$$q_u = \frac{4eV}{mr_0^2\omega^2} \quad (3)$$

In the above equations describing the motion of an ion with mass m and charge e within the quadrupole rods with effective radius r_0^2 between the electrodes, a_u being proportional to the DC voltage U and q_u being proportional to the RF amplitude V applied with the frequency ω . The solution of this equation results in the stability diagram in **Figure 11** which shows the regions where the trajectory through the quadrupole for ions with particular m/z ratios is stable.^[96]

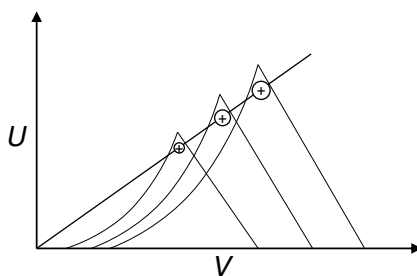


Figure 11: Schematic Mathieu stability diagram for a quadrupole mass analyzer. Stable regions for ions of different sizes depending on DC offset voltage U and RF amplitude V are shown. Ramping U and V at a constant ratio allows scanning for different ions along a working line through the origin as shown.^[96]

The quadrupole mass analyzer can either be operated at set voltages, allowing only a particular ion or a range of ions to pass which is therefore termed single ion monitoring (SIM), or the voltages can be ramped at a constant ratio to scan along an entire mass range to acquire full scan mass spectra. Quadrupoles are generally operated with unit mass resolution, resulting in a full width at half maximum (FWHM) of $0.7 m/z$.^[96]

Quadrupoles are often used together with other mass analyzers for tandem MS at low resolution in the form of triple quadrupole mass spectrometers or high resolution quadrupole time of flight (QTOF) and Orbitrap mass spectrometers.^[86] High resolution mass spectrometers generally achieve a mass resolution $R > 10000$, with R commonly defined as the m/z value divided by the full width at half maximum (FWHM) of a peak in an

MS spectrum $R = \frac{m/z}{\text{FWHM}}$.^[97] While QTOF mass spectrometers generally do not exceed $R = 100000$, they are capable of scanning at very high rates.^[94,98] On the other hand, Orbitrap mass spectrometers became very popular for the analysis of biomolecules due to their ability to achieve resolutions of $R = 1000000$ and high mass accuracy $\text{ppm} < 1$ ^[99], but have considerably lower scan rates compared to QTOFs.^[100,101]

The Orbitrap analyzer is made up of an inner electrode to which a voltage is applied and an outer barrel shaped electrode maintained at virtual ground and functions vastly different from other ion traps that use RF field to trap ions.^[102]

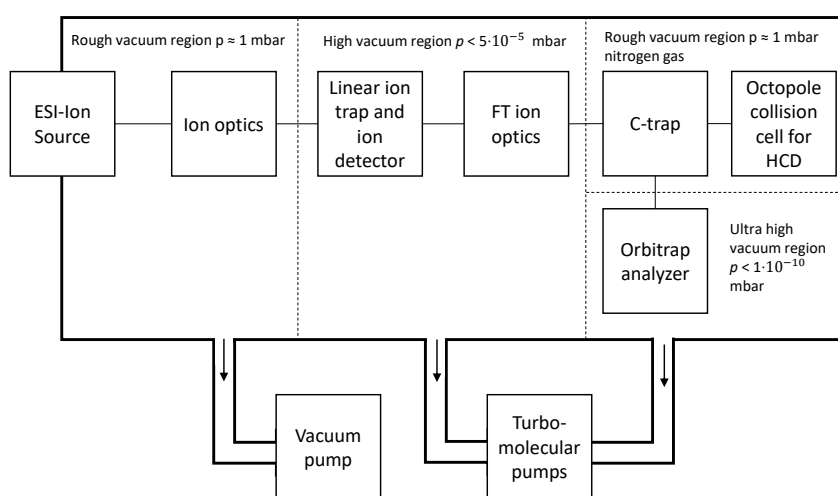


Figure 12: Schematic overview of the components of an LTQ Orbitrap XL mass spectrometer. The vacuum regions are achieved by differential pumping of fore vacuum pumps and turbomolecular pumps. The C-trap is an RF only trap used for pulsing ion packets into the Orbitrap analyzer.^[103]

Ions entering the Orbitrap are trapped in an electrical field and oscillate harmonically along the z axis of the analyzer depending on their m/z ratio. Time dependent detection of this oscillation by an image current detector results in a transient signal that yields the mass spectrum after Fourier transformation with increasing resolution and signal to noise depending on the time the transient is acquired.^[104,105] As a single scan with sufficiently high resolution requires recording a transient longer than a hundred milliseconds even on modern high field Orbitraps, most Orbitrap mass spectrometers such as the LTQ Orbitrap XL are operated together with an ion trap that allows faster scan rate at lower resolution and enables acquisition of tandem MS^n spectra.^[100]

1.4.3 Proteomics

For the analysis of proteins two different approaches are common: A top-down approach where intact protein is directly introduced into an LC-MS system and analyzed^[106] or a bottom-up approach where the protein or a mixture of proteins is digested with a protease and the resulting peptides are then analyzed by LC-MS^[107]. In both cases the mass spectrometer operates in a similar way by performing a precursor scan determining the accurate precursor mass with an accuracy of 15 ppm for intact proteins or 5 ppm for peptides or better at high resolution.^[108,109] The precursor scan is followed by tandem MS fragmentations of selected ions to gain sequence information of peptide or protein ions isolated.^[110] The structural information depends strongly on the type of fragmentation technique used. For instance collision induced dissociation (CID) in the ion trap can be acquired at a fast scan rate but suffer from a low mass cut off while higher energy collision induced dissociation (HCD) in the multipole fragmentation cell results in ions over the entire m/z range but needs to be analyzed by the slower Orbitrap analyzer.^[111] Other common fragmentation techniques such as electron transfer dissociation (ETD)^[112] or ultraviolet photodissociation (UVPD)^[113] offer different fragmentation selectivity.

The precursor selection for MS2 can be performed in a data dependent mode, e.g. selecting the most intense precursors,^[110] or in a data independent mode, e.g. fragmenting only specific ions chosen before the experiment or all ions present, giving better quantitative results^[114]. While top-down analysis has the advantage of requiring less sample preparation, making it easier to conserve post translational modifications, it is inherently more difficult to separate proteins by LC than peptides.^[115] Additionally, proteins have more complex MS spectra with different charge states and their spectra show worse signal to noise ratios than those of peptides.^[106]

For this reason, bottom-up approaches are the most common, since they are easier to perform and easier to analyze in complex mixtures.^[116] With the aid of high resolution mass spectrometers, like the LTQ Orbitrap XL, even complex mixtures, such as cell lysates, containing entire proteomes, can be analyzed by mass spectrometry based bottom-up proteomics^[117]. In complex cases like proteomics, the analysis can no longer be performed manually in a reasonable fashion because a single experiment can generate millions of spectra within an hour. To tackle this challenge, the results are analyzed statistically by comparing the experimental spectra to theoretical fragment spectra from a protein database versus a decoy data set. This database is generally derived from sequenced genomes and and decoy data is often generated by inverting the protein sequences of this protein data base.^[118]

In order to aid quantification, the introduction of labels in form of isotopes or mass tags are available, but label-free quantification also shows reasonable and in some cases even better results.^[119] For the complex data analysis requiring extensive bioinformatics knowledge robust open source programs such as MaxQuant^[120] and the Perseus suite^[121] are available, enabling end users with little knowhow to perform this complex analysis themselves. A complete bottom up proteomics workflow for a label free analysis is summarized in **Figure 13**.

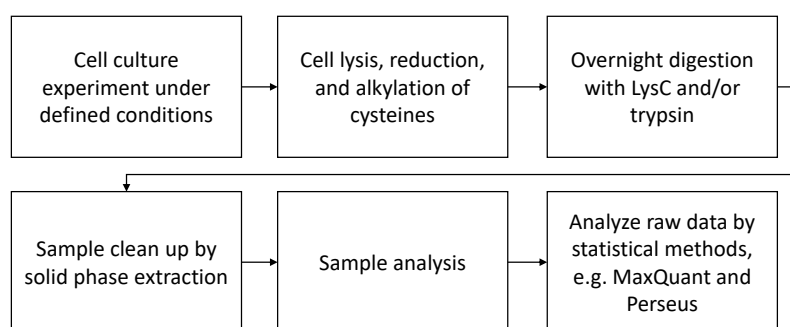


Figure 13: Flowchart for a typical workflow of a label-free bottom up proteomics analysis: After a cell culture experiment, cells are lysed, proteins denatured, reduced, and cysteines are alkylated to avoid disulfidebonds. Overnight digestion with a protease, such as trypsin is followed by a sample clean up by solid phase extraction and sample analysis by LC-MS. The raw data is analyzed by statistical methods, e.g. by using MaxQuant and Perseus.^[116]

1.4.4 Footprinting of proteins

Protein footprinting is an MS-based approach to study higher order protein structures. In this method a covalent label is introduced to the solvent accessible surface area of proteins followed by MS analysis to determine the position of the introduced labels.^[122] Most commonly, protein footprinting is performed using hydrogen deuterium exchange (HDX) where the replacement of the backbone amide hydrogens by the deuterium in D₂O is monitored over a set period of time typically ranging from several minutes to hours.^[123,124] After quenching at different time points, the protein samples are typically digested using pepsin and analyzed by LC-MS according to a bottom-up approach. The HDX kinetic derived from this analysis allows conclusions about the solvent accessibility and involvement in higher order structures of the pepsin peptides.^[125] A limitation of this method is the limited resolution to the peptide level because during MS₂ analysis deuterium can scramble between amides making it difficult to pinpoint their location to a amino acid residue^[126]. Another disadvantage is the reversible nature of the deuterium label which restrains the conditions for protein digestion, limiting the options to pepsin which yield less reproducible results than trypsin or other proteases, making the analysis more difficult^[127].

Another commonly used covalent label in protein footprinting are hydroxy radicals. Unlike deuterium labels, hydroxy radicals lead to an irreversible oxidation of the side chains of virtually all amino acids within proteins although reactivity depends on the amino acid residue.^[128] This allows the use of proteases with reproducible cleavage such as trypsin. The resolution of this method can be as detailed as the amino acid residues level since during MS₂ analysis the labels introduced by oxidation are stable and do not scramble like deuterium.^[129] However, oxidative protein footprinting typically requires generation of hydroxy radicals for only a short period of time on the millisecond scale to avoid overlabeling

resulting in defolding of the protein and labeling of the thereby newly exposed sites.^[130] In order to achieve this, typically excimer lasers^[131], gamma-ray water radiolysis^[132] or synchrotron water radiolysis^[133] is employed. These methods commonly require special equipment that is not accessible to most labs. Alternative approaches such as Fenton-based chemistry that uses Fe(II)-EDTA to generate hydroxy radicals from H₂O₂ in a redox system can also be used but results in longer labeling times of several seconds to minutes which can lead to overlabeling of proteins.^[122,134] However, there were instances where Fenton based approaches were successfully used to study protein protein complexes.^[135]

2 Aim

The cell biological background for FKBP51 is still unclear. The aim of this thesis is therefore the development of chemical tools to explore the function of FKBP51 *in cellulo* by synthesizing and coupling photoreactive warheads to FKBP51 ligands to generate photoaffinity labels for FKBP51. Furthermore, a large scale synthesis of SAFit2 needs to be developed to supply sufficient SAFit2 for *in vivo* studies. Since some FKBP51 have opposing functions, selective chemical tools addressing only particular FKBP51 are required to fully elucidate their biochemical mechanism. For this reason, both pan selective as well as FKBP51 selective chemical tools will be synthesized and characterized according to **Figure 14**. The specific goals of this thesis are:

- 1) The gram scale synthesis of SAFit2 and a negative control compound to meet the existing demand for a FKBP51 selective chemical tool for *in vivo* studies.
- 2) Exploring a new potential group of linear FKBP51 selective ligands based on the SAFit macrocycle structure.
- 3) The synthesis of photoreactive FKBP51 ligands to identify off targets and proteins interacting with FKBP51 in human cells by photoaffinity labeling.
- 4) The development of LC-MS based methods to analyze proteins and the tools synthesized above including intact protein mass measurements, top-down analysis as well as a bottom-up proteomics pipeline.

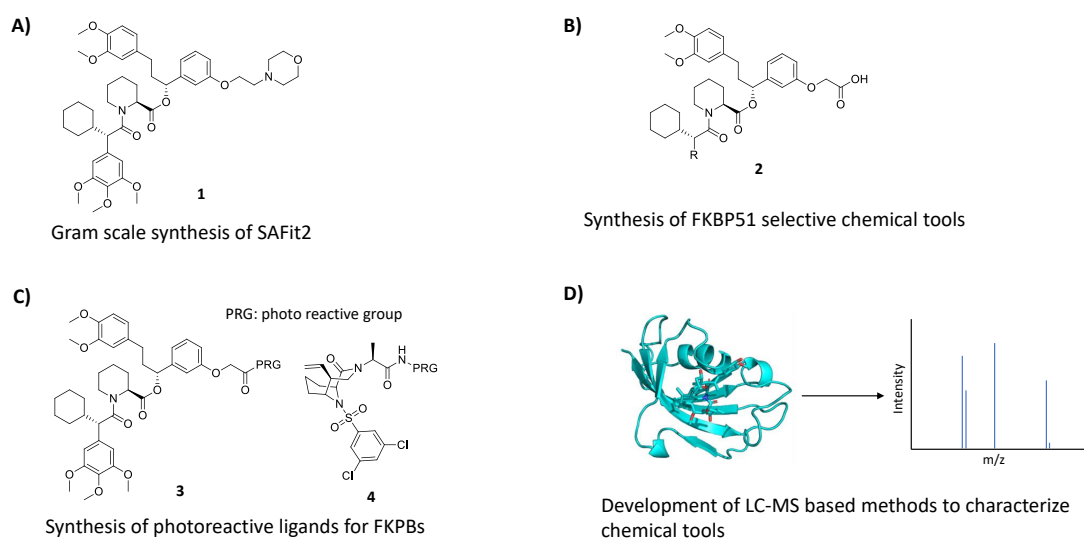


Figure 14: Main projects planned to conduct in this thesis: **A)** Large scale synthesis of FKBP51 selective ligand SAFit2 (**1**), **B)** Development and synthesis of FKBP51 selective chemical tools based on the general structure **2**, **C)** Development and synthesis of photoreactive FKBP ligands for photoaffinity labeling based on the general structure **3** und **4**, **D)** Development of LC-MS based methods to characterize the synthesized chemical tools in this thesis.

3 Results and discussion

3.1 Gram scale synthesis of SAFit ligands

As mentioned previously, SAFit2 is currently the most advanced chemical tool for selectively exploring FKBP51 and its biological function *in vivo*. For this reason, the synthesis of SAFit ligands and the required building blocks were optimized and alternate synthesis routes were explored to meet the rising demand of SAFit ligands shown in **Figure 15**.

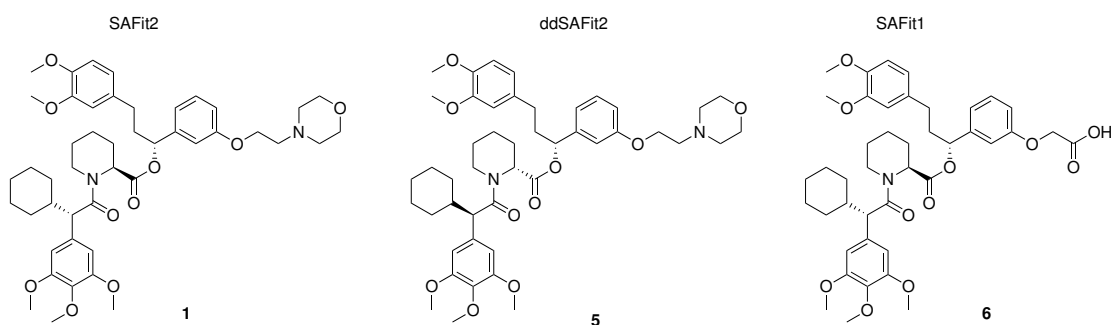
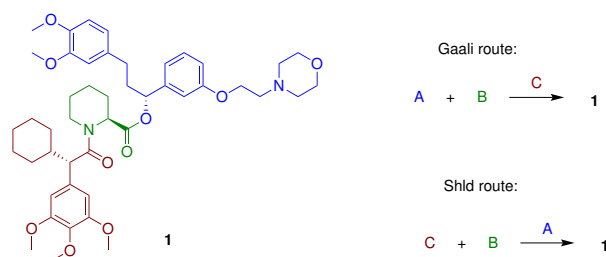


Figure 15: SAFit ligands required for *in vivo* and *in vitro* experiments scheduled for gram scale synthesis: SAFit2 **1**, the negative control compound ddSAFit2 **5** with two inverted stereocenters, and SAFit1 **6**.

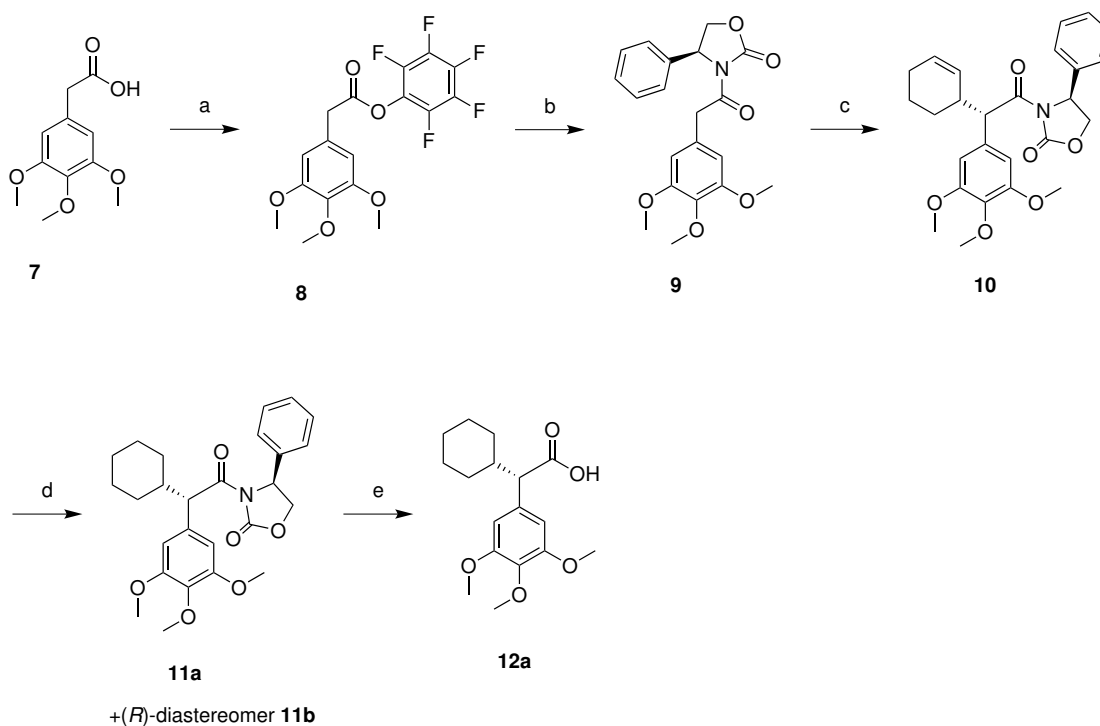
At the beginning of this endeavor two different synthesis routes were known to synthesize SAFit like ligands from the three building blocks they are made of: the original SAFit2 synthesis route^[28] and the scalable synthesis of Shld^[136] shown in **Scheme 1**.



Scheme 1: Known synthesis routes for SAFit like ligands from the three building blocks, the top group shown in blue (A), the core group shown in green (B) and the bottom group shown in red brown (C) for SAFit2 **1**.

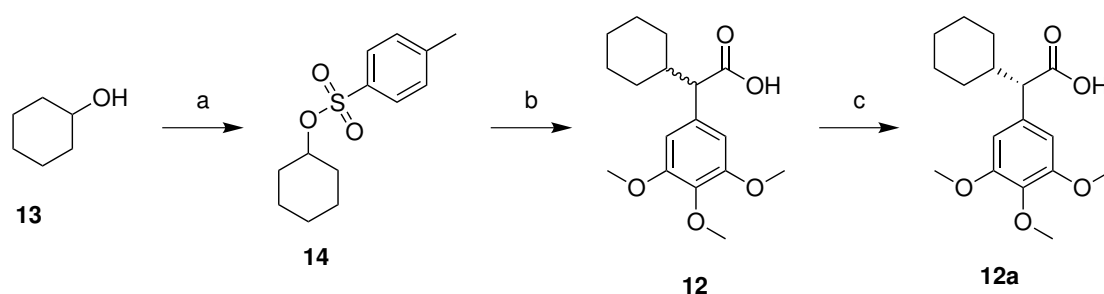
Both synthesis routes commonly require the same building blocks consisting of the top,

bottom and core group, with only the core group requiring some adjustments for the Shld synthesis route. The most challenging part of this synthesis is the bottom group since it requires a stereospecific alkylation that is achieved by using an Evans auxiliary in the SAFit synthesis or a Koga base in the Shld synthesis. As the use of a Koga base for a stereoselective alkylation by previous attempts from other group members were unsuccessful, this only leaves the approach from *Gaali et al.* After some further optimizations of the reaction conditions, such as the temperature, in addition to those conducted by Michael Bauder and Fabian Knaup of the Hausch lab regarding the residue of the Evans auxiliary, the bottom group **12a** was synthesized in multigram scale according to **Scheme 2** in a total yield of 25 %.



Scheme 2: Synthesis of the bottom group starting from commercially available **7** using an optimized protocol of the Gaali route: a) EDC·HCl, DMAP, DCM 0 °C, 74 % yield of **8**, b) 3,4,5-Trimethoxy phenylacetic acid, *n*-BuLi, THF, -78 °C, 76 % yield of **9**, c) LiHMDS, 3-bromo cyclohexene, THF 78 °C, 74 % yield of **10**, d) 1 bar H₂, Pd/C, MeOH, 70 % of **11a** and 19 % of the diastereomer **11b**, e) LiOH/H₂O₂, THF/H₂O 8:5, 0 °C, 87 % yield of **12a**.

While it is certainly possible to synthesize sufficient amounts of the bottom group building block, it is very inefficient as five steps were required although formally a single alkylation step can be sufficient, as was the case in the Shld synthesis. For this reason, a different approach involving alkylation without stereo control, followed by chiral resolution of the racemic bottom group by fractionized crystallization with a chiral amine was performed according to **Scheme 3**.



Scheme 3: Synthesis of racemic bottom group followed by chiral resolution using fractionized crystallization starting from commercially available **13**: a) N-methylimidazole, tosyl chloride, DCM, 0 °C, 93 % yield of **14**, b) NaHMDS, THF, –78 °C, THF, 69 % yield of **12**, c) D-alaninol, MeCN, 16 % yield of **12a**.

D-Alaninol was determined as the most suitable chiral resolving agent by a screening of seven commercially available amines summarized in **Table 1**. The amines were chosen based on their availability and low price.

Table 1: Results of the screening of chiral bases for the fractionized crystallization of **12**. The enantiomeric ratio of *R/S*-isomer of the mother liquor determined by chiral HPLC is given for each combination of base and solvent in presence or absence of 20 % water. n.a. denotes absence of crystals.

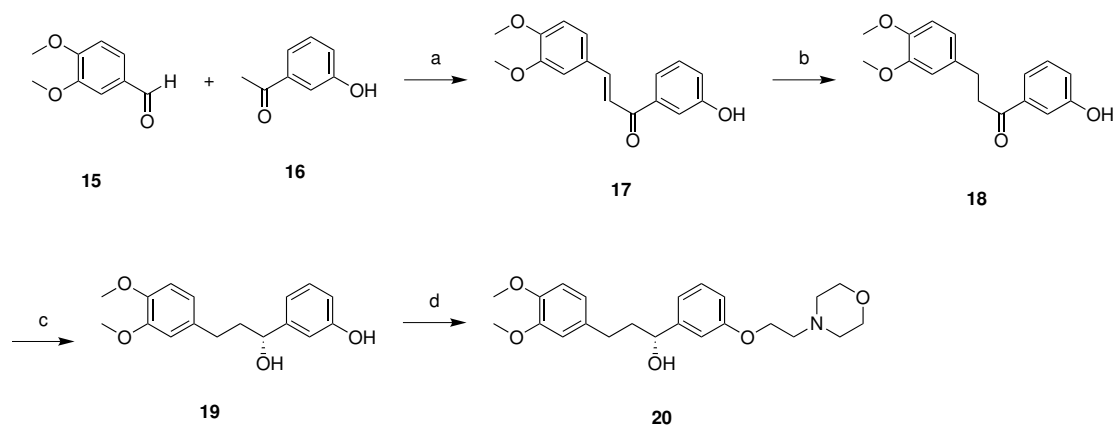
	MeOH	MeOH/H ₂ O	EtOH	EtOH/H ₂ O	iPrOH	iPrOH/H ₂ O	Acetone	Acetone/H ₂ O	THF	THF/H ₂ O	MeCN	MeCN/H ₂ O
Cinchonine	49/51	51/49	51/49	50/50	50/50	50/50	50/50	50/50	n.a.	50/50	25/75	56/44
Quinine	n.a.	n.a.	n.a.	n.a.	50/50	n.a.	73/27	n.a.	n.a.	n.a.	60/40	n.a.
Quinidine	n.a.	50/50	n.a.	n.a.	n.a.	n.a.	n.a.	n.a.	n.a.	n.a.	n.a.	n.a.
L-Proline	n.a.	n.a.	48/52	n.a.	51/49	n.a.	52/48	n.a.	50/50	n.a.	52/48	n.a.
L-Cinchonidine	n.a.	n.a.	59/41	n.a.	62/38	n.a.	54/46	61/39	n.a.	n.a.	61/39	64/36
D-Alaninol	n.a.	n.a.	n.a.	n.a.	n.a.	n.a.	n.a.	n.a.	n.a.	n.a.	67/33	n.a.
L-Lysine	54/46	n.a.	n.a.	n.a.	n.a.	n.a.	n.a.	n.a.	n.a.	n.a.	n.a.	n.a.

After crystallization with the chiral bases overnight at room temperature in various solvent systems, the ratio of enantiomers of the mother liquor was determined by chiral HPLC. Upon reaching an equilibrium state, this ratio is equal to the eutectic point of the crystallization of the diastomeric salts formed between the respective base and the bottom group. This marks the limiting factor to how good each chiral base is at enriching one of the enantiomers, e.g. the higher this ratio is, the less the number of crystallization steps required to reach a specific enantiomeric excess and the higher the yield will be.^[137,138]

D-Alaninol was the only base with suitable solubility in one of the tested solvents with a ratio of enantiomers of 33:67 (*S*)- to (*R*)-isomer that significantly enriched the correct isomer within this screening. Other bases with suitable enantiomeric ratio like Quinine in acetone had extremely poor solubility and were thus impractical to use. In most applications of fractionized crystallization the eutectic enantiomeric ratio achieved is usually 90:10 or higher, indicating the difficulty of the chiral resolution in this case.^[139] Nonetheless, this setup allows a faster, scalable synthesis of the bottom group building block by crystallization that was achieved in multi gram scale. Even though the total yield of 10 % is significantly lower than the 25 % yield of the stereo controlled alkylation, this

synthesis still allows a more time efficient preparation of **12a**.

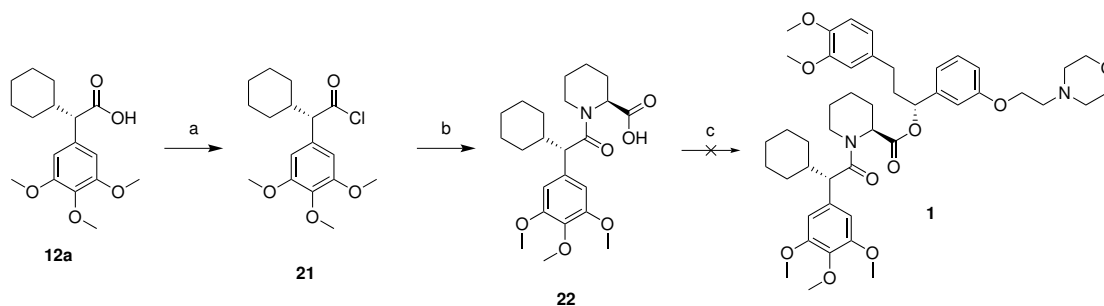
Next, the top group building block was synthesized according to an optimized protocol that was developed together with Andreas Voll from the Hausch lab as shown in **Scheme 4**.



Scheme 4: Synthesis of the SAFit2 top group starting from commercially available aldehyde **15** and ketone **16**: a) KOH, H₂O/EtOH, 0 °C, 99 % yield of **17**, b) Zn/NH₄Ac, MeOH, r.t., 84 % yield of **18**, c) atmospheric H₂, KOtBu, Noyori catalyst, IPA, r.t., 95 % of **19**, d) K₂CO₃, 2-chloroethylmorpholine hydrochloride, MeCN, reflux, quant. yield of **20**. The top group batch for the SAFit2 synthesis was synthesized by Andreas Voll (unpublished results), while the top group batch for ddSAFit2 was synthesized in this thesis with comparable yields except the last step where 78 % yield were achieved.

Notably, this synthesis was completed on multi gram scale without requiring the use of column chromatography and the reduction to the chiral alcohol was performed with atmospheric hydrogen pressure and no longer required an autoclave as the original synthesis did. The total yield for the top group synthesis is 79 % for the batch of Andreas Voll and 62 % were achieved in during this thesis for a smaller batch.

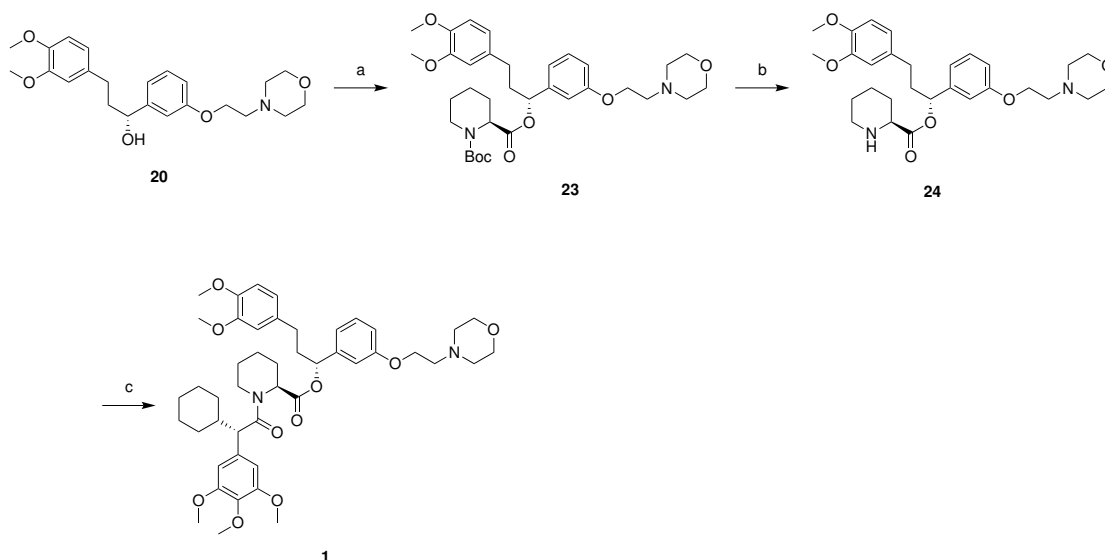
Since the synthesis of the chiral alcohol has the most steps among all building blocks it is the most valuable intermediate and the coupling of the chiral alcohol should preferably be the final steps of the synthesis to minimize the longest linear sequence within this synthesis. This approach was pioneered in the Shld synthesis and also attempted in this work according to the conditions in **Scheme 5**.



Scheme 5: Coupling of the SAFit2 building blocks according to the Shld route, a) SOCl_2 , DCM, 0°C , quant. yield of **21**, b) KOH, dioxane/ H_2O , 0°C , 63% yield of **22**, c) DMAP, DCM, **20**, product **1** could not be isolated in sufficient purity.

Although it is possible to perform the synthesis of SAFit2 in this way the starting material **22** will always epimerize to about 5% during the last esterification step. This happens due to a known mechanism from peptide synthesis via a oxazoline intermediate and could not be avoided in this thesis no matter how the conditions were chosen. Although a purity of 95% is often deemed acceptable for *in vivo* animal experiments the purity is preferable greater than 98%. Unfortunately, the resulting SAFit2 diastereomers are very difficult to separate even when preparative HPLC is used. In addition to the comparably low yields, the Shld synthesis is unsuitable to be adapted for SAFit2. However, the developed synthesis protocol nonetheless turned out very useful for the synthesis of SAFit derivatives with different top groups as performed by Andreas Voll and Michael Bauder and it also allowed separating bottom core group diastereomers **22** which was adapted by Michael Bauder for the synthesis of his macrocyclic SAFit compounds.^[39]

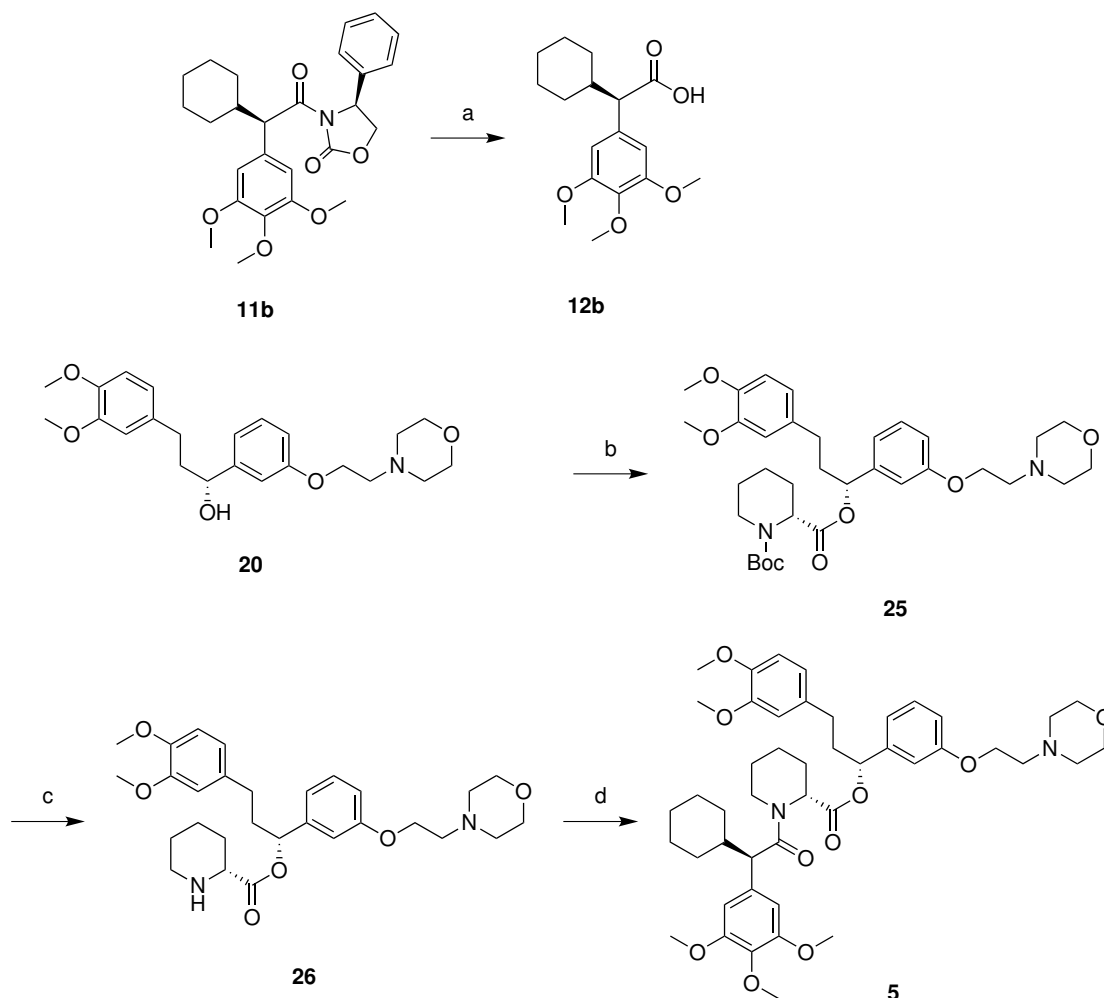
For the synthesis of the SAFit ligands in this thesis, the procedure from *Gaali et al.* was adapted and optimized by using a Boc protective group instead of an Fmoc group resulting in the synthesis route in **Scheme 6** for SAFit2. The top group building block for this synthesis batch was supplied by my colleague Andreas Voll.



Scheme 6: Multi gram synthesis of SAFit2 following the Gaali route, a) EDC·HCl, DMAP, Boc-L-pipecolate, DCM, 0 °C, 97 % yield of **23**, b) DCM/TFA 2:1, r.t., quant. yield of **24**, c) HATU, **12a**, DiPEA, DCM/DMF, r.t., 56 % yield of **1**.

Using this synthesis route, no epimerization occurred and about 20 g high purity (> 99 %) SAFit2 could be synthesized in a single batch with a total yield of 43 %, more than six times as high as the original yield of 6.6 % from *Gaali et al.* and higher than the 39 % reported for Shld using the alternate Shld synthesis route. This amount of SAFit2 is sufficient to meet the demand of SAFit2 for the foreseeable future. By replacing the Fmoc protecting group of the original synthesis by a Boc protecting group, the coupling between top and core group and the successive acidic deprotection was much cleaner allowing easy purification with high yields. The formulation used for *in vivo* experiments in mice was also optimized by increasing the concentration of SAFit2 from 2 mg/mL to 4 mg/mL in PBS containing 4 % EtOH, 5 % Tween80, and 5 % PEG400, enabling the full use of the large amounts of SAFit2 available now. For this formulation SAFit2 is first dissolved in EtOH, PEG400 and Tween80 and then PBS is added until the appropriate concentration is reached. Alternatively, a formulation without ethanol with the original 2 mg/mL was also successfully tested to be soluble using the same procedure without ethanol.

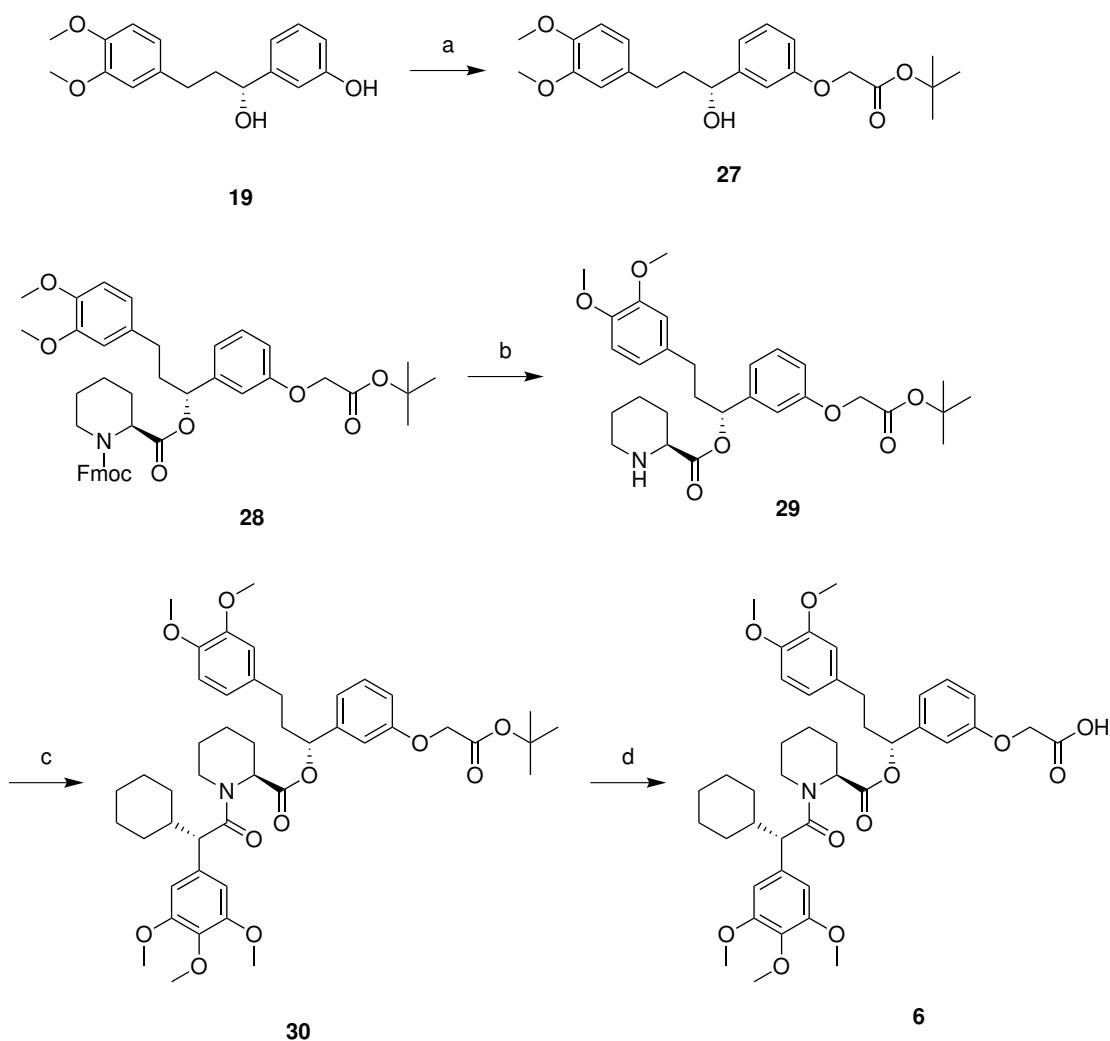
This synthesis was transferred to the the double diastereomer of SAFit2, ddSAFit2, to synthesize large amounts of a negative control compound for *in vivo* studies according to **Scheme 7**.



Scheme 7: Multi gram synthesis of ddSAFit2 starting from the top group **20**, a) LiOH/H₂O₂, THF/H₂O 8:5, 0 °C, 69% yield of **12b**, b) DCC, DMAP, Boc-L-pipecolate, DCM, 0 °C, 78% yield of **25**, c) TFA/DCM 1:2, 0 °C, quant. yield of **26**, d) HATU, **12b**, DiPEA, DCM/DMF, r.t., 78% of **5**.

The yield of the final step for ddSAFit2 was higher than for SAFit2 since an optimized purification protocol for the final step consisting of one preparative HPLC run followed by a flash column chromatography step were used from the beginning to result in about 4 g of inactive ddSAFit2 that serves as a negative non FKBP51 binding control for *in vivo* experiments. The total yield of the synthesis was 50% and a purity of 99%.

The same synthetic procedure was also adapted to synthesize SAFit1 starting with the chiral alcohol **19** according to **Scheme 8**.



Scheme 8: Multi gram synthesis of SAFit1 starting from chiral alcohol **19**, a) K_2CO_3 , *tert*-butyl bromoacetate, MeCN, r.t., 92% yield of **27**, b) DCC, DMAP, Fmoc-*L*-pipecolate, DCM, 0 °C, 89% yield of **28**, c) 4-methylpiperidine/DMF 1:10, r.t., 88% yield of **29**, d) HATU, **12a**, DiPEA, DMF/DCM, r.t., 97% yield of **30**, e) 30% TFA, DCM, r.t., 80% yield of **6**.

For SAFit1 the Fmoc protecting group has to be used because the acidic deprotection of the Boc group would also result in the premature deprotection of the carboxylic acid of the top group. Although this results in less favorable conditions it was still possible to synthesize about 3 g SAFit1 with a total yield of 44% and a purity of 99%.

In order to further elucidate the induced fit binding mechanism of SAFit2 and SAFit derivatives to FKBP51, SAFit2 is analyzed by NMR spectroscopy to learn more about the structure and conformers of SAFit2 in solution while it is not binding to FKBP51. Even though virtually all SAFit derivatives show characteristic rotamers in 1H - and ^{13}C -NMR spectra, they were never analyzed as they are fairly complex. The observed rotamers were

speculated to result from the conformational restraint of the amide bond linking the pipecolate core group and the bottom group. In the case of SAFit2 and SAFit1 these rotamers are very stable and are known to still persist as distinguishable signals in ^1H -spectra at 100°C in DMSO (unpublished results from Michael Bauder of the Hausch lab). In order to analyze the NMR spectra of SAFit2 properly, spectra were recorded with a 700 MHz NMR-spectrometer by Matthias Brauser of the Thiele lab in the course of this thesis. The quality of the resulting spectra was sufficient to assign most proton signals with the help of 2D-NMR ^1H -CLIP COSY^[140], ^1H - ^{13}C -HSQC, ^1H - ^{13}C -HMBC, and ^1H -ROESY at 300 K (see experimental section for spectra). The observed rotamers were indeed confirmed to be the result of the amide bond between bottom and core group as shown by the ROEs of the rotamers of the C_α carbon atoms next to the amide bond as shown in figure Figure 16.

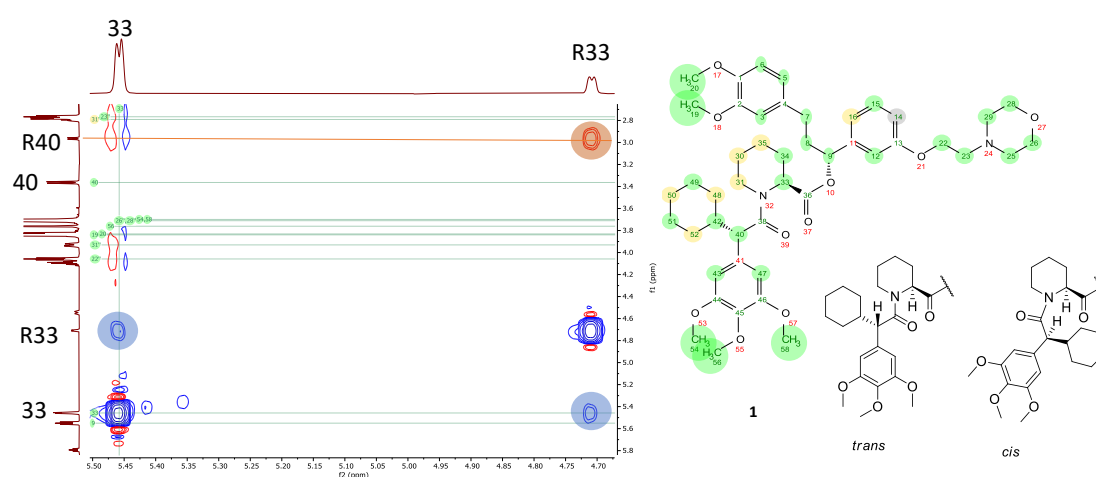


Figure 16: Portion of the ^1H -ROESY with characteristic pipecolate minor rotamer signal of H^{33} and its ROE to the minor rotamer of H^{40} . The corresponding ROE for the major rotamer signals is absent, matching with the *cis* and *trans* isomers of the pipecolate amide bond.

These rotamers are typically found in peptides containing a pipecolate^[141] and it is no surprise for these to be present in SAFit ligands. The ratio of *trans*:*cis* conformers is approximately 3:1 for SAFit2 and 5:1 for SAFit1 as determined from non quantitative ^1H -NMR. This results in a large fraction of the molecule staying in the non binding *cis* conformation explaining the substantial increase in binding affinity of bicyclic FKBP ligands compared to sulfonamides missing the bicyclic bridge of the pipecolate core.^[142] On the basis of the proton assignment in this thesis, it is now possible to determine the entire conformational ensemble using quantitative ROESY techniques to get detailed insights in the structure of SAFit ligands in the future. This in turn will give valuable clues in designing new FKBP51 selective ligands and will explain why previous synthesized ligands had lower binding affinities than expected.

3.2 SAFit1-like lactam derivatives as ligands for FKBP51

In order to explore the possibility of more selective FKBP51 ligands based on the macrocyclic compounds synthesized by Andreas Voll shown in **Figure 17**, a small series based on the linear version of said macrocycles were synthesized.

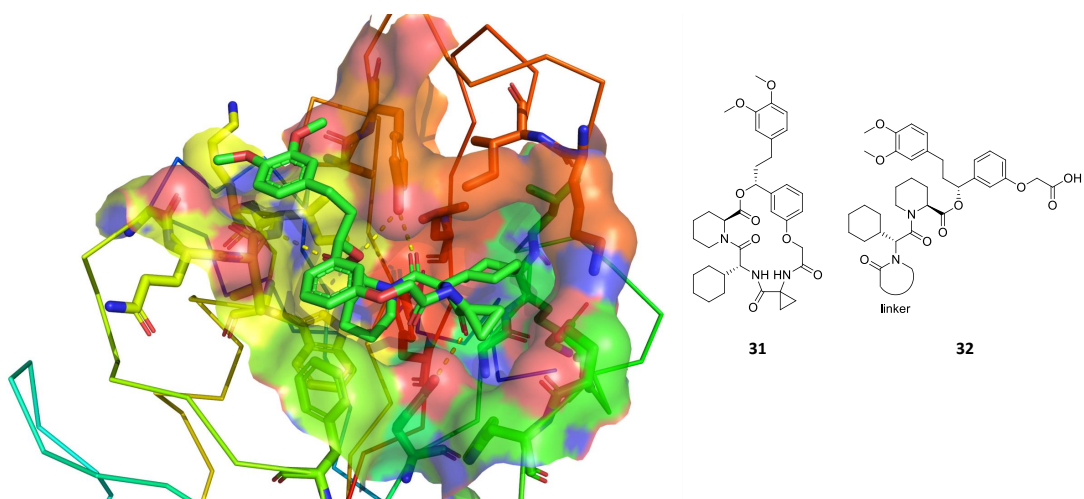
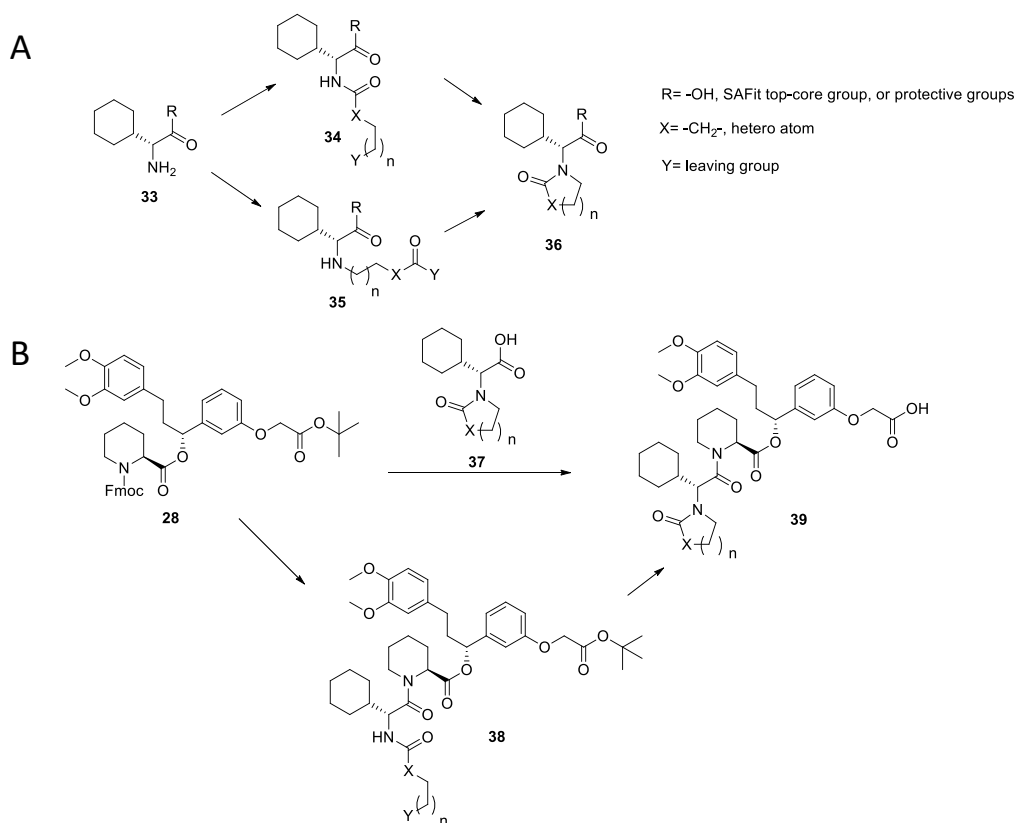


Figure 17: Crystal structure of **31** in complex with FKBP51FK1 (pdb: 7AOU)^[40] and derived structure **32** of linear compounds. Key interactions between **31** and the protein are shown with yellow dashed lines.

The macrocyclic ligands synthesized by Andreas Voll were significantly more selective in binding FKBP51 over FKBP52 and FKBP12, and therefore allow a more targeted analysis of FKBP51. In an attempt to reproduce a similar result with linear molecules derived from SAFit1, a small series of ligand with newly derived lactam and carbamate bottom groups was synthesized. The synthesis routes considered for this approach are summarized in **Scheme 9**.

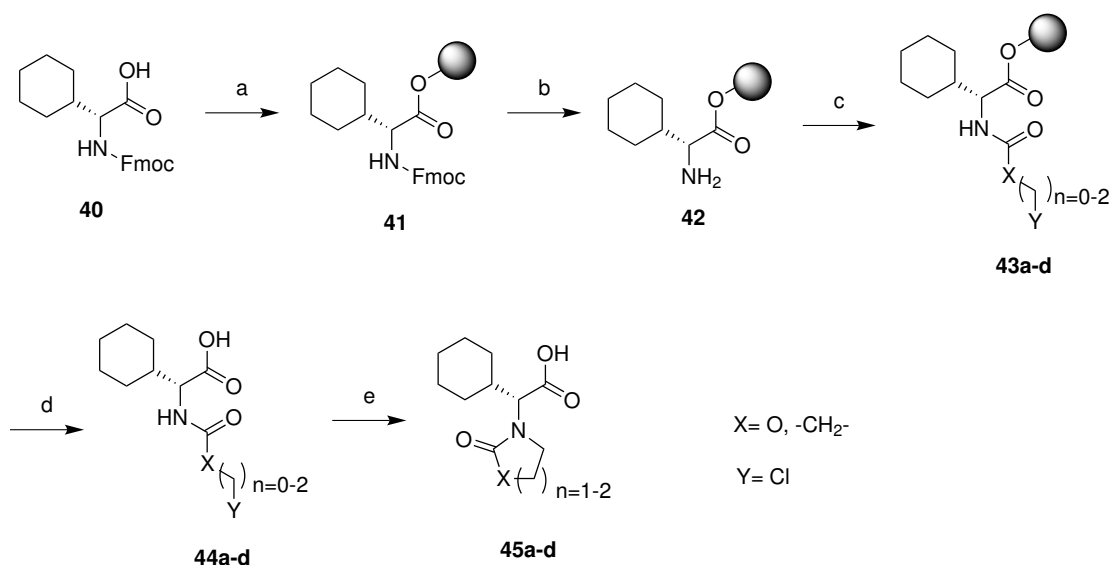


Scheme 9: Synthesis routes considered for lactam and carbamate SAFit1 derivatives: A) Synthesis of the bottom group starting from a precursor **33** by either forming the amide bond or the alkylation of the amine nitrogen first resulting in intermediates **34** and **35**, respectively, followed by cyclization by forming the corresponding other bond leading to **36**. B) Synthesis of new SAFit1 derivatives starting from **28** by either a convergent route by coupling with a separately synthesized bottom group **37** or by a linear route by first synthesizing a linear precursor **38** that is then cyclized into the target compound **39**.

The only feasible synthesis route for the new bottom groups **36** was forming the amide bond first by coupling with an activated carboxylic acid in the form of acid chlorides or similar reactive intermediates. Attempts to first perform alkylation and then the amide bond by e.g. a reductive amination followed by condensation of an ester were not attempted because there was next to no literature present for this type of starting material. Additionally, the other mentioned route yielded sufficient results.

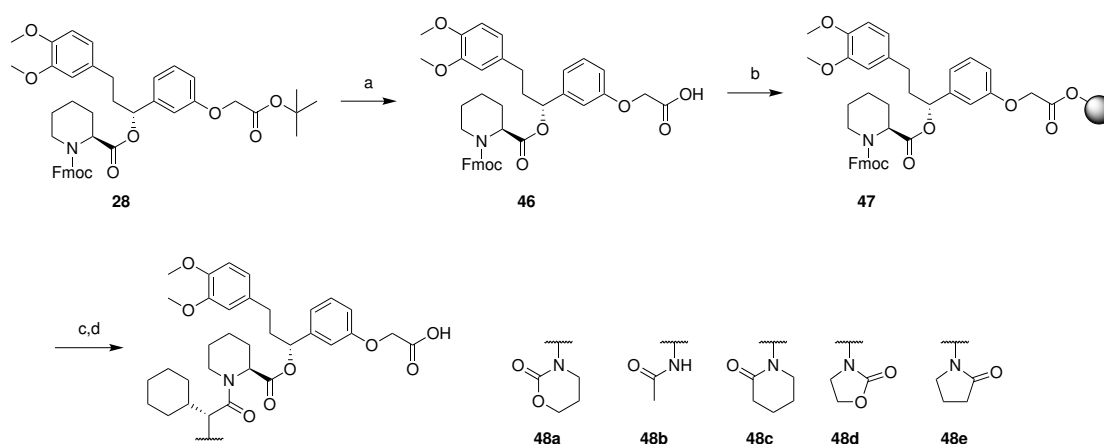
The linear synthesis route for the new SAFit1 derivatives has a very low risk of epimerization via a known oxazoline intermediate as well as no potential for a side reaction to diketopiperazine side product. However, the cyclization of the bottom group required harsh conditions that were not tolerated by the SAFit1 scaffold. For this reason all derivatives were therefore synthesized using a convergent synthesis route with the exception of a control compound requiring no cyclization. The bottom groups were first synthesized according to **Scheme 10** using a solid phase synthesis to allow rapid synthesis and easy

isolation of several bottom groups.



Scheme 10: Synthesis of lactam bottom groups for FKBP51 selective SAlFit1 derivatives starting from **40**, a) CTC-resin, DiPEA, DCM, r.t. resulting in **41**, b) 4-methylpiperidine/DMF 1:5, r.t., resulting in **42**, c) acid chloride, DiPEA, DMF, r.t., resulting in **43a-d**, d) hexafluoro isopropanol/DCM 1:5, r.t., resulting in **44a-d**, e) 1 M KOtBu, DCM, r.t. resulting in bottom groups **45a-d** with yields of 42–55 %.

As the employed chloro trityl resin was not stable under the reaction conditions of the cyclization step of the bottom groups, this final step was performed in solution directly after cleavage from the resin to reliably yield the required bottom groups. The bottom groups were then coupled to the SAlFit1 top core group **46** utilizing solid phase synthesis according to **Scheme 11**.



Scheme 11: Synthesis of SAFit1 derivatives starting from precursor **28**, a) TFA/DCM 1:3, DCM, r.t., quant. yield of **46**, b) CTC resin, DiPEA, DCM, r.t. resulting in **47**, c) 1) 4-methylpiperidine, DMF, 2) HATU, **45a–d**, DiPEA, DMF, r.t. or HATU, Fmoc-Chg-OH, DiPEA, DMF, followed by 4-methylpiperidine, DMF and HATU, acetic acid, DiPEA, DMF d) HFIP/DCM 1:5, r.t., resulting in **48a–e** with 28 – 74 % yield.

The binding affinities for FKBP51 were determined by a fluorescence polarization assay (FPA) and the results are summarized in **Table 2**.

Table 2: Binding affinities of SAFit1 derivatives determined by FPA given as a K_d in μM .

Compound	K_d FKBP51FK1	K_d FKBP52FK1	K_d FKBP12	K_d FKBP12.6
48a	21 ± 18	> 80	> 80	21 ± 36
48b	22 ± 48	> 80	6.1 ± 6.7	> 80
48c	14 ± 9.1	> 80	1.8 ± 0.5	0.92 ± 0.09
48d	20 ± 17	> 80	16 ± 43	12 ± 11
48e	13 ± 6	> 80	> 80	> 80

Unfortunately, the synthesized ligands show only low μM affinity and some are surprisingly active towards FKBP12 and FKBP12.6 instead of FKBP51. This is most likely due to the lactam ring being too constrained to interact with Y57 of FKBP51 as the corresponding part in the macrocycle **31** does. Additionally, the synthesis of the required bottom group moieties is quite difficult and limited by commercially available reagents. For these reasons, this project was no longer pursued after this point. Although these compounds show some value in exploring FKBP12 and FKBP12.6 selective ligands, these two proteins are less relevant drug targets compared to FKBP51. The effort required to synthesize a large library of such ligands to find an optimized compound was deemed too large for the scope of this thesis.

3.3 Analysis of FKBP ligand binding by oxidative footprinting

Although several potential binding partners of FKBP were identified with co-immunoprecipitations (Co-IP) most of them could not be validated. The isolated amounts from human cells are very small and often not pure. However, most *in vitro* validation assays require purified proteins in larger amounts resulting in the inability to validate said protein interactions.

To allow validation and explore the interacting binding surface of potential protein binding partners, an oxidative footprinting method compatible with small amounts of impure sample was developed in a cooperation with Thomas Nehls from the Lermyte lab. This section summarizes published results.^[143] In this method, solvent accessible parts of the protein are oxidized with *in situ* generated hydroxy radicals using Fenton based chemistry. If a protein is binding another protein or ligand, the involved binding surface is no longer accessible and will therefore be less oxidized compared to a control sample of the protein without a binding partner. The proteins are then analyzed by intact mass analysis and a bottom up LC-MS/MS approach after digestion with trypsin. The entire workflow is summarized in **Figure 18**.

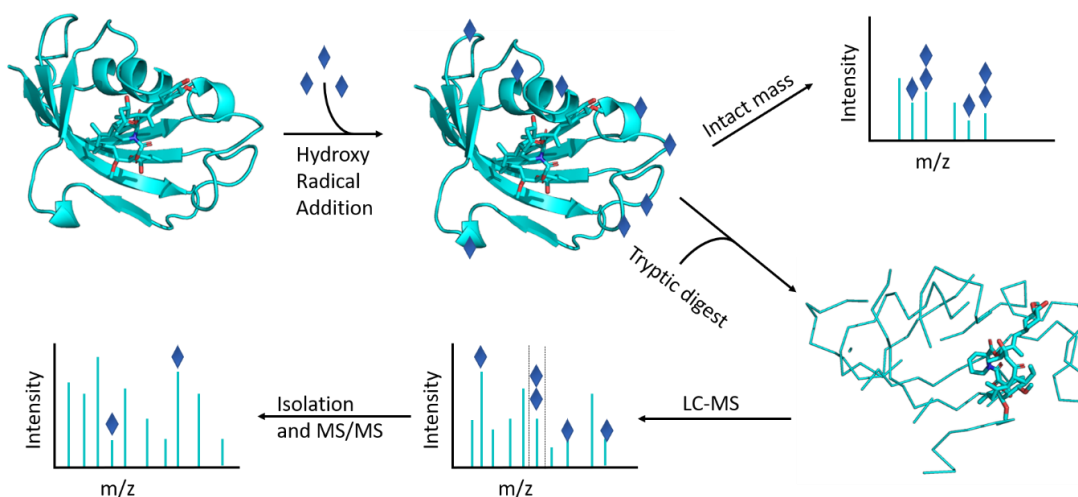


Figure 18: Concept of the oxidative footprinting of proteins to analyze interaction surfaces with binding partners. Proteins are first labeled with hydroxy radicals generated *in situ* by Fenton based chemistry, successive labeling resulting in different oxidized protein species is confirmed by intact mass measurement, the protein is then digested with trypsin and analyzed by LC-MS.^[143]

As a proof of concept this method was first applied to myoglobin which binds a heme group and alcohol dehydrogenase (ADH), a protein that forms tetramers in solution. Both of these are well characterized standard proteins that have literature-known results for oxidative footprinting experiments conducted with UV excimer lasers. The indicated labeling sites in **Figure 19** from our Fenton based oxidative footprinting results are consistent to the literature but also contain different oxidation sites.

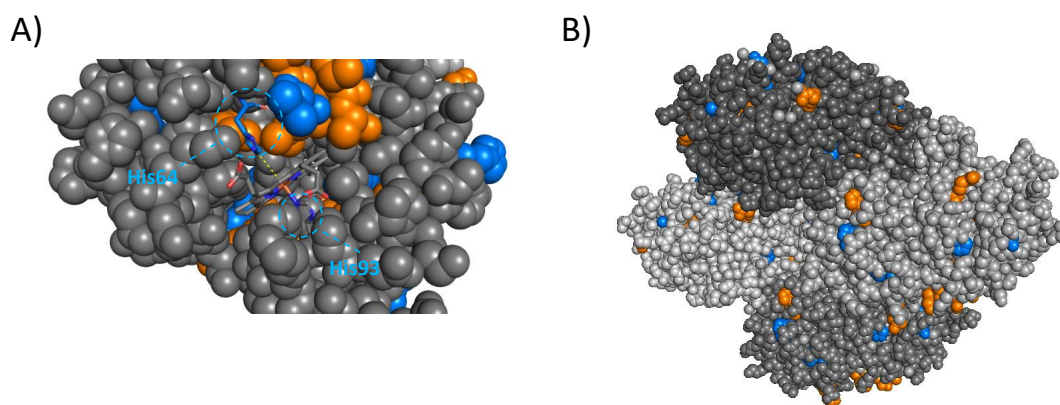


Figure 19: Oxidative footprinting of myoglobin and alcohol dehydrogenase (ADH). Labeled residues are colored blue when they were confirmed in two independent ways (two different oxidations for the same peptide or two oxidized overlapping peptides) and orange when the oxidized peptide was detected only once. A) Crystal structure of *holo*-myoglobin (pdb 1YMB) with labeling sites indicated, B) Crystal structure of ADH Tetramer (pdb 4W6Z) with labeling sites indicated.^[143]

After the first proof of concept, this method was tested to identify the ligand binding pocket of the FKBP51 selective SAFit1 and a FKBP pan selective bicyclic ligand with FKBP51FK1 and FKBP12. The results are shown in **Figure 20**.

The binding region for both proteins and ligands can be clearly identified although the resolution is rather small because the tryptic peptides generated are very large and modifications were only tracked on the peptide level. For this reason, finer details such as the induced fit mechanism were not significantly detected.

In conclusion, this method allowed the approximate detection of binding surfaces of known protein systems. Compared to methods with higher resolution such as NMR, x-ray crystallography and Cryo-EM, the oxidative footprinting is much easier to conduct, faster, and requires much less sample. As this method works the same as bottom up proteomics, this technique requires only 100 ng of a protein mixture to yield results, as long as a nanoLC with a decent mass spectrometer is used. Compared to hydrogen-deuterium exchange (HDX), the oxidative footprinting does not need several time points to derive an exchange kinetic and results in complimentary data solely dependent on solvent accessibility. Fur-

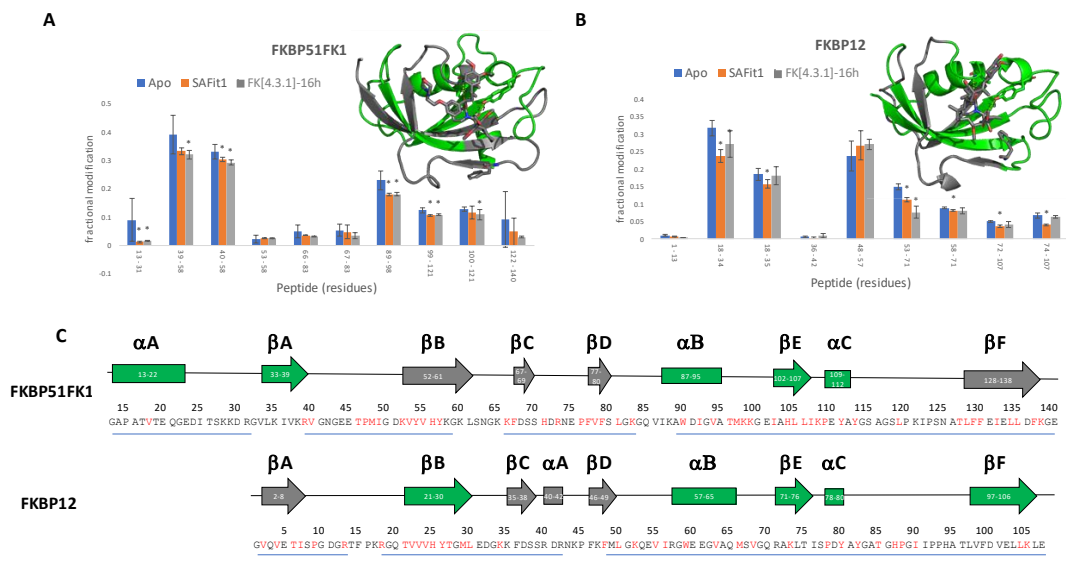


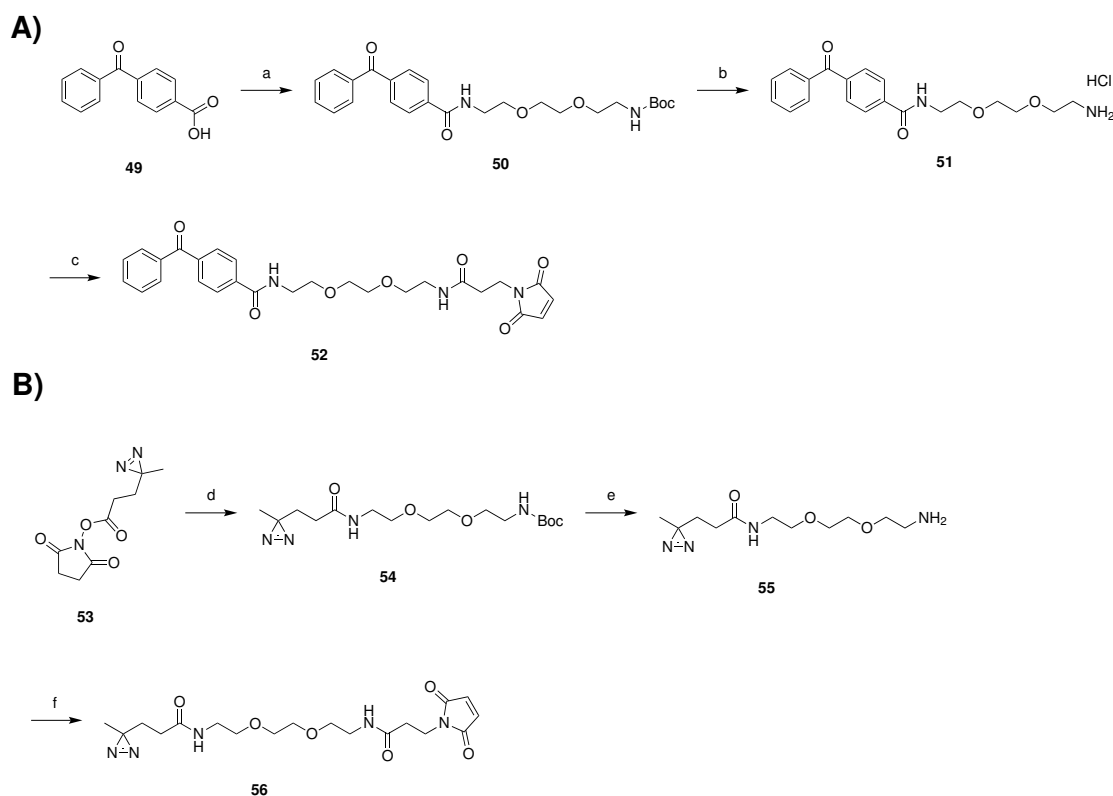
Figure 20: Results of the peptide-level analysis of the FK506-binding proteins: A) fractional oxidative modification of the peptides of FKBP51FK1 for the apo protein as well as SAFit1- and FK[4.3.1]-16h-bound protein, in which statistically significant ($p < 0.05$) differences between ligand-bound and -free states are indicated with an asterisk. Insets show crystal structures with regions that show reduced oxidation after binding of either ligand in green (pdb 4TW7). B) Fractional modification of the peptides of FKBP12 (pdb 1FKJ) for the apo protein as well as ligand-bound states. C) Sequence overview for FKBP51FK1 and FKBP12, with sequence regions covered by the observed peptides underlined. Secondary structure elements are color coded corresponding to the crystal structure. Elements that show reduced oxidation after ligand binding are colored green in Panel (C), and unaffected elements are in gray (same color code as the insets in Panel (A); no regions were observed where ligand binding led to increased oxidative labeling). Detected oxidative labeling sites are colored red in the sequence.^[143]

thermore, it is possible to pinpoint the labeled amino acid using the MS2 spectra which is not possible for deuterium labels as these tend to scramble during tandem MS. Although, this depends on the mass spectrometer and the non optimized state of the MS used for these experiments did only allow this for some exceptions. In future experiments, the oxidative footprinting can be used to validate protein interactions with samples isolated from cell lysate complementary to HDX.

3.4 Photo affinity labels (PALs) to explore FKBP

3.4.1 Cysteine reactive photo crosslinker

Two simple chemical tools consisting of a photo crosslinking warhead and a cysteine reactive group are synthesized according to **Scheme 12**.



The cysteine reactive maleimide can be used to selectively label cysteines of proteins. After the labeling is complete, the photo-crosslinker can be activated at any time by irradiation with UV light leading to covalent crosslinks with binding partners in close proximity. Labeled crosslinks can easily be detected by a visible mass shift in SDS-PAGE or intact protein mass analysis by LC-MS.

The synthesized crosslinkers were successfully used by Maximilian Repity to detect ternary complexes induced upon addition of molecular glues as well as PROTACS. An example for

crosslinks with compound **56** is shown in **Figure 21**. Complete labeling of proteins before crosslinking is determined by intact mass LC-MS (data not shown).

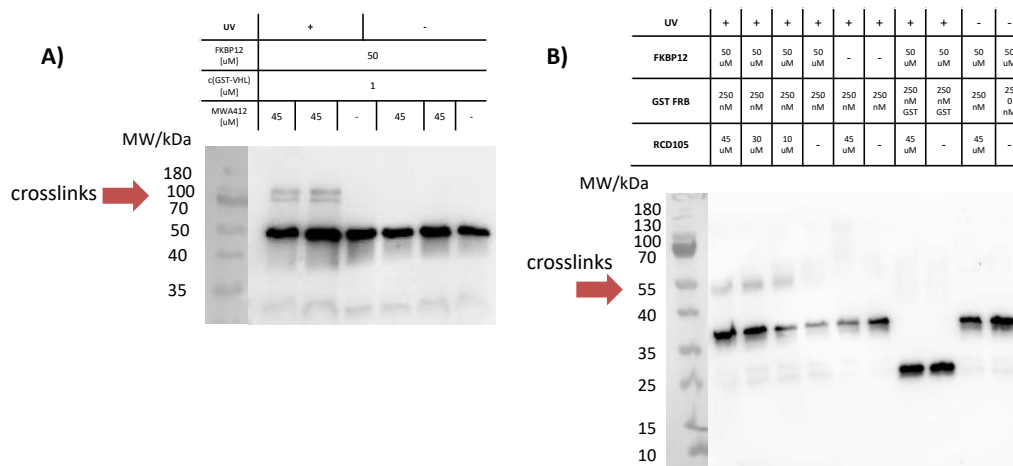


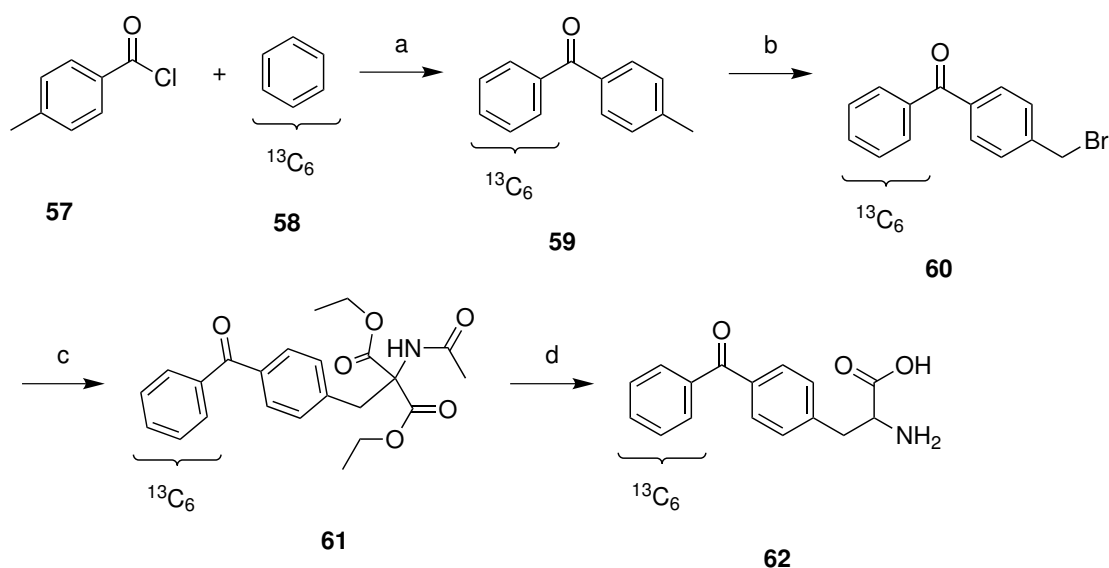
Figure 21: Western blots of crosslinked proteins after labeling with **56**: **A)** Crosslinks of FKBP12 and the VHL complex upon addition of PROTAC MWA412. **B)** Crosslinks between FKBP12 and FRB after addition of the molecular GLUE RCD105. Crosslinks are indicated by a red arrow. (unpublished results by Maximilian Repity)

The diazirine crosslinker showed superior selectivity during crosslinking compared to the benzophenone crosslinker, indicated by the various other bands visible aside from the crosslinked proteins (data not shown). This most likely is due to the much larger size of the benzophenone which may not allow it to stay close enough to the protein surface. For this reason the diazirine crosslinker **56** is the preferred choice in this setup.

The use of crosslinkers allowed detection of the crosslinked product with a distinct mass shift which is far more selective than detecting a fluorescence signal from a FRET assay or another proximity based fluorescence signal. The synthesized cysteine reactive photocrosslinkers have been proven as reliable chemical tools, allowing robust screening of molecular glues as well as detection of induced ternary proteins complexes. The only requirement for their use is a suitable cysteine for labeling via the maleimide group.

3.4.2 Stable isotope labeled pBpa

Photoreactive labels can also be directly introduced into a protein of interest during its biosynthesis within cells by the use of Amber suppression and an unnatural amino acid such as p-benzoyl-L-phenylalanine (pBpa). Cells expressing this modified protein can then be irradiated with UV light to induce crosslinks between the modified protein of interest and protein binding partners in proximity to the label. In order to aid the complex LC-MS data analysis and to provide an internal standard for later quantification, a stable isotope labeled version of this amino acid is synthesized according to **Scheme 13**.



Scheme 13: Synthesis of ^{13}C -labeled pBpa, starting from commercially available **57** and **58**: a) AlCl_3 , CS_2 , 0°C , 75 % yield of **59**, b) AIBN, NBS, chloroform, reflux, 68 % yield of **60**, c) diethyl acetimidomalonate, NaOH/EtOH reflux, 65 % of **61**, d) 6 N HCl reflux, 68 % yield of **62**.

The crosslinks can be detected after cell lysis and FLAG tag enrichment by SDS-PAGE followed by Coomassie staining or western blotting. Alternatively LC-MS analysis allows additional untargeted identification of the crosslinked proteins. **Figure 22** shows the successful crosslinking after incorporation of the synthesized unnatural amino acid from Asat Baischew.

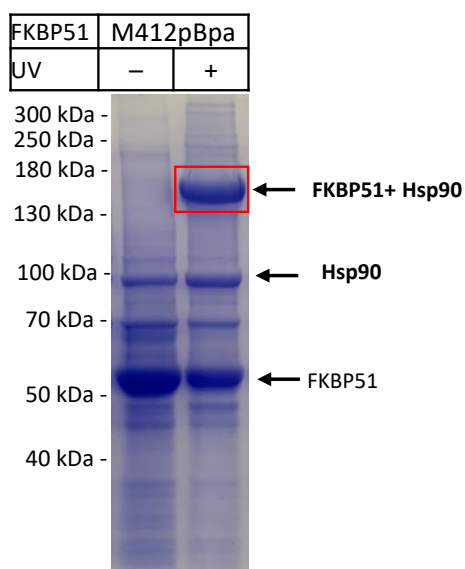
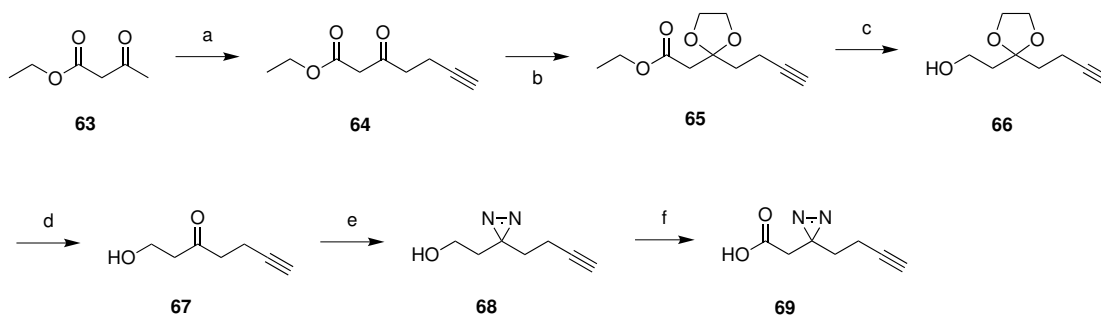


Figure 22: SDS-PAGE after Coomassie staining of a FLAG tag enriched sample with FKBP51-pBpa mutant crosslinks isolated from human cell lysate using the synthesized ^{13}C -labeled compound **62**. (unpublished results by Asat Baischew)

3.4.3 Photo reactive ligands (PRLs) for FKBP5

Synthesis of PRLs for photoaffinity labeling

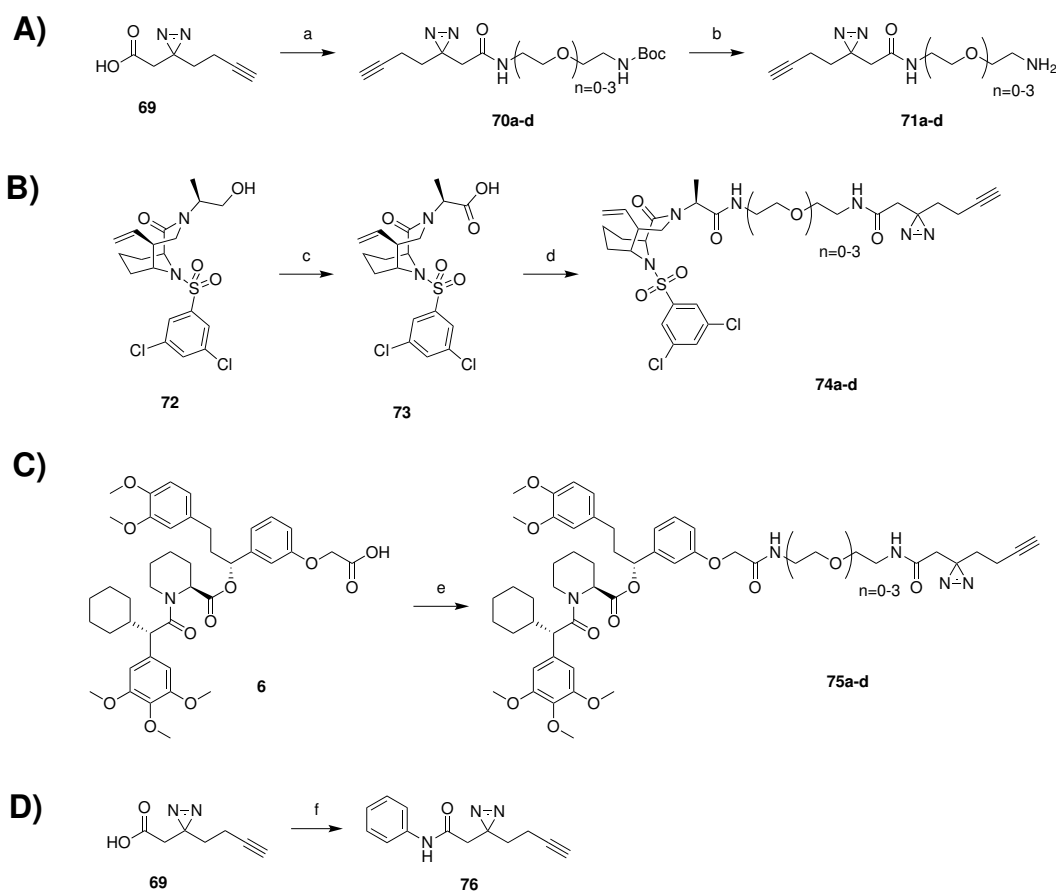
In this section photocrosslinking warheads are directly tethered to protein ligands to detect protein binding partners in proximity to the ligand binding pocket or to find off-targets of previously developed ligands by photoaffinity labeling. Before the actual ligand synthesis can start, a diazirine warhead with a carboxylic acid group with a bioorthogonal alkyne handle is synthesized according to **Scheme 14**.



Scheme 14: Synthesis of the diazirine warhead starting from commercially available starting material **63**: a) 2 eq LDA, 1 eq propargylbromide, THF, -78°C , 68 % yield of **64**, b) pTsOH, ethylene glycol, toluene, reflux, 99 % yield of **65**, c) LAH, THF, 0°C , quant. yield of **66**, d) pTsOH, Acetone, r.t., 58 % yield of **67**, e) 7 M ammonia in MeOH, *tert*-butyl hypochlorite, r.t., 33 % of **68**, f) Jones reagent, acetone, 0°C , 74 % yield of **69**.

The synthesis of the diazirine **69** was the most challenging synthesis in this thesis. Diazirines are usually prepared in an autoclave by condensing liquid ammonia and performing the reaction mostly within liquid ammonia. Use of methanol as a solvent for the same protocols resulted in almost no yield and the reaction mixture was difficult to analyze by LC-MS. Only after acquisition of a new GC-MS system was a precise analysis of the reaction mixture feasible. Furthermore, an optimization of the synthesis by adapting and optimizing an alternate procedure from the literature by adjusting the temperature control of the diazirine formation step was successful.^[144]

Using diazirine **69**, a non binding control compound and a series of FKBP pan-selective and FKBP51-selective photoreactive ligands (PRLs) with different linker size are prepared according to **Scheme 15**.



Scheme 15: Synthesis of PRLs and a non binding control, **A)** synthesis of diazirine linker: a) DIC, HOAt, Boc-linker, DCM, r.t., 71 – 82 % yield of **70a–d**, b) 4 M HCl in dioxane, r.t., 84 %–quant. yield of **71a–d**. **B)** synthesis of pan-selective PRLs starting from **72**, kindly supplied by Patrick Purder: c) Jones reagent, acetone, r.t., 92 % yield of **73**, d) DIC, HOAt, **71a–d**, DCM, r.t., 41 – 56 % yield of **74a–d**. **C)** Synthesis of FKBP51-selective PRLs starting from SAFit1 **6**: e) DIC, HOAt, **71a–d**, DCM, r.t., 30 – 46 % yield of **75a–d**. **D)** Synthesis of the non binding control compound: f) DIC, HOAt, aniline, DCM, r.t., 23 % yield of **76**.

The synthesized ligands were first assessed regarding their binding affinities towards their primary targets FKBP51 and FKBP12 *in vitro* by a fluorescence polarization assay (FPA) performed by Wisley Oki Sugiarto and *in cellulo* by a NanoBRET assay performed and analyzed by Thomas Geiger. The results are shown in **Table 3**.

Table 3: Binding affinities of the synthesized photoreactive ligands given in K_d in nM for fluorescence polarization assay (FPA) *in vitro* and as IC50 in nM a NanoBRET assay in cells.

Compound	linker length n	FPA FKBP51FK1	FPA FKBP12	NanoBRET FKBP51	NanoBRET FKBP12
74a	0	11 ± 1.1	0.60 ± 0.08	76 ± 8.4	14.1 ± 2.6
74b	1	12 ± 1.1	0.69 ± 0.13	124 ± 10	30.5 ± 4.2
74c	2	19 ± 1.7	0.57 ± 0.07	81 ± 12	19.1 ± 1.8
74d	3	32 ± 6.0	1.60 ± 0.20	163 ± 18	38.1 ± 5.8
75a	0	42 ± 5.9	1666 ± 28	1028 ± 84	2994 ± 327
75b	1	56 ± 8.3	228 ± 109	1046 ± 74	2774 ± 504
75c	2	41 ± 6.4	314 ± 72	814 ± 83	2939 ± 335
75d	3	44 ± 7.8	38 ± 114	748 ± 55	2895 ± 458
76	n.a.	> 80000	> 80000	> 10000	> 10000

The data clearly shows that all PRLs are strongly binding both proteins with nanomolar binding affinity in most cases. Selectivity also seems to remain unchanged, except for some compounds, compared to the precursors. Most importantly all compounds are cell permeable. The negative control compound **76** shows no binding affinity as intended.

Reaction optimization for crosslinking and copper catalyzed click reaction using compound **74b**

In the next step, the UV irradiation time required for complete conversion of the diazirine warhead is determined in a time course experiment *in vitro* by incubating FKBP12 with two equivalents of compound **74b**. After complete conversion of the diazirine was determined by LC-MS relative to the starting concentration, the resulting protein mixture is labeled with a biotin azide in a click reaction and analyzed by LC-MS to confirm literature known reaction conditions.^[145] The results are summarized in **Figure 23**.

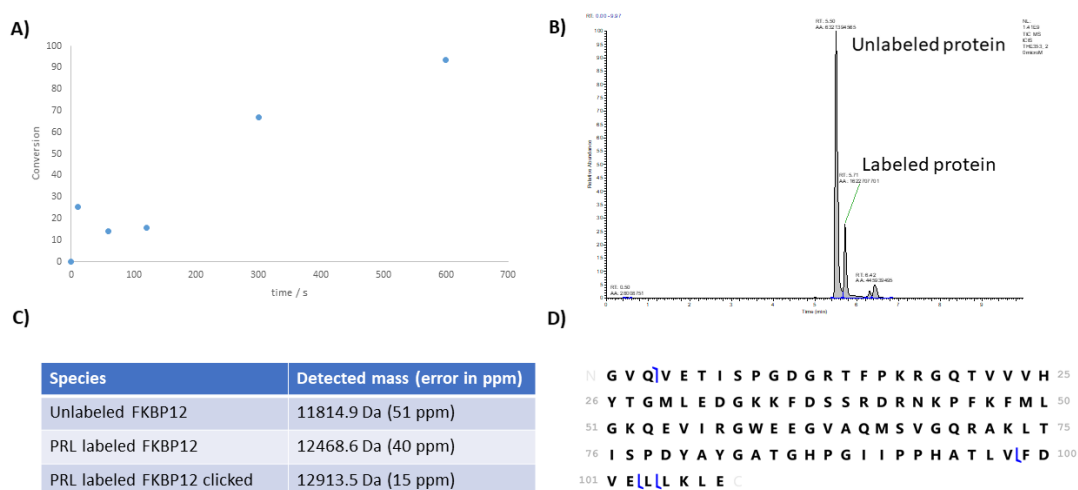


Figure 23: **A)** Conversion of the PRL **74b** in dependence of the UV irradiation time determined by LC-MS relative to the starting concentration at $t = 0$. **B)** TIC of the LC-MS analysis of the last time point with showing that about 20 % of the protein was labeled, assuming a neglectable difference in ionization efficiency of labeled and unlabeled protein. **C)** Summary of the detected intact protein masses after labeling with **74b** and the biotin azide after the click reaction. **D)** Annotated sequence of the FKBP12 construct with found fragment masses from top-down analysis.

Although it was possible to confirm the protein sequence by top down analysis, the MS2 spectra show only low signal to noise, resulting in merely four matched fragment masses. This is insufficient to determine the position on the label but more than enough to validate the identity of the detected protein FKBP12.

The photocrosslinker reacts almost completely within 10 min of UV irradiation as indicated by the almost disappearing signal detected by LC-MS. However, to adjust for the zero order kinetic depending on UV intensity and differences in the geometry resulting in different UV exposure of the sample container, incubation time was increased to 20 min for *in vitro* experiments. Sensitive experiments in cells were incubated for 5 min to minimize the bias in protein expression introduced from UV irradiation.

The conversion of the click reaction was determined to be complete after 60 min by intact protein mass LC-MS as the unreacted labeled protein mass can no longer be detected. This confirms the literature conditions as sufficient since only the product mass and the mass of unmodified FKBP12 was detected.

Validation of crosslinking for all PRLs at low protein concentration

In a next step, the labeling capabilities of all PRL at low concentrations and the detectability of crosslinked protein is assessed. This is necessary to check, since the effective ligand concentration in cells may be much lower than the initial one used. Furthermore, at higher concentrations the PRL may no longer be selective, making it necessary to utilize them at lower concentrations. All PRLs are tested with FKBP12 as a binding model at a concentration of 100 nM and treated with 20 min of UV irradiation at 365 nm. Analysis is performed using by LC-MS and **Table 4** summarizes the results.

Table 4: Observed crosslinking events of PRLs with FKBP12 at a protein concentration of 100 nM by intact mass analysis analog to **Figure 22 B**). Detected crosslinks are noted with a +, absence of crosslinks with a -.

Compound	FKBP12
74a	+
74b	+
74c	+
74d	+
75a	+
75b	+
75c	+
75d	+
76	-

In summary, all PRLs can crosslink to FKBP12 at a concentration of 100 nM with a twofold ligand excess, except the non binding control **76** which is working as intended. The employed LC-MS method is also able to reliably detect the protein crosslinks without requiring a concentration of the sample. The observed labeling efficiencies with about 20 % are sufficient to detect crosslinked proteins after an enrichment step.

PRLs crosslinking in cells

For a proof of concept, the photoreactive FKBP ligands compound **74b** and the negative control **76** were tested in an *in cellulo* setup by incubating both compounds under the same conditions as the nanoBret assay followed by UV irradiation and lysis of the cells. Crosslinked proteins were labeled using the biotin azide (see experimental section) via a copper catalyzed click reaction, enriched by a pull down on streptavidine agarose beads, digested with trypsin directly on the beads and then analyzed by LC-MS.

The required LC-MS method was developed in this thesis using an LTQ Orbitrap XL mass spectrometer that was manually calibrated and tuned using the manufacturers calmix solution leading to an increase in signal to noise of over tenfold compared to the previous state used for the oxidative footprinting. Notably, ion trap performance for MS2 spectra was significantly improved to the point that reasonable MS2 spectra can be obtained for all peptides visible in the precursor scan, allowing their identification.

After acceptable performance close to the instrument specification was achieved using a conventional LC system with a 2.1 mm inner diameter column, the method was transferred to a newly acquired easy nLC1200 nano LC system with an *in house* packed 75 μm inner diameter capillary column with a tapered tip supplied by Georg Tascher from the Münch lab of the Goethe University Frankfurt. The immense increase in data quality in regards to sensitivity and chromatographic resolution can clearly be observed from the base peak chromatograms of the streptavidine pull down protein digest of compound **74b** shown in **Figure 24**.

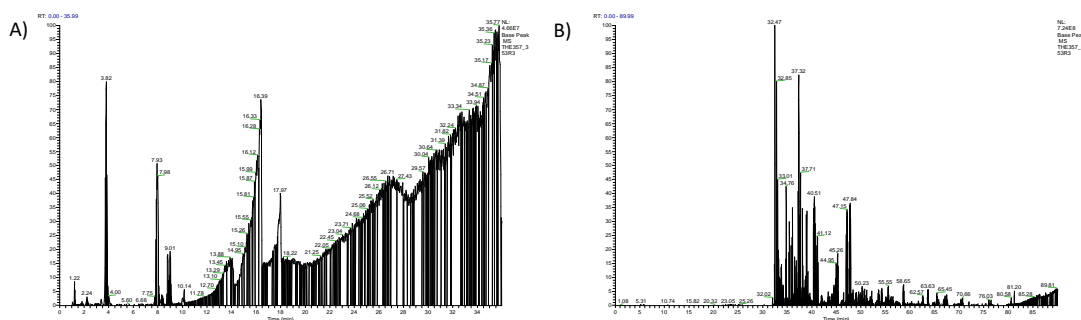
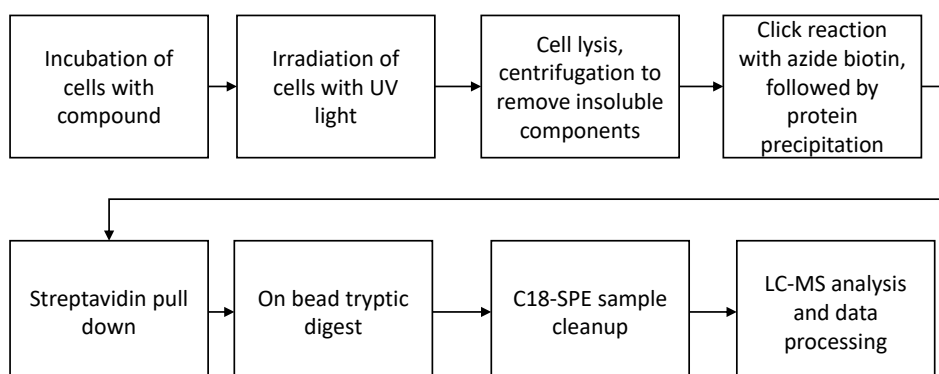


Figure 24: Base peak chromatograms of a streptavidine pull down digest of compound **74b** of an LC-MS run with A) a 20 μL injection on a 2.1 mm column with a conventional LC and B) a 1 μL injection of the same mixture with a 75 μm inner diameter capillary column with a tapered tip and an easy nLC1200 nano LC system.

With an optimized nano LC-MS method in hand, the digested samples from the streptavidin pull down are analyzed by a top 10 data dependent LC-MS analysis, e.g. the ten most abundant precursor signals are selected and fragmented in the ion trap. The raw data is then analyzed with MaxQuant and further processed with Perseus. The entire workflow and the results of the enrichment are shown in **Figure 25**.

A)



B)

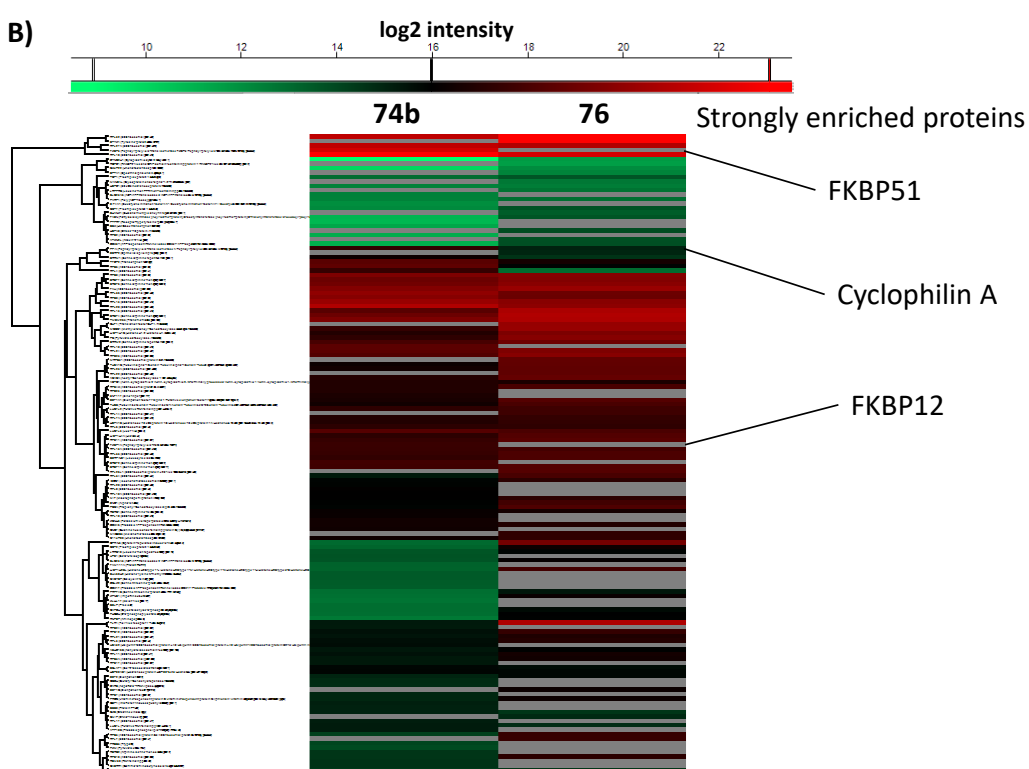


Figure 25: A) Workflow for identification of FKBP interaction partners and ligand binding off targets using photoreactive FKBP ligands and a biotin streptavidine pull down. B) Hierarchical cluster analysis of compound **74b** and the negative control compound **76** using the Perseus software, log₂ iBAQ intensity of the proteins is indicated by a color code, gray areas indicate no protein was detected in the sample. Strongly enriched proteins by **74b** are labeled with the protein name.

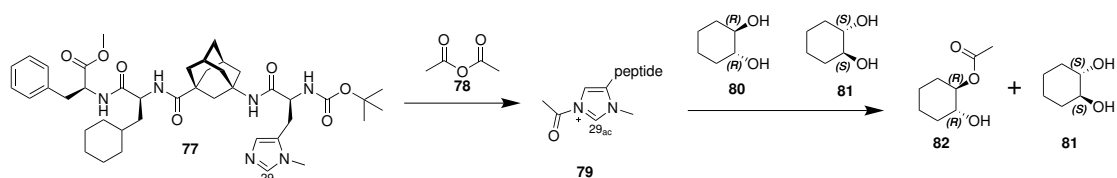
Even though the experimental conditions of the biochemical part of this experiment were not optimized, it was possible to identify several drastically enriched proteins of photocrosslinker **74b** compared to the negative control **76**, like FKBP12, FKBP51 and

cyclophilin A. While the first two are not a surprise, the photocrosslinker **74b** was not meant to have any affinity for cyclophilin A. Since this protein may share potential binding partners of FKBP, such as HSP90, a follow up experiment should investigate whether the photocrosslinker has an affinity for cyclophilin A by using purified protein. Otherwise, it will not be possible to clearly tell which proteins are directly bound by photocrosslinkers and which proteins are only in complex with proteins binding the photocrosslinkers.

In general, there is still a big room for improvements for this method as the current results were generated with a provisional nano ion source that only allowed pressures of up to 500 bar and no temperature control of the column. Additionally, the experiment was only performed in one replicate and the results should be confirmed to be statistically significant by performing the experiment in a triplicate to exclude false positive or false negative results. Nonetheless, the LC-MS performance was significantly enhanced compared to previous results with conventional LCs as was shown in **Figure 24** and the results serve as a good proof of concept for this method.

3.5 Analysis of a tetrapeptidic organocatalyst

In a cooperation with Matthias Brauser from the Thiele lab, a tetrapeptidic organo-catalyst **77** catalyzing a stereoselective acetylation with anhydrides **78** of diols according to **Scheme 16**, was analyzed by HR-MS using an LTQ Orbitrap XL mass spectrometer by the author of this thesis. This section is part of an unpublished manuscript.



Scheme 16: Stereoselective acetylation of diols: The tetrapeptide **77** forms intermediate **79** with anhydride **78** catalyzing enantioselective acetylation of the mixture **80** and **81** leading to **82** and enantiopure **81**. (unpublished results)

Although this particular catalyst and the acetylation reaction has been known for quite some time^[146], the details regarding the reaction mechanism are still unknown. The currently best model for this mechanism is the formation of the acetylated tetrapeptide intermediate **77** that transfers the acetyl group by an unknown mechanism onto the diol **80** resulting in the acetylated isomer **82** and the enantiopure diol **81** with an *ee* of greater 99 %.

As a first step, the tetrapeptide was analyzed with acetic anhydride in DCM with 1 % acetic acid by direct infusion nano ESI-MS in the positive ion mode. The formed acetylated tetrapeptide **79** can be clearly detected with the second highest intensity after the tetrapeptide ion itself as shown in **Figure 26**.

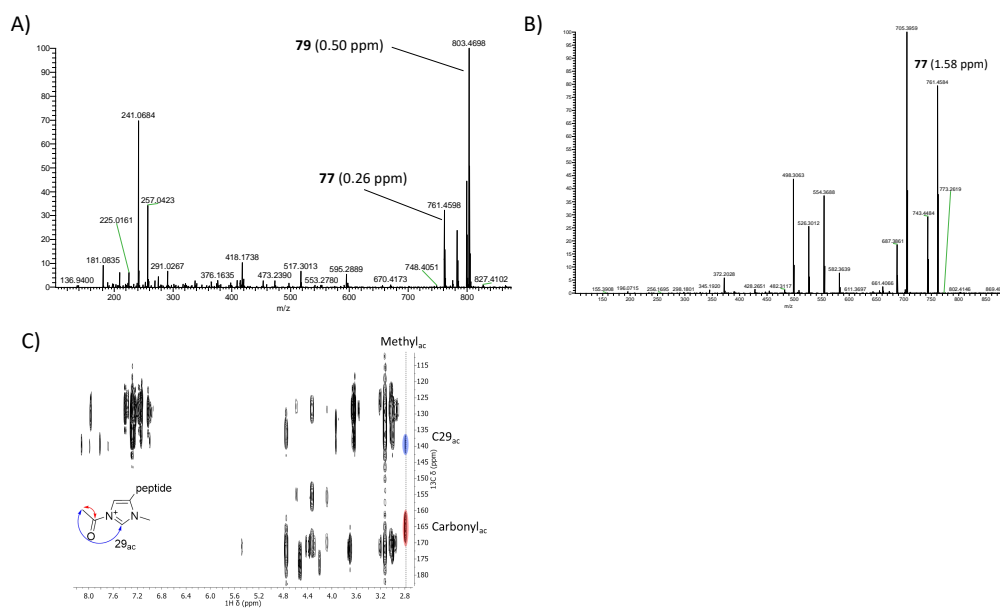


Figure 26: A) ESI MS spectrum of tetrapeptide **77** and acetic anhydride in excess in DCM with 1 % acetic acid. B) HCD spectrum of the intermediate **79** ion, $m/z = 803.47$. C) ^1H - ^{13}C -HMBC and ^1H -NOESY spectra of the intermediate **79** measured by Matthias Brauser. (unpublished results)

Isolation and CID fragmentation of the acetylated tetrapeptide results in fragments matching the structure and therefore confirm its identity. The existence of the intermediate **77** was then confirmed by NMR experiments conducted by Matthias Brauser. For isobutyric and pivalyl anhydride the same intermediate cations could be detected (data not shown).

Additionally, in negative ESI MS of a solution of tetrapeptide, acetic anhydride, and the (*R,R*)-diol in DCM with 1 % acetic acid, a complex of the acetylated diol and the tetrapeptide was detected and confirmed by isolation and HCD fragmentation as shown in **Figure 27**. Since in ESI MS the ionization efficiency not only strongly varies from analyte to analyte but also is significantly effected by the matrix, the total composition of the mixture an analyte is ionized in, quantification of the signals of said complex and the individual components to derive a binding constant are not possible in a meaningful manner. As an alternative, it is possible to isolate the complex in the mass spectrometer and perform tandem MS while slowly ramping up the collision energy used. The remaining precursor signal is then plotted against a sigmoidal curve similar that can be related to the stability of the complex, similar to binding curves. While the normalized collision energy (NCE) at which half of the precursor signal remains (NCE50) is not very meaningful on its own it can be related to the NCE50 of the tetrapeptide adduct ion with acetic acid.

Since acetic acid should not have any significant binding affinity, the complex of the tetrapeptide and acetylated diol should have a significant increase if there are any polar interactions or hydrogen bonds present. Indeed a difference of 1 NCE was detected indicating a hydrogen bond which is reasonable for this complex. Aside from this however,

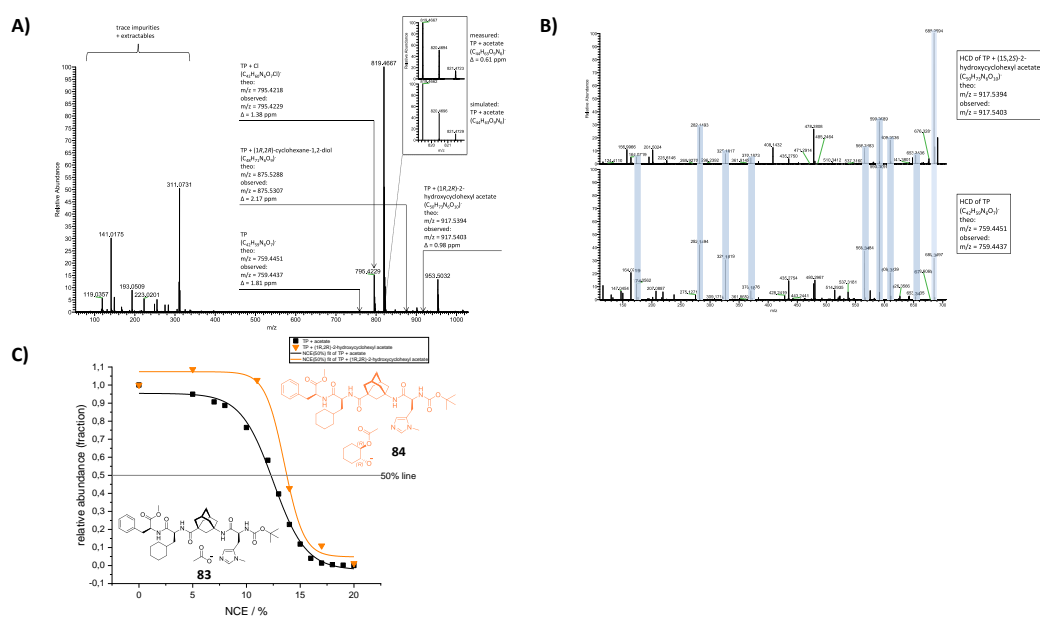


Figure 27: A) Negative mode ESI MS spectrum of tetrapeptide **77** and acetic anhydride and diol **80** in excess in DCM with 1% acetic acid. B) HCD of the tetrapeptide **77** and the complex of tetrapeptide and acetylated diol. C) NCE50 curves of the tetrapeptide acetic acid ion (**83**, black) and the tetrapeptide complex with the acetylated diol (**84**, orange) using HCD. (unpublished results)

it is not possible to detect where such a hydrogen bond is present because only collision activated dissociation techniques, that break weak non covalent bonds long before covalent bonds, are available on the used mass spectrometer. With more sophisticated fragmentation techniques such as ultra violet photo dissociation (UVPD) fragmentation of the precursor with selectively breaking covalent bonds while conserving weaker non covalent bonds may be possible for this cause to narrow down the location of a potential hydrogen bond. Furthermore, in the MS analysis any solvent effects no longer exist, as the measurement takes place in the gas phase which may give significantly deviating results from analysis in solution such as NMR measurements.

4 Conclusion

In this thesis, several chemical tools were successfully developed as summarized in **Figure 28**. Starting with the gram scale synthesis of SAFit2, the best chemical tool available at the start of this thesis, an efficient synthesis with a yield above 40 % over the longest linear sequence was achieved on a 20 g scale with a high purity (> 99 %), meeting the demand of the foreseeable future. On the basis of macrocycles, a new class of linear SAFit1 derivatives was explored that turned out to be more active for FKBP12 and FKBP12.6. Even though the synthesis was discontinued for time efficiency reasons, the ligands synthesized serve as a starting point for potentially potent FKBP12 and FKBP12.6 selective SAFit like ligands.

The most potent chemical tools developed in this thesis are the photocrosslinkers that are either intended to directly label a protein via a reactive side chain such as a cysteine or are based on ligands with a photoreactive warhead that crosslink proteins in proximity to the ligand binding site. This allows detection of molecular glues with superior selectivity and less artifacts compared to previous FRET assays and allows exploring the FKBP interactome in cells.

Complementary to the chemical tools LC-MS based methods for their analysis were developed. This included general purpose techniques such as intact mass measurements of proteins by LC-MS, as well as more sophisticated methods such as the oxidative footprinting and a bottom-up proteomics pipeline allowing qualitative analysis of relevant samples with some quantitative capabilities.

This thesis therefore set the foundation by developing all tools required to study the interactome of FKBP12 and related proteins in human cell lines as well as in macrophages to find new Mips relevant for infectivity.

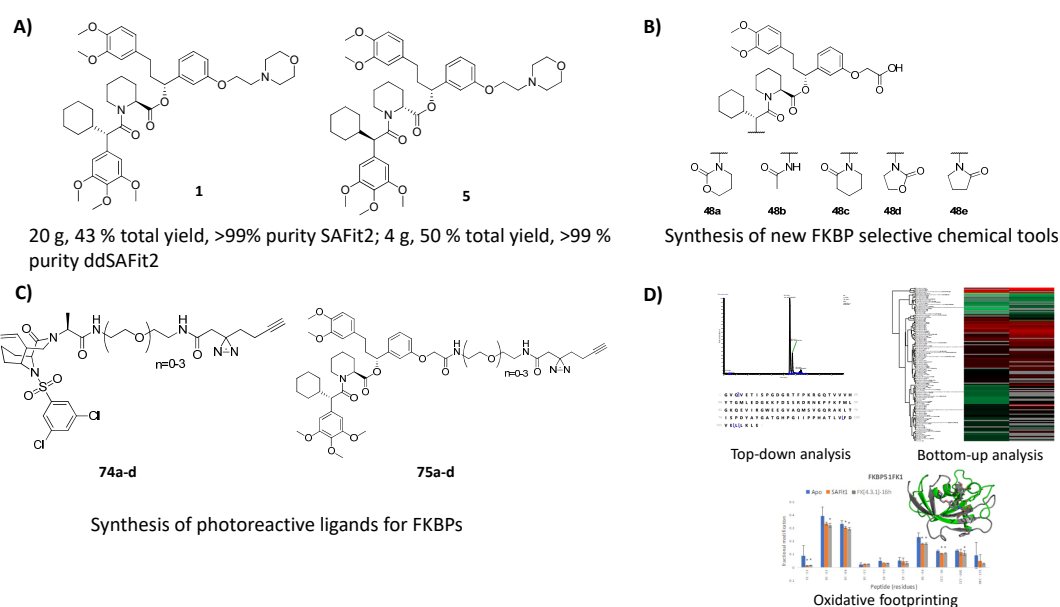


Figure 28: Overview of synthesized chemical tools and developed LC-MS methods for their characterization.

5 Materials and methods

5.1 NMR

^1H -, ^{13}C -NMR spectra were recorded at the NMR department of chemistry of the Technische Universität Darmstadt (TUD) on a Bruker AC 300, AR300 or DRX500 and at the Thiele lab by Johann Primozic and Matthias Brauser on a Bruker Avance III 600 MHz and Bruker Avance III HD 700 MHz spectrometer. Chemical shifts for ^1H and ^{13}C are given in ppm (δ) relative to the tetramethylsilane (TMS) internal standard. Deuterated chloroform (CDCl_3) and methanol (CD_3OD , denoted as MeOD) were used as solvents and the spectra calibrated according to their corresponding peak. The multiplicities are abbreviated as follows: singlet (s), doublet (d), triplet (t), quartet (q), doublet of doublets (dd), multiplet (m).

5.2 HRMS

HRMS spectra were acquired on an LTQ Orbitrap XL that was calibrated using the calmix solution of the manufacturer at least a week before the measurements were conducted.

5.3 LC-MS

Pump: Beckman System Gold 125 Solvent Module
Detector: Beckman System Gold 199 Detector Module
Column: YMC Pack Pro C8, 100×4.6 mm, $3 \mu\text{m}$
Solvent A: 95 % H_2O , 5 % MeCN, 0.1 % Formic acid
Solvent B: 95 % MeCN, 5 % H_2O , 0.1 % Formic acid
Method: 0-100 % B in 19 min, 1 mL/min
MS: LCQ Deca XP Plus
Ionization: ESI
Purity is determined by UV detection at 220 nm and given in percent.

5.4 HPLC

Pump: Dionex System Summit Pump
Detector: UVD380
Column: Phenomenex Jupiter $4 \mu\text{m}$ Proteo 90 Å, 250×4.6 mm

Solvent A: 95 % H₂O, 5 % MeCN, 0.1 % TFA
Solvent B: 95 % MeCN, 5 % H₂O, 0.1 % TFA
Method: 0-100 % B in 20 min, 1.5 mL/min
Purity is determined by UV detection at 220 nm and given in percent.

5.5 Chiral HPLC

Pump: Beckman System Gold 125S Solvent Module
Detector: Beckman System Gold Diode Array Detector Module 168
Column: Daicel chemical industries Ltd, Chiralcel OD-H, Normal Phase analytical column, 250 × 4.6 mm, 5 μm
Solvent A: *n*-Heptane
Solvent B: *iso*-Propanol
Method: isocratic 1 mL/min, percent B given for each compound.
Purity is determined by UV detection at 220 nm and given in percent.

5.6 UHPLC-MS

UHPLCMS measurements were performed on an Agilent 1260 infinity II system consisting out of a flexible pump, a Vialsampler, a multicolumn compartment with a column oven, a DAD detector, and a 6125B MSD. Data was acquired with a 50 x2.1 mm, 1.9 μm EC-C18 Poroshell 120 column using a gradient starting with an isocratic hold of 0.2 min at 5 % solvent B up to 100 % solvent B over 1.8min followed by a hold for 1 min with solvent A being water with 0.1 % formic acid and solvent B acetonitrile with 1 % formic acid.
Purity is determined by UV detection at 220 nm and given in percent.

5.7 GC-MS

GC-MS measurements were performed on an Agilent 8890 GC quipped with an 5976 single quadrupole MSD with an EI ion source and a 7693A automatic liquid sampler, using a 30 m x 0.25 mm, 0.25 μm HP-5ms column operated with 5.0 helium gas. Samples are introduced with a pulsed split injection with an inlet temperature of 280 °C and analyzed at a constant flow rate of 1.5 mL/min with a temperature gradient starting at 60 °C with an isocratic hold for 2 min, followed by a linear gradient to 320 °C over 7 min with a 1 min isocratic hold at 320 °C.

5.8 Flash chromatography

Flash chromatography is performed using an Isolera system from Biotage using the flash columns from the manufacturer with DAD-UV detection. If not mentioned otherwise,

separations are performed with a linear 10 column volume gradient.

5.9 Manual column chromatography

Manual column chromatography was performed using Kieselgel 60 from Roth, 0.04 – 0.063 mm.

5.10 Preparative HPLC

Preparative HPLC is performed on an Interchim Puriflash 5.250 system with UV detection. Purifications are performed using a Luna 250 x 21.2 mm, 5 μ m C18 column with a 100 Å pore size using a gradient from 5 % B to 100 % B in ten column volumes at a flow rate of 30 mL/min unless mentioned otherwise. Solvent A is water with 0.1 % TFA and solvent B acetonitrile with 0.1 % TFA.

5.11 Solvents and reagents

Reagents were obtained from TCI chemicals, abcr, Sigma Aldrich, Alfa Aesar, Fluka, Merck, Novabiochem, Carl Roth, Bachem, Acros Organics and Oxchem and used without further purification. Compound **72** was kindly provided by my colleague Patrick Purder.

tert.-Butyl hypochlorite is prepared briefly before it is used by the following procedure: 34.3 mL (67.5 mmol, 1.0 eq) 12 % sodium hypochlorite solution in H₂O are poured into a 100 mL Erlenmeyer flask and cooled to 0 °C in an ice bath. 6.45 mL (67.5 mmol, 1.0 eq) *tert.*-butanol are added to the aforementioned solution followed by 4.2 mL (74.2 mmol, 1.1 eq) acetic acid. The mixture is stirred for 3 min at 0 °C and then poured into a separatory funnel. The aqueous phase is discarded and the oily organic phase is washed first with saturated sodium carbonate solution, then with water. The crude product is dried over calcium chloride to yield the product as a yellow oil that smells strongly like chlorine. The yield is not determined and the crude product is used quickly. Remaining product and solutions that came into contact with it are quenched using sodium thiosulfate.

5.12 FKBP protein constructs

All FKBP protein constructs used in this thesis were kindly provided by Christian Meyners. Proteins were expressed and purified as previously described.^[16,39]

5.13 Fluorescence polarization assay

Fluorescence polarization assays were performed by Wisely Oki Sugiarto. K_d values were determined from the raw data with GraphpadPrism 6.0 by the author of this thesis by the procedure previously described.^[16,39]

5.14 NanoBRET assay

The NanoBRET assay was performed and the raw data was analyzed by Thomas Geiger as described previously.^[56]

5.15 Protein LCMS

5.15.1 Oxidative footprinting

The oxidative footprinting was performed as previously described.^[143] The instrument parameters were:

LC-MS/MS analysis was performed with an LTQ Orbitrap XL controlled by Xcalibur 2.1 and a micro-LC system consisting of a Micro Pro syringe pump from Eldex Laboratories and an Endurance autosampler (Spark Holland, Emmen, the Netherlands) controlled by the Endurance software. Acquisitions were started upon injection by contact closure.

Samples (5 μ L) were injected with a flushed loop injection and peptides were separated on a ZORBAX StableBond C18, 0.3 x 150 mm, 3.5 μ m column (Agilent, Santa Clara, CA, USA) at a flow rate of 5 μ L/min using the following gradient: linear gradient from 5 % B to 60 % B in 60 min, 10 min linear gradient to 100 %B, 10 min at 100 % B isocratic, followed by re-equilibration at 5 %B for 15 min, with solvent A being water with 0.1 % formic acid and solvent B being acetonitrile with 0.1 % formic acid.

The mass spectrometer was operated in a data dependent mode with a precursor scan in the Orbitrap with a resolution of 60,000 at m/z 400 followed by fragmentation of peptide ions with a charge state of 2 or larger giving rise to the four most intense signals in the ion trap using CID with a normalized collision energy of 25. Dynamic exclusion was enabled and set to a repeat count of 2 with a repeat duration of 30 s, the exclusion list size was 200 and the exclusion duration was 50 s. The ESI source was operated with 10 units of sheath gas flow rate, a spray voltage of 4 kV, a capillary temperature of 300 °C, a capillary voltage of 3 V, and tube lens set to 30.

For intact mass measurements and for native MS, including the experiments with different concentrations of acetonitrile, 10 μ L of sample was loaded into a glass needle that was pulled to a tip of ca. 1- μ m orifice diameter with a P97 Flaming/Brown type micropipette puller (Sutter Instrument Co., Novato, CA, USA), starting from 1.2-mm thin-walled glass capillaries (World Precision Instruments, Friedberg, Germany). Ionisation was then performed using a in house built nano-electrospray source that was coupled to the LTQ Orbitrap XL instrument.

5.15.2 Intact protein mass measurements by LC-MS

Intact protein mass measurements were performed using a 1100 Agilent system consisting out of a quaternary pump and a vial sampler coupled to an LTQ Orbitrap XL mass spectrometer operating in high mass range full scan mode scanning from 200 m/z-4000 m/z with resolution of 60000 at 400 m/z. AGC is set to 1×10^6 with a maximum injection time of 500 ms and one microscan. Typically 5 μ L of sample are injected using into the LC-MS system and separated on a TOSOH bioscience TSK gel C4 2 x 50 mm, 3 μ m column at a

flow rate of 0.35 mL/min starting at 5 % solvent B, increasing over 7 min to 100 % solvent B, with a 3 min isocratic hold at 100 % B, followed by re-equilibration for 3.5 min at 5 % B with the solvent being the same used for the oxidative footprinting.

5.15.3 Top down analysis

Top down analysis of proteins is conducted the same as intact protein mass measurements by LC-MS with the difference that the mass spectrometer is operated in data dependent mode with a precursor scan run with the conditions as described previously, followed by fragmentation of the most abundant ion, by HCD with a NCE of 25 with a maximum injection time of 180 ms and 5 microscans with an AGC of 1×10^{-5} .

Protein mass spectra are deconvoluted using UniDec^[147] and fragment spectra matched with theoretical fragment masses using ProSight Lite^[148].

5.15.4 Bottom up proteomics

For bottom up proteomics measurements the same LTQ Orbitrap XL from the oxidative footprinting was used with optimized parameters. The helium and nitrogen gas flow into the Orbitrap is regulated, so that the pressure increases approximately by 0.3×10^{-10} mbar in the FT analyzer region and 0.2×10^{-5} mbar in the ion trap region so that the instrument tests for isolation and fragmentation, as well as for the resolution pass. The electron multiplier of the ion trap is then recalibrated, before the FT ion optics are manually tuned to achieve maximum signal quality of the injected calibration mixture of the manufacturer. Parameters are further optimized by performing the automatic FT transmission calibration afterwards.

The mass spectrometer is operated in a data dependent top 10 mode, performing one precursor scan at a resolution of 60000 at 400 m/z with maximum injection time of 500 ms and the AGC is set to 1×10^6 , followed by 10 data dependent CID scans of the ten most intense ions in the ion trap with a maximum injection time of 100 ms and the AGC is set to 1×10^4 .

Samples are then analyzed by either a linear gradient from 5 % B to 60 % B in 30 min on a C18, 2.1 x 150 mm, 3.5 μ m Zorbax column with the previous described Agilent 1100 LC System or using an in house bomb loaded capillary with ReproSil-pur C18 1.9 μ m silica column with a tapered tip provided by Georg Tascher with an easy nLC1200 system using a 90 min gradient starting at 0 % B to 40 % B in 50 min to a 60 % B in 20 min and then to 100 % B in 10 min followed by a 10 min hold at 100 % B. The column is equilibrated with 3 μ L pure A and sample was loaded at a constant pressure of 500 bar. Solvent A consists of water with 0.1 % formic acid and solvent B consists of 80 % acetonitrile, 19.9 % water and 0.1 % formic acid. For the nanoLC an in house built nano ion source is used where a high voltage of 2 kV are applied to the T-union connecting the LC to the analytical column. The mass spectrometer is controlled using Xcalibur version 2.1 and the nanoLC is controlled using Xcalibur 4.2.

The raw data is analyzed using MaxQuant^[120] version 2.0.1 using the Swiss-Prot data base with the default settings. The data is then filtered and visualized with Perseus^[121] Version 2.0.3.

5.16 General procedures

5.16.1 Organic synthesis

Reactions are performed in an oven dried round bottom flask under Ar atmosphere if not mentioned otherwise. If indicated, degassing of solvents is performed by bubbling Ar gas through the solution for 15 min.

General procedure for synthesis of photoreactive ligands (PRLs) and cysteine-reactive linkers

- Coupling to linker: The diazirine or benzophenone with a free acid (1 eq) is dissolved in the minimum amount of DCM and mixed with the respective N-Boc-diamine linker (1.1 eq) and 1-Hydroxy-7-azabenzotriazol (HOAt, 1.1 eq). The reaction is started by addition of DIC (1.1 eq) and the mixture is stirred for 1 h at room temperature. After volatiles are removed under reduced pressure, the crude product is purified.
- Boc deprotection: The diazirine-Boc-linker (1 eq) is dissolved in 4 M HCl in dioxane (100 eq) and stirred for 1 h at room temperature. After volatiles are removed under reduced pressure, the crude product is used without further purification.
- Ligand coupling: The deprotected diazirine linker (1 eq), the ligand (1 eq) and HOAt (1.1 eq) are dissolved in the minimum amount of DCM. The reaction is started by addition of DIC (1.1 eq) and the mixture is stirred for 1 h at room temperature. After volatiles are removed under reduced pressure, the crude product is purified.

5.16.2 Solid phase synthesis

- Resin loading: 2-Chlorotriethyl chloride resin (2 eq) is placed into a oven dried flask and swelled for 30 min in DCM under Ar atmosphere at room temperature. The acid to load (2 eq) is dissolved in the minimum amount of DCM, mixed with DiPEA (3 eq), and added to the resin. The resin is stirred overnight before adding 100 μ L MeOH and DiPEA (2 eq) to cap the resin. After filtering and washing the resin three times with DMF and three times with DCM, the resin is dried in a desiccator overnight and the loading l in mmol/g of the resin is determined gravimetric according to **Equation 4** from the mass of the loaded resin m_{total} in mg, the mass of the resin before loading m_{resin} in mg, and the molecular weight of the loaded acid M_{acid} in g/mol:

$$l = \frac{(m_{\text{total}} - m_{\text{resin}}) \cdot 10^3}{(M_{\text{acid}} - 36.46) \cdot m_{\text{total}}} \quad (4)$$

- Test cleavage: An analytical portion of resin is transferred into a polypropylene vial and incubated with 0.5 mL of a 20 % 1,1,1,3,3,3-hexafluoro-2-propanol (HFIP) for 15 min while shaking at room temperature. Volatiles are removed with a gentle stream of argon gas and 0.5 mL of a mixture of MeCN/water/formic acid 1:1:0.01 are added to the dried resin and briefly sonicated. The resin is filtered off and the sample is analyzed by LC-MS.

-
- 3) Fmoc-deprotection: The resin is incubated while shaking for 10 min with 20 % 4-methylpiperidine in DMF and then washed once with DMF. This is repeated three times and after the third time the resin is washed three with times DMF and three times with DCM.
 - 4) Cleavage from resin: The resin is incubated with 20 % HFIP in DCM for 10 min while shaking at room temperature. The liquid phase is filtered into a flask and the resin is washed once with DCM. This procedure is repeated three times. Volatiles are then removed to yield the cleaved product.

Synthesis of lactam bottom groups

- a) (*R*)-2-((((9H-fluoren-9-yl)methoxy)carbonyl)amino)-2-cyclohexylacetic acid is loaded onto the resin according to the procedure 1).
- b) The resin is transferred into a syringe with a filter frit and the Fmoc-group is deprotected according to the procedure 3). Complete conversion is determined by a test cleavage described in procedure 2).
- c) Coupling of acid chlorides: Acid chloride (3 eq) is dissolved in the minimum amount of DCM, mixed with DiPEA (6 eq), added to the resin from b) and incubated while shaking for 30 min. The resin is washed three times with DMF and three times with DCM. Complete conversion is determined by 2).
- d) The intermediate is cleaved from the resin according to 4) to afford the free acid.
 - e) Cyclization is induced by redissolving the free acid in 10 mL/mmol DCM, adding 3 eq of 1 M KOtBu in HOtBu and stirring the mixture for 1 h at room temperature. Volatiles are then removed under reduced pressure to yield the crude product.

Synthesis of SAFit1 derivatives

- a) SAFit1 top core group is loaded onto the resin according to 1).
- b) The resin is transferred into a syringe with a filter frit and the Fmoc-group is deprotected according to the procedure 3). Complete conversion is determined by a test cleavage described in procedure 2).
- c) The lactam bottom group or (*R*)-2-((((9H-fluoren-9-yl)methoxy)carbonyl)amino)-2-cyclohexylacetic acid (1.1 eq) are dissolved in the minimum amount of DMF, mixed with HATU (1.1 eq), HOAt (2 eq) and DiPEA (3 eq) and the mixture is incubated with the resin while shaking at room temperature overnight. The resin is washed three times with DMF and three times with DCM. Complete conversion is determined by 2). In the case of (*R*)-2-((((9H-fluoren-9-yl)methoxy)carbonyl)amino)-2-cyclohexylacetic acid, the Fmoc group is deprotected according to 3) and acetic acid (3 eq) dissolved in the minimum amount of DMF with HATU (2 eq) and DiPEA (3 eq) is incubated for 2 h with the resin. The resin is washed three times with DMF and three times with DCM. Complete conversion is determined by 2).
- d) The compounds are cleaved from the resin according to 4) to yield the crude products.

6 Experimental procedures

6.1 Crosslinking of PRL in vitro

UV irradiation time optimization

FKBP12 is diluted from a stock solution provided by Christian Meyners to 10x the final concentration in ammonium acetate, PRL **74b** is diluted 100x the final concentration in MeCN and then diluted to 10x the final concentration in ammonium acetate.

40 μ L Ammonium acetate, 5 μ L 10x FKBP12 stock, and 5 μ L 10x **74b** are mixed in a well of a translucent 96 well plate from Greiner to a final concentration of 10 μ M protein and 20 μ M ligand. After 15 min of incubation, the wells are irradiated for 0 s, 10 s, 30 s, 1 min, 2 min, 5 min, and 10 min with UV light at 365 nm using a 100 W UV lamp.

The samples are transferred from the well plate into 350 μ L insert glass vials and analyzed by LC-MS intact mass and top down analysis as described. Between each injection a washing gradient using water/IPA from 5 % IPA to 100 % over 3 min and then back to 5 % IPA again over 3 min is run to flush remaining protein out of the system.

Crosslinking screen with FKBP12

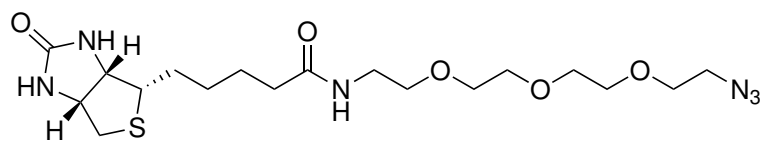
FKBP12 protein stock solution is diluted to 100x the final concentration in 200 mM ammonium acetate. DMSO stock solution of the ligand is diluted 100x the final concentration in MeCN.

98 μ L ammonium acetate, 1 μ L 100x FKBP12, and 1 μ L 100x ligand are mixed in the wells of a translucent 96 well plate from Greiner (part no. 650101) to a final concentration of 100 nM protein and 200 nM ligand. After 15 min of incubation, the wells are irradiated for 20 min. The samples are transferred from the well plate into 350 μ L insert glass vials from Agilent and analyzed by LC-MS.

Clicking of PEG-biotin-azide

Protein is diluted to 100x the final concentration in 200 mM ammonium acetate buffer, ligand is diluted 100x the final concentration in MeCN.

38 μ L 200 mM ammonium acetate buffer, 1 μ L 100x FKBP12, and 1 μ L 100x ligand are diluted in each well of a translucent 96 well plate from Greiner to a final concentration of 10 μ M protein and 200 μ M ligand. After 15 min of incubation, the wells are irradiated for 20 min at 365 nm with a 100 W UV lamp. The samples are transferred from the well plate into 350 μ L insert glass vials from Agilent and analyzed by LCMS to confirm the crosslink. Samples are then reacted with a mixture of commercially available Biotin PEG3 azide from Sigma Aldrich **85** (100 μ M), copper (II) sulfate (250 μ M), THPTA (250 μ M), and sodium ascorbate (2.5 mM) for 90 min at 24 °C while shaking. The product is analyzed by LC-MS.



85

6.2 Crosslinking of PRL in HEK cells

HEK293T cells are grown in 10 cm plates (Sarstedt, no. 83.3902) to 90 % confluency and incubated with 10 μ M **74b** or **76** for 2 h in DMEM+10 % FBS +1 % P/S. Following incubation, the cells were irradiated for 5 min with a 365 nm UV lamp at 4 °C. The cells were harvested, washed with PBS and then lysed for 20 min at 4 °C in 1 mL NETN lysis buffer+protease inhibitor cocktail (Roche, 04 693 124 001) . The lysate was cleared by centrifugation and adjusted to approximately 1 mg/mL protein concentration. This part was performed by my colleague Thomas Geiger.

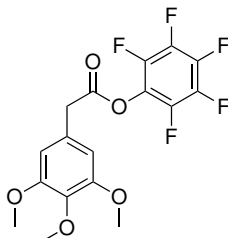
The two samples are then reacted with a mixture of Biotin PEG3 azide **85** (100 μ M), copper (II) sulfate (250 μ M), THPTA (250 μ M), and sodium ascorbate (2.5 mM) for 90 min at 24 °C while shaking. The reaction was quenched by addition of 1 mL of MeOH followed by precipitation at -80 °C overnight. Proteins were pelleted by centrifugation (20 000 g, 10 min, 4 °C). The supernatant was discarded and the pellets were dried briefly with nitrogen gas.

The pellets were resuspended in 500 μ L 1 % SDS in PBS with brief sonication (less than 1 min). Streptavidin agarose resin (200 μ L, washed 3x with 1 mL PBS) was added to each sample and incubated for 18 h at 24 °C with rotation. The beads are washed with 1 % SDS in PBS (1 mL), 8 M urea in PBS (3x1 mL), and 50 mM TEAB (3x1 mL). The beads are suspended in 225 μ L 50 mM TEAB and reduced and alkylated by adding 5 μ L 0.5 M TCEP (final concentration 10 mM) and 20 μ L 0.5 M chloroacetamide (final concentration 40 μ M) for 60 min at 37 °C. The beads are centrifuged, the supernatant is removed and the beads are resuspended in 350 μ L 0.5 M guanidine HCl in 50 mM TEAB pH 8.5. 3.5 μ L of 1 mg/mL MS grade trypsin (1:100 ratio trypsin:protein) is added and the mixture is incubated for 12 h at 37 °C. The reaction is quenched by adding 3.5 μ L TFA and the sample is cleaned up using reverse phase solid phase extraction (Discovery® DSC-18 SPE Tube, 52602-U, Sigma Aldrich) according to the manufacturers instructions. The solvent is removed in a Speedvac at 60 °C for 2 h. Samples are then redissolved in 0.1 % formic acid in water and analyzed by LC-MS with the bottom up proteomics method. Raw files are analyzed with MaxQuant 2.0.1 and the implemented Andromeda search engine with the human Swiss-Prot database. For the searches, tryptic digestion and the default settings for MS and MS/MS spectra were applied. The false discovery rate (FDR) was set to 1 %, minimal LFQ ratio count was set to 2 and the match between run features was enabled.

Further data filtering and visualization was performed using Perseus 2.0.3. First, contaminants, reverse hits and proteins only identified by modified peptides were removed. The remaining hits were then log₂ transformed and visualized by hierarchical clustering of **74b** and negative control **76**.

6.3 Organic syntheses

Perfluorophenyl 2-(3,4,5-trimethoxyphenyl)acetate



Chemical Formula: C₁₇H₁₃F₅O₅

Exact Mass: 392.07

Molecular Weight: 392.27

8

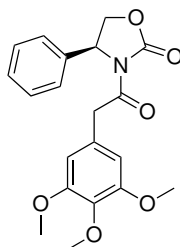
50 g (221 mmol, 1.0 eq) 3,4,5-trimethoxyphenylacetic acid, 40.7 g (221 mmol, 1.0 eq) pentafluorophenol, and 4.96 g (44.2 mmol, 0.2 eq) DMAP are dissolved in 500 mL DCM and cooled to 0 °C, 46.6 g (243 mmol, 1.1 eq) EDC·HCl are added and the mixture is stirred overnight at room temperature. After quenching the reaction by adding brine, the mixture is extracted three times using DCM, the combined organic phases are washed twice with 1 M HCl, dried over MgSO₄, and volatiles are removed under reduced pressure. The crude product is recrystallized from MeOH to yield 64.2 g (74 %) as a white solid.

¹H-NMR (500 MHz, CDCl₃): δ 6.57 (s, 2H), 3.90 (s, 2H), 3.88 (s, 6H), 3.85 (s, 3H).

¹³C-NMR (126 MHz, CDCl₃): δ 153.2, 136.4, 127.9, 106.4, 60.8, 56.1.

LC-MS: *t*_R = 13.43 min (99 %), *m/z*: calculated = 393.08 [M+H]⁺, found = 393.07 [M+H]⁺.

(S)-4-Phenyl-3-(2-(3,4,5-trimethoxyphenyl)acetyl)oxazolidin-2-one



Chemical Formula: C₂₀H₂₁NO₆

Exact Mass: 371.14

Molecular Weight: 371.38

9

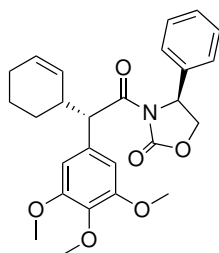
28.19 g (173 mmol, 1.1 eq) Evans auxiliary are dissolved in 620 mL THF and cooled to -78°C . 68.0 mL (173 mmol, 1.1 eq) *n*-butyl lithium are slowly added and the mixture is stirred for 15 min. 61.6 g (157 mmol, 1.0 eq) of **8** are added and the mixture is stirred for 2 h at -78°C before the reaction is quenched by addition of isopropyl alcohol (IPA). The mixture was extracted with EA, dried over MgSO₄, and volatiles are removed under reduced pressure. The crude product is purified by flash column chromatography (Cy/EA gradient) to yield 40.0 g (67%) as a white solid.

¹H-NMR (500 MHz, CDCl₃): δ 7.37 – 7.28 (m, 3H), 7.23 – 7.15 (m, 2H), 6.45 (s, 2H), 5.43 (dd, *J* = 8.8, 4.0 Hz, 1H), 4.69 (t, *J* = 8.9 Hz, 1H), 4.30 – 4.23 (m, 2H), 4.16 (d, *J* = 14.8 Hz, 1H), 3.82 (s, 3H), 3.77 (s, 6H).

¹³C-NMR (126 MHz, CDCl₃): δ 170.6, 153.7, 153.3, 138.8, 137.3, 134.1, 129.2, 128.9, 126.1, 106.8, 70.0, 61.0, 57.9, 56.2, 41.8.

UHPLC-MS: *t*_R = 1.98 min (96%), *m/z*: calculated = 372.15 [M+H]⁺, found = 372.2 [M+H]⁺.

(S)-3-((S)-2-((S)-Cyclohex-2-en-1-yl)-2-(3,4,5-trimethoxyphenyl)acetyl)-4-phenyloxazolidin-2-one



Chemical Formula: C₂₆H₂₉NO₆

Exact Mass: 451.20

Molecular Weight: 451.51

10

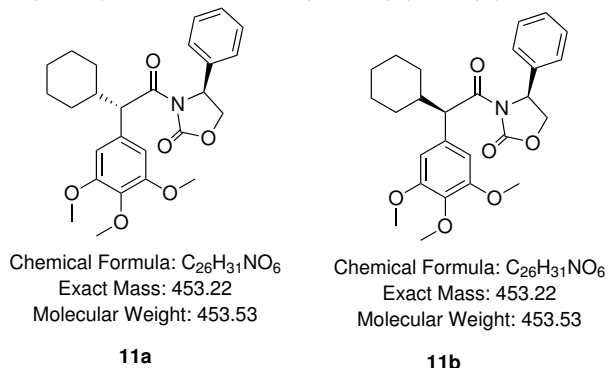
40.0 g (108 mmol, 1.0 eq) **9** are dissolved in 240 mL THF and cooled to 78 °C. 118 mL (118 mmol, 1.1 eq) of 1 M LiHMDS are added and the mixture is stirred for 2 h at -78 °C. 18.9 mL (162 mmol, 1.5 eq) 3-bromocyclohexene are added and the mixture is stirred for another 2 h before the reaction is quenched by addition of NH₄Cl solution. The mixture was extracted with EA, dried over MgSO₄, and volatiles are removed under reduced pressure. The crude product is purified by flash column chromatography (Cy/EA gradient) to yield 35.9 g (74 %) as a white solid as a mixture of diastereomers.

¹H-NMR (500 MHz, CDCl₃): δ 7.43 – 7.37 (m, 2H), 7.36 – 7.30 (m, 3H), 6.67 (d, J = 8.7 Hz, 2H), 5.61 (dq, J = 9.7, 4.6, 1.8 Hz, 1H), 5.36 (ddd, J = 9.2, 5.6, 3.7 Hz, 1H), 5.04 (dq, J = 10.2, 2.3 Hz, 1H), 4.83 (d, J = 11.3 Hz, 1H), 4.57 (td, J = 8.9, 3.2 Hz, 1H), 4.20 (ddd, J = 8.9, 3.8, 2.1 Hz, 1H), 3.83 (d, J = 2.8 Hz, 6H), 3.81 (d, J = 0.7 Hz, 3H), 2.80 (ddp, J = 16.1, 7.7, 2.6 Hz, 1H), 1.93 (ddq, J = 12.4, 5.9, 3.3 Hz, 2H), 1.70 – 1.58 (m, 1H), 1.49 – 1.28 (m, 2H), 1.11 (tdd, J = 12.7, 6.2, 2.6 Hz, 1H).

¹³C-NMR (126 MHz, CDCl₃): δ 173.5, 153.5, 153.4, 153.2, 139.4, 139.4, 137.4, 132.7, 132.6, 129.4, 129.2, 129.1, 128.9, 128.8, 128.5, 128.0, 126.1, 126.0, 106.4, 106.2, 69.5, 69.5, 60.8, 58.2, 58.2, 56.2, 56.2, 53.6, 53.4, 39.7, 39.6, 27.6, 26.1, 25.3, 25.2, 21.1, 20.4.

UHPLC-MS: *t*_R = 1.150 min (99 %), *m/z*: calculated = 452.21 [M+H]⁺, found = 452.2 [M+H]⁺.

(S)-3-((S)-2-Cyclohexyl-2-(3,4,5-trimethoxyphenyl)acetyl)-4-phenyloxazolidin-2-one and (S)-3-((R)-2-cyclohexyl-2-(3,4,5-trimethoxyphenyl)acetyl)-4-phenyloxazolidin-2-one



23.2 g (51.4 mmol, 1.0 eq) **10** are dissolved in 220 mL MeOH and the mixture is degassed with Ar for 15 min before 2.73 g (2.57 mmol, 0.05 eq) Pd/C are added. The mixture is then saturated with hydrogen gas for 15 min before the flask is sealed with a rubber septum and equipped with a hydrogen balloon. The reaction is stirred overnight at room temperature and then stopped by degassing the solution for 15 min with Ar before filtering over silica. Volatiles are removed under reduced pressure. The crude product is purified by flash column chromatography (Cy/EA gradient) to yield **11a** 16.38 g (70 %) as a white solid and **11b** 4.38 g (19 %) as a white solid.

11a

¹H-NMR (500 MHz, CDCl₃): δ 7.46 – 7.26 (m, 5H), 5.36 (dd, J = 8.8, 3.6 Hz, 1H), 4.79 (d, J = 10.8 Hz, 1H), 4.58 (t, J = 8.8 Hz, 1H), 4.21 (dd, J = 8.9, 3.6 Hz, 1H), 3.84 (s, 6H), 3.82 (s, 3H), 2.08 – 1.89 (m, 1H), 1.58 (d, J = 16.1 Hz, 4H), 1.36 – 1.20 (m, 3H), 1.09 (d, J = 8.3 Hz, 2H), 1.01 – 0.62 (m, 1H).

¹³C-NMR (126 MHz, CDCl₃): δ 174.0, 153.7, 153.1, 139.5, 137.2, 133.2, 129.3, 128.9, 126.0, 106.2, 69.5, 61.0, 58.3, 56.2, 54.7, 42.2, 31.5, 30.3, 26.4, 26.0, 25.9.

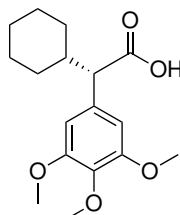
UHPLC-MS: *t*_R = 1.238 min (99 %), *m/z*: calculated = 454.23 [M+H]⁺, found = 454.2 [M+H]⁺.

11b

¹H-NMR (500 MHz, CDCl₃): δ 7.22 – 7.12 (m, 3H), 6.85 – 6.79 (m, 2H), 6.27 (s, 2H), 5.44 (dd, J = 9.0, 5.0 Hz, 1H), 4.72 (d, J = 10.7 Hz, 1H), 4.68 – 4.58 (m, 1H), 3.83 (s, 3H), 3.63 (s, 6H), 2.05 – 1.92 (m, 1H), 1.85 (dt, J = 12.4, 3.1 Hz, 1H), 1.70 (dt, J = 14.7, 3.9 Hz, 1H), 1.65 – 1.57 (m, 3H), 1.35 – 1.20 (m, 2H), 1.20 – 1.07 (m, 2H), 1.02 (tdd, J = 12.4, 10.8, 3.6 Hz, 1H), 0.82 (qd, J = 11.8, 3.0 Hz, 1H).

¹³C-NMR (126 MHz, CDCl₃): δ 172.7, 153.3, 153.0, 138.4, 137.1, 132.1, 128.8, 128.5, 125.9, 106.0, 69.5, 60.9, 57.9, 56.0, 55.9, 39.8, 32.4, 30.3, 26.5, 26.1, 26.1.

UHPLC-MS: *t*_R = 1.186 min (99 %), *m/z*: calculated = 454.23 [M+H]⁺, found = 454.2 [M+H]⁺.

(S)-2-Cyclohexyl-2-(3,4,5-trimethoxyphenyl)acetic acidChemical Formula: C₁₇H₂₄O₅

Exact Mass: 308.16

Molecular Weight: 308.37

12a

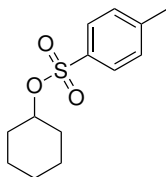
16.38 g (36.1 mmol, 1.0 eq) **11a** are dissolved in 160 mL THF and added to a mixture of 2.59 g (108 mmol, 3.0 eq) LiOH and 18.4 mL (181 mmol, 5.0 eq) H₂O₂ dissolved in 80 mL water. The mixture is stirred overnight at room temperature before the reaction is quenched by addition of 1 M HCl. The mixture is extracted with ether, dried over MgSO₄, and the solvent is removed under reduced pressure. The crude product is purified by flash column chromatography (Cy/EA+1 % of formic acid gradient) to yield 9.7 g (87 %) as a pale yellow solid.

¹H-NMR (500 MHz, CDCl₃): δ 6.54 (s, 2H), 3.84 (s, 6H), 3.82 (s, 3H), 3.12 (d, J = 10.7 Hz, 1H), 1.95 (tt, J = 11.0, 3.3 Hz, 1H), 1.92 – 1.86 (m, 1H), 1.79 – 1.71 (m, 1H), 1.64 (dq, J = 8.0, 3.9 Hz, 2H), 1.43 – 1.34 (m, 1H), 1.34 – 1.24 (m, 1H), 1.22 – 1.13 (m, 2H), 1.07 (tdd, J = 12.6, 10.8, 3.5 Hz, 1H), 0.81 – 0.69 (m, 1H).

¹³C-NMR (126 MHz, CDCl₃): δ 180.0, 153.3, 137.5, 133.0, 105.8, 60.9, 59.1, 56.3, 41.0, 32.0, 30.4, 26.4, 26.0.

UHPLC-MS: *t*_R = 1.863 min (99 %), *m/z*: calculated = 309.2 [M+H]⁺, found = 309.2 [M+H]⁺.

Cyclohexyl 4-methylbenzenesulfonate



Chemical Formula: C₁₃H₁₈O₃S

Exact Mass: 254.10

Molecular Weight: 254.35

14

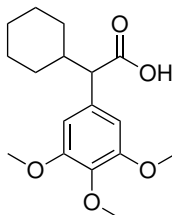
76.1 g (399 mmol, 1.0 eq) *p*-Toluenesulfonyl chloride are dissolved in 500 mL DCM and the mixture is cooled to 0 °C. 42.1 mL (399 mmol, 1.0 eq) cyclohexanol and 98.4 g (1200 mmol, 3.0 eq) N-methylimidazole are added subsequently. The mixture is stirred overnight at room temperature before it is quenched by addition of diluted HCl. The mixture is extracted with DCM, dried over MgSO₄, and the solvent is removed under reduced pressure. The crude product is purified by recrystallization from *n*-heptane to yield 94.5 g (93 %) as a white solid.

¹H-NMR (500 MHz, CDCl₃): δ 7.78 (d, 2H), 7.32 (d, J = 7.9 Hz, 2H), 4.49 (tt, J = 8.7, 3.7 Hz, 1H), 2.43 (s, 3H), 1.81 – 1.65 (m, 4H), 1.57 – 1.40 (m, 3H), 1.33 – 1.19 (m, 3H).

¹³C-NMR (126 MHz, CDCl₃): δ 144.4, 134.9, 129.8, 127.7, 81.8, 32.4, 24.9, 23.5, 21.7.

UHPLC-MS: *t*_R = 2.164 min (99%), *m/z*: calculated = 277.1 [M+Na]⁺, found = 277.0 [M+Na]⁺.

2-Cyclohexyl-2-(3,4,5-trimethoxyphenyl)acetic acid



Chemical Formula: C₁₇H₂₄O₅

Exact Mass: 308.16

Molecular Weight: 308.37

12

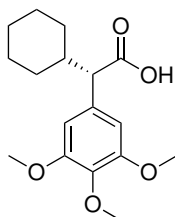
37.0 g (164 mmol, 1.0 eq) 3,4,5-trimethoxyphenylacetic acid are dissolved in 300 mL THF and the mixture is cooled to -78°C . 360 mL (360 mmol, 2.2 eq) 1 M NaHMDS are added and the mixture is stirred for 10 min before 41.6 g (164 mmol, 1.0 eq) **14** dissolved in 50 mL THF are added. The mixture is stirred overnight for 1 h at -78°C and then overnight at room temperature before it is quenched by addition of diluted HCl. The mixture is extracted with ether, dried over MgSO₄, and the solvent is removed under reduced pressure. The crude product is purified by recrystallization of the sodium salt by refluxing in an aqueous NaOH/EtOH mixture. The Na salt is then redissolved in water, acidified by addition of 3 M HCl, extracted with DCM, dried over MgSO₄, and the solvent is removed under reduced pressure to yield 34.7 g (69%) as a pale yellow solid.

¹H-NMR (500 MHz, CDCl₃): δ 6.54 (s, 2H), 3.84 (s, 6H), 3.82 (s, 3H), 3.12 (d, J = 10.7 Hz, 1H), 1.95 (tt, J = 11.0, 3.3 Hz, 1H), 1.92 – 1.86 (m, 1H), 1.79 – 1.71 (m, 1H), 1.64 (dq, J = 8.0, 3.9 Hz, 2H), 1.43 – 1.34 (m, 1H), 1.34 – 1.24 (m, 1H), 1.22 – 1.13 (m, 2H), 1.07 (tdd, J = 12.6, 10.8, 3.5 Hz, 1H), 0.81 – 0.69 (m, 1H).

¹³C-NMR (126 MHz, CDCl₃): δ 180.0, 153.3, 137.5, 133.0, 105.8, 60.9, 59.1, 56.3, 41.0, 32.0, 30.4, 26.4, 26.0.

LC-MS: $t_{\text{R}} = 11.77$ min (99%), m/z: calculated = 309.17 [M+H]⁺, found = 309.16 [M+H]⁺.

(S)-2-Cyclohexyl-2-(3,4,5-trimethoxyphenyl)acetic acid using fractionized crystallization



Chemical Formula: C₁₇H₂₄O₅

Exact Mass: 308.16

Molecular Weight: 308.37

12a

51.6 g (167 mmol, 1.0 eq) **11** are dissolved in 500 mL MeCN and 6.5 mL (83.7 mmol, 0.5 eq) D-Alaninol are added. The mixture is heated to reflux and then allowed to cool to room temperature while stirring. After the crystallization is complete, the solid is filtered and the enantiomeric ratio is determined by chiral HPLC. This process is repeated five times until sufficient *ee* was achieved. The enriched enantiomer is redissolved in water, acidified by addition of 3 M HCl, extracted with DCM, dried over MgSO₄, and volatiles are removed under reduced pressure to yield 8.45 g (16 %) as a white solid.

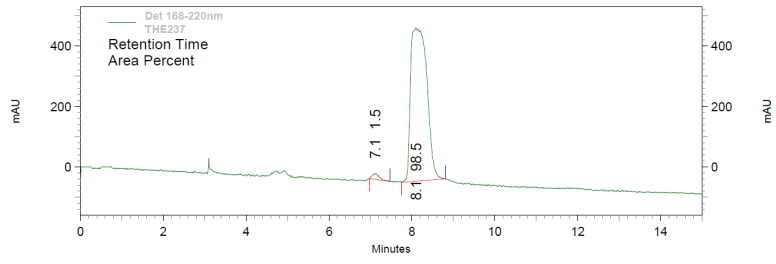
¹H-NMR (500 MHz, CDCl₃): see **12**.

¹³C-NMR (126 MHz, CDCl₃): see **12**.

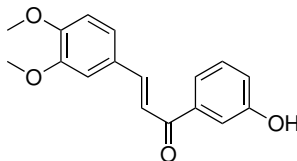
Chiral HPLC (10 % B): *t*_R = 6.70 min (97 %) purity, (97 %) *ee*.

Chiral bases for crystallization were screened by incubating 40 mg **11** with 1 eq of base in the respective solvent overnight. A sample is taken from the mother liquor and analyzed by chiral HPLC.

Chiral HPLC, UV 220 nm



(E)-3-(3,4-Dimethoxyphenyl)-1-(3-hydroxyphenyl)prop-2-en-1-one



Chemical Formula: C₁₇H₁₆O₄

Exact Mass: 284.10

Molecular Weight: 284.31

17

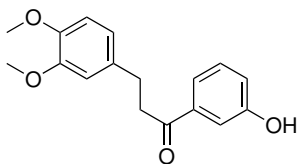
9.0 g (54.2 mmol, 1.0 eq) 3,4-Dimethoxybenzaldehyde and 7.37 g (54.2 mmol, 1.0 eq) 3-hydroxyacetophenone are dissolved in 90 mL EtOH and the mixture is cooled to 0 °C. 24.5 g (217 mmol, 4.0 eq) potassium hydroxide are dissolved in 60 mL water and to the aforementioned mixture. The mixture is stirred for 2 h and then quenched by adding ice and then 3 M HCl until a pH of 2 is reached. The mixture is crystallized from the quenched reaction mixture to yield 15.3 g (99%) as a yellow solid.

¹H-NMR (500 MHz, CDCl₃): δ 7.77 (dd, J = 15.6, 1.4 Hz, 1H), 7.67 – 7.59 (m, 1H), 7.56 (d, J = 7.7 Hz, 1H), 7.40 – 7.33 (m, 2H), 7.22 (dt, J = 8.4, 1.8 Hz, 1H), 7.15 (t, J = 1.8 Hz, 1H), 7.13 – 7.07 (m, 1H), 6.89 (dd, J = 8.3, 1.5 Hz, 1H), 6.64 (s, 1H), 3.94 (s, 3H), 3.93 (s, 3H).

¹³C-NMR (126 MHz, CDCl₃): δ 190.9, 156.6, 151.7, 149.4, 145.7, 139.9, 130.0, 127.9, 123.5, 120.9, 120.3, 120.0, 115.3, 111.3, 110.3, 56.2, 56.1.

UHPLC-MS: *t*_R = 1.753 min (99%), *m/z*: calculated = 285.11 [M+H]⁺, found = 285.2 [M+H]⁺.

3-(3,4-Dimethoxyphenyl)-1-(3-hydroxyphenyl)propan-1-one



Chemical Formula: C₁₇H₁₈O₄

Exact Mass: 286.12

Molecular Weight: 286.32

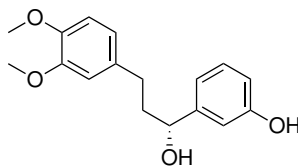
18

14.0 g (215 mmol, 10 eq) zinc and 16.5 g (215 mmol, 10 eq) ammonium acetate are suspended in 100 mL MeOH. 6.1 g (21.5 mmol, 1.0 eq) **17** are dissolved in 100 mL MeOH and added dropwise to the aforementioned mixture. The solids are filtered, washed with MeOH and the crude product is precipitated from the filtrate by addition of water. The crude product is purified by recrystallization from water/methanol to yield 5.17 g (84 %) as a white solid.

¹H-NMR (500 MHz, CDCl₃): δ 7.54 (dd, J = 2.7, 1.6 Hz, 1H), 7.49 (dq, J = 7.9, 1.2 Hz, 1H), 7.31 (td, J = 8.0, 1.1 Hz, 1H), 7.08 (ddd, J = 8.0, 2.6, 0.9 Hz, 1H), 6.83 – 6.73 (m, 3H), 6.63 (d, J = 42.6 Hz, 1H), 3.84 (s, 3H), 3.84 (s, 3H), 3.26 (dd, J = 8.3, 6.9 Hz, 2H), 3.05 – 2.97 (m, 2H).

¹³C-NMR (126 MHz, CDCl₃): δ 200.4, 156.6, 149.0, 147.5, 138.3, 133.9, 130.0, 120.8, 120.6, 120.3, 114.7, 112.1, 111.6, 56.1, 56.0, 40.9, 30.0.

UHPLC-MS: *t*_R = 1.778 min (98 %), *m/z*: calculated = 287.13 [M+H]⁺, found = 287.2 [M+H]⁺.

(R)-3-(3-(3,4-Dimethoxyphenyl)-1-hydroxypropyl)phenolChemical Formula: C₁₇H₂₀O₄

Exact Mass: 288.14

Molecular Weight: 288.34

19

9.70 g (33.9 mmol, 1 eq) **18** and 50.8 mL (50.8 mmol, 1.5 eq) 1 M potassium butoxide were dissolved in 100 mL IPA. The mixture was degassed with Ar and 270 mg (0.27 mmol, 0.01 eq) RuCl₂[(S)-dm-segphos][(S)-daipen] were added. The mixture was saturated with hydrogen for 15 min before the flask was sealed with a rubber septum and equipped with a hydrogen balloon. The mixture is stirred for 72 h before the reaction is stopped by degassing with Ar and removing volatiles under reduced pressure. The crude product is purified by recrystallization DCM to yield 9.28 g (95 %) as a white solid.

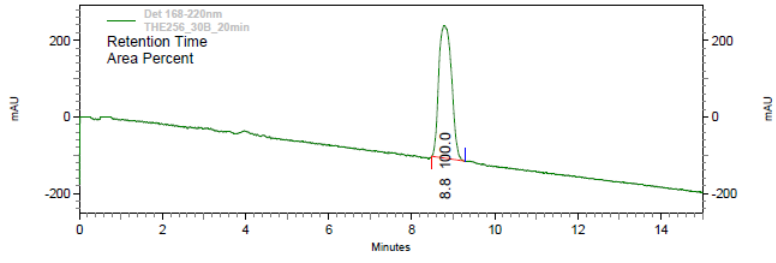
¹H-NMR (500 MHz, CDCl₃): δ 7.14 (t, J = 7.8 Hz, 1H), 6.86 (t, J = 2.0 Hz, 1H), 6.79 (d, J = 7.7 Hz, 1H), 6.76 – 6.70 (m, 2H), 6.69 – 6.61 (m, 2H), 4.58 (dd, J = 7.6, 5.4 Hz, 1H), 3.80 (s, 3H), 3.78 (s, 3H), 2.71 – 2.47 (m, 2H), 2.13 – 1.85 (m, 2H).

¹³C-NMR (126 MHz, CDCl₃): δ 156.3, 148.9, 147.2, 146.1, 134.4, 129.8, 120.4, 118.2, 114.9, 112.9, 112.1, 111.5, 74.0, 56.0, 55.9, 40.3, 31.6.

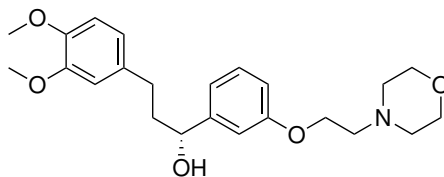
LC-MS: *t*_R = 9.87 min (99 %), *m/z*: calculated = 271.13 [M+H-H₂O]⁺, found = 271.26 [M+H-H₂O]⁺.

Chiral HPLC (30 % B): *t*_R = 8.78 min (>99 %) *ee*

Chiral HPLC, UV 220 nm



(R)-3-(3,4-Dimethoxyphenyl)-1-(3-(2-morpholinoethoxy)phenyl)propan-1-ol



Chemical Formula: C₂₃H₃₁NO₅

Exact Mass: 401.22

Molecular Weight: 401.50

20

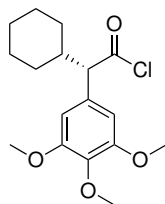
3.33 g (11.5 mmol, 1 eq) **19**, 2.15 g (11.5 mmol, 1 eq) 2-chloroethylmorpholine hydrochloride, and 6.38 g (66.1 mmol, 4 eq) potassium carbonate are suspended in 50 mL MeCN. The suspension is refluxed for 24 h before the reaction is stopped by filtering off the solids and removing volatiles under reduced pressure. The crude product is purified by manual silica column (EA/TEA/MeOH 100:3:1) to yield 3.60 g (78 %) as a yellow oil.

¹H-NMR (500 MHz, CDCl₃): δ 7.28 – 7.21 (m, 1H), 6.92 (dt, J = 6.6, 1.4 Hz, 2H), 6.83 – 6.79 (m, 1H), 6.79 – 6.77 (m, 1H), 6.75 – 6.69 (m, 2H), 4.65 (dd, J = 7.9, 5.2 Hz, 1H), 4.15 – 4.06 (m, 2H), 3.85 (s, 3H), 3.84 (s, 3H), 3.74 – 3.68 (m, 4H), 2.78 (td, J = 5.7, 1.2 Hz, 2H), 2.75 – 2.56 (m, 2H), 2.58 – 2.53 (m, 4H), 2.14 – 1.93 (m, 2H).

¹³C-NMR (126 MHz, CDCl₃): δ 159.1, 149.0, 147.3, 146.6, 134.5, 129.6, 120.3, 118.6, 113.7, 112.3, 111.9, 111.4, 73.8, 67.0, 65.9, 57.8, 56.1, 56.0, 54.2, 40.7, 31.8.

UHPLC-MS: *t*_R = 1.358 min (98 %), *m/z*: calculated = 402.23 [M+H]⁺, found = 402.2 [M+H]⁺.

(S)-2-Cyclohexyl-2-(3,4,5-trimethoxyphenyl)acetyl chloride



Chemical Formula: C₁₇H₂₃ClO₄

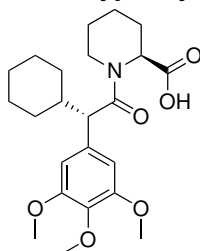
Exact Mass: 326.13

Molecular Weight: 326.82

21

1.00 g (3.24 mmol, 1 eq) **11a** are dissolved in 5 mL DCM and the mixture is cooled to 0 °C. 2.00 mL (4.05 mmol, 1.25 eq) 2 M oxalyl chloride in DCM are added with 50 µL DMF. The mixture is stirred for 2 h at 0 °C before the reaction is stopped by removing volatiles under reduced pressure. The crude product (1.06 g quant.) is used without further purification.

(S)-1-((S)-2-Cyclohexyl-2-(3,4,5-trimethoxyphenyl)acetyl)piperidine-2-carboxylic acid



Chemical Formula: C₂₃H₃₃NO₆

Exact Mass: 419.23

Molecular Weight: 419.51

22

0.96 g (7.42 mmol, 1.1 eq) *L*-pipecolid acid are dissolved in 13.5 mL of a 1 M KOH solution and cooled to 0 °C. 2.20 g (6.74 mmol, 1.0 eq) **21** dissolved in 20 mL dioxane are added and the mixture is stirred overnight at room temperature before the reaction is quenched by adding diluted HCl. The mixture is extracted with DCM, dried with MgSO₄, and volatiles are removed under reduced pressure. The crude product is purified by manual silica column (DCM/MeOH/FA 200:1:2) to yield 1.79 g (63 %) as a white solid.

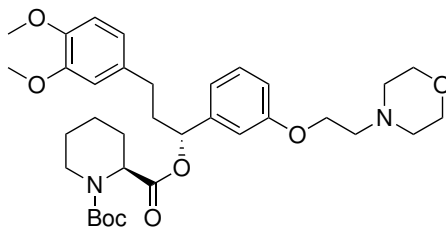
¹H-NMR (500 MHz, CDCl₃): δ 9.18 (s, 1H), 6.44 (s, 1H), 6.43 (s, 2H), 5.33 – 5.27 (m, 1H), 4.78 (d, J = 5.6 Hz, 0H), 4.60 (d, J = 13.7 Hz, 0H), 3.89 (d, J = 14.1 Hz, 1H), 3.82 (s, 3H), 3.81 (s, 3H), 3.79 (s, 6H), 3.35 (d, J = 9.5 Hz, 1H), 3.12 (d, J = 9.6 Hz, 0H), 2.99 – 2.87 (m, 1H), 2.71 – 2.56 (m, 0H), 2.27 – 2.20 (m, 1H), 2.07 (dt, J = 21.5, 11.2 Hz, 2H), 1.87 (dd, J = 30.8, 12.6 Hz, 2H), 1.76 – 1.52 (m, 9H), 1.52 – 0.99 (m, 7H), 0.97 – 0.87 (m, 1H), 0.76 (tt, J = 17.7, 9.3 Hz, 2H).

¹³C-NMR (126 MHz, CDCl₃): δ 176.1, 175.9, 175.9, 173.7, 173.7, 172.3, 153.4, 153.1, 137.0, 136.9, 134.3, 133.2, 105.8, 105.3, 61.0, 60.9, 56.4, 56.4, 56.2, 55.8, 55.5, 52.4, 43.7, 41.3, 41.2, 39.7, 33.0, 32.9, 30.8, 30.7, 26.8, 26.6, 26.6, 26.4, 26.3, 26.2, 25.4, 24.5, 21.0, 20.9.

UHPLC-MS: *t*_R = 2.002 min (99 %), m/z: calculated = 420.24 [M+H]⁺, found = 420.2 [M+H]⁺.

(S)-1-Tert-butyl

**2-((R)-3-(3,4-dimethoxyphenyl)-1-(3-(2-morpholinoethoxy)phenyl)propyl)
piperidine-1,2-dicarboxylate**



Chemical Formula: C₃₄H₄₈N₂O₈

Exact Mass: 612.34

Molecular Weight: 612.75

23

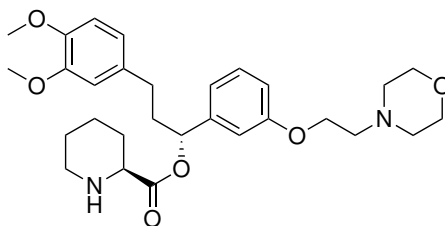
31.3 g (77.8 mmol, 1.0 eq) **20**, 18.74 g (81.7 mmol, 1.05 eq) (*S*)-*N*-Boc-pipecolate, and 1.90 g (15.6 mmol, 0.2 eq) DMAP are dissolved in 350 mL DCM. The mixture is cooled to 0 °C and 15.7 g (81.7 mmol, 1.05 eq) EDC·HCl are added. The mixture is stirred overnight at room temperature before the reaction is quenched by addition of brine. The mixture is extracted with DCM, dried with MgSO₄, and volatiles are removed under reduced pressure. The crude product is purified by flash column chromatography (Cy/EA+3 % TEA) to yield 42.2 g (97 %) as a pale yellow oil.

¹H-NMR (500 MHz, CDCl₃): δ 7.24 (t, *J* = 8.2 Hz, 2H), 6.91 (d, *J* = 7.8 Hz, 2H), 6.87 (s, 2H), 6.82 (d, *J* = 8.2 Hz, 1H), 6.77 (d, *J* = 8.1 Hz, 1H), 6.67 (q, *J* = 6.6 Hz, 3H), 5.76 (s, 1H), 5.04 – 4.89 (m, 1H), 4.75 (d, *J* = 6.0 Hz, 1H), 4.10 (p, *J* = 6.3 Hz, 5H), 4.06 – 3.90 (m, 1H), 3.84 (d, *J* = 2.5 Hz, 9H), 3.80 – 3.68 (m, 7H), 2.79 (t, *J* = 5.7 Hz, 3H), 2.67 – 2.42 (m, 4H), 2.25 (dd, *J* = 26.2, 13.2 Hz, 4H), 2.04 (d, *J* = 8.3 Hz, 4H), 1.77 – 1.55 (m, 5H), 1.47 (s, 6H), 1.36 (d, *J* = 7.2 Hz, 7H), 1.22 – 1.02 (m, 1H).

¹³C-NMR (126 MHz, CDCl₃): δ 171.5, 171.2, 158.9, 155.5, 149.0, 147.5, 141.9, 133.8, 133.6, 129.7, 120.3, 119.2, 114.2, 114.0, 113.1, 111.8, 111.4, 80.0, 76.2, 67.0, 65.9, 60.5, 57.8, 56.0, 55.9, 55.9, 55.1, 54.2, 54.0, 49.2, 42.3, 41.2, 38.4, 38.2, 34.1, 31.5, 31.2, 28.5, 28.4, 26.9, 25.7, 25.1, 25.0, 24.7, 21.1, 21.0, 20.8, 14.3.

UHPLC-MS: *t*_R = 2.072 min (99%), *m/z*: calculated = 613.35 [M+H]⁺, found = 613.4 [M+H]⁺.

(S)-(R)-3-(3,4-Dimethoxyphenyl)-1-(3-(2-morpholinoethoxy)phenyl)propyl piperidine-2-carboxylate



Chemical Formula: C₂₉H₄₀N₂O₆

Exact Mass: 512.29

Molecular Weight: 512.64

24

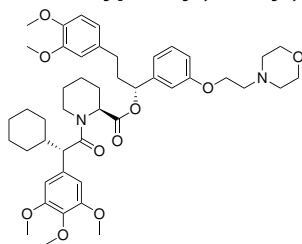
42.2 g (68.9 mmol, 1.0 eq) **23** are dissolved in 40 mL of DCM and 20 mL TFA. The mixture is stirred for 2 h at room temperature before the reaction is quenched by addition of NaHCO₃. The mixture is extracted with DCM, dried with MgSO₄, and volatiles are removed under reduced pressure. The crude product (35.3 g quant.) is used without further purification.

¹H-NMR (500 MHz, CDCl₃): δ 7.22 – 7.15 (m, 1H), 6.86 (d, J = 7.6 Hz, 1H), 6.82 (d, J = 2.5 Hz, 1H), 6.77 (dd, J = 8.2, 2.5 Hz, 1H), 6.73 (d, J = 8.1 Hz, 1H), 6.65 – 6.56 (m, 2H), 5.70 (dd, J = 8.1, 5.5 Hz, 1H), 4.04 (t, J = 5.6 Hz, 2H), 3.80 (s, 3H), 3.79 (s, 3H), 3.68 (t, J = 4.5 Hz, 4H), 3.32 (dd, J = 10.1, 3.3 Hz, 1H), 3.02 (dt, J = 12.2, 3.8 Hz, 1H), 2.74 (t, J = 5.8 Hz, 2H), 2.65 – 2.54 (m, 1H), 2.54 – 2.44 (m, 6H), 2.18 (ddt, J = 14.7, 9.0, 4.2 Hz, 1H), 2.05 – 1.94 (m, 2H), 1.75 (dt, J = 8.5, 4.8 Hz, 1H), 1.59 – 1.48 (m, 2H), 1.47 – 1.36 (m, 2H), 1.16 – 0.96 (m, 1H).

¹³C-NMR (126 MHz, CDCl₃): δ 172.8, 158.8, 148.8, 147.3, 141.8, 133.6, 129.5, 120.1, 120.1, 119.0, 119.0, 113.8, 113.0, 111.7, 111.7, 111.3, 75.5, 67.0, 66.9, 65.7, 58.7, 57.6, 55.9, 55.8, 55.8, 54.1, 52.9, 45.9, 45.6, 38.0, 33.9, 31.3, 31.3, 29.3, 25.8, 25.7, 25.0, 24.1, 9.3, 8.1.

UHPLC-MS: *t*_R = 1.302 min (98%), *m/z*: calculated = 513.30 [M+H]⁺, found = 513.2 [M+H]⁺.

**(S)-(R)-3-(3,4-Dimethoxyphenyl)-1-(3-(2-morpholinoethoxy)phenyl)propyl
1-((S)-2-cyclohexyl-2-(3,4,5-trimethoxyphenyl)acetyl)piperidine-2-carboxylate**



Chemical Formula: C₄₆H₆₂N₂O₁₀
Exact Mass: 802.44
Molecular Weight: 802.99

1

13.4 g (43.3 mmol, 1.0 eq) **12**, 18.1 g (47.6 mmol, 1.1 eq) HATU, and 30.2 mL (173 mmol, 4.0 eq) DiPEA are dissolved in 20 mL of DMF. The mixture is stirred for 30 min at room temperature before 33.3 g (64.9 mmol, 1.5 eq) **24** dissolved in 250 mL DCM are added. The mixture is stirred overnight at room temperature before the reaction is quenched by addition of brine. The mixture is extracted with DCM, dried with MgSO₄, and volatiles are removed under reduced pressure. The crude product is purified by preparative HPLC and flash column chromatography (Cy/EA+3% TEA) to yield 19.5 g (56%) as a white solid.

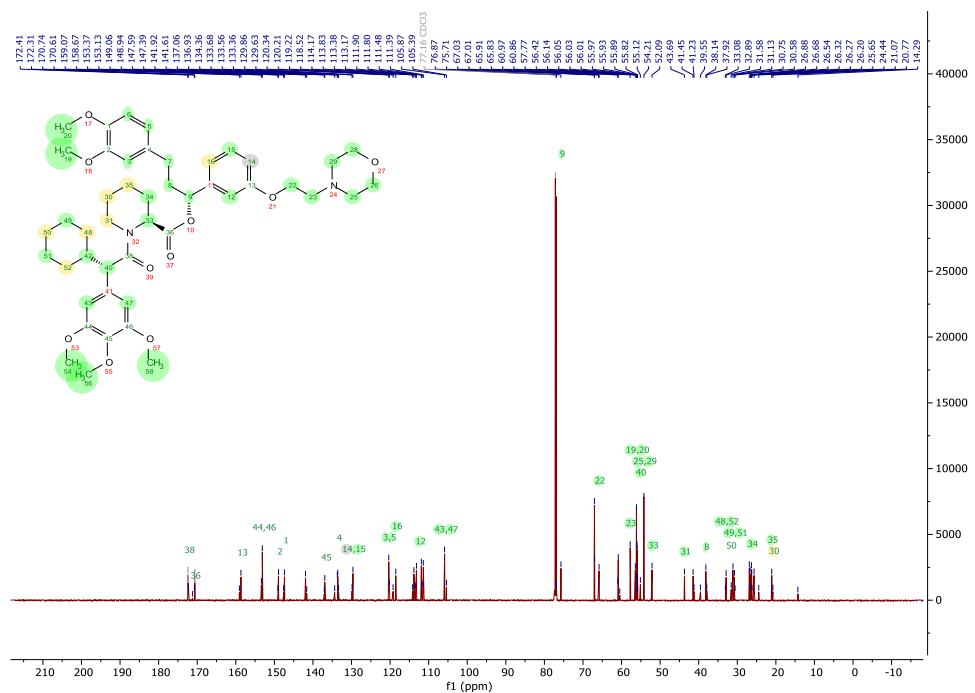
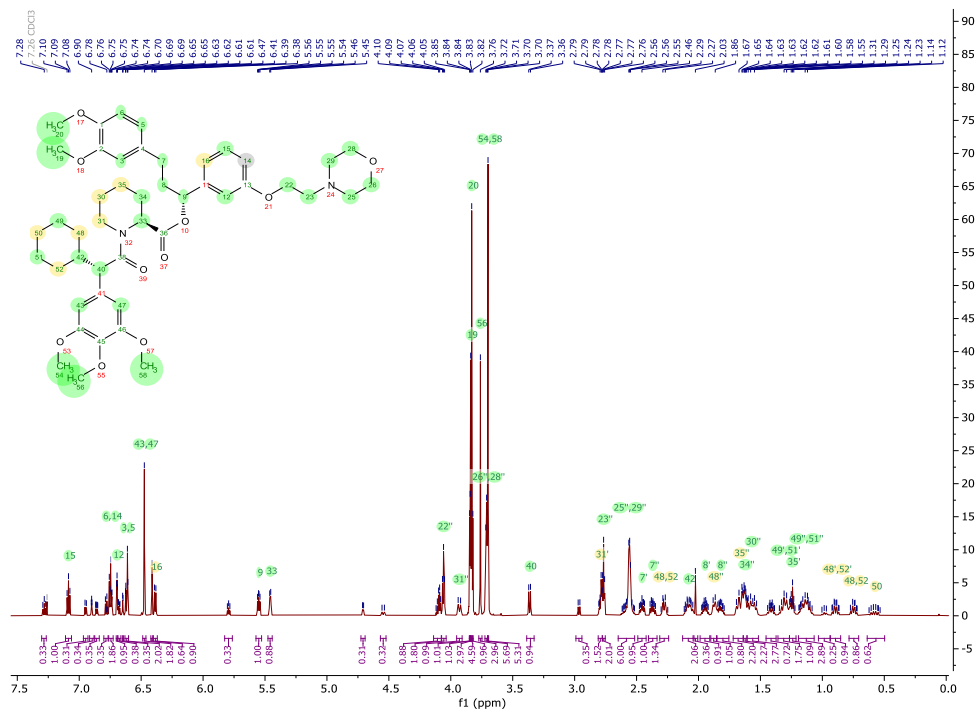
¹H-NMR (700 MHz, CDCl₃): δ 7.28 (t, J = 7.9 Hz, 0H), 7.09 (t, J = 7.9 Hz, 1H), 6.95 (d, J = 7.6 Hz, 0H), 6.90 (t, J = 2.1 Hz, 0H), 6.88 – 6.84 (m, 0H), 6.78 (d, J = 8.2 Hz, 0H), 6.76 – 6.73 (m, 2H), 6.69 (t, J = 2.0 Hz, 1H), 6.68 (dd, J = 8.2, 2.0 Hz, 0H), 6.65 (d, J = 2.0 Hz, 0H), 6.63 – 6.60 (m, 2H), 6.47 (s, 2H), 6.41 (s, 1H), 6.39 (d, J = 7.6 Hz, 1H), 5.79 (t, J = 7.0 Hz, 0H), 5.55 (dd, J = 8.2, 5.5 Hz, 1H), 5.46 (d, J = 5.6 Hz, 1H), 4.71 (d, J = 5.8 Hz, 0H), 4.55 (d, J = 13.6 Hz, 0H), 4.14 – 4.08 (m, 1H), 4.06 (t, J = 5.7 Hz, 2H), 3.93 (d, J = 13.6 Hz, 1H), 3.85 (s, 1H), 3.84 (s, 1H), 3.84 (s, 3H), 3.83 (s, 5H), 3.82 (s, 1H), 3.76 (s, 3H), 3.71 (t, J = 4.7 Hz, 6H), 3.70 (s, 5H), 3.36 (d, J = 9.8 Hz, 1H), 2.96 (d, J = 9.7 Hz, 0H), 2.81 – 2.78 (m, 1H), 2.77 (t, J = 5.7 Hz, 2H), 2.65 – 2.52 (m, 6H), 2.46 (ddd, J = 14.4, 9.4, 5.3 Hz, 1H), 2.37 (ddd, J = 13.9, 9.1, 7.0 Hz, 1H), 2.28 (d, J = 13.7 Hz, 1H), 2.13 – 2.04 (m, 2H), 2.03 (s, 0H), 1.95 (dtd, J = 14.0, 8.7, 5.3 Hz, 1H), 1.87 (d, J = 11.9 Hz, 1H), 1.85 – 1.75 (m, 1H), 1.72 – 1.64 (m, 2H), 1.64 – 1.61 (m, 2H), 1.61 – 1.52 (m, 2H), 1.45 – 1.37 (m, 1H), 1.36 – 1.27 (m, 2H), 1.27 – 1.21 (m, 1H), 1.19 – 1.07 (m, 3H), 0.99 (t, J = 12.6 Hz, 0H), 0.89 (qd, J = 12.5, 3.5 Hz, 1H), 0.78 – 0.71 (m, 1H), 0.64 – 0.50 (m, 1H).

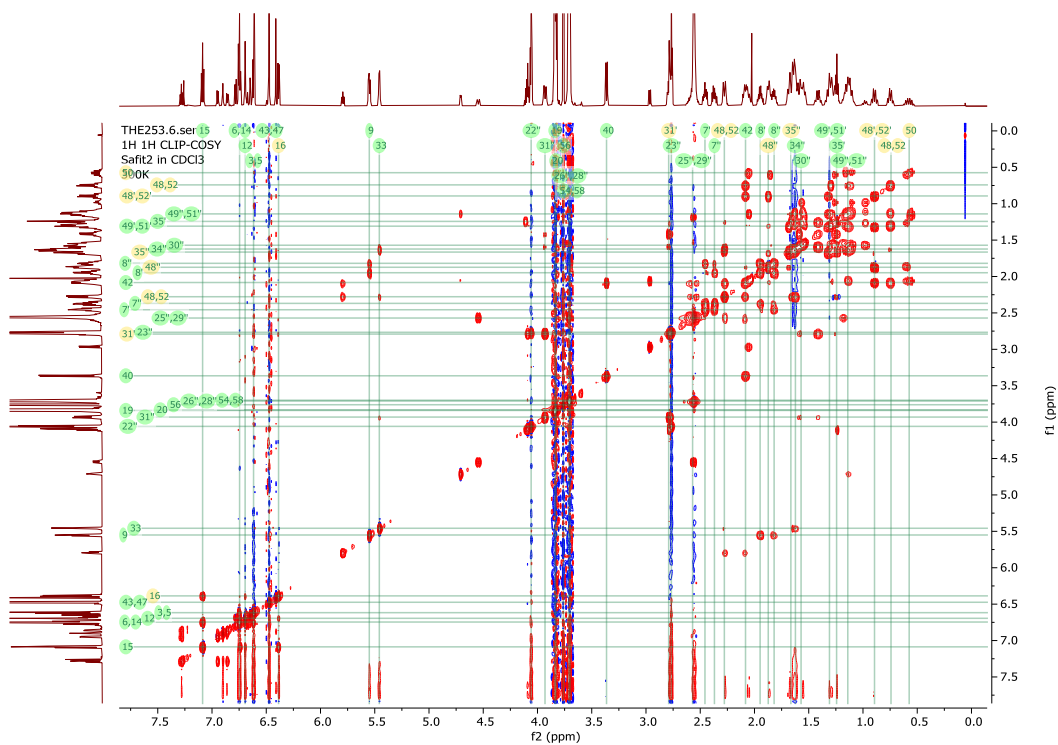
¹³C-NMR (176 MHz, CDCl₃): δ 172.4, 172.3, 171.2, 170.7, 170.6, 159.1, 158.7, 153.4, 153.1, 149.1, 148.9, 147.6, 147.4, 141.9, 141.6, 137.1, 136.9, 134.4, 133.7, 133.6, 133.4, 129.9, 129.6, 120.3, 120.2, 119.2, 118.5, 114.2, 113.8, 113.4, 113.2, 111.9, 111.8, 111.5, 111.4, 105.9, 105.4, 76.9, 75.7, 67.0, 67.0, 65.9, 65.8, 61.0, 60.9, 60.5, 57.8, 56.4, 56.1, 56.0, 56.0, 56.0, 56.0, 55.9, 55.9, 55.8, 55.1, 54.2, 52.1, 43.7, 41.5, 41.2, 39.5, 38.1, 37.9, 33.1, 32.9, 31.6, 31.1, 30.8, 30.6, 26.9, 26.7, 26.5, 26.3, 26.3, 26.2, 25.6, 24.4, 21.1, 21.1, 20.8, 14.3.

UHPLC-MS: *t*_R = 1.614 min (> 99%), m/z: calculated = 803.45 [M+H]⁺, found = 803.4 [M+H]⁺.

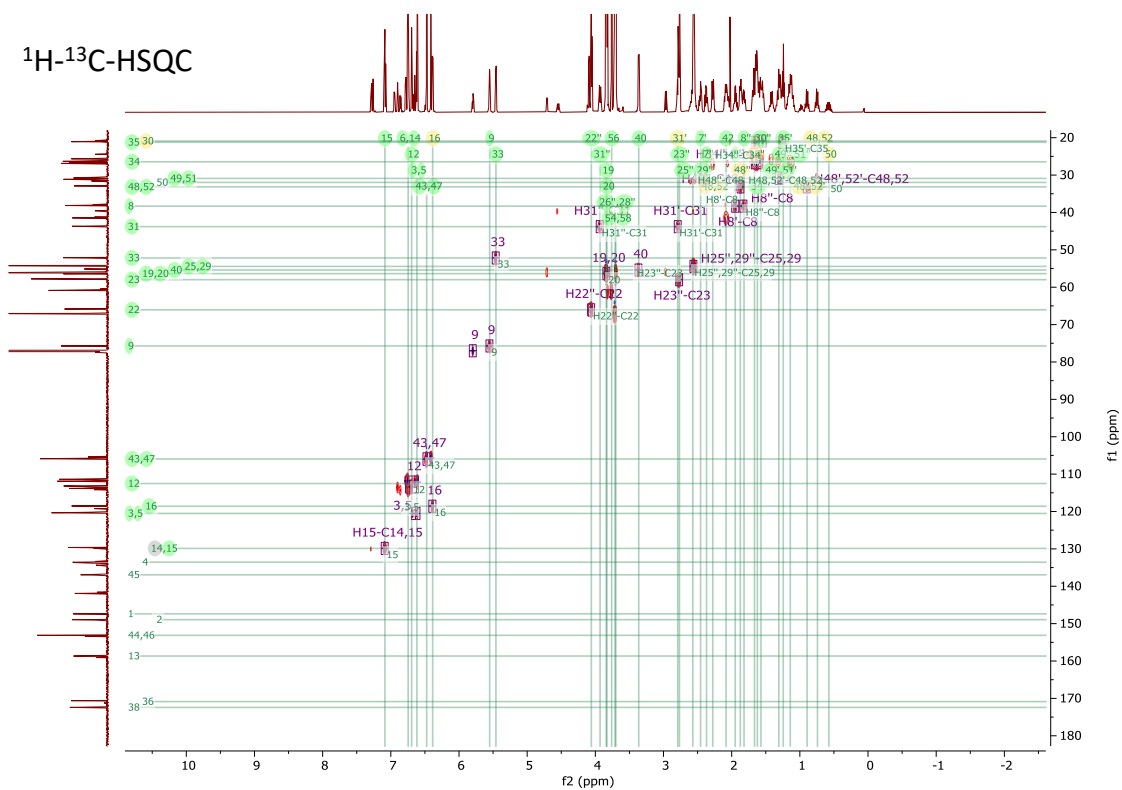
HRMS: $m/z = 803.4465 [M+H]^+$ (1.55 ppm error)

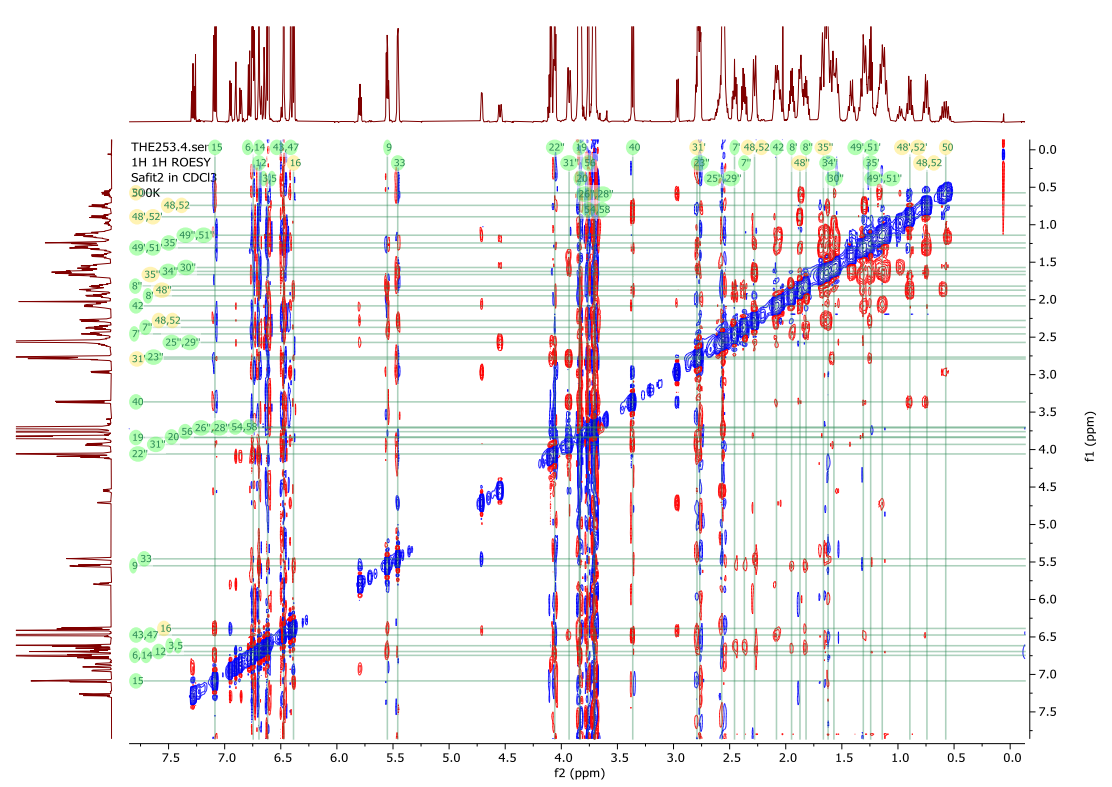
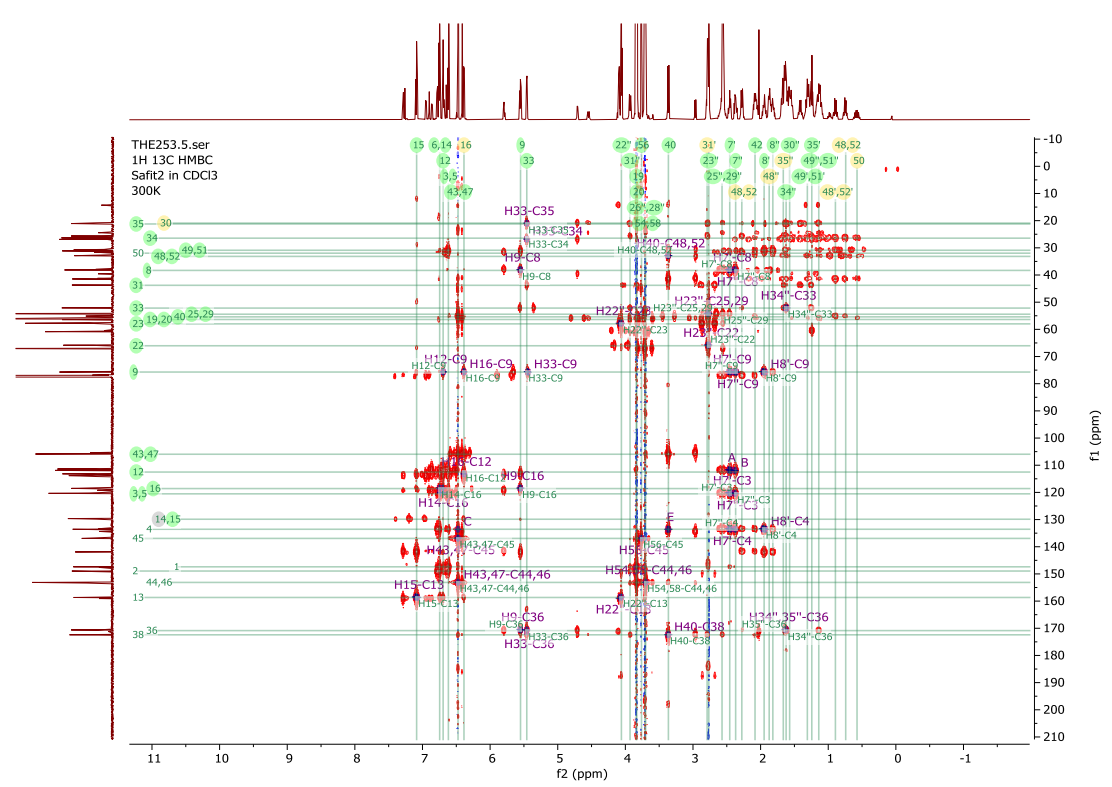
NMR spectra with suggested, incomplete assignments:





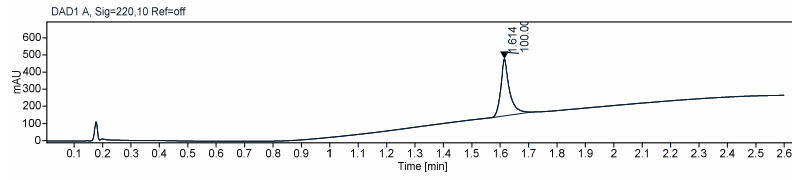
$^1\text{H}-^{13}\text{C}$ -HSQC



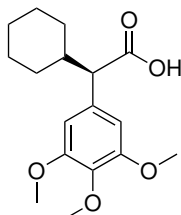




UHPLC, UV 220 nm



(R)-2-Cyclohexyl-2-(3,4,5-trimethoxyphenyl)acetic acid



Chemical Formula: C₁₇H₂₄O₅

Exact Mass: 308.16

Molecular Weight: 308.37

11b

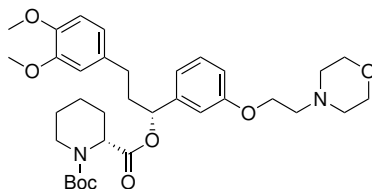
4.34 g (9.57 mmol, 1.0 eq) **11b** are dissolved in 80 mL THF. The mixture is cooled to 0 °C and 0.69 g (28.7 mmol, 3.0 eq) LiOH and 4.89 mL (47.9 mmol, 5.0 eq) H₂O₂ dissolved in 50 mL are added. The mixture is stirred overnight at room temperature before the reaction is quenched by addition of diluted HCl. The mixture is extracted with EA, dried with MgSO₄, and volatiles are removed under reduced pressure. The crude product is purified by flash column chromatography (DCM/MeOH+1 % FA) to yield 2.03 g (69 %) as a white solid.

¹H-NMR (500 MHz, CDCl₃): δ 6.54 (s, 2H), 3.84 (s, 6H), 3.82 (s, 3H), 3.12 (d, J = 10.7 Hz, 1H), 2.02 – 1.85 (m, 2H), 1.79 – 1.71 (m, 1H), 1.68 – 1.58 (m, 2H), 1.41 – 1.23 (m, 2H), 1.22 – 1.01 (m, 3H), 0.81 – 0.69 (m, 1H).

¹³C-NMR (126 MHz, CDCl₃): δ 179.9, 153.3, 137.5, 133.0, 129.3, 126.1, 105.8, 61.0, 59.1, 56.3, 41.0, 32.1, 30.4, 26.4, 26.1.

UHPLC-MS: *t*_R = 0.492 min (97%), *m/z*: calculated = 309.18 [M+H]⁺, found = 309.2 [M+H]⁺.

**(R)-1-tert-Butyl
2-((R)-3-(3,4-dimethoxyphenyl)-1-(3-(2-morpholinoethoxy)phenyl)propyl)
piperidine-1,2-dicarboxylate**



Chemical Formula: C₃₄H₄₈N₂O₈

Exact Mass: 612.34

Molecular Weight: 612.75

25

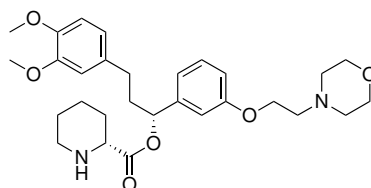
4.00 g (10.0 mmol, 1.0 eq) **20**, 2.40 g (10.5 mmol, 1.05 eq) *R*-N-Boc-pipecolate, and 0.24 g (2.0 mmol, 0.2 eq) DMAP are dissolved in 50 mL DCM. The mixture is cooled to 0 °C and 2.01 g (10.5 mmol, 1.05 eq) DCC are added. The mixture is stirred overnight at room temperature before the reaction is quenched by addition of brine. The mixture is extracted with DCM, dried with MgSO₄, and volatiles are removed under reduced pressure. The crude product is purified by manual column chromatography (EA/TEA/MeOH 100:3:1) to yield 4.78 g (78 %) as a white solid.

¹H-NMR (500 MHz, CDCl₃): δ 7.23 (td, J = 7.9, 5.2 Hz, 1H), 6.90 (q, J = 6.9 Hz, 1H), 6.85 (d, J = 1.8 Hz, 1H), 6.84 – 6.79 (m, 2H), 6.77 (d, J = 8.1 Hz, 1H), 6.68 (dd, J = 8.0, 2.0 Hz, 1H), 6.66 (d, J = 2.0 Hz, 1H), 5.74 (dt, J = 32.3, 6.9 Hz, 1H), 4.98 – 4.88 (m, 1H), 4.77 (s, 0H), 4.09 (t, J = 5.8 Hz, 2H), 3.88 – 3.82 (m, 6H), 3.75 – 3.69 (m, 4H), 2.93 (dt, J = 34.6, 13.1 Hz, 1H), 2.78 (t, J = 5.7 Hz, 2H), 2.66 – 2.47 (m, 6H), 2.22 (qd, J = 15.3, 10.0 Hz, 3H), 2.04 (ddd, J = 16.2, 12.9, 6.4 Hz, 1H), 1.72 – 1.52 (m, 3H), 1.43 (d, J = 32.0 Hz, 11H), 1.22 – 1.02 (m, 1H).

¹³C-NMR (126 MHz, CDCl₃): δ 171.5, 171.3, 159.0, 156.1, 155.4, 149.0, 147.5, 142.3, 141.9, 133.8, 133.7, 129.6, 120.3, 118.8, 114.1, 113.9, 113.2, 112.6, 111.9, 111.5, 80.1, 80.0, 76.2, 76.1, 67.0, 65.9, 57.8, 56.0, 56.0, 55.0, 54.2, 53.9, 42.3, 41.2, 38.5, 38.4, 31.6, 31.4, 28.5, 26.9, 26.8, 24.9, 24.7, 20.8, 20.7.

UHPLC-MS: *t*_R = 1.786 min (97%), *m/z*: calculated = 613.35 [M+H]⁺, found = 613.2 [M+H]⁺.

(R)-(R)-3-(3,4-Dimethoxyphenyl)-1-(3-(2-morpholinoethoxy)phenyl)propyl piperidine-2-carboxylate



Chemical Formula: C₂₉H₄₀N₂O₆

Exact Mass: 512.29

Molecular Weight: 512.64

26

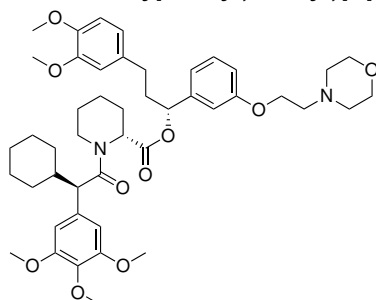
4.78 g (7.8 mmol, 1.0 eq) **25** is dissolved in 24 mL DCM and 12 mL TFA. The mixture is stirred for 1.5 h at room temperature before the mixture was concentrated under reduced pressure and the reaction was neutralized with sodium carbonate. The mixture is extracted with DCM, dried with MgSO₄, and volatiles are removed under reduced pressure. The crude product (4.0 g quant.) is used without further purification.

¹H-NMR (500 MHz, CDCl₃): δ 7.22 (td, J = 7.9, 1.4 Hz, 1H), 6.89 (dt, J = 7.7, 1.3 Hz, 1H), 6.85 (dd, J = 2.6, 1.6 Hz, 1H), 6.80 (ddd, J = 8.2, 2.6, 1.0 Hz, 1H), 6.76 (dd, J = 7.9, 1.4 Hz, 1H), 6.69 – 6.62 (m, 2H), 5.74 (dd, J = 7.9, 5.8 Hz, 1H), 4.08 (td, J = 5.8, 2.3 Hz, 2H), 3.84 (d, J = 1.3 Hz, 3H), 3.83 (d, J = 1.3 Hz, 3H), 3.74 – 3.69 (m, 4H), 3.42 – 3.32 (m, 1H), 3.06 (dt, J = 12.2, 3.7 Hz, 1H), 2.77 (td, J = 5.8, 1.4 Hz, 2H), 2.69 – 2.60 (m, 1H), 2.59 – 2.47 (m, 6H), 2.28 – 2.17 (m, 1H), 2.10 – 1.99 (m, 2H), 1.98 – 1.91 (m, 1H), 1.74 (dq, J = 7.7, 3.4 Hz, 1H), 1.60 – 1.53 (m, 1H), 1.51 – 1.33 (m, 3H).

¹³C-NMR (126 MHz, CDCl₃): δ 172.8, 158.9, 148.9, 147.4, 142.0, 133.7, 129.6, 120.2, 119.0, 113.9, 113.2, 113.1, 111.8, 111.4, 75.7, 67.0, 65.9, 58.7, 57.7, 56.0, 55.9, 54.2, 45.8, 37.9, 31.4, 29.3, 26.0, 24.1.

UHPLC-MS: *t*_R = 1.256 min (97%), *m/z*: calculated = 513.30 [M+H]⁺, found = 513.2 [M+H]⁺.

**(R)-(R)-3-(3,4-Dimethoxyphenyl)-1-(3-(2-morpholinoethoxy)phenyl)propyl
1-((R)-2-cyclohexyl-2-(3,4,5-trimethoxyphenyl)acetyl)piperidine-2-carboxylate**



Chemical Formula: C₄₆H₆₂N₂O₁₀

Exact Mass: 802.44

Molecular Weight: 802.99

5

2.03 g (6.6 mmol, 1.0 eq) **12b**, and 2.63 g (6.9 mmol, 1.05 eq) HATU, and 4.6 mL (26.3 mmol, 4.0 eq) DiPEA are dissolved in 10 mL of DMF. The mixture is stirred for 30 min at room temperature before 4.0 g (7.8 mmol, 1.2 eq) **26** dissolved in 50 mL DCM are added. The mixture is stirred overnight at room temperature before the reaction is quenched by addition of brine. The mixture is extracted with EA, dried with MgSO₄, and volatiles are removed under reduced pressure. The crude product is purified by preparative HPLC and flash column chromatography (Cy/EA+3% TEA) to yield 4.12 g (78%) as a white solid.

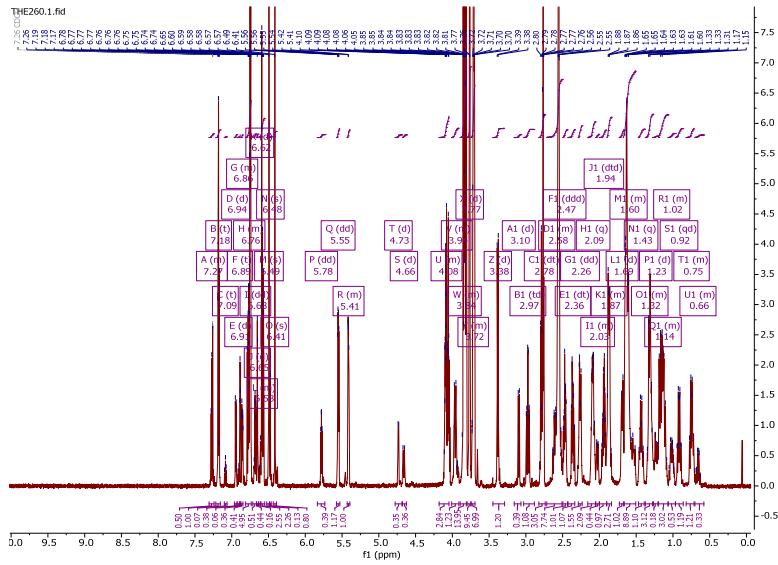
¹H-NMR (700 MHz, CDCl₃): δ 7.29 – 7.25 (m, 0H), 7.18 (t, J = 8.0 Hz, 1H), 6.94 (d, J = 7.6 Hz, 0H), 6.93 – 6.83 (m, 1H), 6.80 – 6.73 (m, 3H), 6.71 – 6.64 (m, 1H), 6.62 – 6.56 (m, 2H), 6.49 (s, 1H), 6.41 (s, 1H), 5.78 (dd, J = 7.9, 6.2 Hz, 0H), 5.55 (dd, J = 8.4, 5.2 Hz, 1H), 5.43 – 5.40 (m, 1H), 4.73 (d, J = 5.6 Hz, 0H), 4.66 (d, J = 13.6 Hz, 0H), 4.12 – 4.02 (m, 2H), 3.96 (d, J = 13.8 Hz, 1H), 3.87 – 3.80 (m, 9H), 3.77 (s, 6H), 3.74 – 3.69 (m, 4H), 3.38 (d, J = 9.8 Hz, 1H), 3.10 (d, J = 9.6 Hz, 0H), 2.97 (td, J = 13.4, 2.9 Hz, 1H), 2.78 (dt, J = 17.0, 5.7 Hz, 2H), 2.65 – 2.51 (m, 5H), 2.47 (ddd, J = 14.3, 9.0, 5.5 Hz, 1H), 2.36 (dt, J = 14.6, 7.8 Hz, 1H), 2.26 (dd, J = 12.0, 4.1 Hz, 1H), 2.15 – 2.02 (m, 2H), 1.98 – 1.85 (m, 3H), 1.74 – 1.50 (m, 5H), 1.43 (q, J = 12.9 Hz, 1H), 1.37 – 1.08 (m, 4H), 1.06 – 0.97 (m, 0H), 0.92 (qd, J = 12.4, 3.5 Hz, 1H), 0.82 – 0.55 (m, 1H).

¹³C-NMR (176 MHz, CDCl₃): δ 172.8, 171.9, 170.6, 170.5, 159.0, 153.4, 153.1, 149.1, 149.0, 147.6, 147.4, 142.3, 141.3, 137.1, 136.9, 134.3, 133.6, 133.6, 133.4, 129.8, 129.7, 120.3, 120.3, 120.2, 119.3, 118.5, 114.1, 113.8, 113.6, 112.7, 111.9, 111.8, 111.5, 111.4, 105.9, 105.4, 77.0, 75.7, 67.0, 67.0, 66.0, 65.9, 61.0, 60.8, 57.8, 57.8, 56.3, 56.2, 56.1, 56.1, 55.9, 55.8, 55.1, 54.2, 54.2, 52.3, 43.7, 41.6, 41.2, 39.7, 38.2, 37.9, 33.2, 32.9, 31.6, 31.3, 30.8, 30.8, 26.9, 26.8, 26.7, 26.7, 26.4, 26.3, 26.3, 26.3, 25.6, 24.6, 21.0, 20.8.

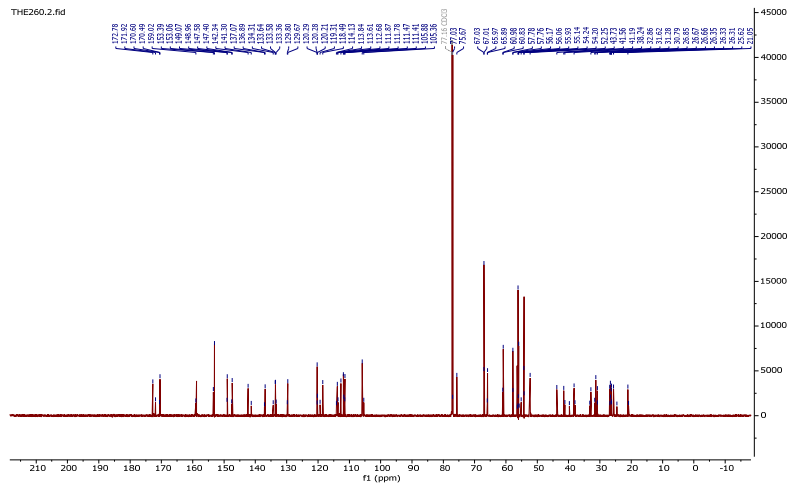
UHPLC-MS: *t*_R = 1.881 min (> 99%), m/z: calculated = 803.45 [M+H]⁺, found = 803.4 [M+H]⁺.

HRMS: m/z = 803.4461 [M+H]⁺ (1.96 ppm error)

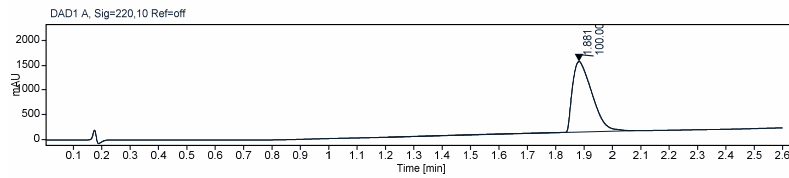
¹H-NMR



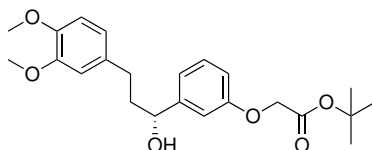
¹³C-NMR



UHPLC, UV 220 nm



(R)-tert-Butyl 2-(3-(3-(3,4-dimethoxyphenyl)-1-hydroxypropyl)phenoxy)acetate



Chemical Formula: C₂₃H₃₀O₆

Exact Mass: 402.20

Molecular Weight: 402.48

27

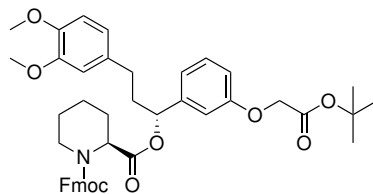
7.09 g (24.6 mmol, 1.0 eq) **19**, 4.0 mL (27.1 mmol, 1.1 eq) *tert*-butyl bromoacetate, and 13.6 g (98.4 mmol, 4.0 eq) potassium carbonate are suspended in 70 mL MeCN. The mixture is stirred overnight at room temperature before the reaction is stopped by filtering off solid and removing volatiles under reduced pressure. The crude product is purified by flash column chromatography (Cy/EA) to yield 9.12 g (92%) as a colourless oil.

¹H-NMR (500 MHz, CDCl₃): δ 7.28 – 7.20 (m, 1H), 6.98 – 6.88 (m, 2H), 6.82 – 6.75 (m, 2H), 6.74 – 6.67 (m, 2H), 4.64 (dd, J = 7.7, 5.3 Hz, 1H), 4.49 (s, 2H), 3.84 (s, 3H), 3.83 (s, 3H), 2.64 (qdd, J = 13.9, 9.3, 6.4 Hz, 2H), 2.26 – 1.83 (m, 2H), 1.47 (s, 9H).

¹³C-NMR (126 MHz, CDCl₃): δ 168.1, 158.2, 148.9, 147.3, 146.6, 134.5, 129.6, 120.3, 119.2, 113.7, 112.3, 111.9, 111.4, 82.4, 73.7, 65.7, 56.0, 55.9, 40.7, 31.7, 28.1, 27.9.

LC-MS: *t*_R = 12.77 min (99%), *m/z*: calculated = 452.20 [M+Na]⁺, found = 452.20 [M+Na]⁺.

**(S)-1-((9H-Fluoren-9-yl)methyl)
2-((R)-1-(3-(2-(tert-butoxy)-2-oxoethoxy)phenyl)-3-(3,4-dimethoxyphenyl)propyl)
piperidine-1,2-dicarboxylate**



Chemical Formula: C₄₄H₄₉NO₉

Exact Mass: 735.34

Molecular Weight: 735.86

28

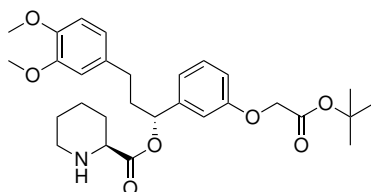
9.12 g (25.7 mmol, 1.0 eq) **27**, 8.76 g (24.9 mmol, 1.1 eq) Fmoc-(S)-pipercolate, and 0.30 g (2.49 mmol, 0.11 eq) DMAP are dissolved in 70 mL DCM. The mixture is cooled to 0 °C and 5.71 g (24.9 mmol, 1.1 eq) DCC are added. The mixture is stirred overnight at room temperature before the reaction is stopped by filtering off solids and removing volatiles under reduced pressure. The crude product is purified by flash column chromatography (Cy/EA) to yield 14.8 g (89 %) as a white solid.

¹H-NMR (500 MHz, CDCl₃): δ 7.80 – 7.68 (m, 2H), 7.59 (t, J = 9.0 Hz, 1H), 7.46 (dd, J = 21.3, 7.5 Hz, 1H), 7.42 – 7.27 (m, 3H), 7.20 (dq, J = 16.1, 8.1 Hz, 2H), 6.99 – 6.86 (m, 2H), 6.77 (dd, J = 35.4, 8.4 Hz, 2H), 6.67 – 6.53 (m, 2H), 5.76 (q, J = 7.6 Hz, 1H), 5.02 (d, J = 5.6 Hz, 1H), 4.88 (d, J = 5.6 Hz, 0H), 4.58 – 4.24 (m, 4H), 4.11 (qt, J = 11.3, 5.7 Hz, 2H), 3.85 – 3.77 (m, 6H), 3.18 – 3.10 (m, 1H), 2.99 (t, J = 13.1 Hz, 0H), 2.49 (dddd, J = 37.0, 22.9, 11.5, 6.4 Hz, 2H), 2.36 – 2.28 (m, 1H), 2.25 – 2.14 (m, 1H), 2.08 – 1.96 (m, 2H), 1.81 – 1.63 (m, 3H), 1.46 (s, 9H), 1.26 (td, J = 7.2, 1.4 Hz, 2H).

¹³C-NMR (126 MHz, CDCl₃): δ 171.2, 171.0, 168.0, 167.9, 158.2, 156.5, 156.0, 148.9, 147.4, 144.2, 144.1, 144.0, 143.9, 141.8, 141.6, 141.4, 133.6, 133.5, 129.8, 127.8, 127.7, 127.2, 127.1, 125.2, 125.0, 120.2, 120.2, 120.1, 119.9, 119.8, 114.0, 113.5, 113.3, 111.8, 111.7, 111.4, 82.4, 76.5, 76.3, 67.9, 65.8, 65.7, 60.5, 56.0, 55.9, 55.0, 54.6, 47.3, 42.1, 42.0, 38.1, 31.2, 28.1, 27.1, 26.9, 24.9, 24.6, 21.1, 20.9, 20.8, 14.3.

LC-MS: *t*_R = 13.83 min (99 %), *m/z*: calculated = 758.34 [M+Na]⁺, found = 758.26 [M+Na]⁺.

(S)-(R)-1-(3-(2-(tert-Butoxy)-2-oxoethoxy)phenyl)-3-(3,4-dimethoxyphenyl)propyl piperidine-2-carboxylate



Chemical Formula: C₂₉H₃₉NO₇
Exact Mass: 513.27
Molecular Weight: 513.62

29

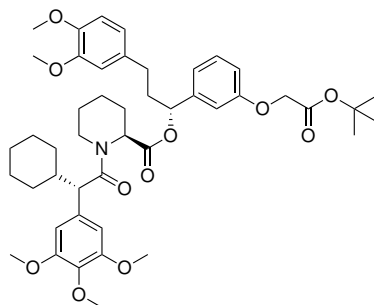
3.08 g (2.27 mmol, 1.0 eq) **28** and 1.50 mL (12.7 mmol, 4.11 eq) 4-methylpiperidine are dissolved in 15 mL DCM. The mixture is stirred 1 h at room temperature before the reaction is quenched by addition of ammonium chloride solution. The mixture is diluted with DCM, washed 4 times with ammonium chloride solution, dried over MgSO₄, and volatiles are removed under reduced pressure. The crude product is purified by flash column chromatography (DCM/MeOH/TEA 100:1:3) to yield 1.39 g (88 %) as a colourless oil.

¹H-NMR (300 MHz, CDCl₃): δ 7.29 – 7.18 (m, 1H), 6.98 – 6.85 (m, 2H), 6.83 – 6.72 (m, 2H), 6.65 (d, J = 7.3 Hz, 2H), 5.76 (dd, J = 7.9, 5.6 Hz, 1H), 5.28 (s, 1H), 4.49 (s, 2H), 3.85 (s, 3H), 3.84 (s, 3H), 3.36 (dd, J = 9.7, 3.3 Hz, 1H), 3.06 (dt, J = 11.9, 3.7 Hz, 1H), 2.71 – 2.43 (m, 3H), 2.33 – 1.95 (m, 4H), 1.78 (tq, J = 5.7, 3.6 Hz, 1H), 1.70 – 1.51 (m, 2H), 1.47 (s, 9H).

¹³C-NMR (78 MHz, CDCl₃): δ 172.8, 168.0, 158.2, 149.0, 147.5, 142.0, 133.7, 129.7, 120.2, 119.9, 113.9, 113.3, 111.8, 111.4, 82.5, 75.5, 65.8, 58.8, 56.0, 56.0, 53.5, 45.7, 38.0, 31.4, 29.3, 28.1, 25.8, 24.2.

LC-MS: *t*_R = 8.40 min (97%), *m/z*: calculated = 514.28 [M+H]⁺, found = 514.33 [M+H]⁺.

**(S)-(R)-1-(3-(2-(tert-Butoxy)-2-oxoethoxy)phenyl)-3-(3,4-dimethoxyphenyl)propyl
1-((S)-2-cyclohexyl-2-(3,4,5-trimethoxyphenyl)acetyl)piperidine-2-carboxylate**



Chemical Formula: C₄₆H₆₁NO₁₁

Exact Mass: 803.42

Molecular Weight: 803.98

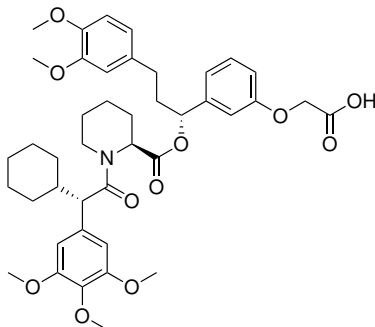
30

1.67 g (5.24 mmol, 1.1 eq) **12**, 3.0 mL (17.24 mmol, 3.5 eq) DiPEA, and 2.06 g (5.42 mmol, 1.1 eq) HATU are dissolved in 20 mL DMF and stirred for 10 min at room temperature. 2.53 g (4.93 mmol, 1.0 eq) **29** are added. The mixture is stirred overnight at room temperature before the reaction is quenched by addition of brine. The mixture is extracted with DCM, dried over MgSO₄, and volatiles are removed under reduced pressure. The crude product is purified by manual column chromatography (Cy/EA 3:1) to yield 3.85 g (97%) as a white solid.

LC-MS: $t_R = 14.39$ min, m/z : calculated = 804.28 [M+H]⁺, found = 804.43 [M+H]⁺.

HPLC: $t_R = 9.56$ min (88%)

2-(3-((R)-1-(((S)-1-((S)-2-Cyclohexyl-2-(3,4,5-trimethoxyphenyl)acetyl)piperidine-2-carbonyloxy)-3-(3,4-dimethoxyphenyl)propyl)phenoxy)acetic acid



Chemical Formula: C₄₂H₅₃NO₁₁

Exact Mass: 747.36

Molecular Weight: 747.87

6

3.85 g (4.79 mmol, 1.0 eq) **30** are dissolved in 12 mL TFA and 40 mL DCM. The mixture is stirred for 1 h before the reaction is quenched by addition of NaHCO₃. The mixture is extracted with DCM, dried over MgSO₄, and volatiles are removed under reduced pressure. The crude product is purified by flash column chromatography (Cy/EA/FA/MeOH 200:100:2:2) to yield 2.85 g (80 %) as a white solid.

¹H-NMR (700 MHz, CDCl₃): δ 7.31 – 7.27 (m, 0H), 7.14 (t, J = 7.9 Hz, 1H), 6.97 (d, J = 7.6 Hz, 0H), 6.90 (h, J = 2.6 Hz, 0H), 6.81 – 6.77 (m, 1H), 6.76 (d, J = 7.9 Hz, 1H), 6.68 (dd, J = 8.2, 2.0 Hz, 0H), 6.67 – 6.63 (m, 4H), 6.61 (d, J = 7.6 Hz, 1H), 6.43 (s, 0H), 6.36 (s, 2H), 5.85 (t, J = 7.0 Hz, 0H), 5.52 (dd, J = 8.6, 5.1 Hz, 1H), 5.47 – 5.41 (m, 1H), 4.76 (d, J = 5.6 Hz, 0H), 4.63 (qd, J = 16.3, 3.9 Hz, 2H), 4.54 (d, J = 13.6 Hz, 0H), 3.88 (d, J = 13.8 Hz, 1H), 3.85 – 3.84 (m, 4H), 3.83 – 3.82 (m, 5H), 3.77 (s, 3H), 3.62 (s, 6H), 3.35 (d, J = 9.5 Hz, 1H), 3.09 (d, J = 9.7 Hz, 0H), 2.83 (td, J = 13.5, 3.0 Hz, 1H), 2.57 (ddd, J = 18.9, 10.1, 5.5 Hz, 1H), 2.46 (ddd, J = 14.0, 9.2, 6.9 Hz, 1H), 2.39 – 2.21 (m, 1H), 2.15 – 1.99 (m, 2H), 1.94 – 1.86 (m, 2H), 1.76 – 1.57 (m, 7H), 1.54 – 1.38 (m, 1H), 1.35 – 1.18 (m, 3H), 1.17 – 0.96 (m, 2H), 0.90 (qd, J = 12.5, 3.5 Hz, 1H), 0.73 (qd, J = 12.1, 3.5 Hz, 1H), 0.63 (qd, J = 12.5, 3.4 Hz, 0H).

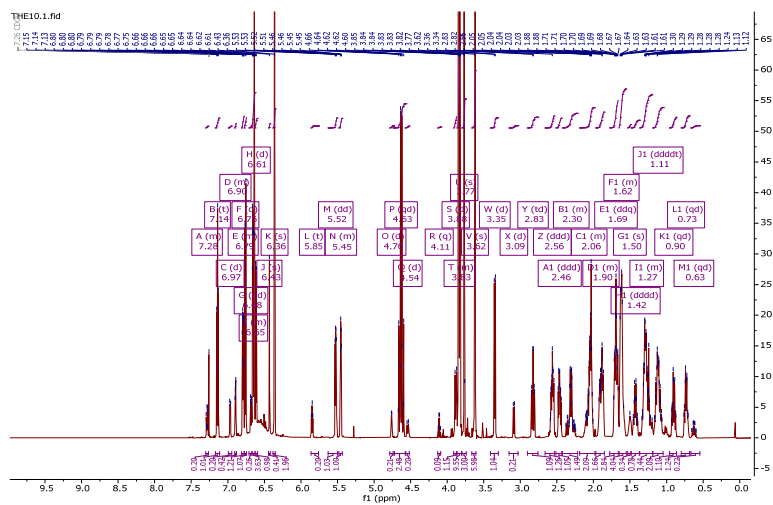
¹³C-NMR (176 MHz, CDCl₃): δ 173.1, 172.9, 171.4, 170.3, 170.2, 158.2, 157.9, 153.4, 153.1, 149.0, 149.0, 147.5, 142.4, 141.4, 137.2, 136.8, 134.1, 133.5, 133.3, 133.0, 130.0, 129.7, 120.6, 120.3, 120.2, 119.7, 115.3, 114.9, 112.5, 111.9, 111.5, 111.5, 110.8, 105.9, 105.4, 76.9, 76.1, 65.5, 65.2, 61.0, 60.9, 56.1, 56.0, 56.0, 56.0, 55.7, 55.4, 52.4, 43.7, 41.2, 41.1, 40.1, 38.2, 37.8, 33.3, 33.0, 31.6, 31.4, 30.7, 30.6, 27.1, 26.7, 26.6, 26.5, 26.3, 26.3, 26.2, 25.5, 24.4, 21.0, 20.6, 14.3.

LC-MS: *t*_R = 14.85 min, *m/z*: calculated = 748.37 [M+H]⁺, found = 748.43 [M+H]⁺.

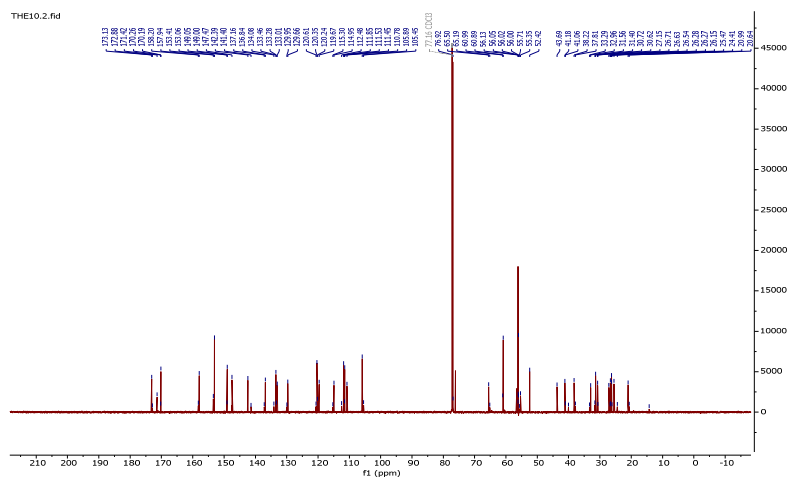
HPLC: *t*_R = 7.49 min (99 %)

HRMS: *m/z* = 748.3691 [M+H]⁺ (0.09 ppm error)

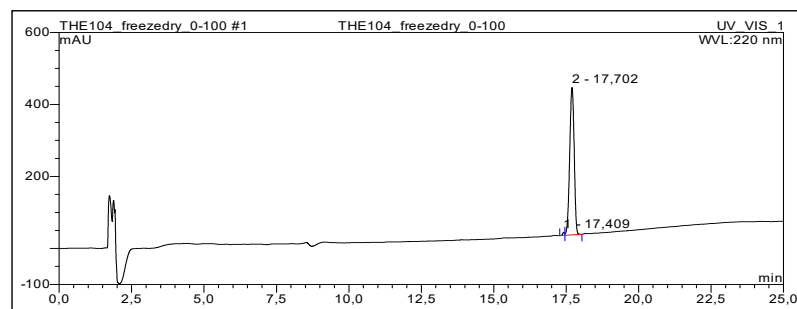
¹H-NMR



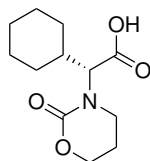
¹³C-NMR



HPLC, UV 220 nm



(R)-2-Cyclohexyl-2-(2-oxo-1,3-oxazinan-3-yl)acetic acid



Chemical Formula: C₁₂H₁₉NO₄

Exact Mass: 241.13

Molecular Weight: 241.28

45a

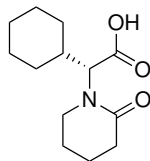
The synthesis is conducted according to general procedure 5.16.2 with 0.66 mmol starting material. The crude product is purified by manual column chromatography (DCM/Me-OH/FA 100:2:1) to yield 88 mg (55 %) as a white solid.

¹H-NMR (300 MHz, CDCl₃): δ 8.66 (s, 1H), 4.33 – 4.23 (m, 3H), 3.50 (dt, J = 12.2, 6.3 Hz, 1H), 3.35 (dt, J = 11.6, 5.9 Hz, 1H), 2.07 (p, J = 5.7 Hz, 3H), 1.75 (dt, J = 23.5, 13.5 Hz, 5H), 1.37 – 1.17 (m, 3H), 1.07 (qd, J = 13.7, 6.0 Hz, 2H).

¹³C-NMR (75 MHz, CDCl₃): δ 173.4, 155.2, 66.9, 66.5, 44.3, 36.0, 30.2, 29.6, 26.2, 25.7, 25.7, 22.3.

LC-MS: *t*_R = 9.35 min (99 %), *m/z*: calculated = 242.14 [M+H]⁺, found = 242.24 [M+H]⁺.

(R)-2-Cyclohexyl-2-(2-oxopiperidin-1-yl)acetic acid



Chemical Formula: C₁₃H₂₁NO₃

Exact Mass: 239.15

Molecular Weight: 239.31

45b

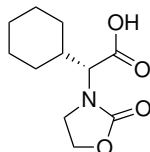
The synthesis is conducted according to general procedure 5.16.2 with 0.66 mmol starting material. The crude product is purified by manual column chromatography (DCM/MeOH/FA 100:1:1) to yield 86 mg (55 %) as a white solid.

¹H-NMR (500 MHz, CDCl₃): δ 3.98 (d, J = 10.9 Hz, 1H), 3.44 – 3.37 (m, 1H), 3.34 (ddd, J = 12.3, 7.5, 5.2 Hz, 1H), 2.57 – 2.41 (m, 2H), 2.28 (qt, J = 11.2, 3.4 Hz, 1H), 1.92 – 1.71 (m, 6H), 1.72 – 1.59 (m, 2H), 1.38 – 1.10 (m, 4H), 1.09 – 0.89 (m, 2H).

¹³C-NMR (126 MHz, CDCl₃): δ 173.6, 171.7, 70.0, 49.9, 35.6, 32.5, 30.2, 29.5, 26.2, 25.7, 25.6, 23.2, 20.4.

LC-MS: *t*_R = 11.63 min (99 %), m/z: calculated = 240.16 [M+H]⁺, found = 240.21 [M+H]⁺.

(R)-2-Cyclohexyl-2-(2-oxooxazolidin-3-yl)acetic acid



Chemical Formula: C₁₁H₁₇NO₄

Exact Mass: 227.12

Molecular Weight: 227.26

45c

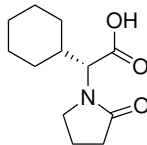
The synthesis is conducted according to general procedure 5.16.2 with 0.49 mmol starting material. The crude product is purified by manual column chromatography (DCM/MeOH/FA 100:2:1) to yield 55 mg (49 %) as a pale yellow solid.

¹H-NMR (500 MHz, CDCl₃): δ 10.58 (s, 1H), 4.42 – 4.30 (m, 2H), 4.27 (d, J = 9.7 Hz, 1H), 3.92 (td, J = 8.9, 7.1 Hz, 1H), 3.58 (td, J = 8.7, 6.8 Hz, 1H), 1.84 (qt, J = 11.0, 3.3 Hz, 1H), 1.78 – 1.72 (m, 3H), 1.69 – 1.62 (m, 2H), 1.32 – 1.02 (m, 5H).

¹³C-NMR (126 MHz, CDCl₃): δ 174.7, 159.1, 62.8, 60.9, 42.1, 37.2, 29.6, 29.5, 26.0, 25.7, 25.6.

LC-MS: *t*_R = 7.78 min (95 %), *m/z*: calculated = 226.15 [M+H]⁺, found = 226.13 [M+H]⁺.

(R)-2-Cyclohexyl-2-(2-oxopyrrolidin-1-yl)acetic acid



Chemical Formula: C₁₂H₁₉NO₃

Exact Mass: 225.14

Molecular Weight: 225.28

45d

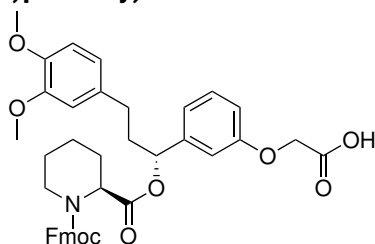
The synthesis is conducted according to general procedure 5.16.2 with 0.30 mmol starting material. The crude product is purified by manual column chromatography (DCM/MeOH/FA 100:1:1) to yield 28 mg (42%) as a pale yellow solid.

¹H-NMR (500 MHz, CDCl₃): δ 9.90 (s, 1H), 4.44 (d, J = 10.2 Hz, 1H), 3.65 (ddd, J = 9.8, 8.1, 6.1 Hz, 1H), 3.41 (ddd, J = 9.9, 8.2, 5.7 Hz, 1H), 2.45 (t, J = 8.1 Hz, 2H), 2.12 – 1.97 (m, 2H), 1.91 (ttt, J = 9.3, 6.5, 3.3 Hz, 1H), 1.81 – 1.70 (m, 3H), 1.68 – 1.61 (m, 1H), 1.60 – 1.48 (m, 1H), 1.33 – 0.93 (m, 5H).

¹³C-NMR (126 MHz, CDCl₃): δ 177.0, 173.4, 60.3, 45.6, 36.8, 31.1, 29.9, 29.5, 26.2, 25.8, 25.7, 18.6.

LC-MS: *t*_R = 11.20 min (87%), *m/z*: calculated = 228.13 [M+H]⁺, found = 228.11 [M+H]⁺.

2-(3-((R)-1-(((S)-1-(((9H-Fluoren-9-yl)methoxy)carbonyl)piperidine-2-carbonyl)oxy)-3-(3,4-dimethoxyphenyl)propyl)phenoxy)acetic acid



Chemical Formula: C₄₀H₄₁NO₉

Exact Mass: 679.28

Molecular Weight: 679.75

40

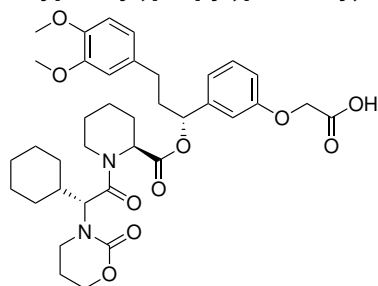
1.00 g (1.36 mmol, 1.0 eq) **12** are dissolved in 5 mL TFA and 10 mL DCM. The mixture is stirred for 1 h at room temperature, before the reaction is quenched by addition of NaHCO₃. The mixture is extracted with EA, dried over MgSO₄, and volatiles are removed under reduced pressure. The crude product is purified by manual column chromatography (Cy/EA/FA 200:300:1) to yield 924 mg (quant.) as a white solid.

¹H-NMR (500 MHz, CDCl₃): δ 7.31 – 7.27 (m, 0H), 7.14 (t, J = 7.9 Hz, 1H), 6.97 (d, J = 7.6 Hz, 0H), 6.90 (h, J = 2.6 Hz, 0H), 6.81 – 6.77 (m, 1H), 6.76 (d, J = 7.9 Hz, 1H), 6.68 (dd, J = 8.2, 2.0 Hz, 0H), 6.67 – 6.63 (m, 4H), 6.61 (d, J = 7.6 Hz, 1H), 6.43 (s, 0H), 6.36 (s, 2H), 5.85 (t, J = 7.0 Hz, 0H), 5.52 (dd, J = 8.6, 5.1 Hz, 1H), 5.47 – 5.41 (m, 1H), 4.76 (d, J = 5.6 Hz, 0H), 4.63 (qd, J = 16.3, 3.9 Hz, 2H), 4.54 (d, J = 13.6 Hz, 0H), 3.88 (d, J = 13.8 Hz, 1H), 3.85 – 3.84 (m, 4H), 3.83 – 3.82 (m, 5H), 3.77 (s, 3H), 3.62 (s, 6H), 3.35 (d, J = 9.5 Hz, 1H), 3.09 (d, J = 9.7 Hz, 0H), 2.83 (td, J = 13.5, 3.0 Hz, 1H), 2.57 (ddd, J = 18.9, 10.1, 5.5 Hz, 1H), 2.46 (ddd, J = 14.0, 9.2, 6.9 Hz, 1H), 2.39 – 2.21 (m, 1H), 2.15 – 1.99 (m, 2H), 1.94 – 1.86 (m, 2H), 1.76 – 1.57 (m, 7H), 1.54 – 1.38 (m, 1H), 1.35 – 1.18 (m, 3H), 1.17 – 0.96 (m, 2H), 0.90 (qd, J = 12.5, 3.5 Hz, 1H), 0.73 (qd, J = 12.1, 3.5 Hz, 1H), 0.63 (qd, J = 12.5, 3.4 Hz, 0H).

¹³C-NMR (126 MHz, CDCl₃): δ 172.2, 170.7, 158.0, 156.9, 149.1, 147.5, 144.0, 143.8, 142.3, 141.4, 133.5, 133.4, 129.9, 127.9, 127.2, 125.1, 120.4, 120.1, 119.8, 115.6, 114.8, 112.9, 111.9, 111.6, 110.7, 76.6, 68.4, 65.4, 56.1, 56.0, 55.0, 54.7, 47.3, 47.2, 42.0, 38.2, 37.9, 31.5, 31.3, 27.1, 26.9, 24.8, 21.2, 20.9, 14.3.

UHPLC-MS: *t*_R = 1.684 min (95 %), *m/z*: calculated = 680.29 [M+H]⁺, found = 680.0 [M+H]⁺.

2-(3-((R)-1-(((S)-1-((R)-2-Cyclohexyl-2-(2-oxo-1,3-oxazinan-3-yl)acetyl)piperidine-2-carbonyloxy)-3-(3,4-dimethoxyphenyl)propyl)phenoxy)acetic acid



Chemical Formula: C₃₇H₄₈N₂O₁₀

Exact Mass: 680.33

Molecular Weight: 680.78

48a

The synthesis is conducted according to general procedure 5.16.2 with 0.15 mmol starting material. The crude product is purified by manual column chromatography (DCM/MeOH/FA 100:1:1) to yield 75 mg (74%) as a pale yellow solid.

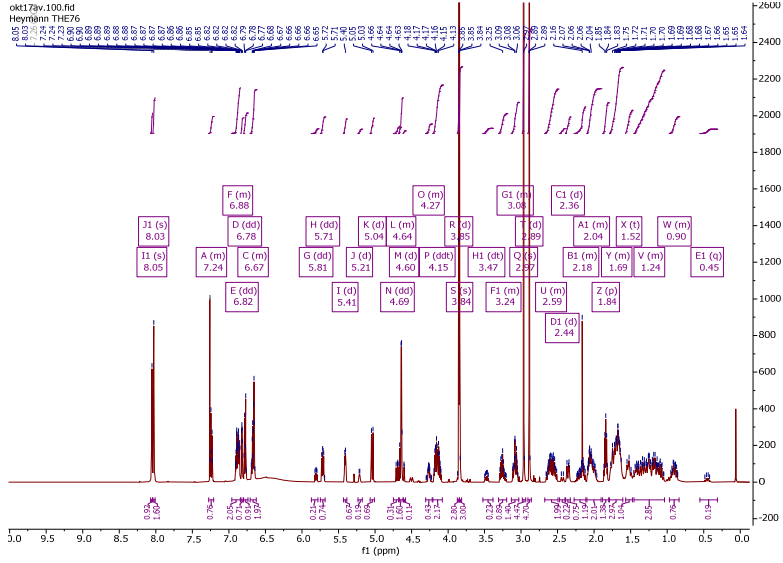
¹H-NMR (500 MHz, CDCl₃): δ 8.04 (d, J = 12.7 Hz, 3H), 7.33 – 7.15 (m, 2H), 6.96 – 6.74 (m, 5H), 6.71 – 6.63 (m, 3H), 5.81 (dd, J = 8.2, 5.4 Hz, 0H), 5.71 (dd, J = 8.2, 5.2 Hz, 1H), 5.41 (d, J = 5.6 Hz, 1H), 5.21 (d, J = 5.3 Hz, 0H), 5.04 (d, J = 10.7 Hz, 1H), 4.77 – 4.56 (m, 3H), 4.31 – 4.22 (m, 1H), 4.15 (ddt, J = 20.2, 10.5, 4.9 Hz, 3H), 3.85 (d, J = 4.3 Hz, 8H), 3.47 (dt, J = 12.0, 5.7 Hz, 0H), 3.31 – 3.20 (m, 1H), 3.13 – 3.03 (m, 2H), 2.97 (s, 6H), 2.89 (d, J = 0.7 Hz, 6H), 2.68 – 2.49 (m, 3H), 2.40 (dd, J = 38.6, 14.0 Hz, 1H), 2.26 – 2.11 (m, 2H), 2.11 – 1.95 (m, 3H), 1.84 (p, J = 5.8 Hz, 2H), 1.81 – 1.60 (m, 4H), 1.60 – 0.78 (m, 7H).

¹³C-NMR (126 MHz, CDCl₃): δ 170.8, 170.3, 170.0, 169.6, 163.2, 163.1, 158.3, 158.1, 154.6, 154.5, 149.1, 147.6, 142.1, 133.5, 129.8, 129.8, 120.3, 120.2, 120.0, 115.9, 115.1, 111.9, 111.6, 111.2, 110.4, 76.5, 76.2, 67.2, 67.1, 65.5, 65.4, 58.9, 56.5, 56.1, 56.0, 56.0, 52.7, 43.9, 40.4, 40.0, 38.5, 38.4, 36.8, 35.8, 35.6, 31.8, 31.6, 31.3, 30.4, 29.9, 28.3, 28.1, 27.0, 26.4, 26.2, 25.8, 25.8, 25.6, 25.1, 22.1, 22.0, 21.3, 21.1.

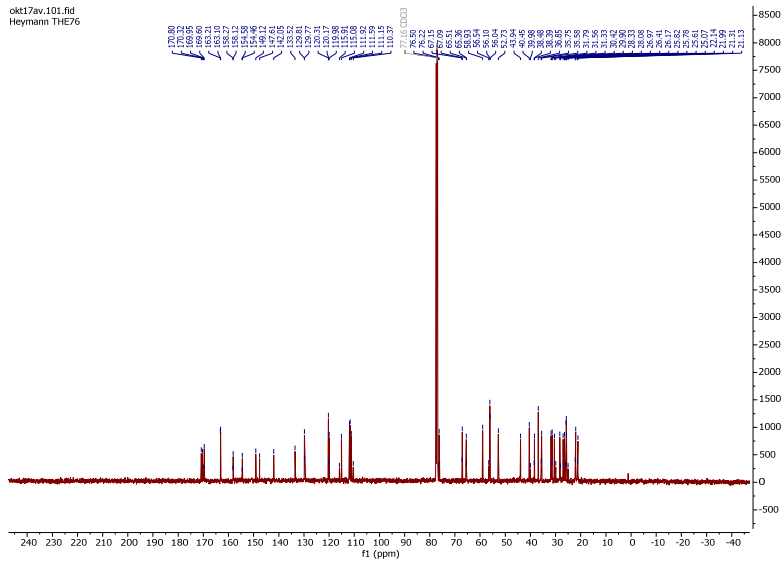
LC-MS: *t*_R = 7.17 min (97%), m/z: calculated = 681.34 [M+H]⁺, found = 681.34 [M+H]⁺.

HRMS: m/z = 681.3379 [M+H]⁺ (0.43 ppm error)

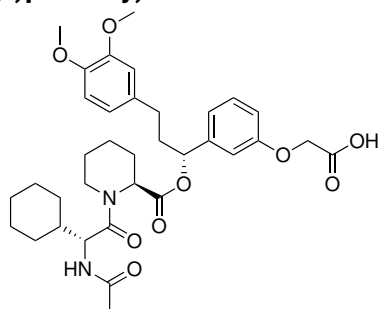
¹H-NMR



¹³C-NMR



2-(3-((R)-1-(((S)-1-((R)-2-Acetamido-2-cyclohexylacetyl)piperidine-2-carbonyloxy)-3-(3,4-dimethoxyphenyl)propyl)phenoxy)acetic acid



Chemical Formula: C₃₅H₄₆N₂O₉

Exact Mass: 638.32

Molecular Weight: 638.75

48b

The synthesis is conducted according to general procedure 5.16.2 with 0.12 mmol starting material using Fmoc-CHg-OH and acetic acid to couple successively. The crude product is purified by manual column chromatography (DCM/MeOH/FA 100:1:1) to yield 22 mg (28 %) as a pale yellow solid.

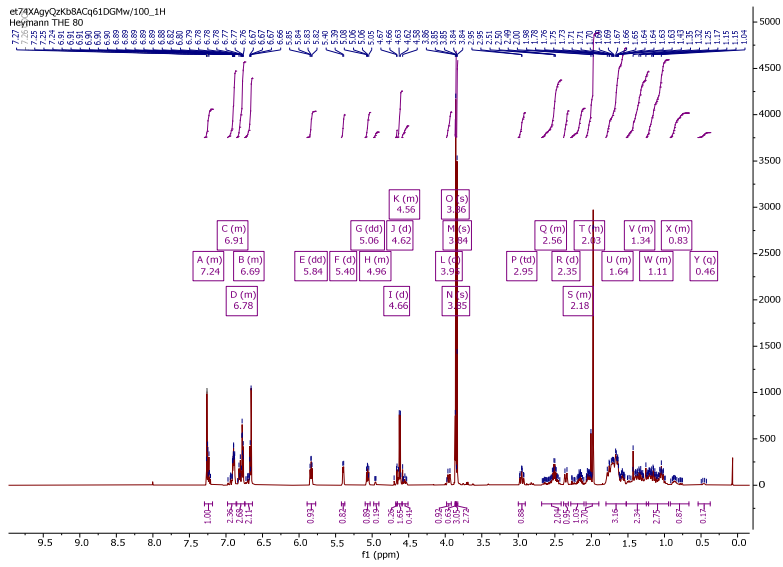
¹H-NMR (500 MHz, CDCl₃): δ 7.29 – 7.18 (m, 1H), 6.98 – 6.86 (m, 2H), 6.85 – 6.74 (m, 3H), 6.74 – 6.64 (m, 2H), 5.84 (dd, J = 7.6, 5.8 Hz, 1H), 5.40 (d, J = 5.4 Hz, 1H), 5.06 (dd, J = 9.2, 6.4 Hz, 1H), 4.98 – 4.91 (m, 0H), 4.66 (d, J = 2.4 Hz, 0H), 4.62 (d, J = 6.8 Hz, 2H), 4.59 – 4.51 (m, 0H), 3.95 (d, J = 14.0 Hz, 1H), 3.86 (s, 1H), 3.85 (s, 3H), 3.84 (s, 3H), 2.95 (td, J = 13.3, 2.7 Hz, 1H), 2.88 – 2.72 (m, 0H), 2.68 – 2.41 (m, 2H), 2.35 (d, J = 13.8 Hz, 1H), 2.28 – 2.10 (m, 1H), 2.07 – 1.90 (m, 4H), 1.80 – 1.52 (m, 8H), 1.52 – 1.20 (m, 4H), 1.25 – 0.94 (m, 5H), 0.92 – 0.66 (m, 1H), 0.46 (q, J = 11.3 Hz, 0H).

¹³C-NMR (126 MHz, CDCl₃): δ 171.7, 171.6, 171.3, 170.9, 170.7, 169.9, 158.5, 158.3, 149.1, 147.6, 141.4, 133.6, 133.4, 129.9, 129.8, 120.7, 120.3, 116.4, 115.9, 112.0, 111.9, 111.6, 111.4, 110.2, 76.5, 76.2, 65.7, 57.2, 56.1, 56.1, 53.3, 52.8, 44.3, 41.6, 40.6, 40.0, 38.5, 37.8, 31.6, 31.0, 30.5, 30.1, 29.5, 28.4, 27.9, 26.7, 26.2, 26.1, 25.9, 25.8, 25.4, 24.8, 23.1, 21.4, 20.9.

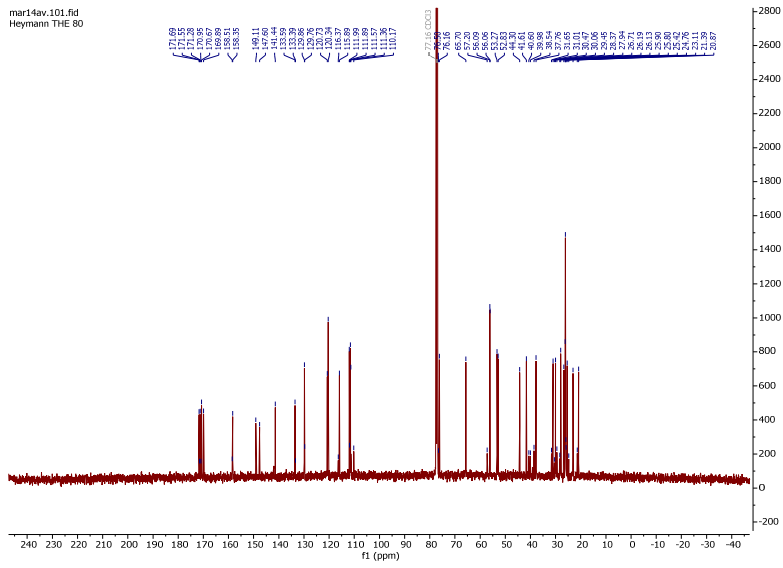
LC-MS: *t*_R = 13.60 min (99 %), *m/z*: calculated = 639.33 [M+H]⁺, found = 639.43 [M+H]⁺.

HRMS: *m/z* = 639.3269 [M+H]⁺ (1.19 ppm error)

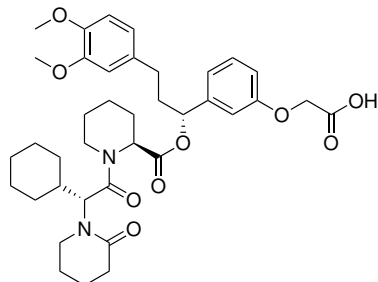
¹H-NMR



¹³C-NMR



2-(3-((R)-1-(((S)-1-((R)-2-Cyclohexyl-2-(2-oxopiperidin-1-yl)acetyl)piperidine-2-carbonyloxy)-3-(3,4-dimethoxyphenyl)propyl)phenoxy)acetic acid



Chemical Formula: C₃₈H₅₀N₂O₉

Exact Mass: 678.35

Molecular Weight: 678.81

48c

The synthesis is conducted according to general procedure 5.16.2 with 0.16 mmol starting material. The crude product is purified by manual column chromatography (DCM/MeOH/FA 100:1:1) to yield 76 mg (70 %) as a pale yellow solid.

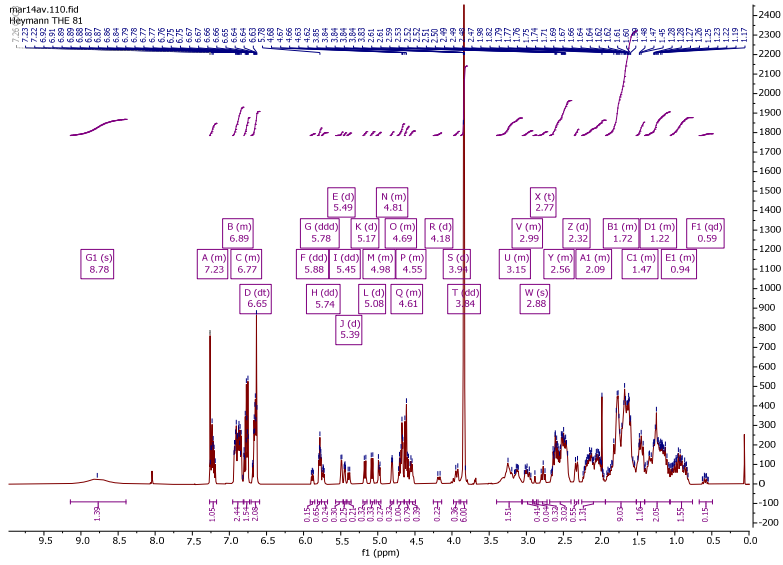
¹H-NMR (500 MHz, CDCl₃): δ 8.78 (s, 1H), 7.27 – 7.17 (m, 1H), 6.96 – 6.81 (m, 2H), 6.80 – 6.73 (m, 2H), 6.65 (dt, J = 10.5, 4.2 Hz, 2H), 5.88 (dd, J = 8.2, 5.1 Hz, 0H), 5.78 (ddd, J = 7.8, 5.6, 2.0 Hz, 1H), 5.74 (dd, J = 8.1, 5.2 Hz, 0H), 5.49 (d, J = 5.2 Hz, 0H), 5.45 (dd, J = 5.9, 2.0 Hz, 1H), 5.39 (d, J = 10.7 Hz, 0H), 5.17 (d, J = 10.6 Hz, 0H), 5.08 (d, J = 10.4 Hz, 1H), 5.02 – 4.96 (m, 0H), 4.83 – 4.79 (m, 0H), 4.74 – 4.65 (m, 1H), 4.64 – 4.58 (m, 1H), 4.57 – 4.50 (m, 0H), 4.18 (d, J = 14.0 Hz, 1H), 3.94 (d, J = 13.8 Hz, 1H), 3.84 (dd, J = 4.4, 1.7 Hz, 6H), 3.40 – 3.06 (m, 2H), 3.06 – 2.72 (m, 1H), 2.68 – 2.40 (m, 4H), 2.32 (d, J = 13.5 Hz, 1H), 2.25 – 1.94 (m, 3H), 1.93 – 1.52 (m, 9H), 1.52 – 1.40 (m, 2H), 1.41 – 1.07 (m, 5H), 1.06 – 0.76 (m, 2H), 0.59 (qd, J = 12.7, 3.2 Hz, 0H).

¹³C-NMR (126 MHz, CDCl₃): δ 171.5, 171.3, 170.5, 170.4, 170.3, 170.0, 169.7, 169.5, 168.9, 168.1, 162.7, 158.6, 158.5, 158.4, 158.1, 149.1, 149.0, 147.6, 147.6, 147.5, 142.1, 142.0, 141.7, 141.5, 133.5, 133.4, 129.8, 129.8, 129.7, 129.5, 120.9, 120.3, 120.2, 120.2, 119.9, 116.9, 116.5, 116.2, 114.8, 111.9, 111.9, 111.8, 111.6, 111.5, 111.4, 110.3, 110.1, 109.3, 76.5, 76.3, 76.1, 75.9, 66.3, 65.7, 65.7, 65.2, 57.3, 57.0, 56.9, 56.8, 56.3, 56.1, 56.0, 56.0, 52.5, 52.5, 44.0, 43.9, 43.4, 43.1, 43.1, 40.2, 40.1, 38.9, 38.9, 38.5, 38.1, 35.9, 35.7, 35.5, 32.1, 32.0, 31.7, 31.6, 31.5, 31.4, 31.3, 30.8, 30.6, 30.5, 30.2, 30.0, 28.4, 28.1, 27.9, 27.7, 26.9, 26.7, 26.4, 26.2, 26.0, 25.9, 25.8, 25.7, 25.3, 25.2, 23.0, 23.0, 22.8, 22.2, 21.9, 21.6, 21.1, 21.0, 20.8, 20.6, 20.0.

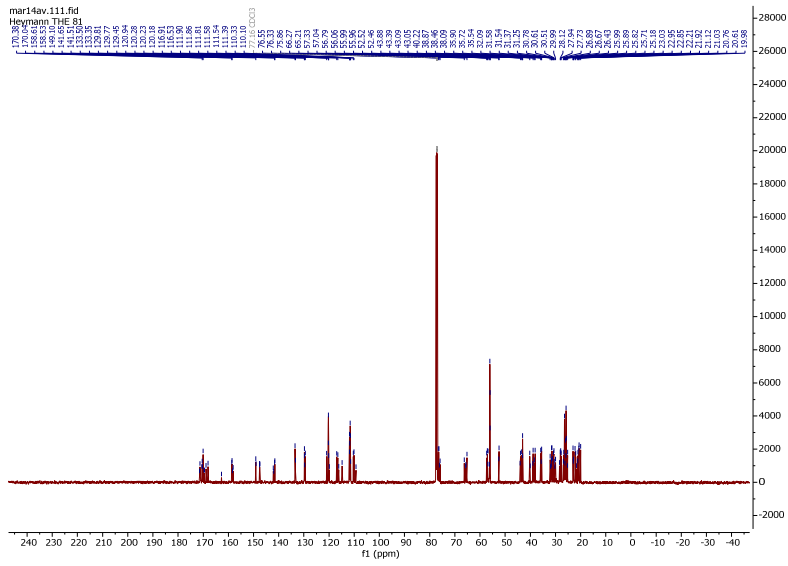
LC-MS: *t*_R = 14.35 min (98%), *m/z*: calculated = 679.36 [M+H]⁺, found = 679.37 [M+H]⁺.

HRMS: *m/z* = 679.3587 [M+H]⁺ (0.35 ppm error)

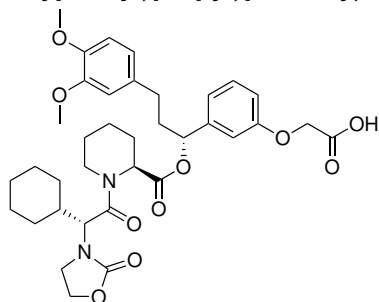
¹H-NMR



¹³C-NMR



2-(3-((R)-1-(((S)-1-((R)-2-Cyclohexyl-2-(2-oxooxazolidin-3-yl)acetyl)piperidine-2-carbonyloxy)-3-(3,4-dimethoxyphenyl)propyl)phenoxy)acetic acid



Chemical Formula: C₃₆H₄₆N₂O₁₀

Exact Mass: 666.32

Molecular Weight: 666.76

48d

The synthesis is conducted according to general procedure 5.16.2 with 0.12 mmol starting material. The crude product is purified by manual column chromatography (DCM/MeOH/FA 100:1:1) to yield 23 mg (29%) as a pale yellow solid.

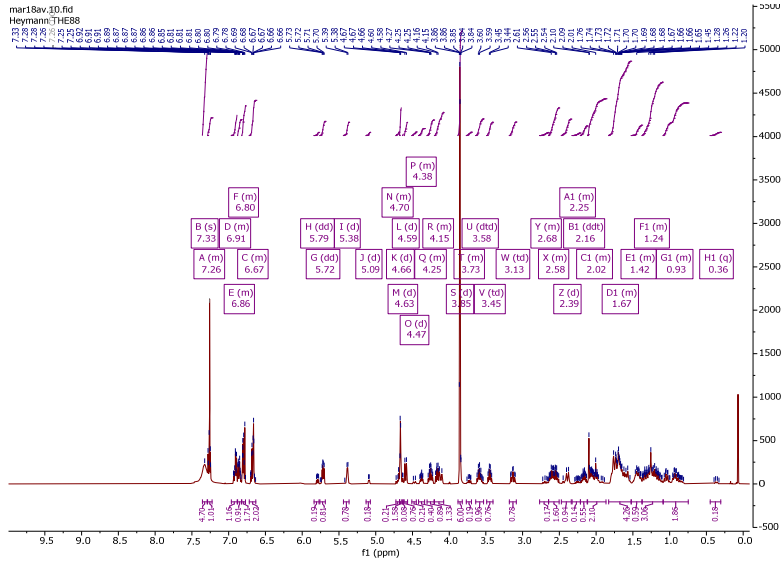
¹H-NMR (500 MHz, CDCl₃): δ 7.33 (s, 1H), 7.29 – 7.23 (m, 1H), 6.96 – 6.89 (m, 1H), 6.88 – 6.82 (m, 1H), 6.82 – 6.77 (m, 2H), 6.72 – 6.63 (m, 2H), 5.79 (dd, J = 8.3, 5.5 Hz, 0H), 5.72 (dd, J = 8.1, 5.3 Hz, 1H), 5.38 (d, J = 5.6 Hz, 1H), 5.09 (d, J = 5.3 Hz, 0H), 4.72 – 4.68 (m, 0H), 4.66 (d, J = 2.2 Hz, 2H), 4.63 (d, J = 1.7 Hz, 0H), 4.59 (d, J = 10.7 Hz, 1H), 4.50 – 4.34 (m, 1H), 4.30 – 4.21 (m, 1H), 4.20 – 4.08 (m, 1H), 3.85 (d, J = 2.5 Hz, 6H), 3.77 – 3.70 (m, 0H), 3.58 (dtd, J = 15.9, 9.2, 6.8 Hz, 1H), 3.45 (td, J = 9.2, 6.9 Hz, 1H), 3.13 (td, J = 13.5, 2.7 Hz, 1H), 2.77 – 2.65 (m, 0H), 2.65 – 2.50 (m, 2H), 2.39 (d, J = 14.1 Hz, 1H), 2.33 – 2.21 (m, 0H), 2.16 (ddt, J = 15.2, 9.0, 4.5 Hz, 1H), 2.12 – 1.87 (m, 2H), 1.83 – 1.52 (m, 7H), 1.52 – 1.37 (m, 1H), 1.37 – 1.09 (m, 5H), 1.09 – 0.75 (m, 2H), 0.36 (q, J = 11.4 Hz, 0H).

¹³C-NMR (126 MHz, CDCl₃): δ 170.0, 169.5, 159.4, 157.9, 149.1, 147.6, 142.0, 141.8, 133.5, 130.0, 129.9, 120.6, 120.4, 120.3, 116.1, 115.1, 111.9, 111.7, 111.2, 110.3, 76.6, 65.4, 65.1, 63.5, 63.4, 57.1, 56.6, 56.4, 56.1, 56.1, 53.0, 44.5, 41.6, 41.4, 40.3, 38.2, 36.3, 36.1, 31.6, 31.3, 29.9, 29.4, 28.8, 28.5, 28.0, 26.9, 26.3, 26.0, 25.6, 25.6, 25.5, 24.7, 21.0.

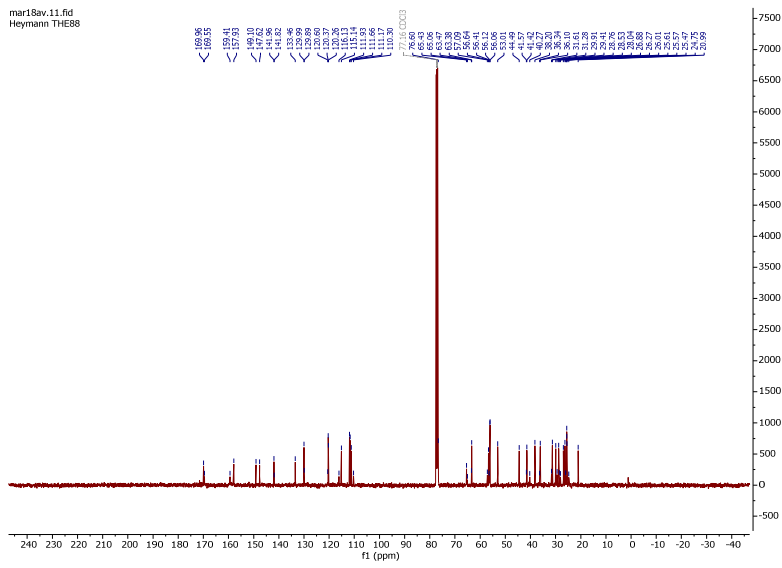
LC-MS: *t*_R = 10.08 min (95%), *m/z*: calculated = 667.33 [M+H]⁺, found = 667.58 [M+H]⁺.

HRMS: *m/z* = 667.3222 [M+H]⁺ (0.54 ppm error)

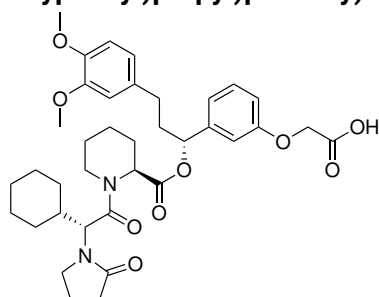
¹H-NMR



¹³C-NMR



2-(3-((R)-1-(((S)-1-((R)-2-Cyclohexyl-2-(2-oxopyrrolidin-1-yl)acetyl)piperidine-2-carbonyloxy)-3-(3,4-dimethoxyphenyl)propyl)phenoxy)acetic acid



Chemical Formula: C₃₇H₄₈N₂O₉

Exact Mass: 664.34

Molecular Weight: 664.79

48e

The synthesis is conducted according to general procedure 5.16.2 with 0.10 mmol starting material. The crude product is purified by manual column chromatography (DCM/MeOH/FA 100:1:1) to yield 42 mg (64 %) as a pale yellow solid.

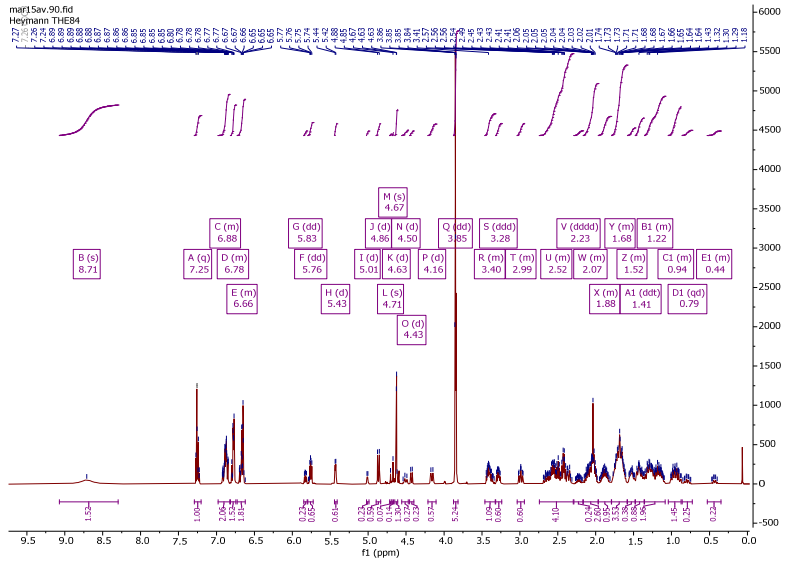
¹H-NMR (500 MHz, CDCl₃): δ 8.71 (s, 1H), 7.25 (q, J = 7.5 Hz, 1H), 6.98 – 6.82 (m, 2H), 6.81 – 6.74 (m, 2H), 6.73 – 6.62 (m, 2H), 5.83 (dd, J = 8.2, 5.3 Hz, 0H), 5.76 (dd, J = 8.0, 5.3 Hz, 1H), 5.43 (d, J = 5.7 Hz, 1H), 5.01 (d, J = 5.2 Hz, 0H), 4.86 (d, J = 10.6 Hz, 1H), 4.81 – 4.65 (m, 1H), 4.63 (d, J = 1.5 Hz, 1H), 4.50 (d, J = 14.1 Hz, 0H), 4.43 (d, J = 10.5 Hz, 0H), 4.16 (d, J = 14.0 Hz, 1H), 3.85 (dd, J = 4.3, 3.0 Hz, 6H), 3.46 – 3.33 (m, 1H), 3.28 (ddd, J = 10.3, 8.2, 5.8 Hz, 1H), 3.04 – 2.94 (m, 1H), 2.74 – 2.30 (m, 5H), 2.23 (dddd, J = 13.5, 12.1, 8.9, 5.0 Hz, 0H), 2.16 – 1.97 (m, 4H), 1.97 – 1.79 (m, 1H), 1.79 – 1.59 (m, 6H), 1.58 – 1.48 (m, 1H), 1.41 (ddt, J = 18.6, 8.8, 6.8 Hz, 2H), 1.36 – 1.08 (m, 4H), 1.04 – 0.87 (m, 2H), 0.79 (qd, J = 12.5, 3.5 Hz, 0H), 0.53 – 0.35 (m, 0H).

¹³C-NMR (126 MHz, CDCl₃): δ 176.5, 176.3, 170.9, 170.7, 170.1, 169.8, 169.0, 168.8, 158.4, 158.1, 149.1, 147.6, 142.1, 142.0, 133.5, 129.9, 129.7, 120.3, 120.3, 120.2, 116.2, 114.8, 111.9, 111.6, 111.6, 111.3, 109.7, 76.5, 76.0, 65.7, 65.5, 56.6, 56.1, 56.0, 55.5, 55.2, 52.7, 44.4, 44.3, 44.3, 40.0, 38.6, 38.5, 36.1, 36.0, 31.6, 31.2, 31.1, 30.9, 30.2, 29.8, 28.7, 28.3, 28.1, 26.9, 26.4, 26.2, 25.7, 25.7, 25.7, 25.6, 25.0, 21.4, 21.1, 18.4.

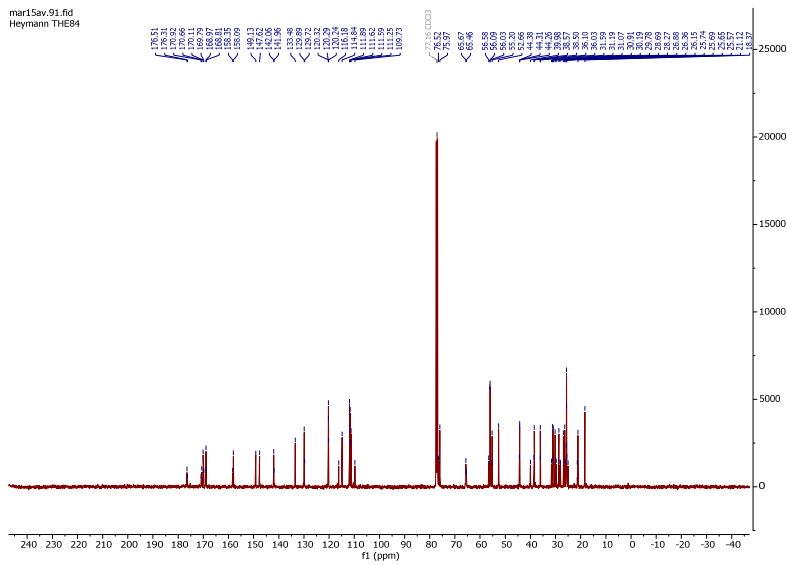
LC-MS: *t*_R = 11.17 min (99%), *m/z*: calculated = 665.35 [M+H]⁺, found = 665.43 [M+H]⁺.

HRMS: *m/z* = 665.3425 [M+H]⁺ (1.14 ppm error)

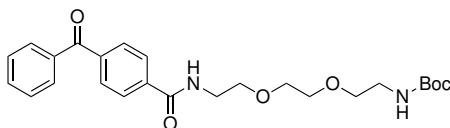
¹H-NMR



¹³C-NMR



tert-Butyl (2-(2-(2-(4-benzoylbenzamido)ethoxy)ethoxy)ethyl)carbamate



Chemical Formula: C₂₅H₃₂N₂O₆

Exact Mass: 456.23

Molecular Weight: 456.53

50

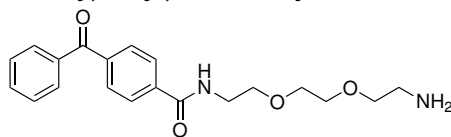
The synthesis is conducted according to general procedure 5.16.1 with 0.20 mmol starting material. The crude product is purified by manual column chromatography (EA/TEA 100:3) to yield 65 mg (71 %) as a white solid.

¹H-NMR (500 MHz, CDCl₃): δ 8.31 (s, 0H), 7.98 (s, 0H), 7.89 (d, J = 7.9 Hz, 2H), 7.80 (d, J = 7.9 Hz, 2H), 7.78 – 7.73 (m, 2H), 7.61 – 7.54 (m, 1H), 7.49 – 7.43 (m, 2H), 7.00 (s, 1H), 5.64 (s, 0H), 5.01 (s, 1H), 3.68 – 3.66 (m, 4H), 3.64 – 3.59 (m, 4H), 3.53 (t, J = 5.7 Hz, 2H), 3.27 (q, J = 5.6 Hz, 2H), 1.41 (s, 9H).

¹³C-NMR (126 MHz, CDCl₃): δ 196.0, 166.7, 157.2, 156.0, 140.1, 137.9, 137.1, 132.9, 130.1, 128.5, 127.1, 79.4, 70.4, 70.3, 69.8, 58.5, 42.0, 40.4, 40.0, 28.5, 23.6, 8.2.

UHPLC-MS: *t*_R = 1.872 min (97%), *m/z*: calculated = 457.24 [M+H]⁺, found = 457.2 [M+H]⁺.

N-(2-(2-(2-Aminoethoxy)ethoxy)ethyl)-4-benzoylbenzamide hydrochloride



Chemical Formula: C₂₀H₂₄N₂O₄

Exact Mass: 356.17

Molecular Weight: 356.42

51

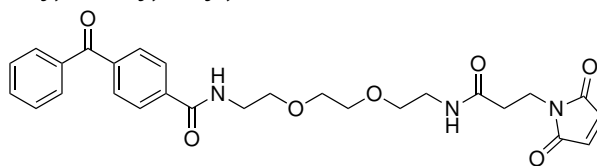
The synthesis is conducted according to general procedure 5.16.1 with 0.14 mmol starting material. The crude product (56 mg quant.) is used without further purification as HCl salt.

¹H-NMR (500 MHz, CDCl₃): δ 8.26 (s, 3H), 8.10 (s, 1H), 8.01 (d, J = 7.8 Hz, 2H), 7.72 (d, J = 7.6 Hz, 2H), 7.71 – 7.65 (m, 2H), 7.53 (t, J = 7.6 Hz, 1H), 7.41 (t, J = 7.6 Hz, 2H), 3.77 – 3.67 (m, 2H), 3.66 (d, J = 0.9 Hz, 4H), 3.57 (s, 4H), 3.15 (s, 2H).

¹³C-NMR (126 MHz, CDCl₃): δ 196.2, 167.1, 139.9, 137.5, 136.9, 133.0, 130.1, 129.9, 128.5, 127.6, 70.2, 70.2, 69.9, 67.1, 66.7, 43.6, 40.2, 39.7, 22.8.

UHPLC-MS: *t*_R = 1.360 min (98%), *m/z*: calculated = 357.18 [M+H]⁺, found = 357.2 [M+H]⁺.

4-Benzoyl-N-(2-(2-(2-(3-(2,5-dioxo-2,5-dihydro-1H-pyrrol-1-yl)propanamido)ethoxy)ethoxy)ethyl)benzamide



Chemical Formula: C₂₇H₂₉N₃O₇

Exact Mass: 507.20

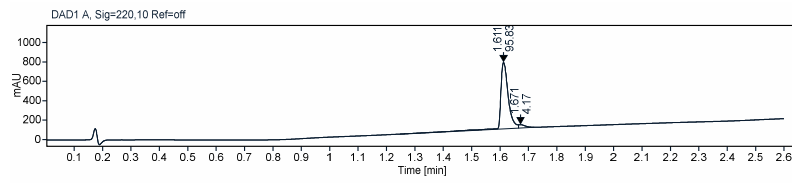
Molecular Weight: 507.54

52

The synthesis is conducted according to general procedure 5.16.1 with 0.10 mmol starting material. The crude product is purified by preparative HPLC to yield 2.3 mg (5 %) as a white solid.

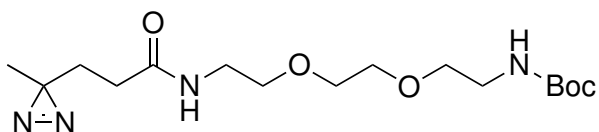
UHPLC-MS: $t_R = 1.611$ min (96 %), m/z : calculated = 508.20 [M+H]⁺, found = 508.2 [M+H]⁺.

UHPLC, UV 220 nm



tert-Butyl

(2-(2-(2-(3-(3-methyl-3H-diazirin-3-yl)propanamido)ethoxy)ethoxy)ethyl)carbamate



Chemical Formula: C₁₆H₃₀N₄O₅

Exact Mass: 358.22

Molecular Weight: 358.43

54

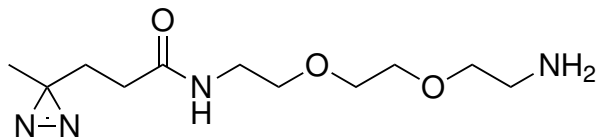
The synthesis is conducted according to general procedure 5.16.1 with 0.22 mmol starting material. The crude product is purified by flash column chromatography (DCM/MeOH) to yield 79 mg (quant.) as a white solid.

¹H-NMR (500 MHz, CDCl₃): δ 6.05 (s, 1H), 4.98 (s, 1H), 3.61 (s, 4H), 3.56 (t, J = 5.1 Hz, 5H), 3.45 (q, J = 5.3 Hz, 3H), 3.32 (t, J = 5.7 Hz, 2H), 2.01 (t, J = 7.6 Hz, 2H), 1.75 (t, J = 7.9 Hz, 2H), 1.45 (s, 9H), 1.02 (s, 3H).

¹³C-NMR (126 MHz, CDCl₃): δ 171.5, 156.1, 79.6, 70.5, 70.4, 70.3, 70.0, 53.1, 46.1, 40.5, 39.4, 30.7, 30.2, 28.6, 25.6.

UHPLC-MS: *t*_R = 1.360 min (91%), *m/z*: calculated = 259.17 [M+H-Boc]⁺, found = 259.2 [M+H-Boc]⁺.

N-(2-(2-(2-Aminoethoxy)ethoxy)ethyl)-3-(3-methyl-3H-diazirin-3-yl)propanamide



Chemical Formula: $C_{11}H_{22}N_4O_3$

Exact Mass: 258.17

Molecular Weight: 258.32

55

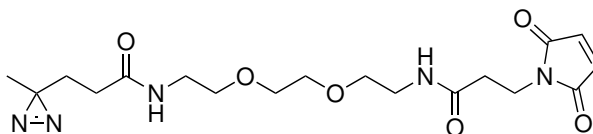
The synthesis is conducted according to general procedure 5.16.1 with 0.22 mmol starting material. The crude product is purified by flash column chromatography (DCM/MeOH+3% TEA) to yield 22 mg (29%) as a white solid.

$^1\text{H-NMR}$ (500 MHz, CDCl_3): δ 3.60 (s, 4H), 3.54 (dt, $J = 6.9, 4.9$ Hz, 4H), 3.47 – 3.37 (m, 2H), 2.88 (t, $J = 5.2$ Hz, 2H), 2.00 (dd, $J = 8.7, 6.8$ Hz, 2H), 1.73 (dd, $J = 8.6, 6.8$ Hz, 2H), 1.01 (s, 3H).

$^{13}\text{C-NMR}$ (126 MHz, CDCl_3): δ 171.6, 72.9, 70.4, 70.1, 70.0, 41.6, 39.4, 30.6, 30.2, 25.6, 20.0.

UHPLC-MS: $t_R = 0.751$ min (99%), m/z : calculated = 259.17 $[\text{M}+\text{H}]^+$, found = 259.2 $[\text{M}+\text{H}]^+$.

3-(2,5-Dioxo-2,5-dihydro-1H-pyrrol-1-yl)-N-(2-(2-(2-(3-(3-methyl-3H-diazirin-3-yl)propanamido)ethoxy)ethoxy)ethyl)propanamide



Chemical Formula: C₁₈H₂₇N₅O₆

Exact Mass: 409.20

Molecular Weight: 409.44

56

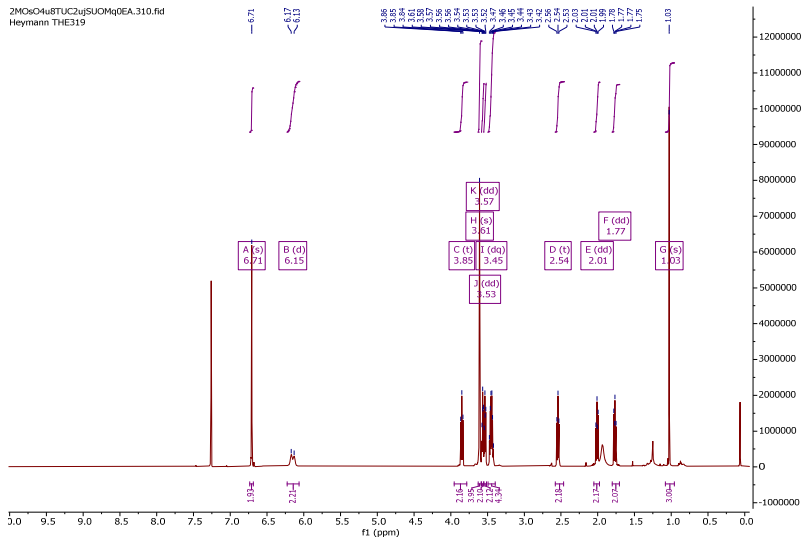
The synthesis is conducted according to general procedure 5.16.1 with 0.08 mmol starting material but with the exception that the reaction is quenched by addition of diluted HCl, extracted with DCM, dried over MgSO₄, and volatiles were removed under reduced pressure. The crude product is purified by preparative HPLC to yield 6 mg (19%) as a white solid.

¹H-NMR (500 MHz, CDCl₃): δ 6.71 (s, 2H), 6.15 (d, J = 19.5 Hz, 2H), 3.85 (t, J = 7.3 Hz, 2H), 3.61 (s, 4H), 3.57 (dd, J = 5.6, 4.7 Hz, 2H), 3.53 (dd, J = 5.6, 4.6 Hz, 2H), 3.45 (dq, J = 10.5, 5.3 Hz, 4H), 2.54 (t, J = 7.3 Hz, 2H), 2.01 (dd, J = 8.6, 6.8 Hz, 2H), 1.77 (dd, J = 8.5, 6.8 Hz, 2H), 1.03 (s, 3H).

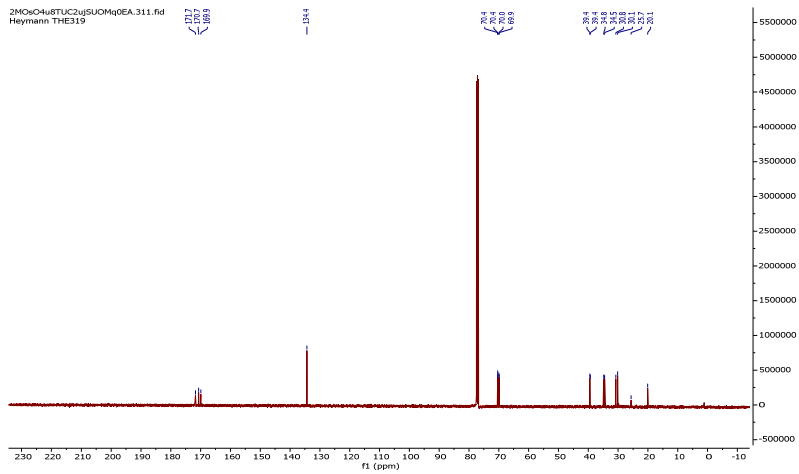
¹³C-NMR (126 MHz, CDCl₃): δ 171.7, 170.7, 169.9, 134.4, 70.4, 70.4, 70.0, 69.9, 39.4, 39.4, 34.8, 34.5, 30.8, 30.1, 25.7, 20.1.

UHPLC-MS: *t*_R = 1.385 min (99%), *m/z*: calculated = 410.21 [M+H]⁺, found = 410.2 [M+H]⁺.

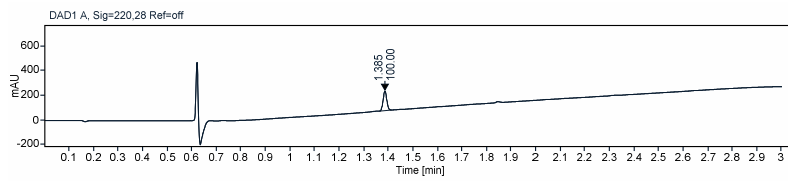
¹H-NMR



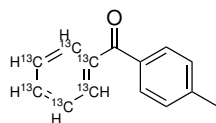
¹³C-NMR



UHPLC, UV 220 nm



¹³C₆-Phenyl(*p*-tolyl)methanone



Chemical Formula: C₈¹³C₆H₁₂O

Exact Mass: 202.11

Molecular Weight: 202.20

59

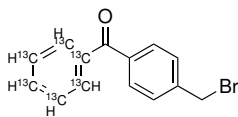
1.14 mL (11.9 mmol, 1.0 eq) labeled benzene are added to a suspension of 3.17 g (23.8 mmol, 2.0 eq) AlCl₃ in 5 mL CS₂ at 0 °C. 2.76 g (17.9 mmol, 1.5 eq) *para* toluoyl chloride are added dropwise and the mixture is stirred overnight at room temperature before the reaction is quenched by addition of NaHCO₃. The mixture is extracted with ether, washed with NaHCO₃ dried over MgSO₄, and volatiles are removed under reduced pressure. The crude product is purified by flash column chromatography (Cy/EA) to yield 1.81 g (75 %) as a pale yellow oil.

¹H-NMR (500 MHz, CDCl₃): δ 7.98 – 7.90 (m, 1H), 7.78 – 7.69 (m, 3H), 7.67 – 7.58 (m, 2H), 7.51 – 7.31 (m, 1H), 7.30 – 7.27 (m, 2H), 2.45 (s, 3H).

¹³C-NMR (126 MHz, CDCl₃): δ 143.4, 138.13 (td, J = 56.5, 8.9 Hz), 133.11 – 131.56 (m), 130.07 (ddd, J = 57.4, 54.4, 9.5 Hz), 129.1, 128.95 – 127.56 (m), 21.8.

UHPLC-MS: *t*_R = 1.564 min (72%), *m/z*: calculated = 203.13 [M+H]⁺, found = 203.0 [M+H]⁺.

¹³C₆-(4-(Bromomethyl)phenyl)(phenyl)methanone



Chemical Formula: C₈¹³C₆H₁₁BrO

Exact Mass: 280.02

Molecular Weight: 281.10

60

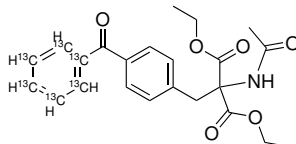
1.61 g (7.96 mmol, 1.0 eq) **59**, 1.56 g (8.76 mmol, 1.1 eq) NBS, and 0.07 g (0.40 mmol, 0.05 eq) AIBN are dissolved in 20 mL chloroform and refluxed overnight. The mixture is filtered and volatiles are removed under reduced pressure. The crude product is purified by preparative HPLC to yield 0.98 g (44 %) as a white solid.

¹H-NMR (500 MHz, CDCl₃): δ 7.95 (ddt, J = 11.9, 8.9, 5.4 Hz, 1H), 7.83 – 7.70 (m, 3H), 7.63 (dq, J = 8.6, 5.6, 2.0 Hz, 2H), 7.55 – 7.47 (m, 2H), 7.47 – 7.39 (m, 0H), 7.32 (dtd, J = 13.2, 8.9, 6.4 Hz, 1H), 4.53 (s, 2H).

¹³C-NMR (126 MHz, CDCl₃): δ 196.3, 195.8, 142.2, 137.47 (td, J = 56.4, 8.9 Hz), 132.66 (td, J = 54.1, 8.9 Hz), 130.6, 130.09 (ddd, J = 57.6, 54.4, 9.2 Hz), 129.0, 128.97 – 127.72 (m), 32.4.

UHPLC-MS: *t_R* = 0.742 min (93 %), *m/z*: calculated = 283.02 [M+H]⁺, found = 283.0 [M+H]⁺.

¹³C₆-Diethyl 2-acetamido-2-(4-benzoylbenzyl)malonate



Chemical Formula: C₁₇¹³C₆H₂₅NO₆

Exact Mass: 417.19

Molecular Weight: 417.40

61

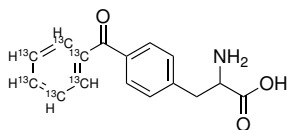
0.14 g (7.96 mmol, 1.0 eq) sodium are dissolved in 40 mL EtOH and 2.26 g (8.32 mmol, 2.0 eq) diethyl acetimidomalonate are added. The mixture is refluxed for 10 min, before 1.17 g (4.16 mmol, 1.0 eq) **60** are added. The mixture is refluxed overnight before the reaction is quenched by adding 1 M HCl. The mixture is extracted with EA, dried over MgSO₄, and volatiles are removed under reduced pressure. The crude product is purified by flash column chromatography (Cy/EA) to yield 1.13 g (65 %) as a white solid.

¹H-NMR (500 MHz, CDCl₃): δ 7.90 (dd, J = 9.0, 5.3 Hz, 1H), 7.76 – 7.66 (m, 3H), 7.60 (qd, J = 9.1, 4.0 Hz, 2H), 7.47 – 7.27 (m, 1H), 7.14 – 7.09 (m, 2H), 6.57 (s, 1H), 4.34 – 4.19 (m, 4H), 3.73 (s, 2H), 2.02 (d, J = 0.8 Hz, 3H), 1.29 (td, J = 7.1, 0.8 Hz, 6H).

¹³C-NMR (126 MHz, CDCl₃): δ 196.6, 196.1, 169.3, 167.4, 140.4, 137.65 (td, J = 56.3, 8.8 Hz), 132.47 (td, J = 54.3, 9.0 Hz), 130.2, 130.00 (ddd, J = 57.5, 54.3, 9.1 Hz), 129.07 – 127.63 (m), 67.1, 62.9, 56.6, 37.9, 23.1, 14.1.

UHPLC-MS: *t*_R = 1.605 min (98 %), *m/z*: calculated = 418.20 [M+H]⁺, found = 418.0 [M+H]⁺.

¹³C₆-2-Amino-3-(4-benzoylphenyl)propanoic acid



Chemical Formula: C₁₀¹³C₆H₁₅NO₃

Exact Mass: 275.13

Molecular Weight: 275.25

62

1.17 g (2.80 mmol, 1.0 eq) **61** are suspended in 40 mL 6 M HCl and refluxed overnight, before the mixture is neutralized by addition of 3 M NaOH. The mixture is flash frozen with liquid nitrogen and freeze dried. The crude product is purified by preparative HPLC to yield 0.52 g (68 %) as a white solid.

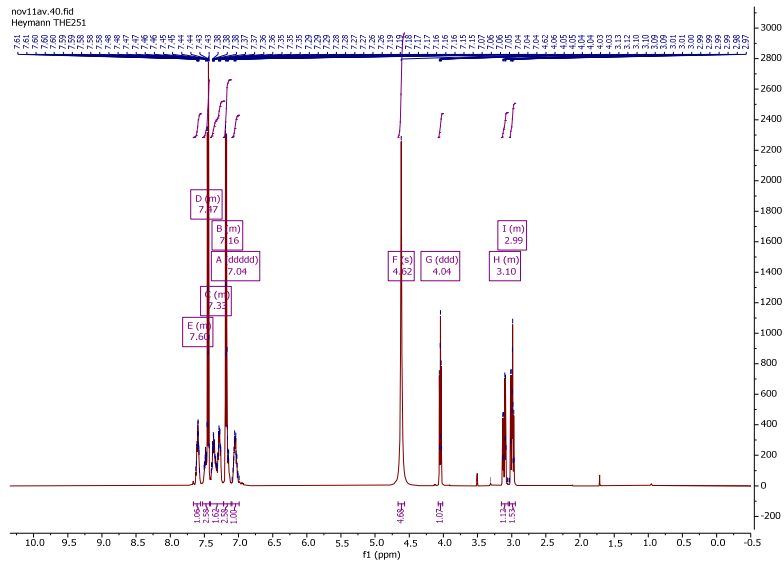
¹H-NMR (500 MHz, MeOD): δ 7.66 – 7.55 (m, 1H), 7.53 – 7.42 (m, 3H), 7.41 – 7.22 (m, 2H), 7.22 – 7.11 (m, 3H), 7.04 (dddd, J = 11.0, 9.1, 7.4, 3.9, 2.1 Hz, 1H), 4.04 (ddd, J = 7.8, 5.8, 1.9 Hz, 1H), 3.15 – 3.05 (m, 1H), 3.03 – 2.95 (m, 2H).

¹³C-NMR (126 MHz, MeOD): δ 198.3, 197.9, 171.0, 140.9, 138.65 (td, J = 56.1, 8.9 Hz), 133.90 (td, J = 53.2, 8.9 Hz), 131.6, 131.54 – 130.37 (m), 130.7, 130.19 – 128.51 (m), 54.9, 37.2.

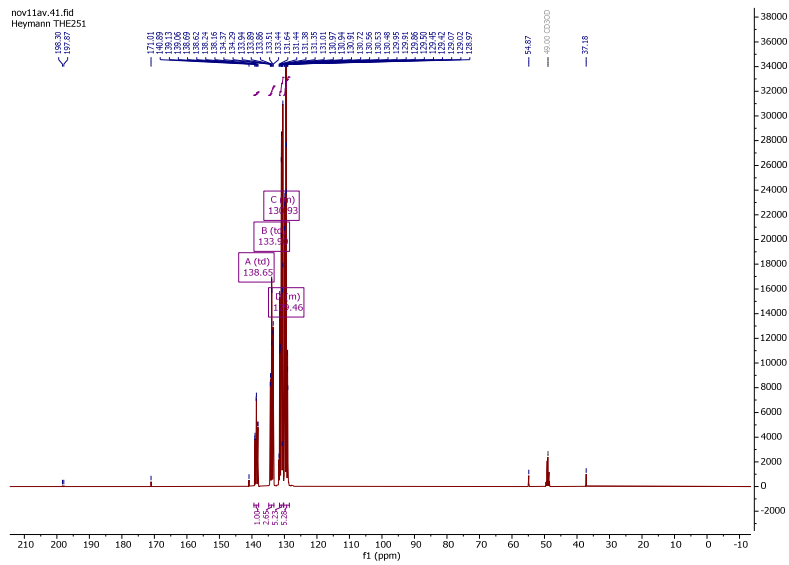
UHPLC-MS: t_R = 1.332 min (98 %), m/z: calculated = 276.14 [M+H]⁺, found = 276.2 [M+H]⁺.

HRMS: m/z = 276.1326 [M+H]⁺ (0.08 ppm error)

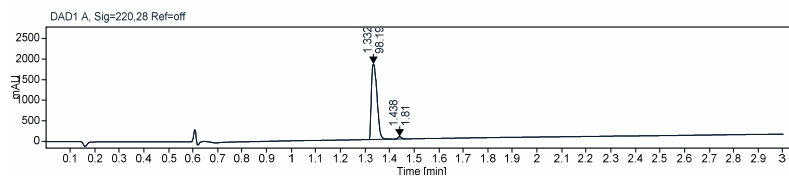
¹H-NMR



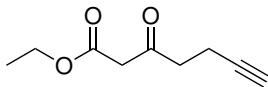
¹³C-NMR



UHPLC, UV 220 nm



Ethyl 3-oxohept-6-ynoate



Chemical Formula: C₉H₁₂O₃

Exact Mass: 168.08

Molecular Weight: 168.19

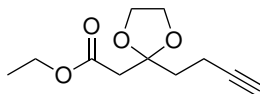
64

17.23 mL (123 mmol, 2.0 eq) diisopropylamine are dissolved in 130 mL dry THF and cooled down to 0 °C. 49.2 mL (123 mmol, 2.0 eq) 2.5 M *n*-butyl lithium in hexanes are slowly added and the mixture is stirred for 10 min before 7.77 mL (61.5 mmol, 1.0 eq) ethyl acetoacetate are added dropwise followed by 6.85 mL (61.5 mmol, 1.0 eq) 80 wt-% propargylbromide in toluene. The mixture is stirred for 30 min until the reaction is quenched by addition of saturated ammonium chloride solution. The mixture is extracted with ether, dried over MgSO₄, and volatiles are removed under reduced pressure. The crude product is purified by flash column chromatography (Cy/EA) to yield 7.06 g (68 %) as a yellow oil.

¹H-NMR (500 MHz, CDCl₃): δ 4.24 – 4.16 (m, 2H), 3.46 (s, 2H), 2.81 (dd, J = 7.7, 6.8 Hz, 2H), 2.51 – 2.45 (m, 2H), 1.96 (t, J = 2.6 Hz, 1H), 1.28 (t, J = 7.2 Hz, 3H).

¹³C-NMR (126 MHz, CDCl₃): δ 200.6, 167.0, 82.7, 69.1, 61.7, 49.4, 41.8, 14.2, 13.0.

UHPLC-MS: *t*_R = 1.664 min (48 %), *m/z*: calculated = 169.09 [M+H]⁺, found = 169.0 [M+H]⁺.

Ethyl 2-(2-(but-3-yn-1-yl)-1,3-dioxolan-2-yl)acetateChemical Formula: C₁₁H₁₆O₄

Exact Mass: 212.10

Molecular Weight: 212.24

65

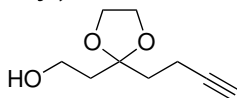
14.2 g (84.4 mmol, 1.0 eq) **64**, 14.1 mL (253 mmol, 3.0 eq) ethylene glycol, and 0.8 g (4.22 mmol, 0.05 eq) *p*TsOH are dissolved in 140 mL toluene and refluxed for 10 h with a Dean Stark trap. The mixture is washed with NaHCO₃, extracted with ether, dried over MgSO₄, and volatiles are removed under reduced pressure. The crude product (17.67 g, 99%) is used without further purification.

¹H-NMR (500 MHz, CDCl₃): δ 4.15 (q, J = 7.2 Hz, 2H), 4.06 – 3.93 (m, 4H), 2.65 (s, 2H), 2.30 (ddd, J = 8.0, 6.6, 2.7 Hz, 2H), 2.19 – 2.07 (m, 2H), 1.93 (t, J = 2.7 Hz, 1H), 1.59 (s, 0H), 1.27 (t, J = 7.1 Hz, 3H).

¹³C-NMR (126 MHz, CDCl₃): δ 169.3, 108.4, 84.1, 68.2, 65.4, 60.8, 42.9, 36.6, 14.3, 13.0.

HRMS: m/z = 213.1121 [M+H]⁺ (0.26 ppm error)

2-(2-(But-3-yn-1-yl)-1,3-dioxolan-2-yl)ethanol



Chemical Formula: C₉H₁₄O₃

Exact Mass: 170.09

Molecular Weight: 170.21

66

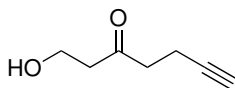
21.7 mL (21.7 mmol, 1.0 eq) LAH is added to a solution of 4.61 g (21.7 mmol, 1.0 eq) **65** in 40 mL dry THF at 0 °C. After stirring for 30 min at room temperature, the mixture is quenched by adding 20 mL of Rochelles salt, extracted with ether, dried over MgSO₄, and volatiles are removed under reduced pressure. The crude product (3.70 g, quant.) is used without further purification.

¹H-NMR (500 MHz, CDCl₃): δ 4.05 – 4.00 (m, 2H), 4.00 – 3.95 (m, 2H), 3.75 (t, J = 5.5 Hz, 2H), 2.63 (s, 1H), 2.32 – 2.21 (m, 2H), 1.94 (ddd, J = 5.6, 3.0, 1.1 Hz, 4H), 1.92 (s, 1H).

¹³C-NMR (126 MHz, CDCl₃): δ 111.2, 84.1, 68.4, 65.1, 58.9, 38.4, 36.0, 13.3.

HRMS: m/z = 171.1014 [M+H]⁺ (1.00 ppm error)

1-Hydroxyhept-6-yn-3-one



Chemical Formula: C₇H₁₀O₂

Exact Mass: 126.07

Molecular Weight: 126.15

67

3.20 g (18.8 mmol, 1.0 eq) **66** and 0.89 g (4.70 mmol, 0.25 eq) *p*TsOH are dissolved in 40 mL acetone. After stirring for 2 h at room temperature, the reaction is quenched by adding 50 mL of NaHCO₃. The mixture is extracted with ether, dried over MgSO₄, and volatiles are removed under reduced pressure. The crude product is purified by distillation (68 °C at 0.13 mbar) and flash column chromatography (Cy/EA) to yield 4.35 g (58 %) as a colourless oil.

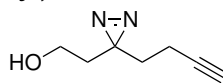
¹H-NMR (500 MHz, CDCl₃): δ 3.87 (q, *J* = 5.7 Hz, 2H), 2.75 – 2.66 (m, 4H), 2.47 (td, *J* = 7.2, 2.6 Hz, 2H), 2.35 – 2.29 (m, 1H), 1.96 (t, *J* = 2.7 Hz, 1H).

¹³C-NMR (126 MHz, CDCl₃): δ 209.2, 82.9, 69.1, 57.9, 44.7, 41.9, 13.0.

UHPLC-MS: *t*_R = 0.965 min (16 %), *m/z*: calculated = 127.08 [M+H]⁺, found = 127.0 [M+H]⁺.

GC-MS: *t*_R = 4.164 min (77 %), *m/z*: calculated = 127.07 [M]^{•+}, found = 127.07 [M]^{•+}.

2-(3-(But-3-yn-1-yl)-3H-diazirin-3-yl)ethanol



Chemical Formula: C₇H₁₀N₂O

Exact Mass: 138.08

Molecular Weight: 138.17

68

500 mg (3.96 mmol, 1.0 eq) **67** are dissolved in 5.7 mL (39.6 mmol, 10 eq) 7 M ammonia in methanol and cooled down to 0 °C. 1.3 mL (11.9 mmol, 3.0 eq) *tert.*-butyl hypochlorite dissolved in 6.5 mL *tert.*-butanol are added carefully to the aforementioned solution. The mixture is stirred for 4 h at room temperature, degassed for 20 min with nitrogen gas, cooled to 0 °C, and a second portion of 0.7 mL (5.90 mmol, 1.5 eq) *tert.*-butyl hypochlorite dissolved in 3.5 mL *tert.*-butanol are added. The mixture is stirred for 30 min at room temperature before the reaction is quenched by addition of thiosulfate solution. The mixture is extracted with ether, dried over MgSO₄, and volatiles are removed under reduced pressure. The crude product is purified by flash column chromatography (Cy/EA) to yield 182 mg (33 %) as a yellow oil.

¹H-NMR (500 MHz, CDCl₃): δ 7.25 (t, J = 6.3 Hz, 2H), 5.80 (td, J = 7.4, 2.5 Hz, 2H), 5.76 (t, J = 2.6 Hz, 1H), 5.50 – 5.42 (m, 4H), 5.34 (s, 1H).

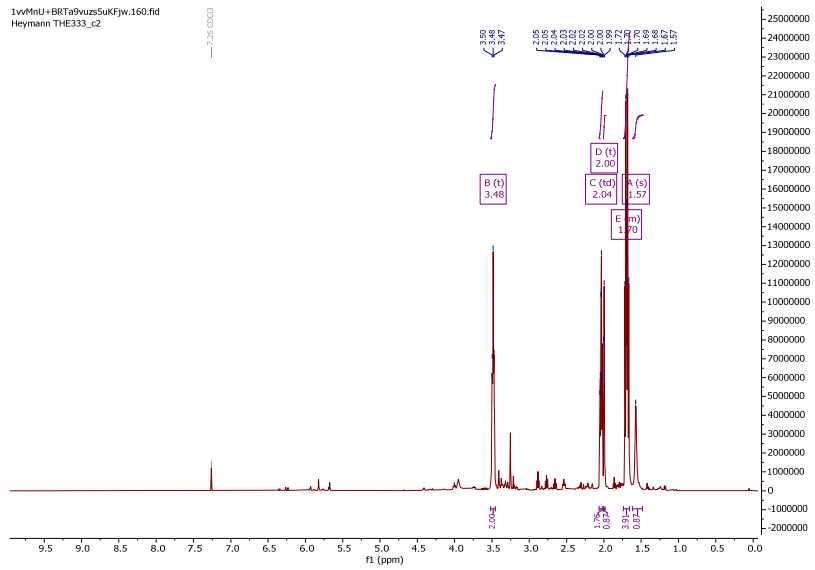
¹³C-NMR (126 MHz, CDCl₃): δ 83.0, 69.4, 57.5, 35.6, 32.8, 26.7, 13.4.

UHPLC-MS: *t*_R = 1.341 min (81 %), *m/z*: calculated = 139.09 [M+H]⁺, found = 139.0 [M+H]⁺.

GC-MS: *t*_R = 3.554 min (98 %), *m/z*: calculated = 138.08 [M]^{•+}, found = only fragments visible, e.g. -[N₂H].

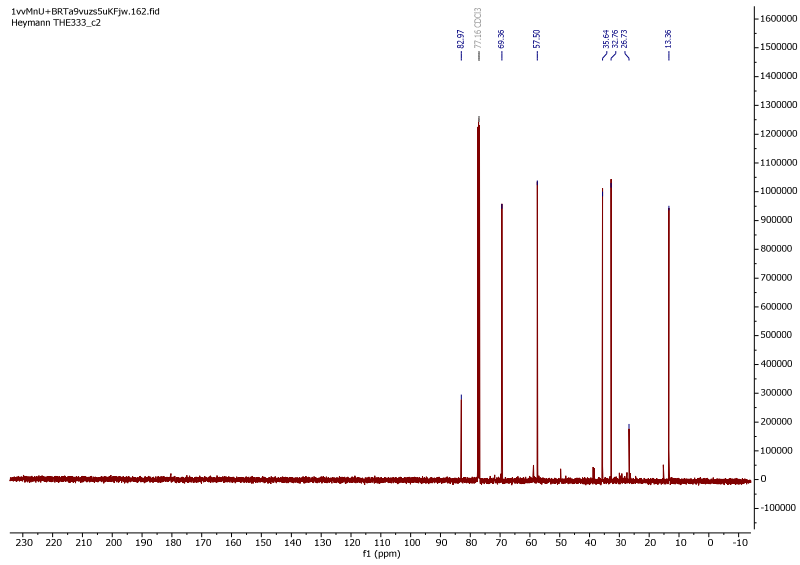
¹H-NMR

1vwMnU+BRtA9vuzSukFjw.160.fid
Heymann THE333_c2

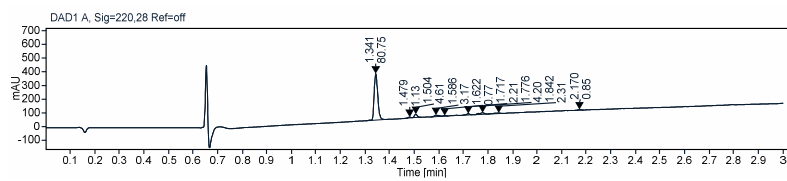


¹³C-NMR

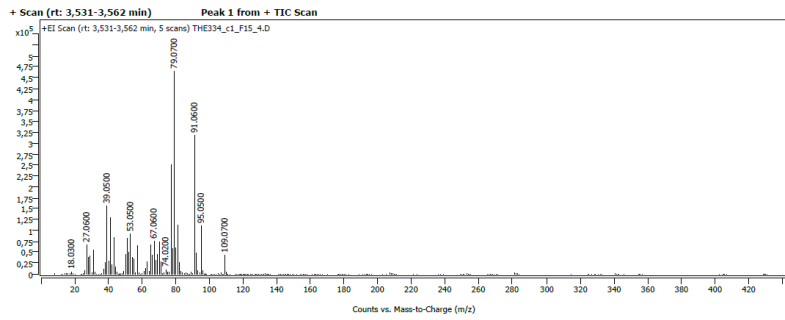
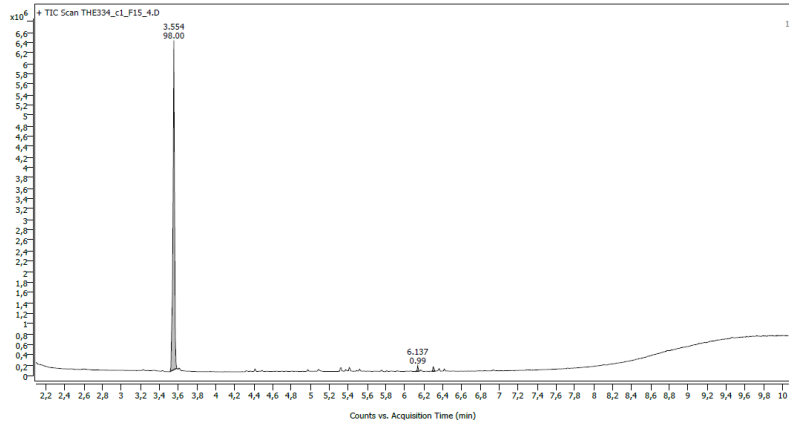
1vwMnU+BRtA9vuzSukFjw.162.fid
Heymann THE333_c2



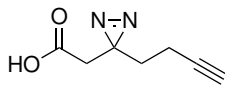
UHPLC, UV 220 nm



TIC GC-MS and scan at 3.554 min



2-(3-(But-3-yn-1-yl)-3H-diazirin-3-yl)acetic acid



Chemical Formula: C₇H₈N₂O₂

Exact Mass: 152.06

Molecular Weight: 152.15

69

165 mg (1.19 mmol, 1.0 eq) **68** are dissolved in 5 mL acetone and cooled down to 0 °C. 1.2 mL (2.39 mmol, 2.0 eq) Jones reagent are added slowly to the aforementioned solution. The mixture is stirred for 2 h before the reaction is quenched by addition of IPA. The mixture is extracted with EA, dried over Na₂SO₄, and volatiles are removed under reduced pressure. The crude product is purified by flash column chromatography (Cy/EA+1 % FA) to yield 133 mg (73 %) as a yellow oil.

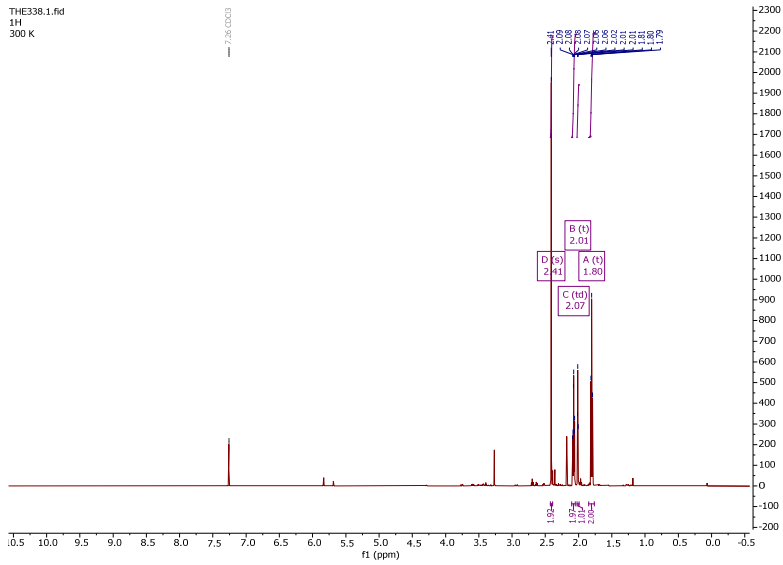
¹H-NMR (500 MHz, CDCl₃): δ 2.41 (s, 2H), 2.07 (td, J = 7.4, 2.7 Hz, 2H), 2.01 (t, J = 2.6 Hz, 1H), 1.80 (t, J = 7.4 Hz, 2H).

¹³C-NMR (126 MHz, CDCl₃): δ 175.1, 82.5, 69.7, 39.5, 32.1, 25.3, 13.4.

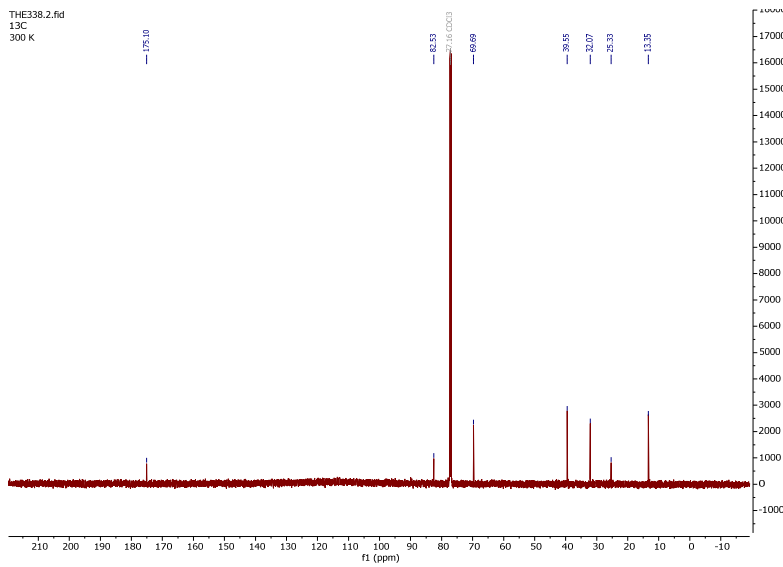
UHPLC-MS: *t*_R = 1.388 min (78 %), *m/z*: calculated = 153.07 [M+H]⁺, found = 153.0 [M+H]⁺.

GC-MS: *t*_R = 4.185 min (93 %), *m/z*: calculated = 152.06 [M]^{•+}, found = only fragments visible, e.g. -[N₂H].

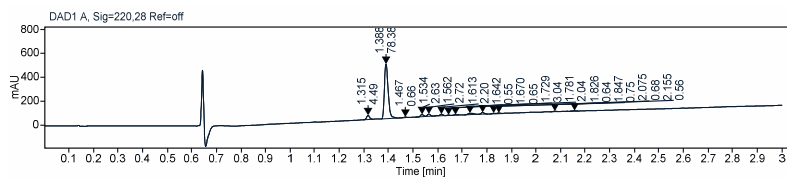
¹H-NMR



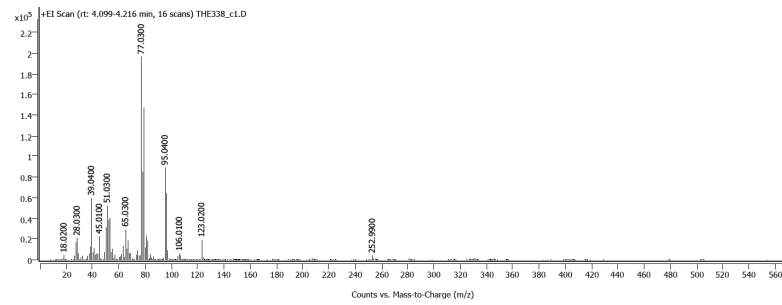
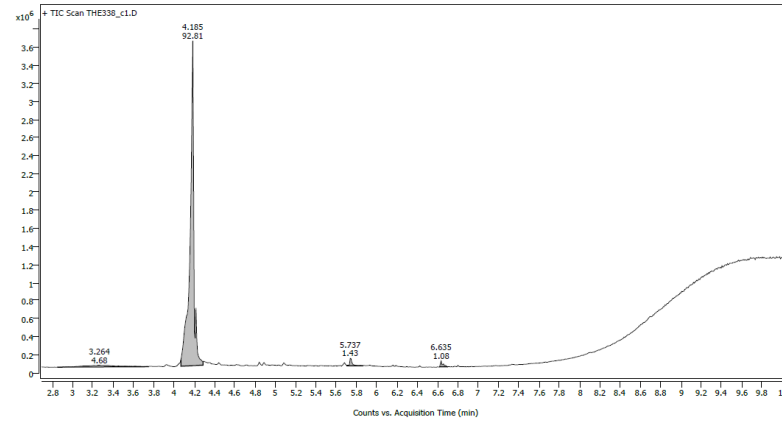
¹³C-NMR



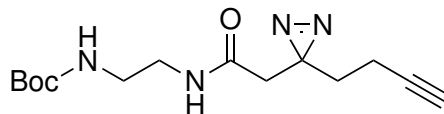
UHPLC, UV 220 nm



TIC GC-MS and scan at 4.185 min



tert-Butyl (2-(2-(3-(but-3-yn-1-yl)-3H-diazirin-3-yl)acetamido)ethyl)carbamate



Chemical Formula: C₁₄H₂₂N₄O₃

Exact Mass: 294.17

Molecular Weight: 294.35

70a

The synthesis is conducted according to the general procedure 5.16.1 using 0.20 mmol **69** as starting material. The crude product is purified by flash column chromatography (DCM/MeOH) to yield 47 mg (81 %) as a pale yellow oil.

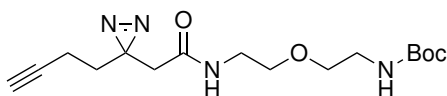
¹H-NMR (600 MHz, CDCl₃): δ 6.46 (s, 1H), 4.90 (s, 1H), 3.37 (q, J = 5.4 Hz, 2H), 3.29 (t, J = 5.9 Hz, 2H), 2.25 (s, 2H), 2.07 (td, J = 7.3, 2.7 Hz, 2H), 2.02 (t, J = 2.7 Hz, 1H), 1.78 (t, J = 7.3 Hz, 2H), 1.44 (s, 9H).

¹³C-NMR (151 MHz, CDCl₃): δ 168.3, 82.8, 69.6, 41.7, 32.2, 28.5, 26.0, 13.4.

UHPLC-MS: *t*_R = 1.671 min (88 %), *m/z*: calculated = 195.13 [M+H-Boc]⁺, found = 195.2 [M+H-Boc]⁺.

tert-Butyl

(2-(2-(2-(3-(but-3-yn-1-yl)-3H-diazirin-3-yl)acetamido)ethoxy)ethyl)carbamate



Chemical Formula: C₁₆H₂₆N₄O₄

Exact Mass: 338.20

Molecular Weight: 338.40

70b

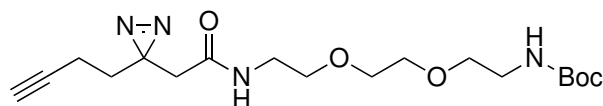
The synthesis is conducted according to the general procedure 5.16.1 using 0.20 mmol **69** as starting material. The crude product is purified by flash column chromatography (DCM/MeOH) to yield 55 mg (82%) as a pale yellow oil.

¹H-NMR (600 MHz, CDCl₃): δ 6.27 (s, 1H), 4.90 (s, 1H), 3.53 (dt, J = 8.2, 5.1 Hz, 4H), 3.46 (q, J = 5.2 Hz, 2H), 3.32 (d, J = 5.5 Hz, 2H), 2.29 (s, 2H), 2.08 (td, J = 7.3, 2.6 Hz, 2H), 2.02 (t, J = 2.6 Hz, 1H), 1.78 (t, J = 7.3 Hz, 2H), 1.44 (s, 9H).

¹³C-NMR (151 MHz, CDCl₃): δ 167.8, 69.6, 41.6, 39.5, 32.2, 28.6, 13.4.

UHPLC-MS: *t*_R = 1.721 min (91%), *m/z*: calculated = 239.15 [M+H-Boc]⁺, found = 239.2 [M+H-Boc]⁺.

tert-Butyl (2-(2-(2-(2-(3-(but-3-yn-1-yl)-3H-diazirin-3-yl)acetamido)ethoxy)ethoxy)ethyl)carbamate



Chemical Formula: C₁₈H₃₀N₄O₅

Exact Mass: 382.22

Molecular Weight: 382.45

70c

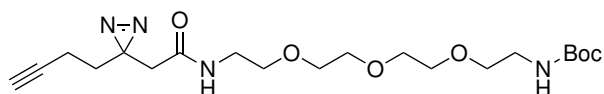
The synthesis is conducted according to the general procedure 5.16.1 using 0.20 mmol **69** as starting material. The crude product is purified by flash column chromatography (DCM/MeOH) to yield 53 mg (71 %) as a colourless oil.

¹H-NMR (600 MHz, CDCl₃): δ 6.24 (s, 1H), 4.95 (s, 1H), 3.72 – 3.53 (m, 7H), 3.47 (q, J = 5.3 Hz, 2H), 3.32 (s, 2H), 2.26 (s, 2H), 2.07 (td, J = 7.4, 2.6 Hz, 2H), 1.78 (t, J = 7.4 Hz, 2H), 1.61 (s, 1H), 1.44 (s, 9H).

¹³C-NMR (151 MHz, CDCl₃): δ 70.2, 69.9, 41.3, 40.1, 39.3, 34.5, 32.0, 28.3, 22.0, 13.1.

UHPLC-MS: *t*_R = 1.732 min (87%), *m/z*: calculated = 283.18 [M+H-Boc]⁺, found = 283.2 [M+H-Boc]⁺.

tert-Butyl (1-(3-(but-3-yn-1-yl)-3H-diazirin-3-yl)-2-oxo-6,9,12-trioxa-3-azatetradecan-14-yl)carbamate



Chemical Formula: C₂₀H₃₄N₄O₆

Exact Mass: 426.25

Molecular Weight: 426.51

70d

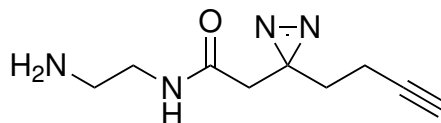
The synthesis is conducted according to the general procedure 5.16.1 using 0.20 mmol **69** as starting material. The crude product is purified by flash column chromatography (DCM/MeOH) to yield 60 mg (71 %) as a colourless oil.

¹H-NMR (600 MHz, CDCl₃): δ 6.31 (s, 1H), 5.02 (s, 1H), 3.68 – 3.61 (m, 8H), 3.56 (dt, J = 18.1, 5.1 Hz, 4H), 3.47 (d, J = 5.7 Hz, 2H), 3.31 (s, 2H), 2.25 (s, 1H), 2.07 (td, J = 7.3, 2.6 Hz, 2H), 1.78 (t, J = 7.3 Hz, 2H), 1.60 (s, 2H), 1.44 (s, 9H).

¹³C-NMR (151 MHz, CDCl₃): δ 70.4, 70.2, 41.4, 40.3, 39.3, 32.0, 28.5, 13.3.

UHPLC-MS: *t*_R = 1.739 min (83 %), *m/z*: calculated = 327.21 [M+H-Boc]⁺, found = 327.2 [M+H-Boc]⁺.

N-(2-Aminoethyl)-2-(3-(but-3-yn-1-yl)-3H-diazirin-3-yl)acetamide



Chemical Formula: C₉H₁₄N₄O

Exact Mass: 194.12

Molecular Weight: 194.23

71a

The synthesis is conducted according to the general procedure 5.16.1 using 0.16 mmol **70a** as starting material. The crude product is used without further purification with a yield of 26 mg (84 %) as a yellow oil.

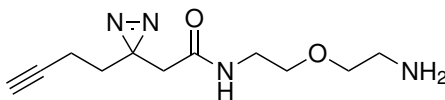
¹H-NMR (600 MHz, CDCl₃): δ 6.18 (s, 1H), 5.30 (s, 1H), 3.32 (q, J = 5.8 Hz, 2H), 2.86 (t, J = 5.9 Hz, 2H), 2.28 (s, 2H), 2.08 (td, J = 7.3, 2.6 Hz, 2H), 2.02 (t, J = 2.6 Hz, 1H), 1.78 (t, J = 7.3 Hz, 2H).

¹³C-NMR (151 MHz, CDCl₃): δ 53.5, 41.9, 41.6, 41.3, 32.2, 13.1.

UHPLC-MS: *t*_R = 0.772 min (*n.d.*), *m/z*: calculated = 195.13 [M+H]⁺, found = 195.2 [M+H]⁺.

GC-MS: *t*_R = 6.159 min (80 %), *m/z*: calculated = 194.12 [M]^{•+}, found = 194.04.

N-(2-(2-Aminoethoxy)ethyl)-2-(3-(but-3-yn-1-yl)-3H-diazirin-3-yl)acetamide



Chemical Formula: C₁₁H₁₈N₄O₂

Exact Mass: 238.14

Molecular Weight: 238.29

71b

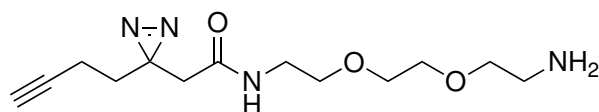
The synthesis is conducted according to the general procedure 5.16.1 using 0.16 mmol **70b** as starting material. The crude product is used without further purification with a yield of 36 mg (92 %) as a yellow oil.

¹H-NMR (600 MHz, CDCl₃): δ 6.18 (s, 1H), 5.30 (s, 1H), 3.32 (q, J = 5.8 Hz, 2H), 2.86 (t, J = 5.9 Hz, 2H), 2.28 (s, 2H), 2.08 (td, J = 7.3, 2.6 Hz, 2H), 2.02 (t, J = 2.6 Hz, 1H), 1.78 (t, J = 7.3 Hz, 2H).

¹³C-NMR (151 MHz, CDCl₃): δ 73.0, 69.4, 53.2, 41.6, 41.6, 39.3, 31.9, 13.1.

UHPLC-MS: *t*_R = 0.898 min (63 %), *m/z*: calculated = 239.15 [M+H]⁺, found = 239.2 [M+H]⁺.

N-(2-(2-(2-Aminoethoxy)ethoxy)ethyl)-2-(3-(but-3-yn-1-yl)-3H-diazirin-3-yl)acetamide



Chemical Formula: C₁₃H₂₂N₄O₃

Exact Mass: 282.17

Molecular Weight: 282.34

71c

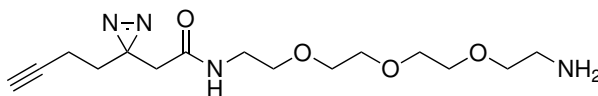
The synthesis is conducted according to the general procedure 5.16.1 using 0.14 mmol **70c** as starting material. The crude product is used without further purification with a yield of 36 mg (92%) as a yellow oil.

¹H-NMR (600 MHz, CDCl₃): δ 6.69 (s, 1H), 3.63 (s, 4H), 3.56 (dt, J = 15.7, 4.9 Hz, 4H), 3.49 – 3.43 (m, 2H), 2.88 (t, J = 5.2 Hz, 2H), 2.27 (s, 2H), 2.10 – 2.01 (m, 2H), 1.78 (t, J = 7.3 Hz, 4H).

¹³C-NMR (151 MHz, CDCl₃): δ 73.0, 70.0, 69.7, 53.2, 41.6, 41.3, 39.3, 32.2, 13.1.

UHPLC-MS: *t*_R = 1.035 min (61%), *m/z*: calculated = 283.18 [M+H]⁺, found = 283.2 [M+H]⁺.

N-(2-(2-(2-(2-Aminoethoxy)ethoxy)ethoxy)ethyl)-2-(3-(but-3-yn-1-yl)-3H-diazirin-3-yl)acetamide



Chemical Formula: C₁₅H₂₆N₄O₄

Exact Mass: 326.20

Molecular Weight: 326.39

71d

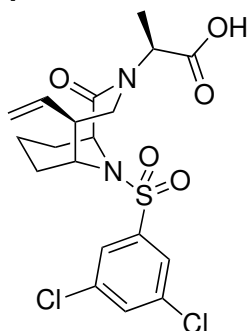
The synthesis is conducted according to the general procedure 5.16.1 using 0.14 mmol **70d** as starting material. The crude product is used without further purification with a yield of 46 mg (quant.) as a yellow oil.

¹H-NMR (600 MHz, CDCl₃): δ 7.20 (s, 1H), 5.30 (s, 1H), 3.68 – 3.60 (m, 9H), 3.54 (dt, J = 15.4, 4.9 Hz, 4H), 3.45 (q, J = 5.2 Hz, 2H), 2.85 (t, J = 5.1 Hz, 2H), 2.25 (s, 2H), 2.07 (td, J = 7.4, 2.6 Hz, 2H), 2.02 (t, J = 2.6 Hz, 1H), 1.79 (t, J = 7.4 Hz, 2H).

¹³C-NMR (151 MHz, CDCl₃): δ 73.0, 70.4, 70.0, 69.1, 53.2, 41.6, 41.3, 39.3, 32.2, 13.1.

UHPLC-MS: *t*_R = 1.446 min (77%), *m/z*: calculated = 327.21 [M+H]⁺, found = 327.2 [M+H]⁺.

(2S)-2-((5S)-10-((3,5-Dichlorophenyl)sulfonyl)-2-oxo-5-vinyl-3,10-diazabicyclo[4.3.1]decan-3-yl)propanoic acid



Chemical Formula: C₁₉H₂₂Cl₂N₂O₅S

Exact Mass: 460.06

Molecular Weight: 461.36

73

310 mg (0.69 mmol, 1.0 eq) **72**, kindly provided by Patrick Purder, are dissolved in 10 mL acetone and cooled down to 0 °C. 0.7 mL (1.39 mmol, 2.0 eq) Jones reagent are added slowly to the aforementioned solution. The mixture is stirred for 2 h before the reaction is quenched by addition of IPA. The mixture is extracted with EA, dried over MgSO₄, and volatiles are removed under reduced pressure. The crude product is purified by flash column chromatography (Cy/EA+1 % FA) to yield 293 mg (92 %) as a white solid.

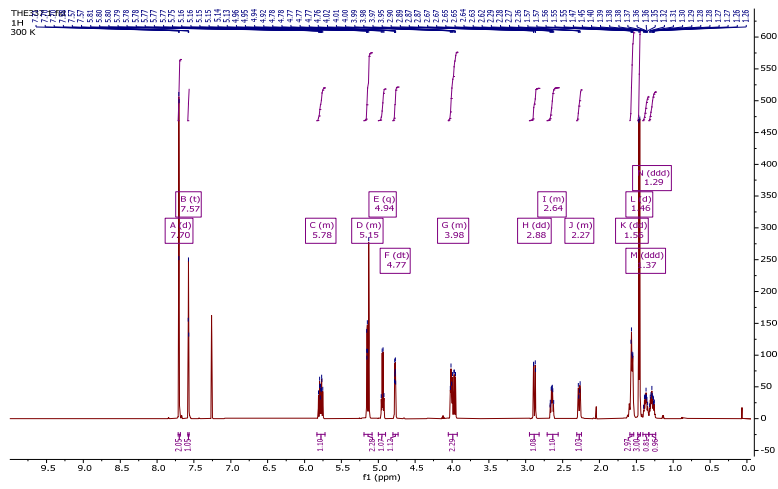
¹H-NMR (600 MHz, CDCl₃): δ 7.70 (d, J = 1.8 Hz, 2H), 7.57 (t, J = 1.8 Hz, 1H), 5.83 – 5.72 (m, 1H), 5.19 – 5.08 (m, 2H), 4.94 (q, J = 7.0 Hz, 1H), 4.77 (dt, J = 6.0, 1.9 Hz, 1H), 4.05 – 3.93 (m, 2H), 2.88 (dd, J = 14.7, 1.9 Hz, 1H), 2.71 – 2.56 (m, 1H), 2.31 – 2.24 (m, 1H), 1.56 (dd, J = 11.4, 3.9 Hz, 3H), 1.46 (d, J = 7.1 Hz, 3H), 1.37 (ddd, J = 12.8, 10.0, 6.3 Hz, 1H), 1.29 (ddd, J = 13.8, 11.8, 6.0 Hz, 1H).

¹³C-NMR (151 MHz, CDCl₃): δ 175.5, 170.5, 144.0, 137.2, 136.6, 133.0, 125.1, 117.3, 57.6, 56.9, 55.2, 50.2, 49.8, 28.0, 26.6, 15.6, 14.6.

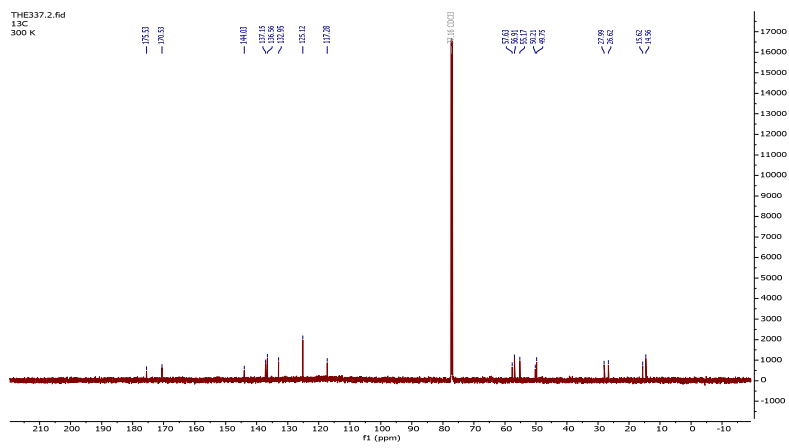
UHPLC-MS: *t*_R = 2.077 min (95 %), *m/z*: calculated = 461.07 [M+H]⁺, found = 461.0 [M+H]⁺.

HRMS: *m/z* = 461.0693 [M+H]⁺ (1.33 ppm error)

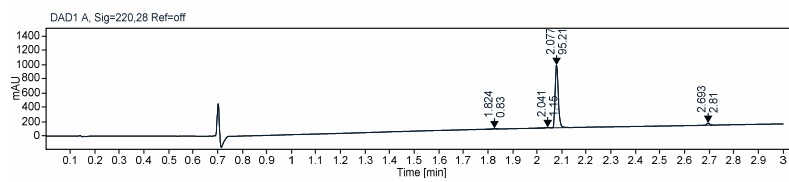
¹H-NMR



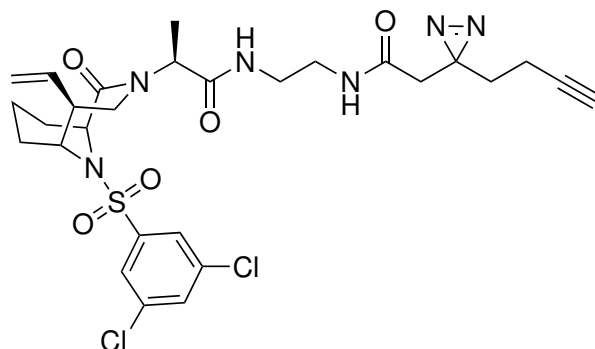
¹³C-NMR



UHPLC, UV 220 nm



(2S)-N-(2-(2-(3-(But-3-yn-1-yl)-3H-diazirin-3-yl)acetamido)ethyl)-2-((5S)-10-((3,5-dichlorophenyl)sulfonyl)-2-oxo-5-vinyl-3,10-diazabicyclo[4.3.1]decan-3-yl)propanamide



Chemical Formula: C₂₈H₃₄Cl₂N₆O₅S

Exact Mass: 636.17

Molecular Weight: 637.58

74a

The synthesis is conducted according to the general procedure 5.16.1 using 0.06 mmol **73** and **71a** as starting materials. The crude product is purified by preparative HPLC and flash column chromatography (DCM/MeCN+1 % FA) 16 mg (41 %) as a white solid.

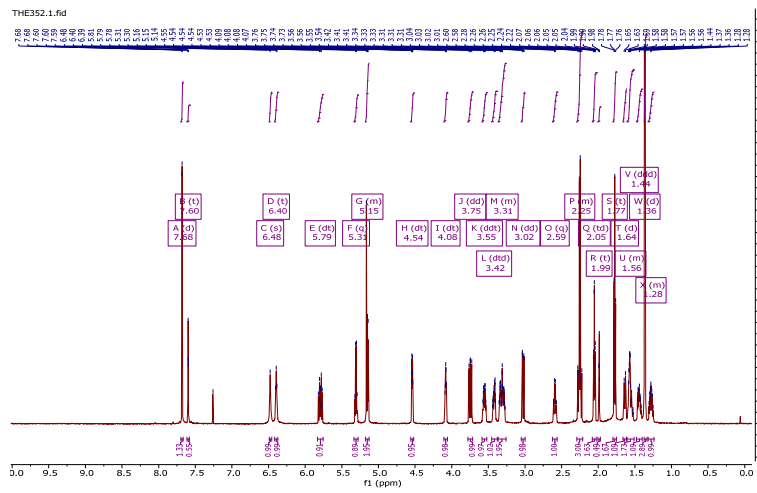
¹H-NMR (700 MHz, CDCl₃): δ 7.68 (d, J = 1.8 Hz, 1H), 7.60 (t, J = 1.8 Hz, 1H), 6.48 (s, 1H), 6.40 (t, J = 6.0 Hz, 1H), 5.79 (dt, J = 17.2, 9.3 Hz, 1H), 5.31 (q, J = 6.9 Hz, 1H), 5.18 – 5.13 (m, 2H), 4.54 (dt, J = 6.6, 2.0 Hz, 1H), 4.08 (dt, J = 6.6, 3.2 Hz, 1H), 3.75 (dd, J = 14.7, 10.8 Hz, 1H), 3.55 (ddt, J = 14.0, 7.0, 3.6 Hz, 1H), 3.42 (dtd, J = 10.9, 5.7, 2.7 Hz, 1H), 3.37 – 3.26 (m, 2H), 3.02 (dd, J = 14.6, 1.9 Hz, 1H), 2.59 (q, J = 8.8 Hz, 1H), 2.29 – 2.21 (m, 3H), 2.05 (td, J = 7.4, 2.6 Hz, 2H), 1.99 (t, J = 2.6 Hz, 0H), 1.77 (t, J = 7.4 Hz, 2H), 1.64 (d, J = 13.7 Hz, 1H), 1.61 – 1.51 (m, 2H), 1.44 (ddd, J = 17.7, 11.1, 5.2 Hz, 1H), 1.36 (d, J = 7.0 Hz, 3H), 1.32 – 1.24 (m, 1H).

¹³C-NMR (176 MHz, CDCl₃): δ 171.2, 168.3, 143.4, 136.7, 136.5, 133.3, 125.0, 117.8, 82.9, 57.0, 55.4, 54.8, 49.6, 46.9, 41.3, 40.4, 39.6, 32.2, 27.5, 26.7, 26.3, 15.4, 13.4, 13.4.

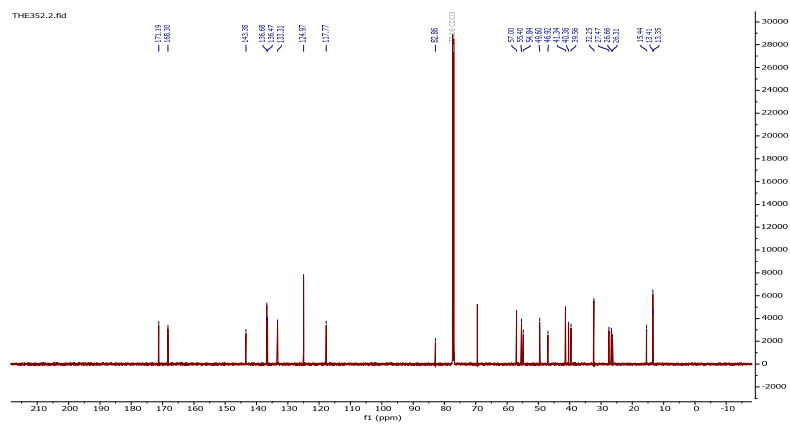
UHPLC-MS: *t*_R = 2.135 min (99 %), *m/z*: calculated = 637.17 [M+H]⁺, found = 637.2 [M+H]⁺.

HRMS: *m/z* = 637.1671 [M+H]⁺ (0.02 ppm error)

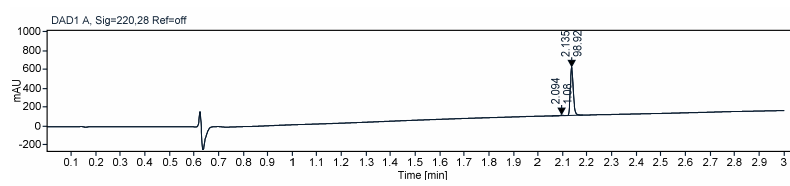
¹H-NMR



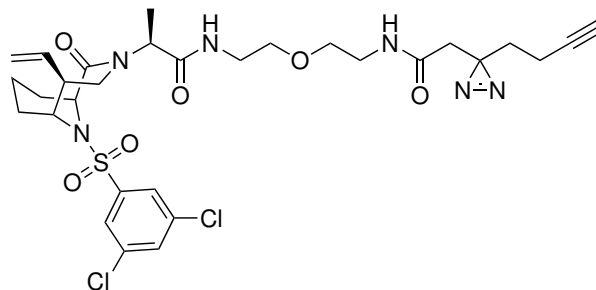
¹³C-NMR



UHPLC, UV 220 nm



(2S)-N-(2-(2-(2-(3-(But-3-yn-1-yl)-3H-diazirin-3-yl)acetamido)ethoxy)ethyl)-2-((5S)-10-((3,5-dichlorophenyl)sulfonyl)-2-oxo-5-vinyl-3,10-diazabicyclo[4.3.1]decan-3-yl)propanamide



Chemical Formula: C₃₀H₃₈Cl₂N₆O₆S

Exact Mass: 680.20

Molecular Weight: 681.63

74b

The synthesis is conducted according to the general procedure 5.16.1 using 0.07 mmol **73** and **71b** as starting materials. The crude product is purified by preparative HPLC and flash column chromatography (DCM/MeCN+1 % FA) 24 mg (49 %) as a white solid.

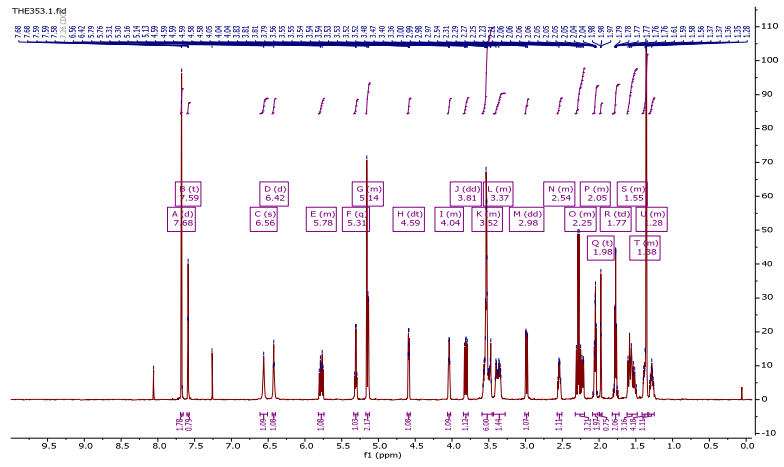
¹H-NMR (700 MHz, CDCl₃): δ 7.68 (d, J = 1.8 Hz, 2H), 7.59 (t, J = 1.8 Hz, 1H), 6.56 (s, 1H), 6.42 (d, J = 6.1 Hz, 1H), 5.82 – 5.74 (m, 1H), 5.31 (q, J = 6.9 Hz, 1H), 5.17 – 5.12 (m, 2H), 4.59 (dt, J = 6.4, 1.9 Hz, 1H), 4.06 – 4.02 (m, 1H), 3.81 (dd, J = 14.8, 10.9 Hz, 1H), 3.59 – 3.45 (m, 6H), 3.44 – 3.28 (m, 1H), 2.98 (dd, J = 14.7, 1.9 Hz, 1H), 2.57 – 2.51 (m, 1H), 2.32 – 2.20 (m, 3H), 2.09 – 2.01 (m, 2H), 1.98 (t, J = 2.6 Hz, 1H), 1.77 (td, J = 7.6, 1.7 Hz, 2H), 1.62 – 1.48 (m, 3H), 1.41 – 1.34 (m, 4H), 1.32 – 1.25 (m, 1H).

¹³C-NMR (176 MHz, CDCl₃): δ 171.3, 170.4, 168.1, 162.3, 143.6, 136.5, 133.2, 124.9, 117.7, 69.6, 69.5, 69.4, 57.1, 55.3, 54.8, 49.9, 46.8, 41.2, 39.6, 39.5, 32.3, 27.7, 26.6, 26.4, 15.4, 13.4, 13.4.

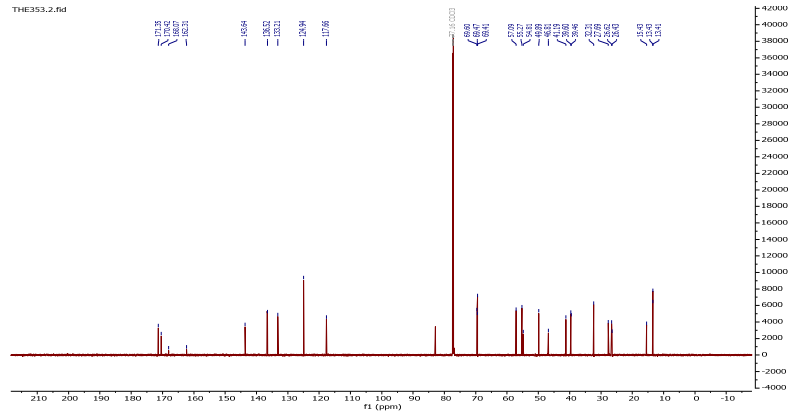
UHPLC-MS: *t*_R = 2.142 min (99%), *m/z*: calculated = 681.20 [M+H]⁺, found = 681.2 [M+H]⁺.

HRMS: *m/z* = 681.2019 [M+H]⁺ (0.71 ppm error)

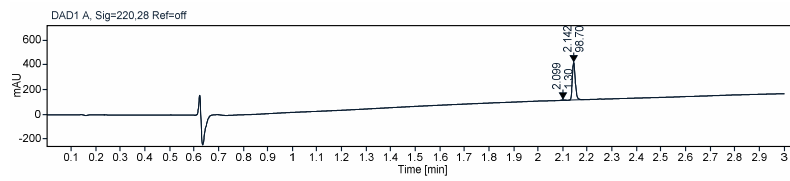
¹H-NMR



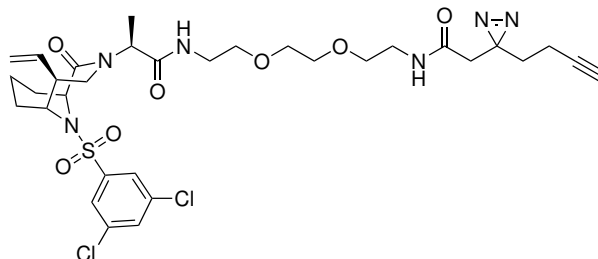
¹³C-NMR



UHPLC, UV 220 nm



(2S)-N-(2-(2-(2-(2-(3-(But-3-yn-1-yl)-3H-diazirin-3-yl)acetamido)ethoxy)ethoxy)ethyl)-2-((5S)-10-((3,5-dichlorophenyl)sulfonyl)-2-oxo-5-vinyl-3,10-diazabicyclo[4.3.1]decan-3-yl)propanamide



Chemical Formula: C₃₂H₄₂Cl₂N₆O₇S

Exact Mass: 724.22

Molecular Weight: 725.68

74c

The synthesis is conducted according to the general procedure 5.16.1 using 0.06 mmol **73** and **71c** as starting materials. The crude product is purified by preparative HPLC and flash column chromatography (DCM/MeCN+1 % FA) 21 mg (48 %) as a white solid.

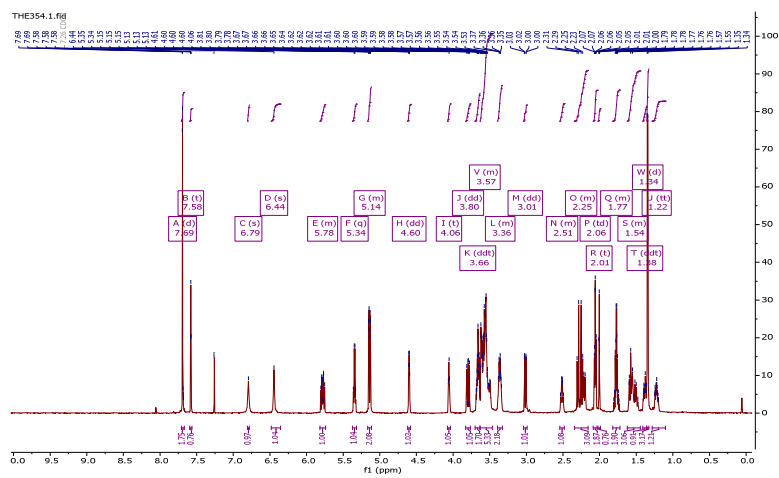
¹H-NMR (700 MHz, CDCl₃): δ 7.69 (d, J = 1.8 Hz, 2H), 7.58 (t, J = 1.8 Hz, 1H), 6.79 (s, 1H), 6.44 (s, 1H), 5.82 – 5.74 (m, 1H), 5.34 (q, J = 6.9 Hz, 1H), 5.16 – 5.11 (m, 2H), 4.60 (dd, J = 5.1, 3.2 Hz, 1H), 4.06 (t, J = 5.8 Hz, 1H), 3.80 (dd, J = 14.8, 10.8 Hz, 1H), 3.66 (ddt, J = 15.0, 9.6, 5.3 Hz, 2H), 3.63 – 3.46 (m, 6H), 3.39 – 3.33 (m, 2H), 3.01 (dd, J = 14.7, 1.9 Hz, 1H), 2.54 – 2.48 (m, 1H), 2.34 – 2.16 (m, 3H), 2.06 (td, J = 7.4, 2.6 Hz, 2H), 2.01 (t, J = 2.6 Hz, 1H), 1.82 – 1.72 (m, 2H), 1.62 – 1.44 (m, 3H), 1.38 (ddt, J = 13.2, 8.6, 4.7 Hz, 1H), 1.34 (d, J = 6.9 Hz, 3H), 1.22 (tt, J = 13.2, 4.9 Hz, 1H).

¹³C-NMR (176 MHz, CDCl₃): δ 171.1, 170.3, 168.0, 143.8, 136.6, 133.1, 125.0, 117.5, 82.9, 70.5, 70.3, 70.0, 69.6, 57.0, 55.3, 54.4, 50.1, 46.5, 41.3, 39.6, 39.5, 32.3, 27.7, 26.6, 26.4, 15.5, 13.5, 13.4.

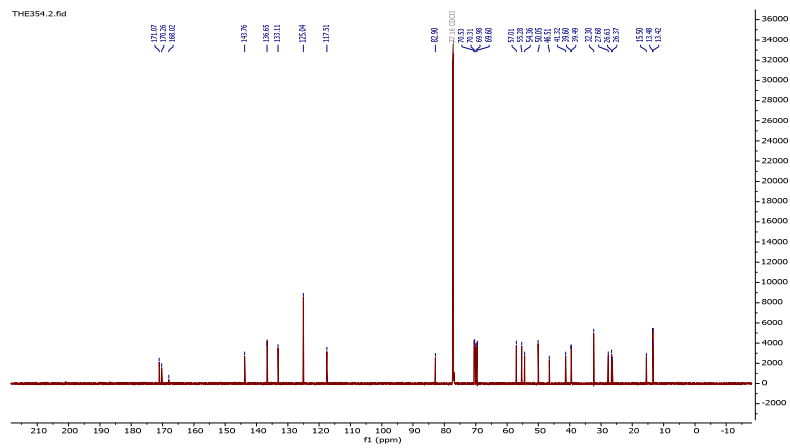
UHPLC-MS: *t*_R = 2.163 min (96 %), *m/z*: calculated = 725.23 [M+H]⁺, found = 725.20 [M+H]⁺.

HRMS: *m/z* = 725.2289 [M+H]⁺ (0.54 ppm error)

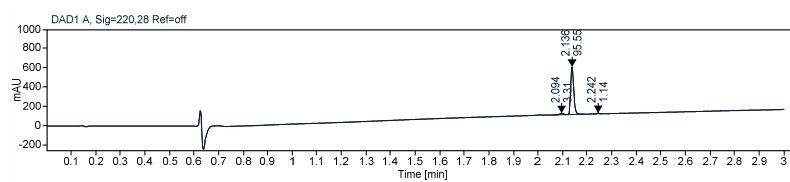
¹H-NMR



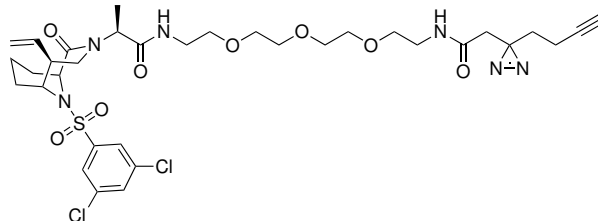
¹³C-NMR



UHPLC, UV 220 nm



(2S)-N-(1-(3-(But-3-yn-1-yl)-3H-diazirin-3-yl)-2-oxo-6,9,12-trioxa-3-azatetradecan-14-yl)-2-((5S)-10-((3,5-dichlorophenyl)sulfonyl)-2-oxo-5-vinyl-3,10-diazabicyclo[4.3.1]decan-3-yl)propanamide



Chemical Formula: C₃₄H₄₆Cl₂N₆O₈S

Exact Mass: 768.25

Molecular Weight: 769.74

74d

The synthesis is conducted according to the general procedure 5.16.1 using 0.06 mmol **73** and **71d** as starting materials. The crude product is purified by preparative HPLC and flash column chromatography (DCM/MeCN+1 % FA) 29 mg (56 %) as a white solid.

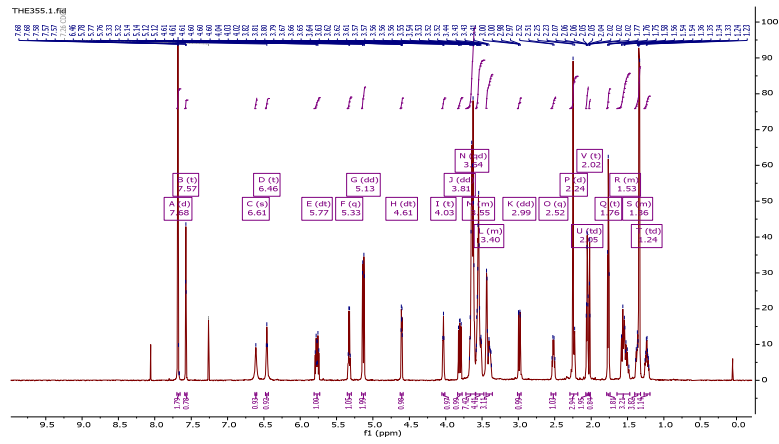
¹H-NMR (700 MHz, CDCl₃): δ 7.68 (d, J = 1.8 Hz, 2H), 7.57 (t, J = 1.8 Hz, 1H), 6.61 (s, 1H), 6.46 (t, J = 5.6 Hz, 1H), 5.77 (dt, J = 17.1, 9.3 Hz, 1H), 5.33 (q, J = 6.9 Hz, 1H), 5.13 (dd, J = 13.8, 3.2 Hz, 2H), 4.61 (dt, J = 6.2, 1.9 Hz, 1H), 4.03 (t, J = 5.6 Hz, 1H), 3.81 (dd, J = 14.8, 10.8 Hz, 1H), 3.64 (qd, J = 9.4, 4.1 Hz, 7H), 3.59 – 3.48 (m, 4H), 3.45 – 3.36 (m, 3H), 2.99 (dd, J = 14.8, 1.8 Hz, 1H), 2.52 (q, J = 8.8 Hz, 1H), 2.24 (d, J = 14.8 Hz, 3H), 2.05 (td, J = 7.4, 2.6 Hz, 2H), 2.02 (t, J = 2.6 Hz, 1H), 1.76 (t, J = 7.4 Hz, 2H), 1.64 – 1.47 (m, 3H), 1.40 – 1.32 (m, 4H), 1.24 (td, J = 13.2, 6.7 Hz, 1H).

¹³C-NMR (176 MHz, CDCl₃): δ 171.0, 170.3, 168.0, 143.8, 136.7, 133.1, 125.0, 117.5, 82.9, 70.6, 70.6, 70.5, 70.5, 70.4, 69.8, 69.7, 69.6, 57.0, 55.2, 54.7, 49.9, 46.8, 41.4, 39.7, 39.5, 32.2, 27.6, 26.5, 26.3, 15.5, 13.6, 13.4.

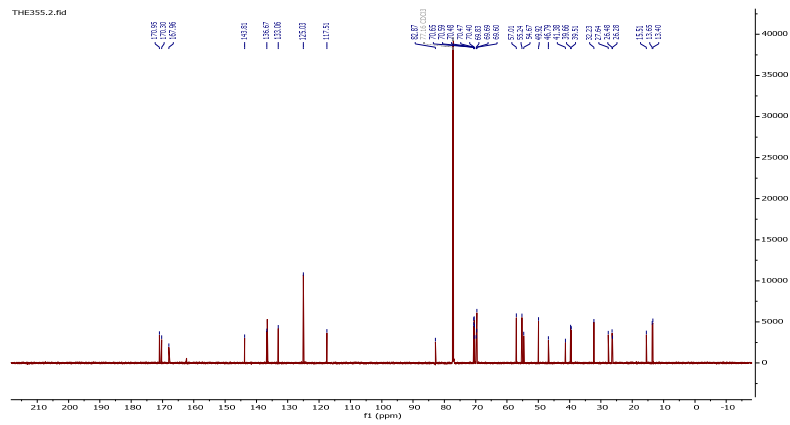
UHPLC-MS: *t*_R = 2.133 min (95 %), *m/z*: calculated = 769.25 [M+H]⁺, found = 769.2 [M+H]⁺.

HRMS: *m/z* = 769.2540 [M+H]⁺ (0.98 ppm error)

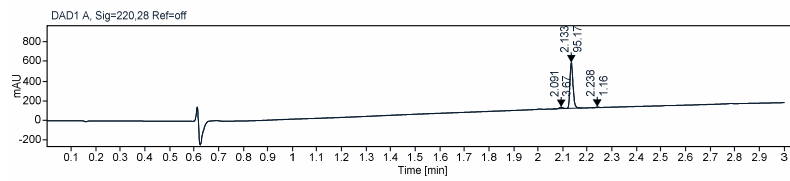
¹H-NMR



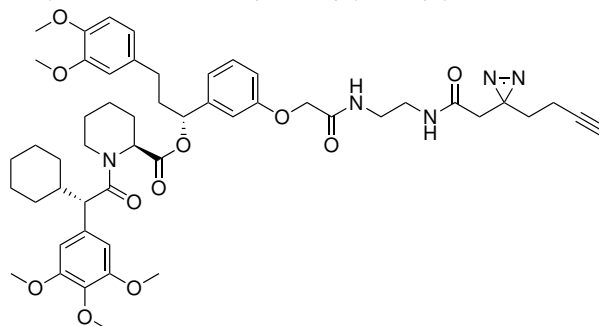
¹³C-NMR



UHPLC, UV 220 nm



**(S)-(R)-1-(3-(2-((2-(2-(3-(But-3-yn-1-yl)-3H-diazirin-3-yl)acetamido)ethyl)amino)-2-oxoethoxy)phenyl)-3-(3,4-dimethoxyphenyl)propyl
1-((S)-2-cyclohexyl-2-(3,4,5-trimethoxyphenyl)acetyl)piperidine-2-carboxylate**



Chemical Formula: C₅₁H₆₅N₅O₁₁

Exact Mass: 923.47

Molecular Weight: 924.09

75a

The synthesis is conducted according to the general procedure 5.16.1 using 0.06 mmol **6** and **71a** as starting materials. The crude product is purified by preparative HPLC and flash column chromatography (DCM/MeCN+1 % FA) 23 mg (40 %) as a white solid.

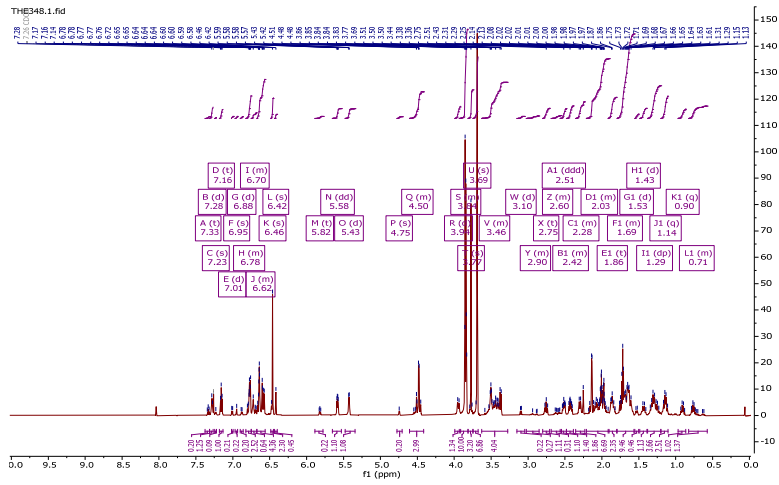
¹H-NMR (700 MHz, CDCl₃): δ 7.33 (t, J = 7.9 Hz, 0H), 7.28 (d, J = 6.3 Hz, 1H), 7.23 (s, 0H), 7.16 (t, J = 7.9 Hz, 1H), 7.01 (d, J = 7.6 Hz, 0H), 6.95 (s, 0H), 6.88 (d, J = 8.5 Hz, 0H), 6.82 – 6.75 (m, 3H), 6.75 – 6.67 (m, 1H), 6.67 – 6.56 (m, 4H), 6.46 (s, 2H), 6.42 (s, 0H), 5.82 (t, J = 6.8 Hz, 0H), 5.58 (dd, J = 8.4, 5.3 Hz, 1H), 5.43 (d, J = 5.7 Hz, 1H), 4.75 (s, 0H), 4.61 – 4.41 (m, 3H), 3.94 (d, J = 13.6 Hz, 1H), 3.93 – 3.81 (m, 10H), 3.77 (s, 3H), 3.69 (s, 7H), 3.63 – 3.28 (m, 4H), 3.10 (d, J = 9.6 Hz, 0H), 3.02 – 2.85 (m, 0H), 2.75 (t, J = 12.9 Hz, 1H), 2.69 – 2.55 (m, 0H), 2.51 (ddd, J = 14.3, 9.3, 5.3 Hz, 1H), 2.48 – 2.38 (m, 1H), 2.35 – 2.23 (m, 2H), 2.21 – 1.90 (m, 7H), 1.86 (t, J = 13.9 Hz, 2H), 1.79 – 1.56 (m, 9H), 1.53 (d, J = 13.1 Hz, 0H), 1.43 (d, J = 13.4 Hz, 1H), 1.29 (dp, J = 25.7, 12.9 Hz, 4H), 1.14 (q, J = 12.9 Hz, 3H), 0.90 (q, J = 12.0 Hz, 1H), 0.82 – 0.57 (m, 1H).

¹³C-NMR (176 MHz, CDCl₃): δ 172.6, 170.6, 169.8, 168.7, 157.4, 153.1, 149.0, 147.5, 142.5, 136.8, 133.7, 133.4, 129.9, 120.4, 120.3, 120.1, 114.0, 113.6, 113.2, 111.9, 111.8, 111.6, 111.5, 105.9, 82.8, 76.6, 75.6, 69.6, 69.5, 67.4, 61.0, 60.9, 56.5, 56.1, 56.1, 56.1, 56.0, 55.2, 52.2, 43.8, 41.5, 41.4, 41.2, 40.4, 40.3, 39.4, 38.2, 32.9, 32.2, 32.2, 31.3, 30.8, 26.8, 26.7, 26.3, 26.3, 26.1, 25.6, 21.1, 13.4, 13.4.

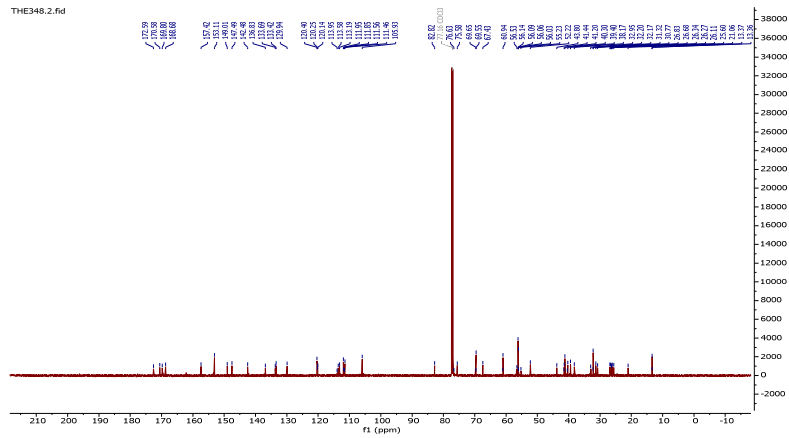
UHPLC-MS: *t*_R = 2.340 min (99 %), *m/z*: calculated = 924.47 [M+H]⁺, found = 924.4 [M+H]⁺.

HRMS: *m/z* = 924.4736 [M+H]⁺ (1.84 ppm error)

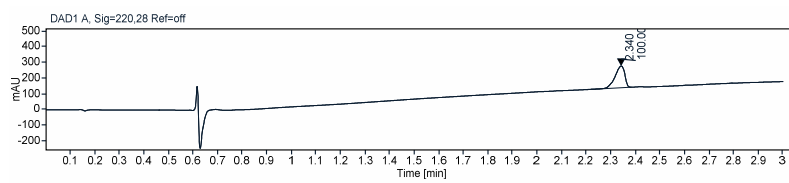
¹H-NMR



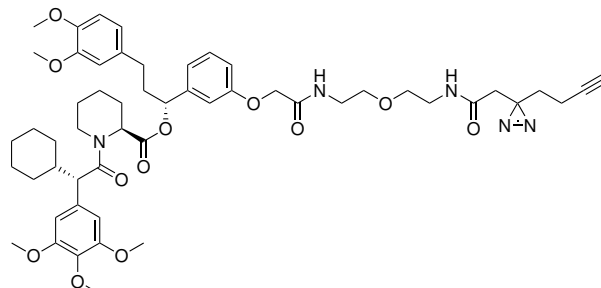
¹³C-NMR



UHPLC, UV 220 nm



**(S)-(R)-1-(3-(2-((2-(2-(2-(3-(But-3-yn-1-yl)-3H-diazirin-3-yl)acetamido)ethoxy)ethyl)amino)-2-oxoethoxy)phenyl)-3-(3,4-dimethoxyphenyl)propyl
1-((S)-2-cyclohexyl-2-(3,4,5-trimethoxyphenyl)acetyl)piperidine-2-carboxylate**



Chemical Formula: $C_{53}H_{69}N_5O_{12}$
Exact Mass: 967.49
Molecular Weight: 968.14

75b

The synthesis is conducted according to the general procedure 5.16.1 using 0.07 mmol **6** and **71b** as starting materials. The crude product is purified by preparative HPLC and flash column chromatography (DCM/MeCN+1 % FA) 32 mg (46 %) as a white solid.

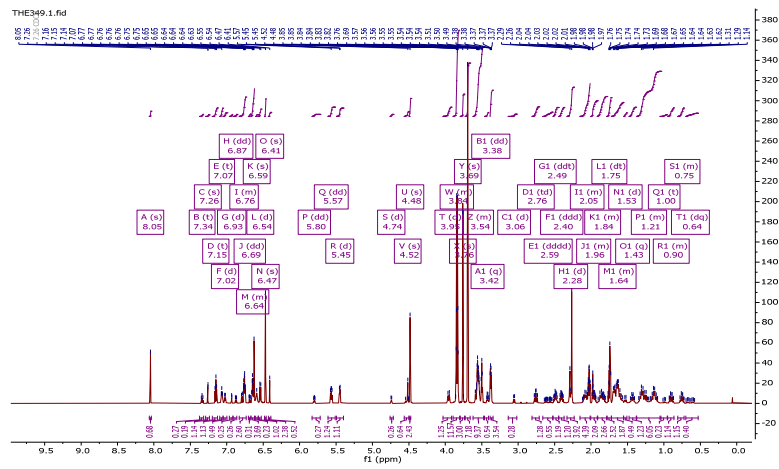
$^1\text{H-NMR}$ (700 MHz, CDCl_3): δ 8.05 (s, 1H), 7.34 (t, $J = 8.0$ Hz, 0H), 7.26 (s, 0H), 7.15 (t, $J = 7.9$ Hz, 1H), 7.07 (t, $J = 5.8$ Hz, 1H), 7.02 (d, $J = 7.2$ Hz, 0H), 6.93 (d, $J = 2.4$ Hz, 0H), 6.87 (dd, $J = 8.1, 2.5$ Hz, 0H), 6.83 – 6.73 (m, 3H), 6.69 (dd, $J = 8.1, 2.0$ Hz, 0H), 6.67 – 6.62 (m, 4H), 6.59 (s, 0H), 6.54 (d, $J = 7.7$ Hz, 1H), 6.47 (s, 2H), 6.41 (s, 1H), 5.80 (dd, $J = 7.7, 6.2$ Hz, 0H), 5.57 (dd, $J = 8.4, 5.4$ Hz, 1H), 5.45 (d, $J = 5.6$ Hz, 1H), 4.74 (d, $J = 5.7$ Hz, 0H), 4.52 (s, 1H), 4.48 (s, 2H), 3.95 (d, $J = 13.6$ Hz, 1H), 3.89 – 3.80 (m, 12H), 3.76 (s, 3H), 3.69 (s, 7H), 3.62 – 3.48 (m, 9H), 3.42 (q, $J = 5.3$ Hz, 1H), 3.38 (dd, $J = 7.6, 2.5$ Hz, 4H), 3.06 (d, $J = 9.7$ Hz, 0H), 2.76 (td, $J = 13.3, 2.9$ Hz, 1H), 2.59 (dddd, $J = 42.5, 14.3, 9.5, 5.9$ Hz, 1H), 2.49 (ddt, $J = 13.3, 9.4, 4.7$ Hz, 1H), 2.40 (ddd, $J = 13.7, 8.7, 6.9$ Hz, 1H), 2.28 (d, $J = 18.7$ Hz, 4H), 2.15 – 2.01 (m, 4H), 2.00 – 1.91 (m, 2H), 1.92 – 1.78 (m, 3H), 1.75 (dt, $J = 9.4, 7.5$ Hz, 3H), 1.72 – 1.56 (m, 2H), 1.53 (d, $J = 12.5$ Hz, 0H), 1.43 (q, $J = 13.0$ Hz, 1H), 1.37 – 1.04 (m, 6H), 1.00 (t, $J = 12.6$ Hz, 0H), 0.95 – 0.86 (m, 1H), 0.81 – 0.72 (m, 1H), 0.64 (dq, $J = 46.9, 11.9$ Hz, 0H).

$^{13}\text{C-NMR}$ (176 MHz, CDCl_3): δ 172.7, 170.6, 170.6, 168.7, 168.3, 162.7, 157.4, 157.2, 153.5, 149.1, 149.0, 147.7, 147.5, 142.1, 137.2, 136.9, 134.2, 133.6, 133.4, 133.2, 130.3, 130.0, 120.4, 120.2, 120.1, 114.1, 114.0, 113.6, 113.5, 111.9, 111.8, 111.5, 111.5, 105.9, 105.4, 82.8, 82.8, 76.7, 75.5, 69.8, 69.8, 69.5, 69.5, 69.4, 67.5, 67.4, 60.9, 56.5, 56.1, 56.1, 56.0, 55.9, 55.2, 52.2, 43.8, 41.4, 41.3, 41.2, 39.8, 39.6, 39.5, 38.9, 38.9, 38.1, 37.9, 33.2, 32.9, 32.2, 31.6, 31.2, 30.7, 30.7, 26.8, 26.7, 26.6, 26.6, 26.3, 26.2, 26.2, 25.6, 24.5, 21.0, 20.7, 13.3.

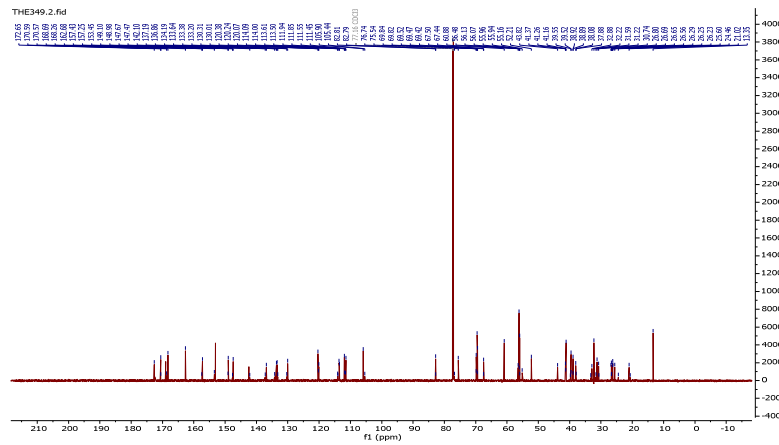
UHPLC-MS: $t_R = 2.335$ min (98 %), m/z : calculated = 968.50 $[\text{M}+\text{H}]^+$, found = 968.4 $[\text{M}+\text{H}]^+$.

HRMS: $m/z = 968.5002$ $[\text{M}+\text{H}]^+$ (1.41 ppm error)

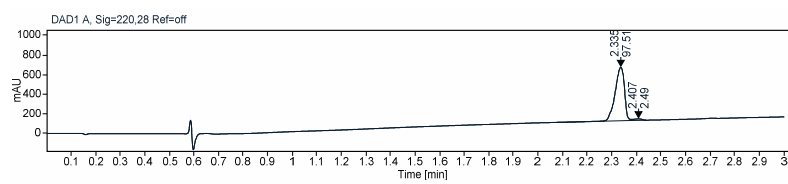
¹H-NMR



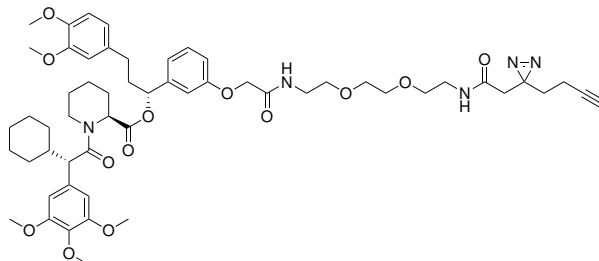
¹³C-NMR



UHPLC, UV 220 nm



**(S)-(R)-1-(3-((14-(3-(But-3-yn-1-yl)-3H-diazirin-3-yl)-2,13-dioxo-6,9-dioxa-3,12-diazatetradecyl)oxy)phenyl)-3-(3,4-dimethoxyphenyl)propyl
1-((S)-2-cyclohexyl-2-(3,4,5-trimethoxyphenyl)acetyl)piperidine-2-carboxylate**



Chemical Formula: C₅₅H₇₃N₅O₁₃

Exact Mass: 1011.52

Molecular Weight: 1012.19

75c

The synthesis is conducted according to the general procedure 5.16.1 using 0.06 mmol **6** and **71c** as starting materials. The crude product is purified by preparative HPLC and flash column chromatography (DCM/MeCN+1 % FA) 23 mg (38 %) as a white solid.

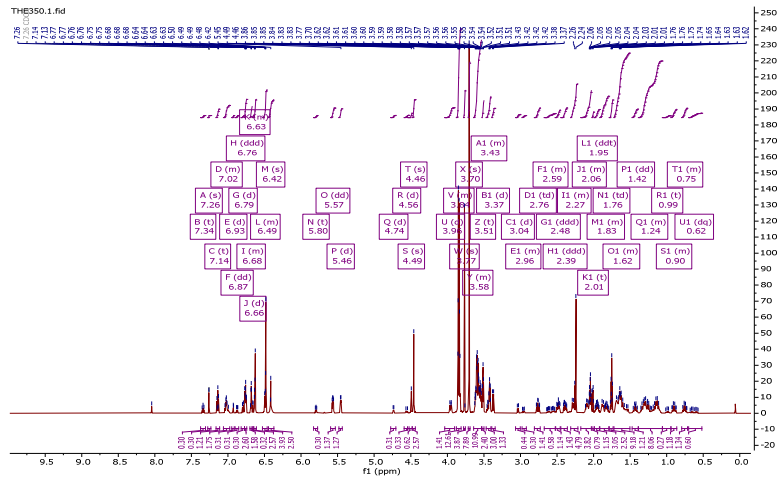
¹H-NMR (700 MHz, CDCl₃): δ 7.34 (t, J = 7.9 Hz, 0H), 7.26 (s, 0H), 7.14 (t, J = 7.9 Hz, 1H), 7.06 – 6.98 (m, 2H), 6.93 (d, J = 2.5 Hz, 0H), 6.87 (dd, J = 8.0, 2.6 Hz, 0H), 6.79 (d, J = 8.1 Hz, 0H), 6.76 (ddd, J = 6.2, 4.8, 2.2 Hz, 3H), 6.70 – 6.67 (m, 2H), 6.66 (d, J = 2.0 Hz, 0H), 6.65 – 6.61 (m, 3H), 6.53 – 6.46 (m, 4H), 6.42 (s, 3H), 5.80 (t, J = 6.9 Hz, 0H), 5.57 (dd, J = 8.3, 5.4 Hz, 1H), 5.46 (d, J = 5.7 Hz, 1H), 4.74 (d, J = 5.7 Hz, 0H), 4.56 (d, J = 13.4 Hz, 0H), 4.49 (s, 1H), 4.46 (s, 3H), 3.96 (d, J = 13.8 Hz, 1H), 3.88 – 3.81 (m, 13H), 3.77 (s, 4H), 3.70 (s, 8H), 3.64 – 3.53 (m, 11H), 3.51 (t, J = 5.2 Hz, 2H), 3.47 – 3.40 (m, 3H), 3.37 (d, J = 9.8 Hz, 1H), 3.04 (d, J = 9.7 Hz, 0H), 2.98 – 2.92 (m, 0H), 2.76 (td, J = 13.3, 2.9 Hz, 1H), 2.67 – 2.52 (m, 1H), 2.48 (ddd, J = 14.4, 9.3, 5.2 Hz, 1H), 2.39 (ddd, J = 14.9, 9.0, 7.0 Hz, 1H), 2.31 – 2.21 (m, 5H), 2.17 – 2.03 (m, 4H), 2.01 (t, J = 2.6 Hz, 1H), 1.95 (ddt, J = 13.9, 8.8, 4.4 Hz, 1H), 1.91 – 1.79 (m, 3H), 1.76 (td, J = 7.4, 4.5 Hz, 3H), 1.72 – 1.50 (m, 9H), 1.42 (dd, J = 15.0, 10.9 Hz, 1H), 1.39 – 1.06 (m, 8H), 0.99 (t, J = 12.6 Hz, 0H), 0.94 – 0.86 (m, 1H), 0.79 – 0.72 (m, 1H), 0.62 (dq, J = 37.4, 11.6 Hz, 1H).

¹³C-NMR (176 MHz, CDCl₃): δ 172.5, 170.7, 168.5, 167.9, 157.5, 157.3, 153.4, 153.2, 149.1, 149.0, 147.5, 142.4, 137.0, 133.7, 133.4, 130.0, 120.4, 120.2, 119.9, 113.7, 113.6, 111.9, 111.8, 111.6, 111.5, 105.9, 105.5, 82.8, 76.8, 75.5, 70.5, 70.3, 69.9, 69.8, 69.8, 69.8, 69.6, 69.6, 67.5, 61.0, 60.9, 56.5, 56.2, 56.1, 56.1, 56.0, 55.9, 55.2, 52.2, 43.8, 41.5, 41.4, 41.4, 39.5, 39.5, 39.0, 38.9, 38.2, 33.2, 32.9, 32.2, 31.6, 31.2, 30.8, 26.8, 26.7, 26.3, 26.3, 25.7, 21.1, 13.4.

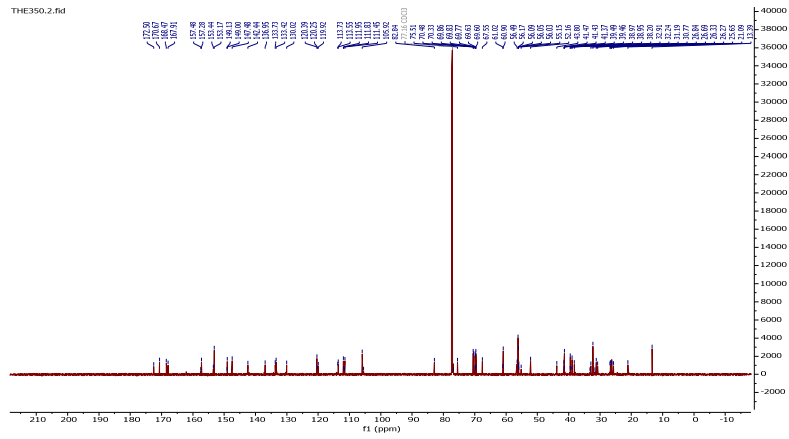
UHPLC-MS: *t*_R = 2.328 min (99 %), *m/z*: calculated = 1012.53 [M+H]⁺, found = 1012.60 [M+H]⁺.

HRMS: *m/z* = 1012.5258 [M+H]⁺ (1.90 ppm error)

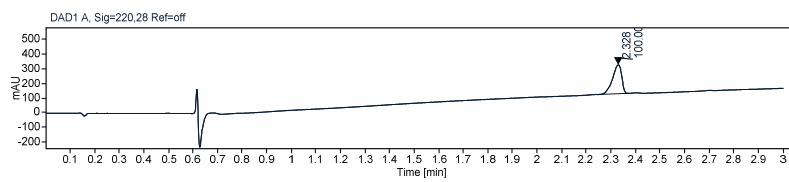
¹H-NMR



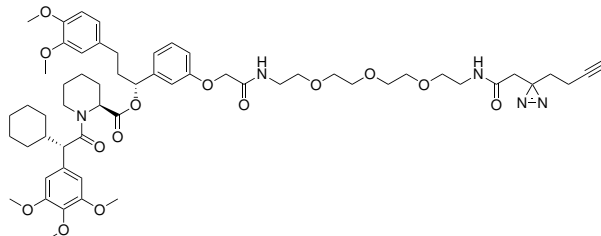
¹³C-NMR



UHPLC, UV 220 nm



**(S)-(R)-1-(3-((17-(3-(But-3-yn-1-yl)-3H-diazirin-3-yl)-2,16-dioxo-6,9,12-trioxa-3,15-diazaheptadecyl)oxy)phenyl)-3-(3,4-dimethoxyphenyl)propyl
1-((S)-2-cyclohexyl-2-(3,4,5-trimethoxyphenyl)acetyl)piperidine-2-carboxylate**



Chemical Formula: C₅₇H₇₇N₅O₁₄
Exact Mass: 1055.55
Molecular Weight: 1056.25

75d

The synthesis is conducted according to the general procedure 5.16.1 using 0.07 mmol **6** and **71d** as starting materials. The crude product is purified by preparative HPLC and flash column chromatography (DCM/MeCN+1 % FA) 21 mg (30 %) as a white solid.

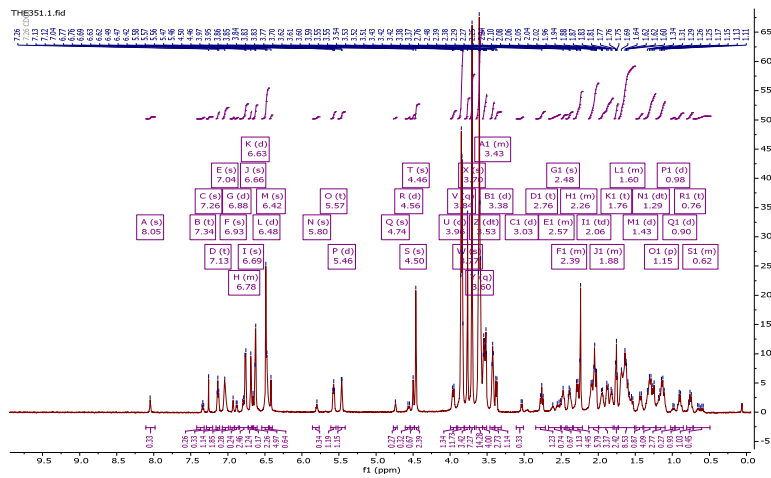
¹H-NMR (700 MHz, CDCl₃): δ 8.05 (s, 0H), 7.34 (t, J = 8.0 Hz, 0H), 7.26 (s, 0H), 7.13 (t, J = 8.0 Hz, 1H), 7.04 (s, 2H), 6.93 (s, 0H), 6.88 (d, J = 8.2 Hz, 0H), 6.84 – 6.73 (m, 2H), 6.69 (s, 1H), 6.66 (s, 0H), 6.63 (d, J = 5.9 Hz, 2H), 6.48 (d, J = 10.5 Hz, 5H), 6.42 (s, 1H), 5.80 (s, 0H), 5.57 (t, J = 6.8 Hz, 1H), 5.46 (d, J = 5.7 Hz, 1H), 4.74 (s, 0H), 4.56 (d, J = 13.4 Hz, 0H), 4.50 (s, 1H), 4.46 (s, 2H), 3.96 (d, J = 13.7 Hz, 1H), 3.84 (q, J = 4.3 Hz, 12H), 3.77 (s, 3H), 3.70 (s, 7H), 3.60 (q, J = 7.1 Hz, 14H), 3.53 (dt, J = 19.7, 5.3 Hz, 4H), 3.46 – 3.40 (m, 3H), 3.38 (d, J = 9.8 Hz, 1H), 3.03 (d, J = 9.4 Hz, 0H), 2.76 (t, J = 13.1 Hz, 1H), 2.67 – 2.51 (m, 1H), 2.48 (s, 1H), 2.44 – 2.35 (m, 1H), 2.34 – 2.21 (m, 4H), 2.06 (td, J = 21.3, 9.8 Hz, 6H), 1.99 – 1.80 (m, 3H), 1.76 (t, J = 7.3 Hz, 2H), 1.73 – 1.51 (m, 9H), 1.43 (d, J = 13.4 Hz, 1H), 1.29 (dt, J = 30.0, 16.1 Hz, 4H), 1.15 (p, J = 13.8 Hz, 3H), 0.98 (d, J = 12.3 Hz, 0H), 0.90 (d, J = 12.4 Hz, 1H), 0.76 (t, J = 12.0 Hz, 1H), 0.72 – 0.49 (m, 0H).

¹³C-NMR (176 MHz, CDCl₃): δ 172.5, 170.6, 168.4, 167.9, 157.3, 153.4, 153.2, 149.0, 147.5, 142.4, 137.0, 133.7, 133.4, 130.0, 120.4, 120.2, 119.9, 113.8, 113.5, 111.9, 111.8, 111.5, 105.9, 105.5, 82.8, 75.5, 70.6, 70.4, 70.4, 69.9, 69.8, 69.8, 69.7, 67.5, 61.0, 60.9, 56.5, 56.2, 56.1, 56.1, 56.0, 56.0, 55.2, 52.2, 43.8, 41.5, 41.4, 39.5, 39.5, 39.0, 38.2, 32.9, 32.2, 31.2, 30.8, 26.8, 26.7, 26.3, 26.3, 26.2, 25.7, 21.1, 13.4.

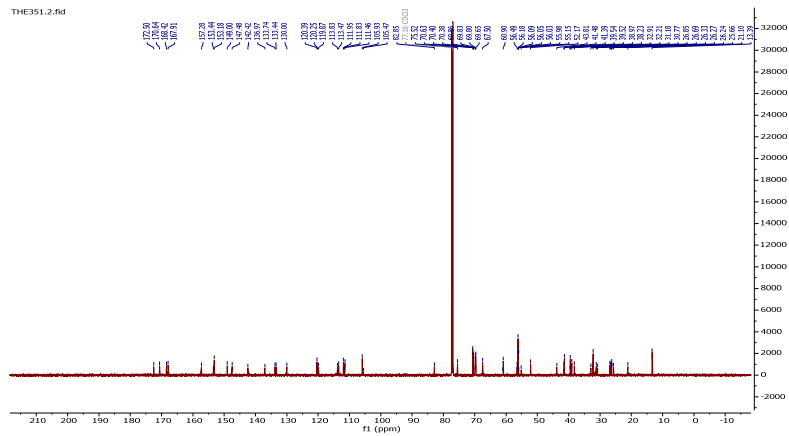
UHPLC-MS: *t*_R = 2.327 min (99 %), *m/z*: calculated = 1056.55 [M+H]⁺, found = 1056.60 [M+H]⁺.

HRMS: *m/z* = 1056.5517 [M+H]⁺ (2.15 ppm error)

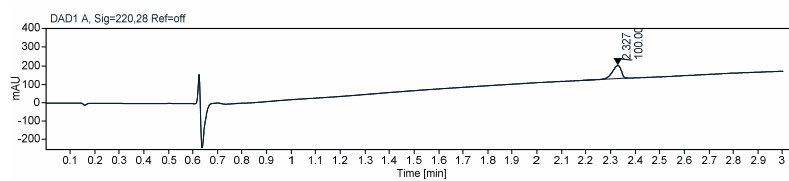
¹H-NMR



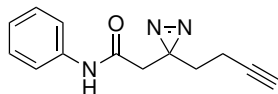
¹³C-NMR



UHPLC, UV 220 nm



2-(3-(but-3-yn-1-yl)-3H-diazirin-3-yl)-N-phenylacetamide



Chemical Formula: C₁₃H₁₃N₃O

Exact Mass: 227.11

Molecular Weight: 227.26

76

The synthesis is conducted according to the general procedure 5.16.1 using 0.33 mmol **69** and aniline as starting materials. The crude product is purified by preparative HPLC and flash column chromatography (DCM/MeCN) 17 mg (23 %) as a white solid.

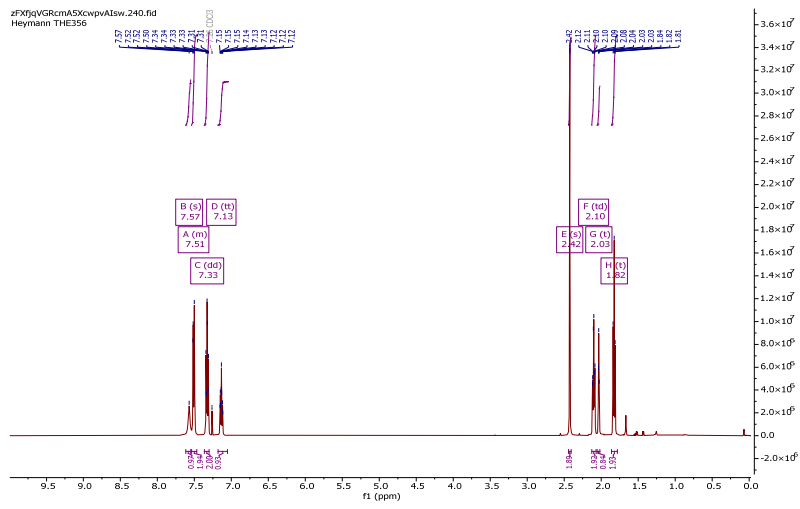
¹H-NMR (500 MHz, CDCl₃): δ 7.57 (s, 1H), 7.54 – 7.47 (m, 2H), 7.33 (dd, J = 8.6, 7.4 Hz, 2H), 7.13 (tt, J = 7.3, 1.2 Hz, 1H), 2.42 (s, 2H), 2.10 (td, J = 7.2, 2.6 Hz, 2H), 2.03 (t, J = 2.7 Hz, 1H), 1.82 (t, J = 7.2 Hz, 2H).

¹³C-NMR (126 MHz, CDCl₃): δ 166.2, 137.4, 129.2, 125.0, 120.4, 82.8, 69.8, 42.7, 32.1, 26.2, 13.4.

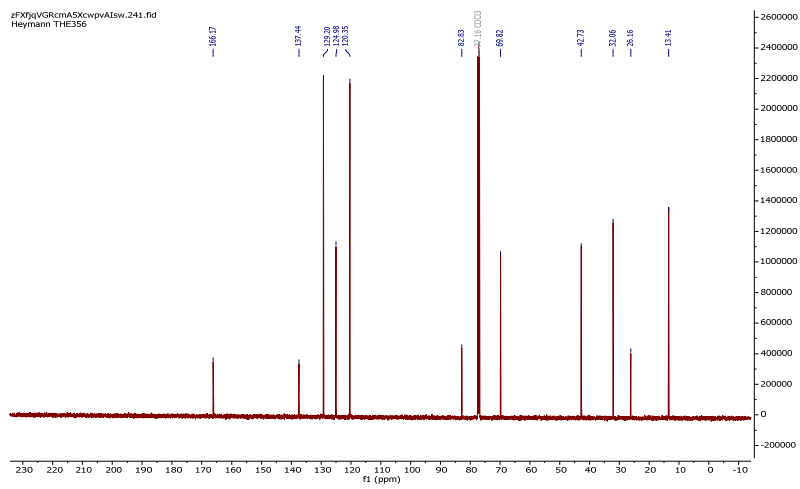
UHPLC-MS: *t*_R = 1.807 min (99 %), *m/z*: calculated = 228.12 [M+H]⁺, found = 228.2 [M+H]⁺.

HRMS: *m/z* = 228.1131 [M+H]⁺ (0.21 ppm error)

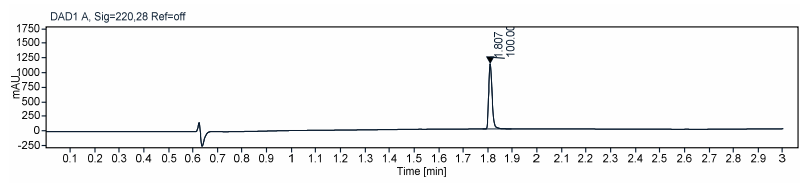
¹H-NMR



¹³C-NMR



UHPLC, UV 220 nm



References

- [1] J. M. Kolos, A. M. Voll, M. Bauder, F. Hausch, *Frontiers in pharmacology* **2018**, *9*, 1425.
- [2] J. Liang, J. Choi, J. Clardy, *Acta crystallographica. Section D Biological crystallography* **1999**, *55*, 736–744.
- [3] J. P. Griffith, J. L. Kim, E. E. Kim, M. D. Sintchak, J. A. Thomson, M. J. Fitzgibbon, M. A. Fleming, P. R. Caron, K. Hsiao, M. A. Navia, *Cell* **1995**, *82*, 507–522.
- [4] C. R. Kissinger, H. E. Parge, D. R. Knighton, C. T. Lewis, L. A. Pelletier, A. Tempczyk, V. J. Kalish, K. D. Tucker, R. E. Showalter, E. W. Moomaw, *Nature* **1995**, *378*, 641–644.
- [5] M. K. Rosen, S. L. Schreiber, *Angewandte Chemie International Edition in English* **1992**, *31*, 384–400.
- [6] L. A. Banaszynski, C. W. Liu, T. J. Wandless, *Journal of the American Chemical Society* **2005**, *127*, 4715–4721.
- [7] A. J. Demetris, J. J. Fung, S. Todo, B. Banner, T. Zerbe, G. Sysyn, T. E. Starzl, *Transplantation proceedings* **1990**, *22*, 25–34.
- [8] R. N. Saunders, M. S. Metcalfe, M. L. Nicholson, *Kidney international* **2001**, *59*, 3–16.
- [9] Z.-H. Zhang, L. X. Li, P. Li, S.-C. Lv, B. Pan, Q. He, *Journal of investigative surgery : the official journal of the Academy of Surgical Research* **2019**, *32*, 632–641.
- [10] Z. Yan, X. Bai, C. Yan, J. Wu, Z. Li, T. Xie, W. Peng, C. Yin, X. Li, S. H. W. Scheres, Y. Shi, N. Yan, *Nature* **2015**, *517*, 50–55.
- [11] T. W. E. Steele, M. Samsó, *Journal of structural biology* **2019**, *205*, 180–188.
- [12] S. Dhindwal, J. Lobo, V. Cabra, D. J. Santiago, A. R. Nayak, K. Dryden, M. Samsó, *Science signaling* **2017**, *10*, DOI 10.1126/scisignal.aai8842.
- [13] W. Shou, B. Aghdasi, D. L. Armstrong, Q. Guo, S. Bao, M. J. Charng, L. M. Mathews, M. D. Schneider, S. L. Hamilton, M. M. Matzuk, *Nature* **1998**, *391*, 489–492.
- [14] X. Sun, J. Wang, X. Yao, W. Zheng, Y. Mao, T. Lan, L. Wang, Y. Sun, X. Zhang, Q. Zhao, J. Zhao, R.-P. Xiao, X. Zhang, G. Ji, Y. Rao, *Cell discovery* **2019**, *5*, 10.
- [15] A. Des Georges, O. B. Clarke, R. Zalk, Q. Yuan, K. J. Condon, R. A. Grassucci, W. A. Hendrickson, A. R. Marks, J. Frank, *Cell* **2016**, *167*, 145–157.e17.
- [16] C. Kozany, A. März, C. Kress, F. Hausch, *Chembiochem : a European journal of chemical biology* **2009**, *10*, 1402–1410.
- [17] C. L. Storer, C. A. Dickey, M. D. Galigniana, T. Rein, M. B. Cox, *Trends in endocrinology and metabolism: TEM* **2011**, *22*, 481–490.

-
- [18] B. M. Dunyak, J. E. Gestwicki, *Journal of medicinal chemistry* **2016**, *59*, 9622–9644.
- [19] D. L. Riggs, P. J. Roberts, S. C. Chirillo, J. Cheung-Flynn, V. Prapapanich, T. Ratajczak, R. Gaber, D. Picard, D. F. Smith, *The EMBO journal* **2003**, *22*, 1158–1167.
- [20] J. C. Young, W. M. Obermann, F. U. Hartl, *The Journal of biological chemistry* **1998**, *273*, 18007–18010.
- [21] J. C. O’Leary, S. Dharia, L. J. Blair, S. Brady, A. G. Johnson, M. Peters, J. Cheung-Flynn, M. B. Cox, G. de Erasquin, E. J. Weeber, U. K. Jinwal, C. A. Dickey, *PLoS one* **2011**, *6*, e24840.
- [22] C. Touma, N. C. Gassen, L. Herrmann, J. Cheung-Flynn, D. R. Büll, I. A. Ionescu, J.-M. Heinzmann, A. Knapman, A. Siebertz, A.-M. Depping, J. Hartmann, F. Hausch, M. V. Schmidt, F. Holsboer, M. Ising, M. B. Cox, U. Schmidt, T. Rein, *Biological psychiatry* **2011**, *70*, 928–936.
- [23] J. Hartmann, K. V. Wagner, C. Liebl, S. H. Scharf, X.-D. Wang, M. Wolf, F. Hausch, T. Rein, U. Schmidt, C. Touma, J. Cheung-Flynn, M. B. Cox, D. F. Smith, F. Holsboer, M. B. Müller, M. V. Schmidt, *Neuropharmacology* **2012**, *62*, 332–339.
- [24] T. Klengel, D. Mehta, C. Anacker, M. Rex-Haffner, J. C. Pruessner, C. M. Pariante, T. W. W. Pace, K. B. Mercer, H. S. Mayberg, B. Bradley, C. B. Nemeroff, F. Holsboer, C. M. Heim, K. J. Ressler, T. Rein, E. B. Binder, *Nature neuroscience* **2013**, *16*, 33–41.
- [25] S. Albu, C. P. N. Romanowski, M. Letizia Curzi, V. Jakubcakova, C. Flachskamm, N. C. Gassen, J. Hartmann, M. V. Schmidt, U. Schmidt, T. Rein, F. Holsboer, F. Hausch, M. Paez-Pereda, M. Kimura, *Journal of sleep research* **2014**, *23*, 176–185.
- [26] L. Hoeijmakers, D. Harbich, B. Schmid, P. J. Lucassen, K. V. Wagner, M. V. Schmidt, J. Hartmann, *PLoS one* **2014**, *9*, e95796.
- [27] A. S. Zannas, M. Jia, K. Hafner, J. Baumert, T. Wiechmann, J. C. Pape, J. Arloth, M. Ködel, S. Martinelli, M. Roitman, S. Röh, A. Haehle, R. T. Emeny, S. Iurato, T. Carrillo-Roa, J. Lahti, K. Räikkönen, J. G. Eriksson, A. J. Drake, M. Waldenberger, S. Wahl, S. Kunze, S. Lucae, B. Bradley, C. Gieger, F. Hausch, A. K. Smith, K. J. Ressler, B. Müller-Myhsok, K.-H. Ladwig, T. Rein, N. C. Gassen, E. B. Binder, *Proceedings of the National Academy of Sciences of the United States of America* **2019**, *116*, 11370–11379.
- [28] S. Gaali, A. Kirschner, S. Cuboni, J. Hartmann, C. Kozany, G. Balsevich, C. Namendorf, P. Fernandez-Vizarra, C. Sippel, A. S. Zannas, R. Draenert, E. B. Binder, O. F. X. Almeida, G. Rühler, M. Uhr, M. V. Schmidt, C. Touma, A. Bracher, F. Hausch, *Nature chemical biology* **2015**, *11*, 33–37.
- [29] L. A. Stechschulte, B. Qiu, M. Warriar, T. D. Hinds, M. Zhang, H. Gu, Y. Xu, S. S. Khuder, L. Russo, S. M. Najjar, B. Lecka-Czernik, W. Yong, E. R. Sanchez, *Endocrinology* **2016**, *157*, 3888–3900.

-
- [30] G. Balsevich, A. S. Häusl, C. W. Meyer, S. Karamihalev, X. Feng, M. L. Pöhlmann, C. Dournes, A. Uribe-Marino, S. Santarelli, C. Labermaier, K. Hafner, T. Mao, M. Breitsamer, M. Theodoropoulou, C. Namendorf, M. Uhr, M. Paez-Pereda, G. Winter, F. Hausch, A. Chen, M. H. Tschöp, T. Rein, N. C. Gassen, M. V. Schmidt, *Nature communications* **2017**, *8*, 1725.
- [31] M. Maiarù, K. K. Tochiki, M. B. Cox, L. V. Annan, C. G. Bell, X. Feng, F. Hausch, S. M. Géranton, *Science translational medicine* **2016**, *8*, 325ra19.
- [32] S. D. Linnstaedt, K. D. Riker, C. A. Rueckeis, K. M. Kutchko, L. Lackey, K. R. McCarthy, Y.-H. Tsai, J. S. Parker, M. C. Kurz, P. L. Hendry, C. Lewandowski, E. Datner, C. Pearson, B. O’Neil, R. Domeier, S. Kaushik, A. Laederach, S. A. McLean, *The Journal of neuroscience : the official journal of the Society for Neuroscience* **2018**, *38*, 8407–8420.
- [33] M. Maiarù, O. B. Morgan, T. Mao, M. Breitsamer, H. Bamber, M. Pöhlmann, M. V. Schmidt, G. Winter, F. Hausch, S. M. Géranton, *Pain* **2018**, *159*, 1224–1234.
- [34] J. Cheung-Flynn, V. Prapapanich, M. B. Cox, D. L. Riggs, C. Suarez-Quian, D. F. Smith, *Molecular endocrinology (Baltimore Md.)* **2005**, *19*, 1654–1666.
- [35] Z. Yang, I. M. Wolf, H. Chen, S. Periyasamy, Z. Chen, W. Yong, S. Shi, W. Zhao, J. Xu, A. Srivastava, E. R. Sánchez, W. Shou, *Molecular endocrinology (Baltimore Md.)* **2006**, *20*, 2682–2694.
- [36] S. Gaali, X. Feng, A. Hähle, C. Sippel, A. Bracher, F. Hausch, *Journal of Medicinal Chemistry* **2016**, *59*, 2410–2422.
- [37] X. Feng, C. Sippel, A. Bracher, F. Hausch, *Journal of Medicinal Chemistry* **2015**, *58*, 7796–7806.
- [38] X. Feng, C. Sippel, F. H. Knaup, A. Bracher, S. Staibano, M. F. Romano, F. Hausch, *Journal of Medicinal Chemistry* **2020**, *63*, 231–240.
- [39] M. Bauder, C. Meyners, P. L. Purder, S. Merz, W. O. Sugiarto, A. M. Voll, T. Heymann, F. Hausch, *Journal of medicinal chemistry* **2021**, *64*, 3320–3349.
- [40] A. M. Voll, C. Meyners, M. C. Taubert, T. Bajaj, T. Heymann, S. Merz, A. Charalampidou, J. Kolos, P. L. Purder, T. M. Geiger, P. Wessig, N. C. Gassen, A. Bracher, F. Hausch, *Angewandte Chemie (International ed. in English)* **2021**, *60*, 13257–13263.
- [41] F. Holsboer, *Neuropsychopharmacology : official publication of the American College of Neuropsychopharmacology* **2000**, *23*, 477–501.
- [42] G. P. Chrousos, A. Vingerhoeds, D. Brandon, C. Eil, M. Pugeat, M. DeVroede, D. L. Loriaux, M. B. Lipsett, *Journal of Clinical Investigation* **1982**, *69*, 1261–1269.
- [43] E. B. Binder, *Psychoneuroendocrinology* **2009**, *34 Suppl 1*, S186–95.
- [44] A. S. Zannas, E. B. Binder, *Genes brain and behavior* **2014**, *13*, 25–37.
- [45] E. T. Tatro, I. P. Everall, M. Kaul, C. L. Achim, *Brain research* **2009**, *1286*, 1–12.
- [46] D. Chen, L. Meng, F. Pei, Y. Zheng, J. Leng, *Journal of clinical neuroscience : official journal of the Neurosurgical Society of Australasia* **2017**, *43*, 39–46.
- [47] C. M. Pariante, A. H. Miller, *Biological psychiatry* **2001**, *49*, 391–404.

-
- [48] K. Lee, A. C. Thwin, C. M. Nadel, E. Tse, S. N. Gates, J. E. Gestwicki, D. R. Southworth, *Molecular cell* **2021**, *81*, 3496–3508.e5.
- [49] N. J. Scheuplein, N. M. Bzdyl, E. A. Kibble, T. Lohr, U. Holzgrabe, M. Sarkar-Tyson, *Journal of Medicinal Chemistry* **2020**, *63*, 13355–13388.
- [50] J. Colgan, M. Asmal, J. Luban, *Genomics* **2000**, *68*, 167–178.
- [51] S. Pomplun, C. Sippel, A. Hähle, D. Tay, K. Shima, A. Klages, C. M. Ünal, B. Rieß, H. T. Toh, G. Hansen, H. S. Yoon, A. Bracher, P. Preiser, J. Rupp, M. Steinert, F. Hausch, *Journal of Medicinal Chemistry* **2018**, *61*, 3660–3673.
- [52] D. A. Holt, J. I. Luengo, D. S. Yamashita, H. J. Oh, A. L. Konialian, H. K. Yen, L. W. Rozamus, M. Brandt, M. J. Bossard, M. A. Levy, D. S. Eggleston, J. Liang, L. W. Schultz, T. J. Stout, J. Clardy, *Journal of the American Chemical Society* **1993**, *115*, 9925–9938.
- [53] D. A. Holt, A. L. Konialian-Beck, H.-J. Oh, H.-K. Yen, L. W. Rozamus, A. J. Krog, K. F. Erhard, E. Ortiz, M. A. Levy, M. Brandt, M. J. Bossard, J. I. Luengo, *Bioorganic & Medicinal Chemistry Letters* **1994**, *4*, 315–320.
- [54] S. Pomplun, Y. Wang, A. Kirschner, C. Kozany, A. Bracher, F. Hausch, *Angewandte Chemie International Edition in English* **2015**, *54*, 345–348.
- [55] R. Gopalakrishnan, C. Kozany, Y. Wang, S. Schneider, B. Hoogeland, A. Bracher, F. Hausch, *Journal of Medicinal Chemistry* **2012**, *55*, 4123–4131.
- [56] M. T. Gnatzy, T. M. Geiger, A. Kuehn, N. Gutfreund, M. Walz, J. M. Kolos, F. Hausch, *Chembiochem : a European journal of chemical biology* **2021**, *22*, 2257–2261.
- [57] A. K. Yudin, *Chemical science* **2015**, *6*, 30–49.
- [58] J. Mallinson, I. Collins, *Future medicinal chemistry* **2012**, *4*, 1409–1438.
- [59] P. K. Mishra, C.-M. Yoo, E. Hong, H. W. Rhee, *Chembiochem : a European journal of chemical biology* **2020**, *21*, 924–932.
- [60] A. L. Mackinnon, J. Taunton, *Current protocols in chemical biology* **2009**, *1*, 55–73.
- [61] H. Guo, Z. Li, *MedChemComm* **2017**, *8*, 1585–1591.
- [62] M. Walko, E. Hewitt, S. E. Radford, A. J. Wilson, *RSC Advances* **2019**, *9*, 7610–7614.
- [63] N. J. Alves, M. M. Champion, J. F. Stefanick, M. W. Handlogten, D. T. Moustakas, Y. Shi, B. F. Shaw, R. M. Navari, T. Kiziltepe, B. Bilgicer, *Biomaterials* **2013**, *34*, 5700–5710.
- [64] A. M. Sadaghiani, S. H. Verhelst, M. Bogyo, *Current opinion in chemical biology* **2007**, *11*, 20–28.
- [65] L. Dubinsky, B. P. Krom, M. M. Meijler, *Bioorganic & medicinal chemistry* **2012**, *20*, 554–570.
- [66] Y. Su, J. Ge, B. Zhu, Y.-G. Zheng, Q. Zhu, S. Q. Yao, *Current opinion in chemical biology* **2013**, *17*, 768–775.
- [67] J. R. Hill, A. A. B. Robertson, *Journal of Medicinal Chemistry* **2018**, *61*, 6945–6963.
- [68] D. P. Murale, S. C. Hong, M. M. Haque, J.-S. Lee, *Proteome science* **2016**, *15*, 14.

-
- [69] K. Yatabe, M. Hisada, Y. Tabuchi, M. Taki, *International journal of molecular sciences* **2018**, *19*, DOI 10.3390/ijms19113682.
- [70] J. W. Chin, A. B. Martin, D. S. King, L. Wang, P. G. Schultz, *Proceedings of the National Academy of Sciences of the United States of America* **2002**, *99*, 11020–11024.
- [71] J. W. Chin, P. G. Schultz, *Chembiochem : a European journal of chemical biology* **2002**, *3*, 1135–1137.
- [72] S. A. Fleming, *Tetrahedron* **1995**, *51*, 12479–12520.
- [73] G. Dormán, G. D. Prestwich, *Biochemistry* **1994**, *33*, 5661–5673.
- [74] J. B. Fenn, M. Mann, C. K. Meng, S. F. Wong, C. M. Whitehouse, *Science (New York N.Y.)* **1989**, *246*, 64–71.
- [75] K. Tanaka, H. Waki, Y. Ido, S. Akita, Y. Yoshida, T. Yoshida, T. Matsuo, *Rapid Communications in Mass Spectrometry* **1988**, *2*, 151–153.
- [76] E. W. Y. Ng, M. Y. M. Wong, T. C. W. Poon, *Topics in current chemistry* **2014**, *336*, 139–175.
- [77] J. J. Pitt, *The Clinical biochemist. Reviews* **2009**, *30*, 19–34.
- [78] A. Sinha, M. Mann, *The Biochemist* **2020**, *42*, 64–69.
- [79] Y. Bian, R. Zheng, F. P. Bayer, C. Wong, Y.-C. Chang, C. Meng, D. P. Zolg, M. Reinecke, J. Zecha, S. Wiechmann, S. Heinzlmeir, J. Scherr, B. Hemmer, M. Baynham, A.-C. Gingras, O. Boychenko, B. Kuster, *Nature communications* **2020**, *11*, 157.
- [80] S. C. Taylor, T. Berkelman, G. Yadav, M. Hammond, *Molecular biotechnology* **2013**, *55*, 217–226.
- [81] W.-J. Qian, J. M. Jacobs, T. Liu, D. G. Camp, R. D. Smith, *Molecular & cellular proteomics : MCP* **2006**, *5*, 1727–1744.
- [82] M. Mann, *Journal of proteome research* **2008**, *7*, 3065.
- [83] N. Iwamoto, T. Shimada, *Pharmacology & therapeutics* **2018**, *185*, 147–154.
- [84] L. Nahar, A. Onder, S. D. Sarker, *Phytochemical analysis : PCA* **2020**, *31*, 413–457.
- [85] Y. V. Karpievitch, A. D. Polpitiya, G. A. Anderson, R. D. Smith, A. R. Dabney, *The annals of applied statistics* **2010**, *4*, 1797–1823.
- [86] C. S. Ho, C. W. Lam, M. H. Chan, R. C. Cheung, L. K. Law, L. C. Lit, K. F. Ng, M. W. Suen, H. L. Tai, *The Clinical biochemist. Reviews* **2003**, *24*, 3–12.
- [87] R. H. Rathod, S. R. Chaudhari, A. S. Patil, A. A. Shirkhedkar, *Future Journal of Pharmaceutical Sciences* **2019**, *5*, 14.
- [88] J. Cielecka-Piontek, P. Zalewski, A. Jelińska, P. Garbacki, *Chromatographia* **2013**, *76*, 1429–1437.
- [89] E. Vasconcelos Soares Maciel, A. L. de Toffoli, E. Sobieski, C. E. Domingues Nazário, F. M. Lanças, *Analytica chimica acta* **2020**, *1103*, 11–31.
- [90] T. H. Walter, R. W. Andrews, *TrAC Trends in Analytical Chemistry* **2014**, *63*, 14–20.
- [91] L. Shan, B. R. Jones, *Biomedical chromatography : BMC* **2022**, e5317.

-
- [92] S. Banerjee, S. Mazumdar, *International journal of analytical chemistry* **2012**, 2012, 282574.
- [93] T. W. Burgoyne, G. M. Hieftje, *Mass Spectrometry Reviews* **1996**, 15, 241–259.
- [94] S. Beck, A. Michalski, O. Raether, M. Lubeck, S. Kaspar, N. Goedecke, C. Baessmann, D. Hornburg, F. Meier, I. Paron, N. A. Kulak, J. Cox, M. Mann, *Molecular & cellular proteomics : MCP* **2015**, 14, 2014–2029.
- [95] K.-H. Jang, S. Bae, J. Woo, S.-W. Kang, N.-S. Lee, Y. U. Jeong, *AIP Advances* **2022**, 12, 015121.
- [96] P. E. Miller, M. B. Denton, *Journal of Chemical Education* **1986**, 63, 617.
- [97] C. Géhin, S. W. Holman, *Analytical Science Advances* **2021**, 2, 142–156.
- [98] A. Garabedian, P. Benigni, C. E. Ramirez, E. S. Baker, T. Liu, R. D. Smith, F. Fernandez-Lima, *Journal of the American Society for Mass Spectrometry* **2018**, 29, 817–826.
- [99] E. M. Schmidt, M. A. Pudenzi, J. M. Santos, C. F. F. Angolini, R. C. L. Pereira, Y. S. Rocha, E. Denisov, E. Damoc, A. Makarov, M. N. Eberlin, *RSC Advances* **2018**, 8, 6183–6191.
- [100] R. A. Zubarev, A. Makarov, *Analytical chemistry* **2013**, 85, 5288–5296.
- [101] D. B. Bekker-Jensen, A. Martínez-Val, S. Steigerwald, P. Rütther, K. L. Fort, T. N. Arrey, A. Harder, A. Makarov, J. V. Olsen, *Molecular & cellular proteomics : MCP* **2020**, 19, 716–729.
- [102] Makarov, *Analytical chemistry* **2000**, 72, 1156–1162.
- [103] R. H. Perry, R. G. Cooks, R. J. Noll, *Mass Spectrometry Reviews* **2008**, 27, 661–699.
- [104] M. Hardman, A. A. Makarov, *Analytical chemistry* **2003**, 75, 1699–1705.
- [105] Q. Hu, R. J. Noll, H. Li, A. Makarov, M. Hardman, R. Graham Cooks, *Journal of mass spectrometry : JMS* **2005**, 40, 430–443.
- [106] A. D. Catherman, O. S. Skinner, N. L. Kelleher, *Biochemical and biophysical research communications* **2014**, 445, 683–693.
- [107] Y. Zhang, B. R. Fonslow, B. Shan, M.-C. Baek, J. R. Yates, *Chemical reviews* **2013**, 113, 2343–2394.
- [108] B. Fan, J. Ma, H. Zhang, Y. Liao, W. Wang, S. Zhang, C. Lu, L. Guo, *Asia-Pacific psychiatry : official journal of the Pacific Rim College of Psychiatrists* **2021**, 13, e12464.
- [109] A. I. Nepomuceno, R. J. Gibson, S. M. Randall, D. C. Muddiman, *Journal of proteome research* **2014**, 13, 777–785.
- [110] P. Barbier Saint Hilaire, K. Rousseau, A. Seyer, S. Dechaumet, A. Damont, C. Junot, F. Fenaille, *Metabolites* **2020**, 10, DOI 10.3390/metabo10040158.
- [111] M. P. Jedrychowski, E. L. Huttlin, W. Haas, M. E. Sowa, R. Rad, S. P. Gygi, *Molecular & cellular proteomics : MCP* **2011**, 10, M111.009910.
- [112] K. L. Fort, C. N. Cramer, V. G. Voinov, Y. V. Vasil'ev, N. I. Lopez, J. S. Beckman, A. J. R. Heck, *Journal of proteome research* **2018**, 17, 926–933.

-
- [113] T. P. Cleland, C. J. DeHart, R. T. Fellers, A. J. VanNispen, J. B. Greer, R. D. LeDuc, W. R. Parker, P. M. Thomas, N. L. Kelleher, J. S. Brodbelt, *Journal of proteome research* **2017**, *16*, 2072–2079.
- [114] L. Reubsaet, M. J. Sweredoski, A. Moradian, *Journal of proteome research* **2019**, *18*, 803–813.
- [115] T. K. Toby, L. Fornelli, K. Srzentić, C. J. DeHart, J. Levitsky, J. Friedewald, N. L. Kelleher, *Nature protocols* **2019**, *14*, 119–152.
- [116] E. J. Dupree, M. Jayathirtha, H. Yorkey, M. Mihasan, B. A. Petre, C. C. Darie, *Proteomes* **2020**, *8*, DOI 10.3390/proteomes8030014.
- [117] G. L. Andrews, R. A. Dean, A. M. Hawkrigde, D. C. Muddiman, *Journal of the American Society for Mass Spectrometry* **2011**, *22*, 773–783.
- [118] Á. Révész, M. G. Milley, K. Nagy, D. Szabó, G. Kalló, É. Csósz, K. Vékey, L. Drahos, *Journal of proteome research* **2021**, *20*, 474–484.
- [119] V. J. Patel, K. Thalassinou, S. E. Slade, J. B. Connolly, A. Crombie, J. C. Murrell, J. H. Scrivens, *Journal of proteome research* **2009**, *8*, 3752–3759.
- [120] J. Cox, M. Mann, *Nature biotechnology* **2008**, *26*, 1367–1372.
- [121] S. Tyanova, T. Temu, P. Sinitcyn, A. Carlson, M. Y. Hein, T. Geiger, M. Mann, J. Cox, *Nature methods* **2016**, *13*, 731–740.
- [122] X. R. Liu, M. M. Zhang, M. L. Gross, *Chemical reviews* **2020**, *120*, 4355–4454.
- [123] A. Hvidt, K. Linderstrøm-Lang, *Biochimica et Biophysica Acta* **1955**, *16*, 168–169.
- [124] S. W. Englander, N. R. Kallenbach, *Quarterly reviews of biophysics* **1983**, *16*, 521–655.
- [125] E. I. James, T. A. Murphree, C. Vorauer, J. R. Engen, M. Guttman, *Chemical reviews* **2021**, DOI 10.1021/acs.chemrev.1c00279.
- [126] Y. Hamuro, J. C. Tomasso, S. J. Coales, *Analytical chemistry* **2008**, *80*, 6785–6790.
- [127] J. Ahn, M.-J. Cao, Y. Q. Yu, J. R. Engen, *Biochimica et Biophysica Acta* **2013**, *1834*, 1222–1229.
- [128] A. McKenzie-Coe, N. S. Montes, L. M. Jones, *Chemical reviews* **2021**, DOI 10.1021/acs.chemrev.1c00432.
- [129] X. R. Liu, D. L. Rempel, M. L. Gross, *Analytical chemistry* **2019**, *91*, 12560–12567.
- [130] J.-Q. Guan, M. R. Chance, *Trends in biochemical sciences* **2005**, *30*, 583–592.
- [131] D. M. Hambly, M. L. Gross, *Journal of the American Society for Mass Spectrometry* **2005**, *16*, 2057–2063.
- [132] B. N. Nukuna, G. Sun, V. E. Anderson, *Free radical biology & medicine* **2004**, *37*, 1203–1213.
- [133] S. D. Maleknia, M. Brenowitz, M. R. Chance, *Analytical chemistry* **1999**, *71*, 3965–3973.
- [134] T. D. Tullius, B. A. Dombroski, *Proceedings of the National Academy of Sciences of the United States of America* **1986**, *83*, 5469–5473.

-
- [135] S. M. Cheal, M. Ng, B. Barrios, Z. Miao, A. K. Kalani, C. F. Meares, *Biochemistry* **2009**, *48*, 4577–4586.
- [136] F. P. Jørgensen, M. Bols, *The Journal of organic chemistry* **2018**, *83*, 6050–6055.
- [137] A. Borghese, V. Libert, T. Zhang, C. A. Alt, *Organic Process Research & Development* **2004**, *8*, 532–534.
- [138] E. Pálovics, D. F. Bánhegyi, E. Fogassy, *Chemistry (Weinheim an der Bergstrasse Germany)* **2020**, *2*, 787–795.
- [139] S. Iwama, K. Kuyama, Y. Mori, K. Manoj, R. G. Gonnade, K. Suzuki, C. E. Hughes, P. A. Williams, K. D. M. Harris, S. Veessler, H. Takahashi, H. Tsue, R. Tamura, *Chemistry (Weinheim an der Bergstrasse Germany)* **2014**, *20*, 10343–10350.
- [140] M. R. M. Koos, G. Kummerlöwe, L. Kaltschnee, C. M. Thiele, B. Luy, *Angewandte Chemie International Edition in English* **2016**, *55*, 7655–7659.
- [141] W.-J. Wu, D. P. Raleigh, *The Journal of organic chemistry* **1998**, *63*, 6689–6698.
- [142] J. M. Kolos, S. Pomplun, S. Jung, B. Rieß, P. L. Purder, A. M. Voll, S. Merz, M. Gnatzy, T. M. Geiger, I. Quist-Løkken, J. Jatzlau, P. Knaus, T. Holien, A. Bracher, C. Meyners, P. Czodrowski, V. Krewald, F. Hausch, *Chemical science* **2021**, *12*, 14758–14765.
- [143] T. Nehls, T. Heymann, C. Meyners, F. Hausch, F. Lermyte, *International journal of molecular sciences* **2021**, *22*, DOI 10.3390/ijms22189927.
- [144] Q. Ibert, M. Cauwel, T. Glachet, T. Tite, P. Le Nahenec–Martel, J.-F. Lohier, P.-Y. Renard, X. Franck, V. Reboul, C. Sabot, *Advanced Synthesis & Catalysis* **2021**, *363*, 4390–4398.
- [145] A. V. West, G. Muncipinto, H.-Y. Wu, A. C. Huang, M. T. Labenski, L. H. Jones, C. M. Woo, *Journal of the American Chemical Society* **2021**, *143*, 6691–6700.
- [146] C. E. Müller, D. Zell, R. Hrdina, R. C. Wende, L. Wanka, S. M. M. Schuler, P. R. Schreiner, *The Journal of organic chemistry* **2013**, *78*, 8465–8484.
- [147] M. T. Marty, A. J. Baldwin, E. G. Marklund, G. K. A. Hochberg, J. L. P. Benesch, C. V. Robinson, *Analytical chemistry* **2015**, *87*, 4370–4376.
- [148] R. T. Fellers, J. B. Greer, B. P. Early, X. Yu, R. D. LeDuc, N. L. Kelleher, P. M. Thomas, *PROTEOMICS* **2015**, *15*, 1235–1238.

Curriculum Vitae

Personal information

Name: Tim Heymann

Date and place of birth: 28th May 1995, Groß-Umstadt

Citizenship: German

Education

12/2018-3/2022

Doctoral thesis in chemistry: Synthesis and mass spectrometry based characterization of chemical tools to explore FK506 binding proteins, Felix Hausch

10/2016-10/2018

Master thesis in chemistry: Synthesis of substituted derivatives of SAFit1, Technical University Darmstadt, Felix Hausch

10/2013-09/2016

Bachelor thesis in chemistry: Synthesis of Nek1 kinase inhibitors on the basis of 3-aminopyrazoles, Boris Schmidt

08/2011-07/2013

A-Level, Ernst-Göbel Schule Höchst